

THESE DE DOCTORAT DE

L'UNIVERSITE DE NANTES

ECOLE DOCTORALE N° 605

Biologie Santé

Spécialité : *Immunovirologie*

Par

Ngoc Khanh NGUYEN

Characterization of BKPyV-specific monoclonal antibodies in kidney transplant recipients after BKPyV reactivation

Thèse présentée et soutenue à Nantes, le 31/03/2021

Unité de recherche :

Centre de Recherche en Transplantation et Immunologie (CRTI), INSERM UMR 1064

Centre de Recherche en Cancérologie et Immunologie Nantes-Angers (CRCINA), INSERM UMR 1232

Rapporteurs avant soutenance :

Samira FAFI-KREMER Professeur des Universités - Praticien Hospitalier, Hôpitaux Universitaires de Strasbourg

Michel COGNE Professeur des Universités - CNRS UMR 7276 / INSERM U 1262, Limoges

Composition du Jury :

Président : Samira FAFI-KREMER Professeur des Universités - Praticien Hospitalier, Hôpitaux Universitaires de Strasbourg

Examineurs : Sophie BROUARD Directrice de Recherche, CRTI UMR 1064, Nantes
Catherine FRANCOIS Maître de Conférences des Universités - Praticien Hospitalier, CHU Amiens Sud
Dorian MCILROY Maître de Conférences des Universités, Université de Nantes
Xavier SAULQUIN Professeur des Universités, Université de Nantes

Dir. de thèse : Dorian MCILROY Maître de Conférences des Universités, Université de Nantes

Co-dir. de thèse : Xavier SAULQUIN Professeur des Universités, Université de Nantes

THESE DE DOCTORAT DE

L'UNIVERSITE DE NANTES

ECOLE DOCTORALE N° 605

Biologie Santé

Spécialité : *Immunovirologie*

Par

Ngoc Khanh NGUYEN

Characterization of BKPyV-specific monoclonal antibodies in kidney transplant recipients after BKPyV reactivation

Thèse présentée et soutenue à Nantes, le 31/03/2021

Unité de recherche :

Centre de Recherche en Transplantation et Immunologie (CRTI), INSERM UMR 1064

Centre de Recherche en Cancérologie et Immunologie Nantes-Angers (CRCINA), INSERM UMR 1232

Rapporteurs avant soutenance :

Samira FAFI-KREMER Professeur des Universités - Praticien Hospitalier, Hôpitaux Universitaires de Strasbourg
Michel COGNE Professeur des Universités - CNRS UMR 7276 / INSERM U 1262, Limoges

Composition du Jury :

Président : Samira FAFI-KREMER Professeur des Universités - Praticien Hospitalier, Hôpitaux Universitaires de Strasbourg

Examineurs : Sophie BROUARD Directrice de Recherche, CRTI UMR 1064, Nantes
Catherine FRANCOIS Maître de Conférences des Universités - Praticien Hospitalier, CHU Amiens Sud
Dorian MCILROY Maître de Conférences des Universités, Université de Nantes
Xavier SAULQUIN Professeur des Universités, Université de Nantes

Dir. de thèse : Dorian MCILROY Maître de Conférences des Universités, Université de Nantes
Co-dir. de thèse : Xavier SAULQUIN Professeur des Universités, Université de Nantes

ACKNOWLEDGEMENT

First and foremost, I would like to express my sincere gratitude to my PhD jury members: **Dr. Samira FAFI-KREMER**, **Dr. Michel COGNE**, **Dr. Catherine FRANCOIS** and **Dr. Sophie BROUARD** for taking your time to read, evaluate my dissertation and to be present in my thesis defense. What a pity that we could not see each other physically for this final meeting other because of the COVID-19 pandemic.

Many thanks to my thesis committee members **Dr. Jacques LEPENDU** and **Dr. Antoine TOUZE** for your useful comments and suggestions.

I am profoundly grateful to my supervisor **Dr. Dorian MCILROY**. Thank you for giving me the opportunity to continue my study as a PhD student. You have consistently supported me not only in the working environment but also in the mental life, especially when France welcomed me with varicella and COVID-19 infections. I truly appreciate your careful and continuous guidance on how to conduct a research, how to get involved in the scientific community, how to prepare a captivating speech, how to stay optimistic towards our projects and so on. I am very grateful for what I have learnt throughout after having worked with you for the last 3 years. Without you, I would not have become the person I am today as a greatly improved version of who I was in 2018.

I am also really grateful to my co-supervisor **Dr. Xavier SAULQUIN**. Although we don't meet quite often, you are always there whenever I need you. You have always been willing and supportive since the first day we met. You have helped me fill in my serious knowledge gap when it comes to immunology, a subject that I did not have a chance to learn during my 4 years of undergraduate education in Vietnam. I appreciate many scientific discussions with you and the valuable experience that I have acquired from

you. You have encouraged me a lot when our project was in trouble. Once again thank you for all of your support, either physical or mental.

This work has been completed in CRTI and CRCINA, so I would like to thank everybody that I have encountered in these two labs as they are the ones who have, in one way or another, contributed to this project.

Laetitia and **Marie-Claire**, many thanks for your contribution to the project. You were really supportive, kind, and friendly. It was a delight working with you.

Karine, Klara, Juliette, thanks for training me on the HPLC technique. **Mike**, you helped me a lot with SPR Biacore, and for that I am much obliged. **Phillippe**, you let me play around with the HCS reader, thank you.

To Viro team in CRTI: **Franck, Céline, Flora, Cécile, Marie, Eléa, Paul**. Many thanks for your supportive, encouraging, considerate, cooperative and friendly working environment.

I won't forget your great help **Jeremie, Cynthia** for the single-cell experiment. I truly appreciate that. A big thank to **Debajyoti, Thomas, Céline, Florian** for helping me with the analysis of single-cell data.

To the PhD students of our "generation" and of the open space 😊 **Marine, Alexandre, Malo, Pière, Marion, Alice, Anaïs, Amélie** for the great time that we have spent together.

Thomas and **Sita**, I'll never forget the time we fought Pokemon bosses together before the first lockdown 😊

Many thanks to **Anh Hòa, Chì Hà** and **Trà My** for the Vietnamese food that you sometimes brought to me. That made me feel less homesick.

Many thanks to all **lab colleagues** in CRTI and CRCINA for your kindness, support and joyful environment. Forgive me if I forget to name someone here, because I have the memory of a goldfish (~.~)'.

A big special thanks to **my parents**. You are always waiting for the day I finish the PhD program and come back home with you. You are my support, my encouragement and my life. I still have 9 months ahead. I'll be home soon.

No words to express my appreciation to **my sisters**. You have been doing your best to take care of mom so that I can concentrate 100% on my writing to finish my PhD journey. And I'm happy to see our mom's conditions becoming better and better day by day.

Finally, special thanks to **Bé Sâu** for being by my side, for your patience and wholehearted support during the last stage of my PhD. I know you have been waiting for this moment for ages. And here it comes 😊.

Again, thank you everyone!!! ❤️❤️❤️

KHANH NGUYEN

CONTENTS

ACKNOWLEDGEMENT	2
CONTENTS.....	5
FIGURES & TABLES	7
ABBREVIATIONS	9
INTRODUCTION.....	10
PART 1: BK POLYOMAVIRUS.....	11
1. History, taxonomy and epidemiology of BK polyomavirus.....	11
1.1. History	11
1.2. Taxonomy.....	12
1.3. Epidemiology & transmission.....	13
2. BK polyomavirus structure.....	16
2.1. BKPyV virion	17
2.2. BKPyV genomic organization.....	18
2.2.1. Non-coding control region (NCCR).....	19
2.2.2. Early coding region.....	20
2.2.3. Late coding region.....	23
2.2.4. MicroRNA (miRNA).....	25
3. BK polyomavirus lifecycle.....	26
3.1. Attachment & Internalization	27
3.2. Intracellular trafficking	28
3.2.1. Targeting endoplasmic reticulum (RE).....	28
3.2.2. Decapsidating & Releasing from ER to cytosol.....	29
3.2.3. Nuclear entry.....	29
3.3. Gene expression & Genome replication.....	30
3.4. Virion assembly & Viral progeny release.....	31
4. Pathogenicity of BK polyomavirus.....	31
4.1. Primary infection & latent state.....	31
4.2. BKPyV reactivation.....	32
4.2.1. In immunocompetent hosts	32
4.2.2. In immunodeficient hosts.....	32
5. BKPyV-associated nephropathy (BKPyVAN)	33
5.1. Risk factors	33
5.2. Diagnosis	35

5.2.	Prevention and Prophylaxis.....	40
5.3.	Current therapeutic approaches.....	41
PART 2: HUMORAL IMMUNE RESPONSE AND ROLES OF B CELLS IN THE RESPONSE AGAINST INFECTIOUS DISEASE.....		44
6.	Humoral immunity and B lymphocytes.....	44
6.1.	Discovery of humoral immunity.....	44
6.2.	Antibodies and their functions.....	44
6.3.	B-cell development: generation, activation and differentiation.....	47
7.	Memory B cell response to secondary infection.....	51
7.1.	Functions of memory B cells.....	51
7.2.	Memory B cell phenotypes and characteristics.....	53
7.3.	Memory B cell localization.....	55
8.	Immune responses to BK polyomavirus.....	56
8.1.	Innate immune response.....	56
8.2.	Adaptive immune response.....	58
8.2.1.	Cellular immunity.....	58
8.2.2.	Humoral immunity.....	60
9.	Neutralizing monoclonal antibodies and viral infections.....	63
9.1.	Introduction.....	63
9.2.	Antibody-mediated neutralization.....	63
9.3.	Neutralizing antibodies and BKPyV infection.....	65
9.4.	Methods for obtaining therapeutic antibodies.....	66
RESEARCH OBJECTIVES.....		69
RESULTS.....		70
PART 1: MedRXiv preprint.....		72
PART 2: Identification of a 41F17-like family of BKPyV-specific bNAbs.....		117
PART 3: Detailed report for patent application.....		127
DISCUSSION.....		146
PART 1: Technical aspects.....		148
PART 2: IgM memory B-cells in BKPyV-specific humoral response in kidney transplant recipients.....		152
PART 3: 41F17-like broadly neutralizing antibodies.....		155
REFERENCES.....		160
RESUME EN FRANCAIS.....		188
ANNEX.....		196

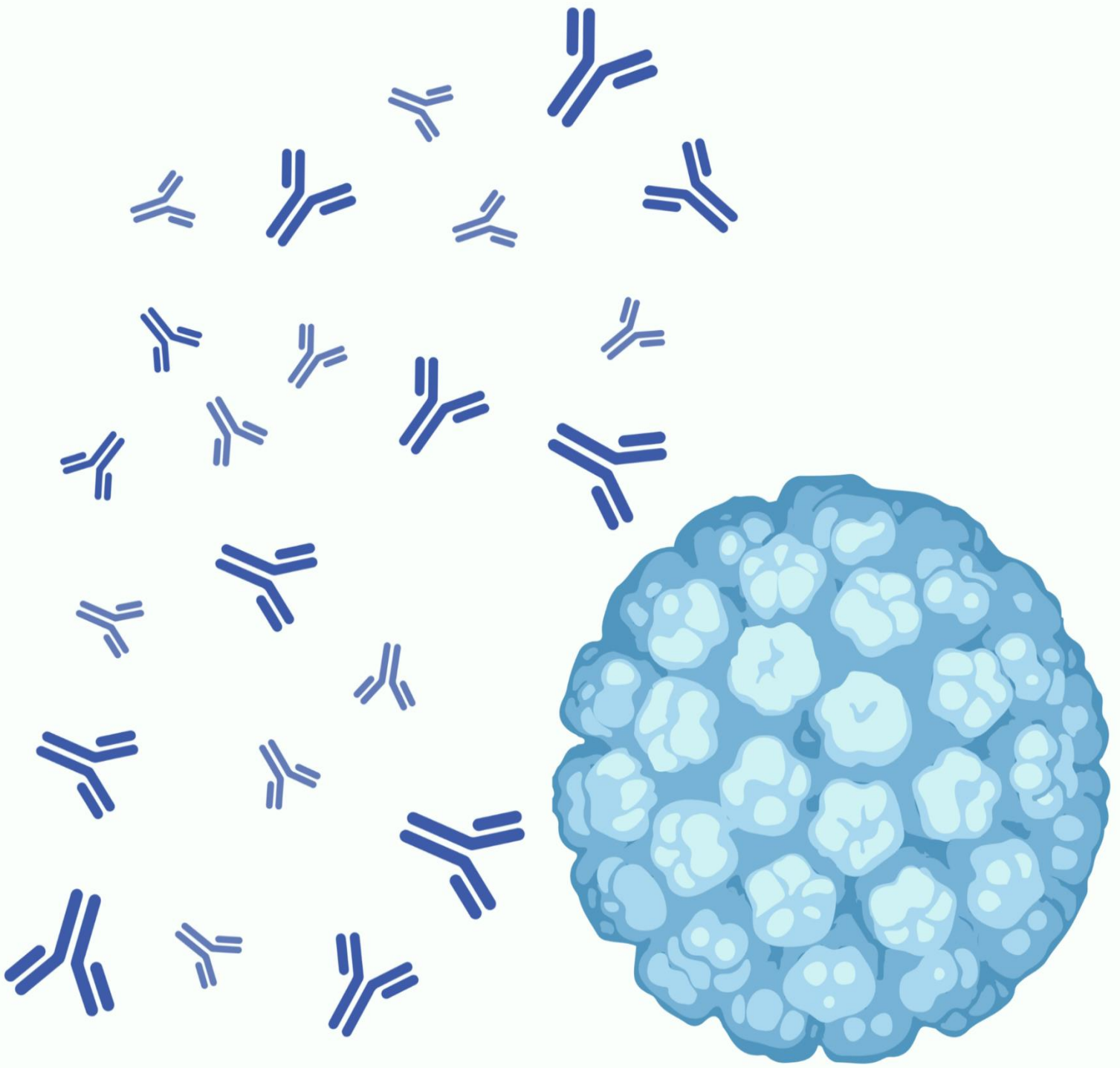
FIGURES & TABLES

Figure 1: BKPyV particles observed in the patient's urine for the first time.	12
Figure 2: Seroprevalence of BK polyomavirus at different ages.....	14
Figure 3: Distribution of four BKPyV subtypes I to IV worldwide.	15
Figure 4: Geographical distribution of four subgroups of BKPyV subtype I.....	16
Figure 5: Structure of BKPyV particles obtained by cryo-electron microscopy	17
Figure 6: BKPyV genome structure.....	18
Figure 7: Schematic representation of NCCR architecture and expression levels of early viral gene region (EVGR) and late viral gene region (LVGR) of different BKPyV strains.	20
Figure 8: Functional domains of BKPyV TAg	22
Figure 9: BKPyV lifecycle	26
Figure 10: Schematic presentation of structures of disialic acid-containing b-series gangliosides GD3, GD2, GD1b and GT1b	27
Figure 11: Risk factors for BKPyV-associated nephropathy in kidney transplant recipients	35
Figure 12: Decoy cells in patients' urine with enlarged nucleus and basophilic intranuclear inclusion, stained with Papanicolaou	36
Figure 13: Negative staining electron microscopy of BKPyV aggregates (Haufen) observed in urine of a BKPyVAN patient	37
Figure 14: Histologic classification system of Polyomavirus nephropathy	39
Figure 15: BKPyV screening and patient management after renal transplantation	40
Figure 16: Immunoglobulin structure	45
Figure 17: VDJ rearrangement of gene segments	48
Figure 18: Different stages of B cell development	49
Figure 19: A schematic of B-cell developmental stages in the spleen	51
Figure 20: Roles of long-lived plasma cells and memory B cells in the secondary response to pathogens	52
Figure 21: Relationship between T cell response and clinical outcomes of BKPyV infection.....	60

Figure 22: Approaches for the generation of fully human therapeutic antibodies	66
Figure 23: CDR3 sequence clustering BKPyV-specific IgG and definition of a 41F17-like family of BNAbs.....	120
Figure 24: Phylogram of Kappa (upper panel) and Lambda (lower panel) light chain SpecB antibodies	121
Figure 25: Neutralization properties of non-41F17-like antibodies on 293TT cells	123
Figure 26: Identification of critical binding residues on the virus capsid by alanine scanning.....	124
Figure 27: Titration of antibody binding to wild-type and mutant gI BKPyV VLP.	125
Figure 28: BCR clustering based on CDR3 properties of IgG isotype.....	155
Figure 29: Neutralization properties of antibody 206 on RS cells	156
Figure 30: Potential broadly neutralizing antibody cluster (red) detected in the phylogram of CDR3 heavy and lambda light chains.	158
Table 1: Diagnosis of BKPyV replication and nephropathy	36

ABBREVIATIONS

aa: amino acid	kDa: kilo Dalton
Ab(s): Antibody(ies)	mAb(s): monoclonal antibody(ies)
BKPyV: BK polyomavirus	MPyV: Murine polyomavirus
BKPyVAN: BK polyomavirus-associated nephropathy	mRNA : messenger RNA
bNAb(s): Broadly neutralizing antibody(ies)	NAb(s): Neutralizing antibody(ies)
bp : base pair	NCCR: Non-coding control region
BSA: Bovine serum albumin	NK : Natural Killer cells
CMV : Cytomegalovirus	PCR: Polymerase chain reaction
CTL(s): Cytotoxic T lymphocyte(s)	PSV(s): Pseudovirus(es)
DC : Dendritic cells	PyVAN: Polyomavirus-associated nephropathy
DNA : Deoxyribonucleic acid	qPCR: Quantitative polymerase chain reaction
dsDNA: double-stranded DNA	RNA : Ribonucleic acid
Fab : Antigen-binding fragments	RT-PCR : Reverse transcription polymerase chain reaction
Fc : Fragment crystallizable	SARS-CoV-2: Severe acute respiratory syndrome coronavirus 2
FBS: Fetal bovine serum	SPR: Surface Plasmon Resonance
GC : Germinal center	ssDNA: single-stranded DNA
HCV: Hepatitis C virus	SV40: Simian virus 40
HEK: Human kidney epithelial	TAg : Large T antigen
HIV: Human immunodeficiency virus	tAg : Small t antigen
HRPTEC(s): human renal proximal tubule epithelial cell(s)	TNF : Tumor necrosis factor
IFN : Interferon	VLP(s): Virus-like particle(s)
Ig : Immunoglobulin	



INTRODUCTION

PART 1: BK POLYOMAVIRUS

1. History, taxonomy and epidemiology of BK polyomavirus

1.1. History

On 17 May 1970, a male patient originating from Sudan was hospitalized in St. Mary's Hospital, London for chronic pyelonephritis, a kind of kidney infection typically caused by bacteria, leading to end-stage renal disease. On 24 June 1970, the patient was transplanted with the left kidney and ureter derived from his brother. On 5 October 1970, the patient was readmitted to hospital due to graft pain and no urine production. Examination revealed a distal ureteric stenosis. The patient's urine was collected for several tests. Cytological methods demonstrated that the majority of mononuclear cells contained a single round intranuclear inclusion. Observing urine with electron microscopy showed a huge number of 40-50 nm diameter virus particles, which had similar morphology to polyoma viruses, a subgroup of what was then known as the Papovavirus group (**Figure 1**). Inoculating the patient's urine onto primary rhesus monkey kidney (M.K.) cells and later with African green monkey kidney (Vero) cells, a slowly-increasing cytopathic effect was seen 18 days after the first passage in MK cells and 109 days after passage into Vero cells. Serological tests were performed and showed that the virus did not cross-react with antisera to other polyoma or human papillomaviruses. It did, however, have a weak cross-reaction with Simian virus 40 (SV40) antisera, the first polyomavirus or vacuolating virus accidentally identified in 1953 from leukemic Ak mice (Gross, 1953). As a result, a new virus was discovered and named B.K., after the initials of the individual from whom the virus was isolated (Gardner et al., 1971).

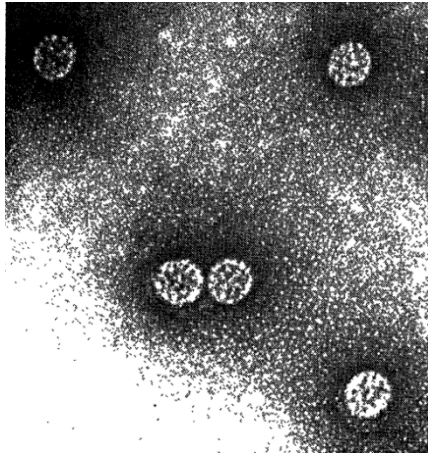


Figure 1: BKPyV particles observed in the patient's urine for the first time.

1.2. Taxonomy

BK virus is a member of human polyomaviruses. BK virus and JC virus were the first two polyomaviruses to be identified that infected human beings. JC virus was isolated in 1971 from the brain tissue of a patient with progressive multifocal leukoencephalopathy, a severe damage of the white matter of the brain at multiple locations (Padgett et al., 1971). Up until 1999, polyomaviruses were classified within the Papovavirus group that consisted of papillomavirus, polyomavirus and vacuolating virus (Melnick, 1962).

In 1999, the seventh Report of the International Committee on Taxonomy of Viruses (ICTV) was published, in which polyomaviruses were split from papillomaviruses to form the two separate families *Polyomaviridae* and *Papillomaviridae* due to their genetic differences. *Polyomavirus* represents the single genus of the family *Polyomaviridae* (Fauquet & Mayo, 2001).

Together with the fast-growing number of polyomaviruses identified, the Polyomaviridae Study Group of the ICTV updated the classification of the family *Polyomaviridae* in 2016, which were based on host specificity, nucleic acid sequence and large T antigen (TAg) coding sequence. Four genera were established, including *Alphapolyomavirus*, *Betapolyomavirus*, *Deltapolyomavirus* and *Gammapolyomavirus*.

The first three genera are known to infect solely mammals and the last one infects birds. In order to avoid arbitrary nomenclature, a standardized species naming system was also proposed by the Polyomaviridae Study Group. Precisely, species are named by the host species followed by *polyomavirus* and a number indicating the order of discovery. *BK polyomavirus* (BKPyV), therefore, has the new species name which is *Human polyomavirus 1* belonging to the genus *Betapolyomavirus* (Calvignac-Spencer et al., 2016). Up to 2019, the family *Polyomaviridae* has 13 human-infecting polyomaviruses, 80 other polyomaviruses and 9 unassigned polyomaviruses (Moens et al., 2017). More recently, the *Polyomaviridae* have been regrouped with the *Papillomaviridae* in the Class *Papovaviricites* (Walker et al., 2020).

1.3. Epidemiology & transmission

BKPyV is a ubiquitous virus throughout the globe. Different serological studies in various populations around the world demonstrated that BKPyV antibodies are detected from early childhood, increasing over time to reach more than 80% seroprevalence in adults and eventually decreasing to approximately 70% among those aged over 50 (Gardner, 1973; Kean et al., 2009; Shah et al., 1973). A study of 1501 adults aged at least 21 from Kean et al. indicated that BKPyV VP1 specific antibodies might be related to age (**Figure 2**) (Kean et al., 2009). Another study on 400 20-59-year-old healthy blood donors in Switzerland revealed the similar tendencies which are 1) IgG seroprevalence for BKPyV reached a peak of 82% in the 20-29-year-old group compared to 71% in the 50-59-year-old group and 2) no IgG seroprevalence difference was found between male and female group (Egli et al., 2009).

Many different routes of BKPyV transmission have been hypothesized. It is most likely that infection with BKPyV is common in early childhood and can be transmitted within the human population via the respiratory route. This hypothesis was strengthened by the detection of BKPyV DNA in tonsillar tissue of children who had acute respiratory disease (Goudsmit et al., 1982), although follow-up studies have found BKPyV

respiratory infections to be infrequent (Sundsford et al., 1994). BKPyV DNA was found in maternal and fetal materials, suggesting that vertical transmission can occur with an estimated prevalence of 4.9%. However, BKPyV infection causes no harm to pregnant women and fetuses (Cheungpasitporn et al., 2018; Pietropaolo et al., 1998), and a careful study of BKPyV genetic subtypes showed that most virus transmission is horizontal (Yogo et al., 2007). Contaminated water or food is also a possible entrance of BKPyV into the human population (Bofill-Mas et al., 2000, 2001). BKPyV is transmissible via organ transplantation as well, especially in kidney transplantation (Andrews et al., 1988). Other potential routes might be sexual transmission and blood transfusion based on the fact that BKPyV DNA is detectable in sperm and blood (Chatterjee et al., 2000; Dolei et al., 2000; Monini et al., 1996). However, further studies are required to determine the frequency of these potential modes of BKPyV transmission in adults. BKPyV primary infection is usually asymptomatic or may cause mild respiratory illness (Goudsmit et al., 1982). Following primo-infection, the virus is possibly transported by peripheral blood leukocytes from the primary site of infection to different sites within the body (Chatterjee et al., 2000), for instance the urinary tract (Heritage et al., 1981) or even central nervous system (Vago et al., 1996) where BKPyV establishes a persistent phase for the whole life of the host.

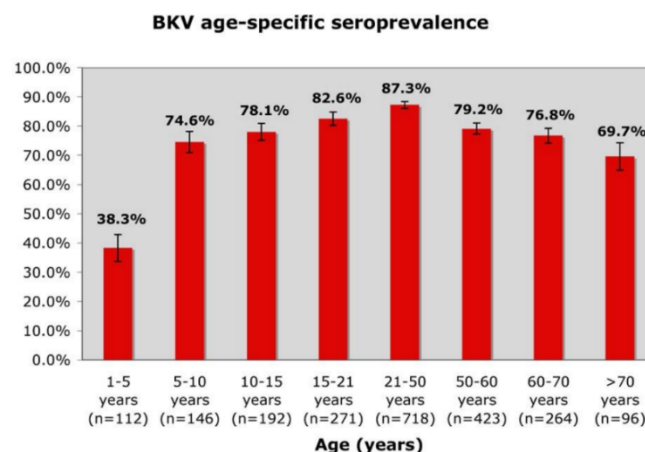


Figure 2: Seroprevalence of BK polyomavirus at different ages (Kean et al., 2009).

BKPyV isolates were classified into four serotypes (Knowles et al., 1989), which were subsequently found to correspond to four genotypes I, II, III and IV based on the polymorphism of residues 61 to 83 within the VP1 protein (Jin, Gibson, Knowles, et al.,

1993). Despite their presence worldwide, the four BKPyV genotypes have distinct geographical distributions (**Figure 3**). More specifically, BKPyV subtype I is widespread throughout the globe with a prevalence rate of 46% to 82%. Subtype IV is found mostly in Europe (39%) and Asia (12-54%) but rarely in Africa (5%). Whereas, subtypes II and III are rarely detected in all geographical areas.

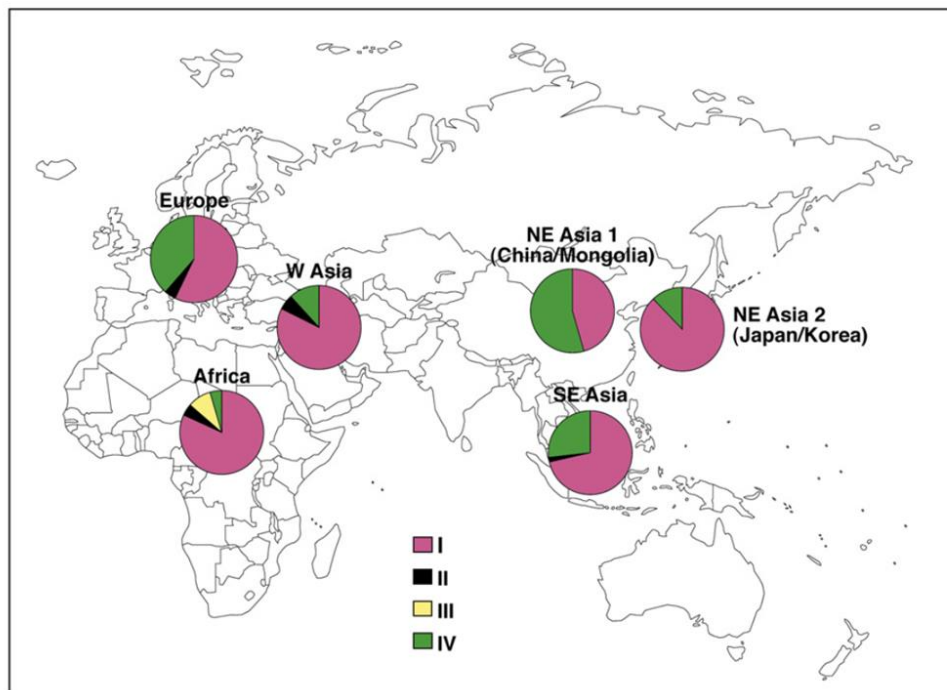


Figure 3: Distribution of four BKPyV subtypes I to IV worldwide (Zheng et al., 2007). Whilst BKPyV subtypes I (46-82%) and IV (5-54%) are the most frequent across the continents, subtype II is restricted to Europe, Africa, West (W) Asia and Southeast (SE) Asia with very low incidences (2-5%). Subtype III is only found in Africa (9%) in the study.

Based on further phylogenetic analysis on nucleotide variations within the typing region, subtype I can be subdivided into four subgroups comprising Ia, Ib-1, Ib-2 and Ic (Nishimoto et al., 2006; Takasaka et al., 2004). In addition, detailed phylogenetic analysis on complete viral DNA sequences revealed that subtype IV isolates can be classified into six subgroups comprising IVa-1, IVa-2, IVb-1, IVb-2, IVc-1 and IVc-2 (Nishimoto et al., 2007). Interestingly, each of these subgroups shows a geographical distribution bias. Subgroup Ia is prevalent in Africa, Ib-1 in Southeast (SE) Asia, Ib-2 in Europe and Ic in Northeast (NE) Asia (**Figure 4**) (Zheng et al., 2007). Concerning the different subgroups of BKPyV subtype IV, all of them except for IVc-2 are prevalent in specific Asian populations. For instance, subgroups IVa-1 and IVc-1 are mainly found in

Southeast Asia and China respectively. Subgroups IVb-1 and IVb-2 have high prevalence in South Korea and Japan. Only subgroup IVc-2 is identified in Europe (Nishimoto et al., 2007).

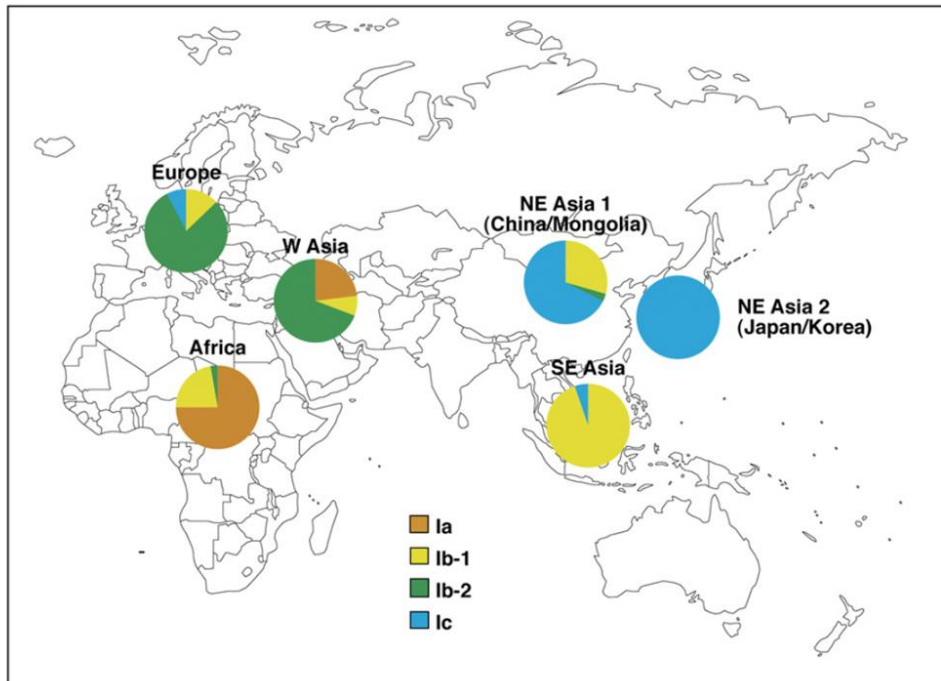


Figure 4: Geographical distribution of four subgroups of BKPyV subtype I (Zheng et al., 2007). Subgroup Ia is predominant in Africa. Subgroup Ib-1 can be detected around the world but most frequently in Southeast (SE) Asia. While Ib-2 is the main subgroup in Europe and West (W) Asia, subgroup Ic shows a geographical distribution biased towards Northeast (NE) Asia.

A study of 178 kidney transplant and bone marrow allograft recipients in Nantes, France showed that subgroups Ib-1 and Ib-2 were the most frequent, accounting for 27.0 % and 51.7% of viruses, respectively. The proportion of subgroup Ia was quite low, at 7.3%. The percentage of subtype IV was slightly higher, at 11.8%. Only 4 out of 178 patients (2.2%) had subtype II BKPyV and no subgroup Ic and subtype III viruses were detected (Michon, 2018).

2. BK polyomavirus structure

As one of the first human polyomaviruses discovered, BKPyV has the typical characteristics of *Polyomaviridae* which are small non-enveloped viruses with a diameter of 40-45 nm. They have circular dsDNA genomes of approximately 5-kilobase

pairs. The viral genome is combined with the cellular histone proteins H2A, H2B, H3 and H4 to form a minichromosome (Moens et al., 2017).

2.1. BKPyV virion

Using high resolution cryo-electron microscopy at subnanometer level, Hurdiss et al. presented the structure of native and infectious BKPyV virions (**Figure 5**). BKPyV particles have a $T = 7d$ icosahedral symmetric structure, containing three structural capsid proteins including surface-exposed VP1, which makes up 80% of the virion, together with VP2 and VP3 which are hidden on the internal face of the capsid. Indeed, BKPyV capsids are composed of 72 pentameric capsomers each containing 5 molecules of VP1 and 1 molecule of either VP2 or VP3 situated in the cavity of VP1 pentamers. Each VP1 has a C-terminal arm that extends to flexibly link the neighboring capsomers together and form the mature capsid (Hurdiss et al., 2016; Rayment et al., 1982). Similar to SV40 (Stehle et al., 1994), the capsid stability of intact BKPyV particles is maintained by the presence of calcium ions and intra- and inter-pentameric disulfide bonds (Nilsson et al., 2005). Because they make up the outer virion surface, VP1 proteins play a crucial role in the attachment to host cells and also in their interactions with antibodies.

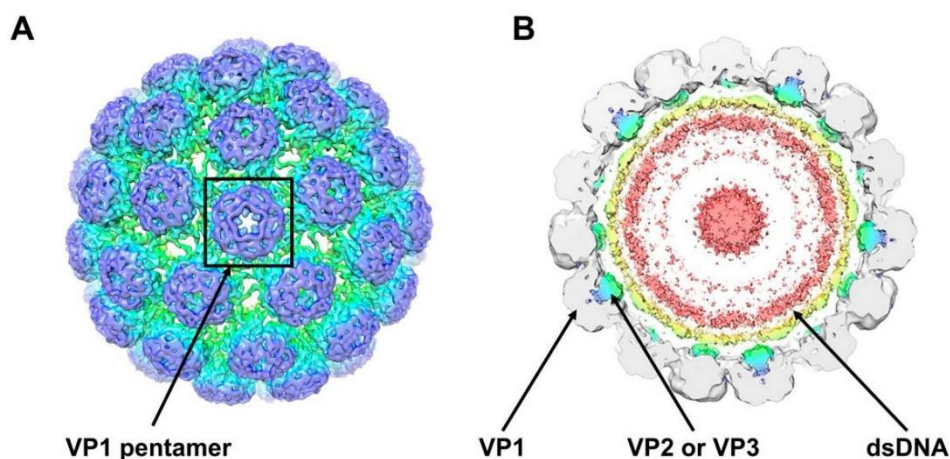


Figure 5: Structure of BKPyV particles obtained by cryo-electron microscopy (Hurdiss et al., 2016). **(A)** External view of the BKPyV virion with VP1 pentamer presented inside the square; **(B)** Internal view of the BKPyV virion at a 40-Å thick slab. Each VP1 penton is associated with one VP2 or VP3 protein to form a capsomer, encapsidating a circular dsDNA molecule.

2.2. BKPyV genomic organization

The genome of BKPyV is a circular double-stranded DNA molecule of approximately 5000 base pairs divided into three functional regions: non-coding control region (NCCR), early coding region and late coding region (**Figure 6**). The protein-coding regions are genetically conserved, whereas the NCCR shows significant variation. In mature BKPyV virions, the genome is complexed with the cellular histones H2A, H2B, H3 and H4 to create a minichromosome containing 20 nucleosomes on the average (Meneguzzi et al., 1978).

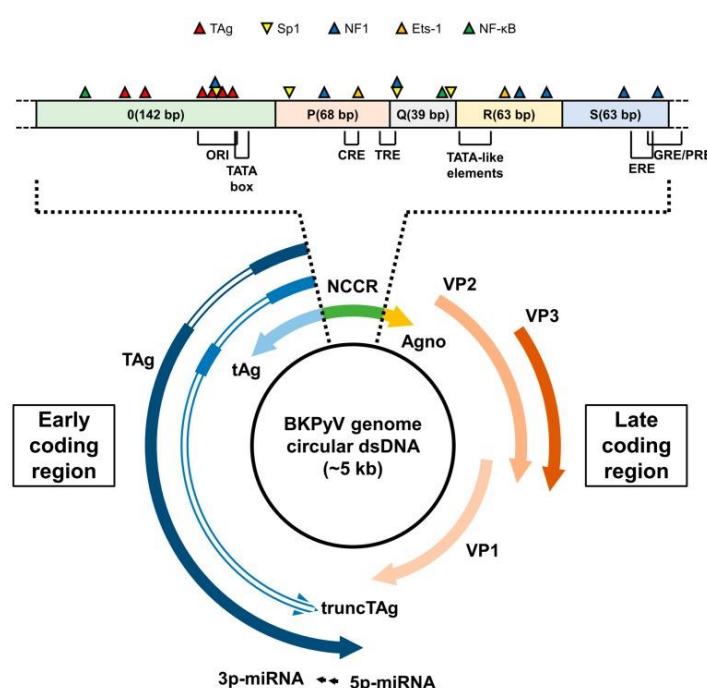


Figure 6: BKPyV genome structure (Helle et al., 2017).

(Bottom) The viral genome is a closed circular dsDNA of roughly 5-kilobase pairs. The viral DNA molecule has three regions: **(1)** the non-coding control region (NCCR) (green, middle top) contains the origin of replication (ori) which initiates bidirectional viral DNA replication; **(2)** the early coding region (left) encodes large T antigen (TAg), small t antigen (tAg) and truncated T antigen (truncTAg); **(3)** the late region (right) encodes structural proteins (VP1, VP2, VP3) together with Agnoprotein.

(Top) NCCR organization of a BKPyV archetype strain. The region is composed of five blocks designated O, P, Q, R and S. Apart from the replication origin (O), it contains a TATA-box, TATA-like elements and various binding sites of regulatory transcription factors including Sp1 (specificity protein 1), NF1 (nuclear factor 1), Ets-1 (protein C-ets-1), NF-κB (nuclear factor kappa-light-chain-enhancer of activated B cells). It also has CRE (cAMP response element), TRE (phorbol ester response element), GRE/PRE (glucocorticoid/progesterone response element) and ERE (estrogen response element) transcription factor binding sites.

2.2.1. Non-coding control region (NCCR)

The NCCR is about 300 - 500 bp in length and localized in between the early and late coding regions. Two forms of NCCR have been described: archetype and rearranged. The archetype NCCR is the predominant form of BKPyV preferentially secreted in the urine and it is considered to be the transmissible form of the virus. During culture *in vitro*, rearranged NCCRs arise as a result of multiple rearrangements of sequences within the region. Due to these modifications, the NCCR is the most variable region of BKPyV genome between different strains (Moens et al., 1995).

The archetype NCCR structure can be classified into five blocks namely O (142 bp), P (68 bp), Q (39 bp), R (63 bp) and S (63 bp) (**Figure 6, top**). The O element is the region situated between the ATG start codon of the early genes and the P block. The O block contains the origin of DNA replication (*ori*) and the TATA box of the early promoter, as well as the binding sites of T antigen and NF- κ B, an inducible transcription factor. The O block is followed by the enhancer elements P, Q, R and S. The P, Q and R blocks contain various transcription factor binding sites where enhancers or suppressors can bind to and modulate the expression of the early and late genes of BKPyV. The S block spans the sequences between the end of the R block and the ATG start codon of the Agno gene. This late leader region is highly conserved between different BKPyV isolates. Interestingly, it contains steroid response units (GRE/PRE and ERE sites in **Figure 6**) (Cubitt, 2006; Moens & Rekvig, 2001; White et al., 2009). Corticosteroids are often used as an anti-rejection treatment in kidney transplant recipients, which was found to have an association with BKPyV reactivation and nephropathy (Hirsch et al., 2002).

As mentioned, the second form of NCCRs comprise rearranged sequences, in which the most frequently occurring modifications are duplications or triplications of the P block including a part of the neighboring O and Q regions. Deletions of any sequences at any position within the P, Q, R or S regions also have been observed (**Figure 7**) (Cubitt, 2006). NCCR rearrangements can occur when the archetype BKPyV propagates in cell culture, showing that rearranged NCCR forms replicate more efficiently in cell culture than

archetype forms (Rubinstein et al., 1991). Moreover, BKPyV with NCCR variants can emerge *in vivo* in immunocompromised kidney transplant recipients, particularly in kidney recipients with prolonged BKPyV viremia and with polyomavirus nephropathy PyVAN (Gosert et al., 2008). Rearranged NCCR strains were demonstrated to have a strong expression of early genes and weak expression of late genes; whereas, archetype NCCR isolates showed the opposite trend (Bethge et al., 2015; Gosert et al., 2008; Martelli et al., 2018).

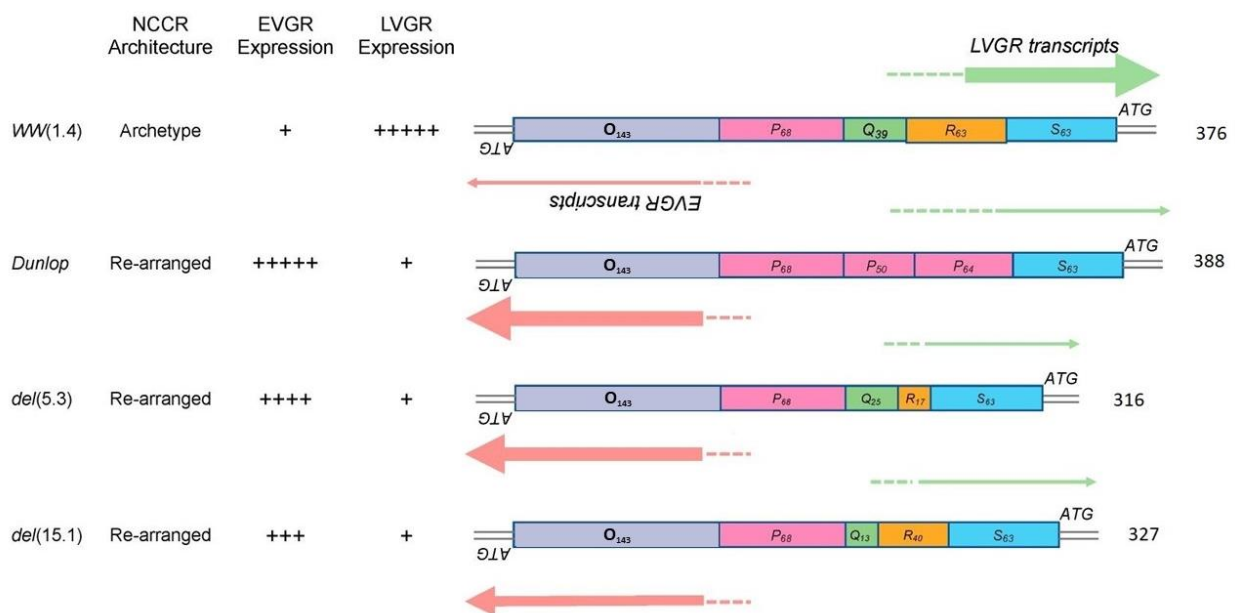


Figure 7: Schematic representation of NCCR architecture and expression levels of early viral gene region (EVGR) and late viral gene region (LVGR) of different BKPyV strains (Adapted from (Martelli et al., 2018)). The NCCR of the archetype BKPyV ww(1.4) is divided into five sequence blocks O (grey), P (pink), Q (green), R (orange) and S (blue). The rearranged NCCRs in: the laboratory-derived Dunlop strain with deletions of Q and R blocks together with triplication of the P block (Henriksen et al., 2015), two clinical strains del(5.3) (Gosert et al., 2008) and del(15.1) (Bethge et al., 2015) containing deletions in the Q and R blocks from kidney transplant patients with nephropathy. Total base pairs of each NCCR are on the right. The relative expression levels of the EVGR and LVGR is presented by the thickness of the red and green arrows (very strong +++++ to weak +).

2.2.2. Early coding region

As the name implies, genes in the early region are transcribed and translated soon after the virus enters host cells. The early coding region is about 2.4-kilobase pair in length and encodes three regulatory proteins: large tumor antigen (TAg), small tumor antigen

(tAg) together with truncated tumor antigen (truncTAg). These proteins are differentially translated by alternative splicing of a common precursor messenger RNA transcript. In detail, removal of the first intron leads to the splicing of the first and second exons, allowing translation of TAg (695 aa, 80 kDa). If the first intron is not removed, the mRNA molecule is translated until reaching the stop codon within the intron resulting in tAg (172 aa, 20 kDa) (Cubitt, 2006). The other alternatively spliced mRNA derived from the excision of a second intron of TAg mRNA encodes truncTAg (136 aa, 17-20 kDa) (**Figure 6, left**) (Abend et al., 2009).

BKPyV TAg is made of 695 amino acids, 529 of which are identical to SV40 TAg, and it is generally thought that BKPyV TAg has the same functions in infected cells as SV40 TAg (Moens & Rekvig, 2001). Although the DNA sequence of early region is variable, the TAg proteins are more highly conserved than the late proteins VP1 VP2/3 and Agno. This is explained by the prevalence of substitutions at the 3rd position in codons of the *TAg* gene, leading to synonymous variants (Luo et al., 2008). TAg is a complex and multifunctional protein that is necessary for regulating viral genome replication and cell cycle progression. It can exert its various functions based on the existence of different regulatory binding domains (**Figure 8**). In detail, like SV40 TAg, BKPyV TAg is able to interact with the retinoblastoma susceptibility protein (pRb), a negative regulator of cell growth, and its family members (p107 and p130) through a highly conserved motif LXCXE (Leucine-X-Cysteine-X-Glutamine). This binding requires both intact pRb-binding domain and intact J domain at the N-terminus. Due to the interaction between TAg and pRb, pRb-E2F complexes are disrupted, resulting in the release of the transcription factor E2F. E2F allows cells to enter S phase, meaning that the cellular DNA synthesis machinery is readily available, and can therefore induce viral DNA replication. The second major target of BKPyV TAg is the cellular tumor suppressor protein p53, the main mediator that controls the host response to DNA damage by inducing G1 arrest and apoptosis. Binding of the TAg to p53 involves the GXXXGK motif (Glycine-X-X-X-Glycine-Lysine) present in the TAg ATPase domain, and leads to inactivation of p53, thus

blocking apoptosis and leading to inappropriate cell proliferation and allowing maximal viral production (Harris et al., 1996; Harris et al., 1998).

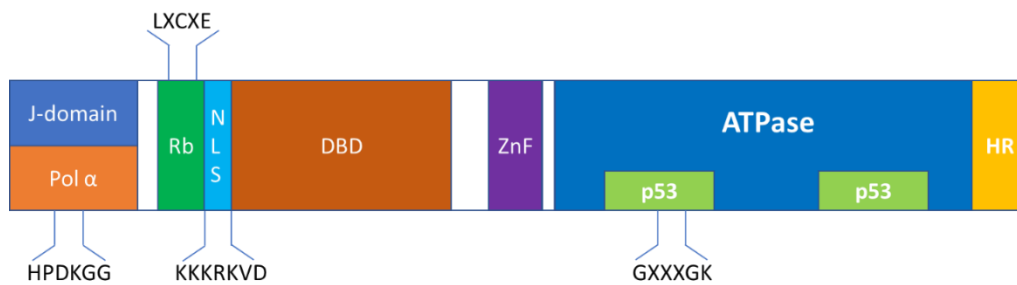


Figure 8: Functional domains of BKPvV TAG (Adapted from (Moens & Rekvig, 2001)). **Pol α** : DNA polymerase α binding site; **J domain**: domain with homology to the DnaJ domain; **Rb**: binding site for the retinoblastoma family members; **DBD**: DNA binding domain; **NLS**: nuclear localization signal domain; **ZnF**: zinc finger binding domain; **ATPase-p53**: ATPase-p53 binding domains; **HR**: host range domain. The one-letter code amino acid is used: H = histidine, P = proline, D = aspartic acid, K = lysine, G = glycine, L = Leucine, C = Cysteine, E = Glutamic acid, R = arginine, V = valine.

The N-terminus of TAG possesses a J domain that shows extensive homology to the DnaJ family of molecular chaperone proteins. The interaction between TAG and the heat shock protein (hsc70) via the HPDKGG motif (Histidine-Proline-Aspartic acid-Lysine-Glycine-Glycine) in the J domain is required for efficient viral application (Moens & Rekvig, 2001). The DNA binding domain recognizes a specific DNA sequence GAGGC present in four copies in the viral *ori* in the NCCR region. The zinc finger binding domain (ZnF) and the ATPase domain of TAG form the enzymatic core of DNA helicase activity which is essential for viral DNA replication (An et al., 2012). Finally, the host range domain (HR) is located at the C-terminus of TAG. This region of SV40 is required for productive viral infection and viral assembly (Stacy et al., 1989). Similar to TAG, truncTAG contains the J domain and the LXCXE motif of pRb binding site, thus it has the corresponding regulatory functions in cell growth and viral replication.

Since they carry a nuclear localization signal (NLS), TAG and truncTAG are primarily located in the nucleus. In contrast, tAg is localized both in the nucleus and the cytoplasm. BKPvV tAg shares the N-terminal J domain with TAG. tAg associates with the catalytic subunit C and regulatory subunit B of protein phosphatase 2A (PP2A), leading to its inactivation which favors cell proliferation and survival (Bennett et al., 2012).

However, the absence of tAg does not impair viral propagation in cell culture (Moens & Rekvig, 2001).

2.2.3. Late coding region

The late coding region is expressed after the onset of viral DNA replication. This region spans 2.3-kilobase pairs and encodes three structural proteins (VP1, VP2 and VP3) and also the agnoprotein. The structural protein transcripts are alternatively spliced from a common precursor mRNA (**Figure 6, right**). Due to the fact that VP2 (351 aa, 38 kDa) and VP3 (232 aa, 27 kDa) have the same mRNA but using different start codons, VP3 is completely identical with the C-terminus of VP2. An addition of 119 aa at the amino terminus of VP3 forms the complete VP2 sequence. Furthermore, VP1 (362 aa, 42 kDa) is translated from a different reading frame and the N-terminus of VP1 overlaps a short sequence of the C-terminus of VP2/VP3. Viral genome packaging and particle formation occurs in the nucleus, so the capsid proteins each carry three functional regions, a DNA binding domain, a protein-protein interaction domain and a nuclear localization signal. VP1 comprises 69% to 84% of the protein mass of the virion; therefore, it is the major capsid protein. VP2 and VP3 are considered minor capsid proteins as they constitute less than 20% of the virion proteins (Moens & Rekvig, 2001; Rayment et al., 1982).

VP1 protein is primarily composed of eight antiparallel β -sheets (B to I), that are joined by loops on the inside and outside of the capsid. The surface-exposed BC, DE, FG and HI loops are highly variable and confer receptor binding specificity (Teunissen et al., 2013). The viral capsid is made of 360 VP1 molecules organized in 72 VP1 pentamers. Each pentamer associates with one copy of either VP2 or VP3 which fills the internal cavity of the VP1 pentamer to form a functional capsomer. In the absence of VP2/VP3, VP1 is able to form virus-like particles (VLPs) resembling native virions and devoid of viral DNA (Salunke et al., 1986). VP1 also has the ability to encapsidate DNA molecules of similar size to the native viral genome, generating pseudoviruses (PSVs) (Gillock et al., 1997). Infectious, though non-replicating PSV can be generated by co-expressing

VP1, VP2 and VP3 in packaging cells, together with a plasmid coding for a reporter gene (Pastrana et al., 2012). The calcium-binding domain and the flexible arm at the C-terminus of VP1 ensure capsid assembly and stability. It was demonstrated that VP1 molecules with truncated C-terminus can form VP1 capsomers but fail to self-associate to form capsids (Garcea et al., 1987). In a similar manner, a point mutation in the calcium-binding region of VP1 prevents capsomer assembly (Haynes et al., 1993). In contrast to VP1, VP2/VP3 proteins are not necessary for viral assembly, and even deletion of VP2/VP3 has no impact on virion stability. However, they are required for the formation of infectious virions (Dean et al., 1995; Nakanishi et al., 2007; Sahli et al., 1993; Teunissen et al., 2013). With regard to VP1 variability, Jin et al. compared VP1 sequences among representative BKPyV strains of each subtypes including four subtype I, four subtypes II, one subtype III and two subtypes IV. They found that the entire coding region of VP1 shares approximately 96% similarity, however, the region spanning amino acids 61-83 (numbering according to BKPyV Dunlop strain) is variable with only about 70% similarity. These hydrophilic residues in the BC loop are considered to be the genomic typing region of BKPyV that distinguishes the four main viral genotypes (Jin, Gibson, Booth, et al., 1993; Jin, Gibson, Knowles, et al., 1993). The receptor binding sites of BKPyV are found to be in the groove between the HI and BC loops. By site-specific mutagenesis within the BC, DE and HI loops of BKPyV VP1, Dugan et al. identified several amino acids that in the BC loop that are important for viral viability and growth. For instance, mutations such as E61A, R64A, G65A, K69A, D79A and K84A prevent BKPyV spread in cell culture (Dugan et al., 2007).

The fourth protein encoded by the viral late transcript is the agnoprotein. It is a small phosphoprotein of 66 amino acids expressed about 36 hours post infection (Moens & Rekvig, 2001; Rinaldo et al., 1998). BKPyV agnoprotein is abundantly expressed *in vitro* in different virus-infected cell lines and *in vivo* in renal tubular epithelial cells of kidney transplant biopsy specimens. The protein resides predominantly in the cytoplasm and in the perinuclear area associated with the outer nuclear membrane. Although it is strongly expressed in infected cells, it is poorly recognized immunologically: fewer than

10% of kidney transplant recipients develop anti-agnoprotein IgG compared to around 60% of patients with anti-TAg IgG and 80% with anti-VP1 IgG (Leuenberger et al., 2007; Rinaldo et al., 1998). BKPyV agnoprotein can be phosphorylated, and phosphorylation of serine 11 plays a critical regulatory role in virus propagation. Replacement of serine 11 with either non-phosphorylatable alanine or phospho-mimicking aspartate reduces the production of infectious viral particles (Johannessen et al., 2008). More recently, Panou et al. have demonstrated that in the absence of agnoprotein, morphologically normal BKPyV virions are still produced and retain their infectivity. However, due to the lack of agnoprotein, BKPyV virions are blocked inside the nucleus of infected cells (Panou et al., 2018). In other words, agnoprotein appears to function as a nuclear egress factor that facilitates virion release by fragmenting the nucleus-surrounding mitochondrial network (Manzetti et al., 2020).

2.2.4. MicroRNA (miRNA)

MicroRNAs (miRNAs) are small non-coding RNAs of 20-22 nucleotides that act as regulatory factors of gene expression through degradation of messenger RNA or translational inhibition. BKPyV encodes one precursor miRNA, bkv-miR-B1, which is complementary to the 3' end of TAg and eventually generates two mature miRNAs: bkv-miR-B1-3p and bkv-miR-B1-5p. The 3p miRNA is conserved between JC and BK polyomaviruses (Broekema & Imperiale, 2013; Li et al., 2014). The BKPyV miRNAs have been demonstrated to inhibit TAg expression in viruses with archetype NCCR, leading to the reduction of viral gene expression and viral DNA replication (Tian et al., 2014). Some studies have shown that BKPyV miRNA expression levels are significantly elevated in kidney transplant patients with biopsy-confirmed PyVAN (Kim et al., 2017; Virtanen et al., 2018), although whether this is a cause or a consequence of the intense virus replication that characterizes PyVAN is not clear. In the SV40 model, mutant viruses that lack miRNA are replication competent, but infected cells are more susceptible to lysis by CTL due to higher levels of TAg expression (Sullivan et al., 2005). Similarly, MPyV mutants lacking miRNA replicate efficiently in cell culture, but show reduced virus

shedding in the urine of infected mice (Burke et al., 2018). Reduced virus shedding reflected more effective immune control of miRNA mutant virus, since viruria was the same in *Rag2*^{-/-} mice for both wild-type and miRNA mutant MPyV.

3. BK polyomavirus lifecycle

The infectious lifecycle of BK polyomavirus starts with the binding of virions to cellular receptors, then entry into the host cell, traffic to the nucleus and initiation of viral gene expression. Following genome replication, new virions are formed and eventually released to complete the viral replication cycle (**Figure 9**). Each step will be described in more detail below.

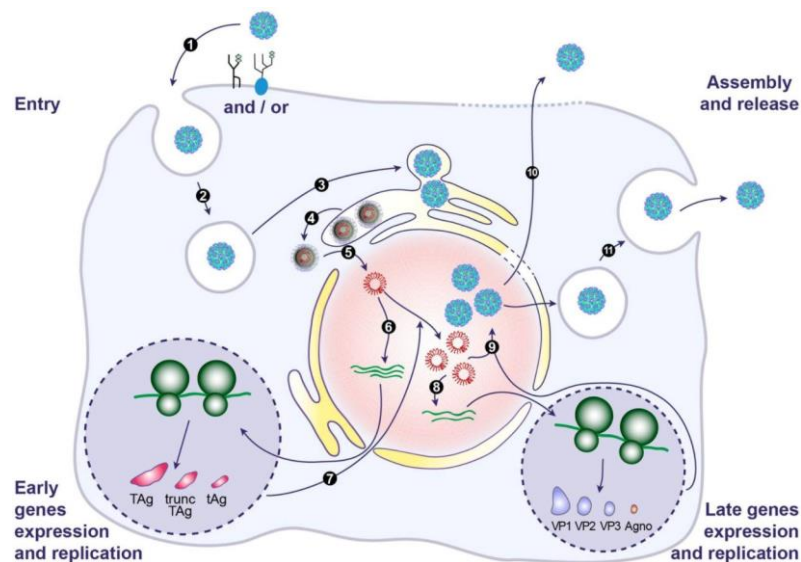


Figure 9: BKPv lifecycle (Helle et al., 2017). Briefly, BKPv initiates its productive infection by binding to ganglioside receptors, especially GT1b and GD1b and/or an N-linked glycoprotein containing $\alpha(2,3)$ -linked sialic acid on the surface of permissive cells (1), subsequent to internalization via caveolae-mediated endocytosis (2) within 4 h. The virus then is carried from late endosomes to endoplasmic reticulum (ER) at roughly 10 h post infection (3). In the ER, the virions are partially uncoated and released to the cytosol thanks to ER-associated degradation (ERAD) machinery (4). The partially disassembled virions are next transported into the nucleus through the nuclear pore with the help of VP2/VP3 NLS and the importin α/β 1 pathway (5). 24 h post infection, the early genes of BKPv are transcribed in the nucleus (6) and translated in the cytosol (7). Viral DNA is replicated, which is followed by the expression of late genes (8). VP1, VP2 and VP3 are translocated into the nucleus where they form themselves into capsids and package newly synthesized double-stranded DNA (9). Finally, progeny virions are released from infected cells via a lytic way (10) or released into the extracellular environment via a non-lytic egress pathway (11).

3.1. Attachment & Internalization

In order to infect cells, BKPyV must attach to its receptors on the host cell surface. Different BKPyV subtypes appear to have distinct cellular entry tropisms (Pastrana et al., 2013), although the molecular mechanisms underlying this observation are not currently known. The primary cell surface receptors used by many polyomaviruses to enter target cells are gangliosides which are sialylated oligosaccharides (glycans) with lipid tails that can be divided into the “a” series and “b” series (O’Hara et al., 2014). It has been demonstrated that all b-series gangliosides (**Figure 10**) can function as cellular receptors of BKPyV, especially GD1b and GT1b. The $\alpha(2,8)$ -disialic acid motif on the right arm of these glycans is required for virus-host cell binding, while the left arm of GD1b and GT1b contributes some additional interaction (Low et al., 2006; Neu et al., 2013). It has also been observed *in vitro* that N-linked glycoprotein containing a terminal $\alpha(2,3)$ -linked sialic acid can be a functional receptor of BKPyV infection of Vero cells (Dugan et al., 2005).

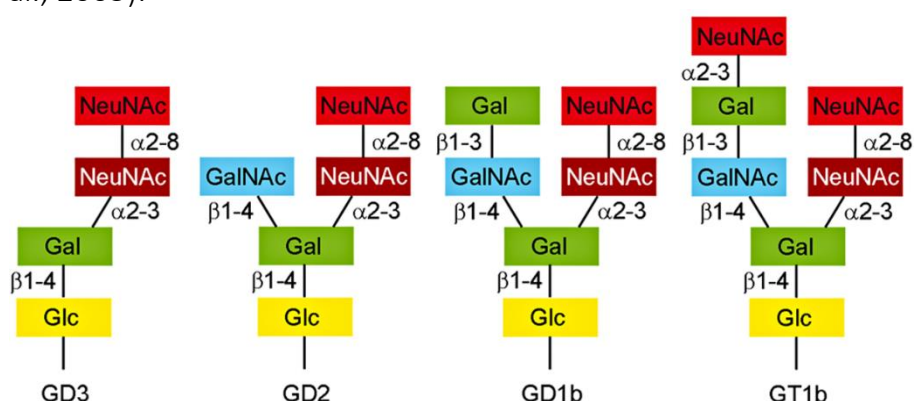


Figure 10: Schematic presentation of structures of disialic acid-containing b-series gangliosides GD3, GD2, GD1b and GT1b (Neu et al., 2013). Abbreviations: Gal = Galactose, Glc = Glucose, NeuNAc = 5-N-acetyl neuraminic acid, GalNAc = N-acetylgalactosamine.

The step following the initial virion attachment to the permissive cell surface is internalization. Since non-enveloped viruses cannot fuse with the host cell membrane, these viruses have used alternative major viral entry pathways including caveolae-mediated, clathrin-mediated, dynamin-dependent and dynamin-independent endocytosis. Endocytic entry is used by a number of naked viruses because 1) this

ensures that virions only enter live cells with active membrane transport, 2) a particle can bind anywhere on the host cell and then be carried through cytoplasmic barriers to reach the perinuclear region, 3) after internalization, no viral proteins remain on the plasma membrane, which reduces the risk of detection by immune system, and finally 4) the low pH conditions in endocytic vesicles can be exploited to activate the penetration program (Pelkmans & Helenius, 2003). While JC polyomavirus enters target cells via a clathrin-dependent pathway (Pho et al., 2000), BK polyomavirus exploits caveolae-mediated endocytosis pathway for uptake into Vero cells. Caveolae (or "little caves") are cholesterol- and sphingolipid-rich smooth invaginations of the plasma membrane with a diameter of 50 to 80 nm (Eash et al., 2004). Studies of BKPyV entry into its main natural target, which are human renal proximal tubule epithelial cells (HRPTEC) showed that the virus uses the same pathway to invade permissive cells and maximally associates with caveolae at 4 h post infection (Moriyama et al., 2007; Moriyama & Sorokin, 2008b). In contrast, a recent report from Zhao et al. failed to reproduce Moriyama's results and pointed out that BKPyV enters HRPTEC in a caveolin- and clathrin-independent pathway (Zhao et al., 2016). Further investigations are therefore still needed in order to definitively determine the BKPyV endocytosis pathways in different cell types.

3.2. Intracellular trafficking

3.2.1. Targeting endoplasmic reticulum (RE)

After being encapsulated by the caveola, BKPyV is trafficked to the late endosome where acidification is essential for BKPyV infection. Low pH conditions are likely to induce conformational changes in the viral capsid, ensuring further virion disassembly and membrane penetration (Jiang et al., 2009; Zhao & Imperiale, 2017). After release from the late endosome, BKPyV-containing vesicles are transported to the ER in Vero and HRPTEC at 8 to 16 h post infection (Jiang et al., 2009). Productive BKPyV infection in Vero cells decreases in the presence of pharmacological drugs that damage the

structural integrity of the microtubule network (Drachenberg et al., 2003; Eash & Atwood, 2005; Moriyama & Sorokin, 2008a), which shows that trafficking of BKPyV requires an intact microtubule network. In contrast BKPyV infection does not apparently depend on intact actin and dynein, a cellular motor protein.

3.2.2. Decapsidating & Releasing from ER to cytosol

Once inside the ER, BKPyV takes advantage of numerous ER lumen proteins including chaperones, disulfide isomerases and disulfide reductase for partial capsid disassembly and egress from the ER to cytosol (Chromy et al., 2006). The evidence for partially disassembled virions is the increased accumulation of accessible VP2/VP3 visualized in the ER. Inside the ER membrane, partially uncoated virions exploit the ER-associated degradation (ERAD) pathway to enter the cytosol (Bennett et al., 2013). Derlin-1, an ER transmembrane protein that detects unfolded/misfolded proteins for proteasome degradation in the cytosol, has been demonstrated to possibly directly take part in carrying BKPyV out of the ER by interacting with VP1 (Jiang et al., 2009). VP1 monomers are also detected in the cytosol following ER trafficking in BKPyV-infected HRPTEC, supporting the idea that BKPyV travels through the ER to the cytosol (Bennett et al., 2013). Together with the ERAD pathway, another critical component that ensures BKPyV productive infection is a functional proteasome which is required until 18 h post infection, a time point after ER trafficking. Proteasome inhibition by lactacystin significantly reduces subsequent TAg expression in infected cells (Jiang et al., 2009), although the precise role of the proteasome in the entry process has yet to be determined.

3.2.3. Nuclear entry

In BKPyV-infected HRPTEC, it has been shown that virion transport from the cytosol to the nucleus through the nuclear pores, is dependent on the nuclear localization signal of the minor capsid proteins VP2/VP3 and the importin α/β 1 pathway (Bennett et al.,

2015). Importins α and $\beta 1$ are adaptor proteins that interact with a nuclear localization signal via certain basic amino acids in the C-terminus of VP2 and VP3. In the context of BKPyV infection, the conserved lysine K200 in VP3 (K319 in VP2) is required for nuclear entry (Bennett et al., 2015).

3.3. Gene expression & Genome replication

Decapsidation is thought to be completed after nuclear entry, after which the BKPyV minichromosome is accessible to host transcription factors. Classical experiments from the 1970s on SV40 lytic infection (Cowan et al., 1973; Lindstrom & Dulbecco, 1972) showed that early expression of the TAg and tAg proteins was required for viral DNA replication, which in turn induced expression of the structural proteins. The lytic infection cycle of BKPyV follows this pattern, with viral gene expression orchestrated by the NCCR. The BKPyV early promoter contains a TATA box motif in the O block, whereas the late promoter lacks a canonical motif, but contains TATA-like elements in the R block (**Figure 6, top**). Thanks to the early promoter, early genes TAg and tAg are transcribed in the nucleus using host RNA polymerase, then translated in the cytoplasm and eventually transported back to the nucleus. The expression of early proteins, especially TAg, plays a central role for viral DNA replication. As described in section 2.2.2, interactions of BKPyV TAg with pRb and p53 proteins trigger cell cycle progression and activation of host DNA synthetic machinery which is required to drive viral genome replication. In addition, TAg is able to bind to the origin of replication in the NCCR and commence bidirectional DNA replication. Briefly, TAg interacts with the core origin in an ATP-dependent way to form a double hexamer which acts like a helicase. Replication protein A (RPA) is then recruited to cover the resulting stretches of single-stranded DNA. In order to facilitate DNA unwinding, topoisomerase I is also recruited to the acting site. In the following step, DNA polymerase α -primase (Pol-prim) interacts with the TAg-RPA-topoisomerase I-DNA complex. Pol-prim synthesizes short RNA primers at the origin, which are elongated by DNA polymerase function of the enzyme complex. Concurrently, Pol-prim switches to DNA polymerase δ (Pol δ). Pol δ , RPA, replication

factor C (RFC) and proliferating cell nuclear antigen (PCNA), all work together for the synthesis of leading strand first, followed by the synthesis of lagging strand to complete viral DNA replication (Tikhanovich & Nasheuer, 2010). Once the viral genome has been replicated, TAg inhibits early gene transcription and stimulates transcription of late genes to express structural proteins VP1, VP2, VP3 and agnoprotein (Eash et al., 2006).

3.4. Virion assembly & Viral progeny release

Capsid proteins expressed in the cytoplasm form capsomers composed of five copies of VP1 associated with one copy of either VP2 or VP3. Capsomers do not associate into higher order structures in the cytoplasm, possibly due to the association of VP1 with cellular chaperon proteins, but are delivered to the nucleus for virion assembly. Import of the structural proteins into the nucleus depends on the NLS of VP1 but does not require the NLS of either VP2 or VP3 (Bennett et al., 2015). The high calcium conditions inside the nucleus favour capsid assembly and stabilization (Chromy et al., 2006), and in MPyV, capsid morphogenesis seems to involve the formation of tubular VP1 structures before the incorporation of chromatinized virus genomes (Erickson et al., 2012). Nuclear export of mature virions is facilitated by the agnoprotein (Johannessen et al., 2011; Panou et al., 2018). Finally, new BKPyV progeny can be released from infected cells in a nonlytic (Evans et al., 2015; Handala et al., 2020) or lytic (Low et al., 2004) manner by 48 h post infection.

4. Pathogenicity of BK polyomavirus

4.1. Primary infection & latent state

In humans, BKPyV primary infection occurs during childhood and the vast majority of cases are subclinical. After infection early in life, a latent infection is established in renal tubular epithelial cells, usually without a significant clinical impact (Wiseman, 2009).

4.2. BKPyV reactivation

BKPyV reactivation from its dormant state can be established by the detection of viral genomes in urine, also called viruria, in both healthy and immunocompromised individuals (Lamarche et al., 2016). BKPyV diseases, which are defined as “cases with histological evidence of BKPyV-mediated organ pathology” (Hirsch & Steiger, 2003), typically develops in immunosuppressed subjects whose immune response against the virus is deficient.

4.2.1. In immunocompetent hosts

BKPyV reactivation in immunocompetent subjects is usually asymptomatic. Egli et al. reported detecting BKPyV genomic DNA in the urine of 28 out of 400 healthy blood donors (7%). The urinary BKPyV load was less than 5 log genome equivalents (GEq)/mL for all subjects and the median viruria was 3.51 log GEq/mL (Egli et al., 2009). BKPyV reactivation during pregnancy was initially detected by the observation that 37% of pregnant women had increased antibody titers against BKPyV (Coleman et al., 1983). More recently, longitudinal analysis has shown that viruria is present in at least 50% of pregnant women (McClure et al., 2012).

4.2.2. In immunodeficient hosts

BKPyV replication and excretion in urine occurs in up to 60% of immunocompromised individuals with an increase of viruria from $< 5 \log_{10}$ GEq/mL to $> 7 \log_{10}$ GEq/mL (Hirsch et al., 2013). This usually leads to the presence of infected cells in the urine or so-called “decoy cells”, which can be seen by urine cytology (Hirsch et al., 2002) and free viral particles which can be observed by direct negative staining electron microscopy (Singh et al., 2009). Despite high-level BKPyV viruria, viremia or BKPyV diseases are rarely present in most solid organ transplant patients (Hirsch & Snydman, 2005). The principal manifestations of BKPyV reactivation mainly occur in kidney transplant patients and

hematopoietic stem cell transplant patients and include adverse clinical outcomes including hemorrhagic cystitis, ureteral stenosis, interstitial nephritis and BKPyV-associated nephropathy (De Gascun & Carr, 2013; Hirsch et al., 2013). Apart from the transplantation context, BKPyV reactivation has also been reported in 21% of patients with AIDS (Markowitz et al., 1993), in patients with multiple sclerosis receiving natalizumab therapy (Loneragan et al., 2009), in 16% of patients with systemic lupus erythematosus (Sundsford et al., 1999), in a six-year-old boy with hyperimmunoglobulin M immunodeficiency (Rosen et al., 1983), in a child with cartilage-hair hypoplasia and Hodgkin's disease (de Silva et al., 1995) and in a patient with Wiskott-Aldrich syndrome (Takemoto et al., 1974).

5. BKPyV-associated nephropathy (BKPyVAN)

In the context of kidney transplantation, the use of immunosuppressive treatment is causally related to the occurrence of active BKPyV replication soon after transplantation. As mentioned above, the evidence of BKPyV reactivation is BKPyV viremia which occurs in up to 60% of kidney transplant recipients, while progression from viremia to viremia is seen in 10-30% of these patients (Hirsch et al., 2013; Krejci et al., 2018; Mengel, 2017). Without any intervention, this can lead to nephropathy, a serious clinical issue of kidney transplantation, which occurs in 1% to 10% of kidney graft patients (Jamboti, 2016; Sharma & Zachariah, 2020). BKPyVAN often causes severe allograft dysfunction in 50% - 80% of patients within 24 months, or even graft loss in 30% - 80% of cases during the subsequent 6 - 60 months (Krejci et al., 2018; Nickeleit et al., 2018).

5.1. Risk factors

Multiple risk factors have been found to contribute to the development of BKPyV reactivation and BKPyVAN, of which the level of immunosuppressive treatment is the most important (Hirsch et al., 2005). Immunosuppression reduction is applied in order

to restrain BKPyV replication and eventually reduce the risk of PyVAN, however, different transplant centres implement different strategies, and there is still no consensus on the optimal method. There are three immunosuppressants that have been used for the majority of kidney transplant recipients, including tacrolimus (a calcineurin inhibitor), mycophenolate (an antiproliferative agent) and corticoids (Hirsch et al., 2005; Krejci et al., 2018). The particular regimen is dependent on transplant centers and each patient's medical history. Patients treated with tacrolimus plus mycophenolate during maintenance immunosuppression therapy have higher risk of BKPyV viremia and BKPyVAN (Suwelack et al., 2012). Furthermore, the higher level of immunosuppressant agents might increase the incidence of BKPyV nephropathy (Cosio et al., 2007). For this reason, plasma levels of immunosuppressive drugs are routinely monitored post kidney transplant, and dosage is adjusted as required.

Several additional risk factors have been documented and can be classified into 3 categories: donor risk factors, recipient risk factors and transplant-associated risk factors (**Figure 11**). Concerning risk factors originating from donors, these include the number of HLA mismatches, deceased donors versus living donors, high BKPyV antibody titers explaining a recent infection, graft load and possibly female gender. Whereas, recipient determinants can include older and male recipient, obesity and low or absent BKPyV-specific antibody titers (Solis et al., 2018). Finally, post-transplantation factors can be the presence of ureteric stents, acute rejection and antirejection treatment, low or absent BKPyV-specific T cell response, and re-transplantation after graft lost (Ambalathingal et al., 2017; Hirsch et al., 2013).

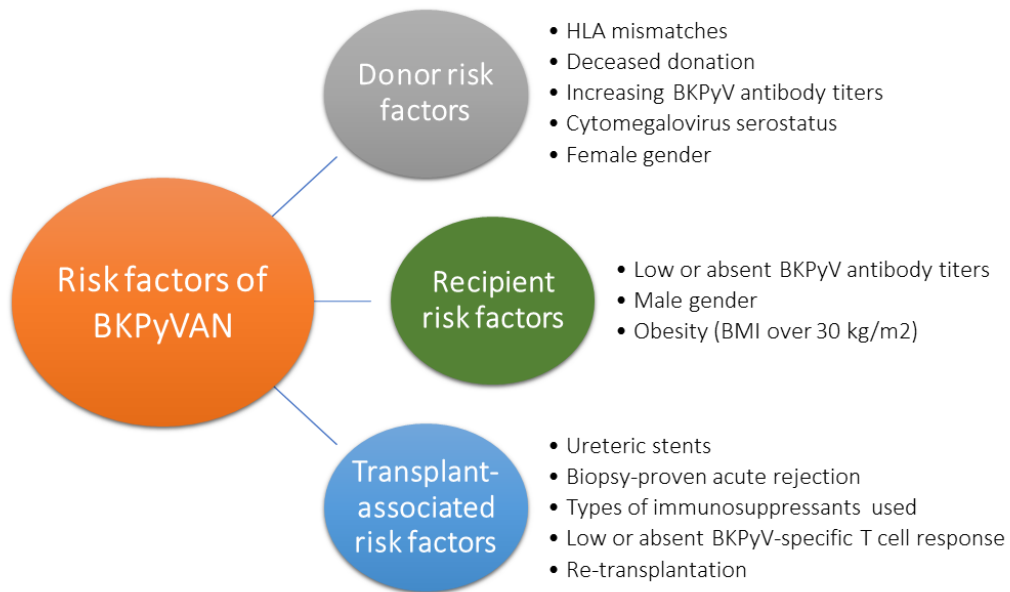


Figure 11: Risk factors for BKPyV-associated nephropathy in kidney transplant recipients (Adapted from (Ambalathingal et al., 2017; Hirsch et al., 2013)). Each of these risk factors can directly or indirectly increase the risk of BKPyV-associated nephropathy.

5.2. Diagnosis

Kidney transplant patients developing BKPyVAN express no specific clinical signs, neither fever nor viral infection symptoms, making diagnosis difficult. Gradually increasing serum creatinine concentration is a biological sign that can be observed in patients with BKPyVAN and can be used to evaluate loss of renal function (Vasudev et al., 2005). However, it is a general indicator of graft dysfunction rather than a specific diagnostic criterion for BKPyVAN (Hirsch et al., 2013). Rather, diagnosis of PyVAN depends on the exploration of viral replication in urine and blood and can only be definitively confirmed by histological examination. An overview of diagnostic criteria is shown in **Table 1** and details are discussed below.

Table 1: Diagnosis of BKPyV replication and nephropathy (Adapted from(Hirsch et al., 2013)).

Test		Diagnosis of BKPyVAN		
		Possible	Presumptive	Proven
Urine	Detection of decoy cells	+	+	+
	Viruria >10 ⁷ copies/μL			
	Detection of polyomavirus-Haufen			
Plasma	Viremia >10 ⁴ copies/μL	-	+	+
Biopsy	Lesions of BKPyV nephropathy, i.e. viral cytopathic changes, interstitial fibrosis	-	-	+
Treatment		No	Yes	Yes

-, not detectable (testing negative); +, detectable (testing positive)

Urinary cytology

Cytological examination of urine is a test to look for BKPyV-infected cells derived from the desquamation of infected renal epithelial cells. These “decoy cells” are observed thanks to Papanicolaou staining and display homogeneous enlarged nuclei due to viral inclusions (**Figure 12**). This test has high sensitivity but positive predictive value is only about 12%. This value can be improved up to 32% if a threshold of > 10 cells is set (Koh et al., 2012; Nankivell et al., 2015). Decoy cells can also be detected in patients who are infected with adenoviruses or Cytomegalovirus (Krejci et al., 2018). Due to its low positive predictive value, testing for decoy cells is not a good diagnostic of BKPyVAN.

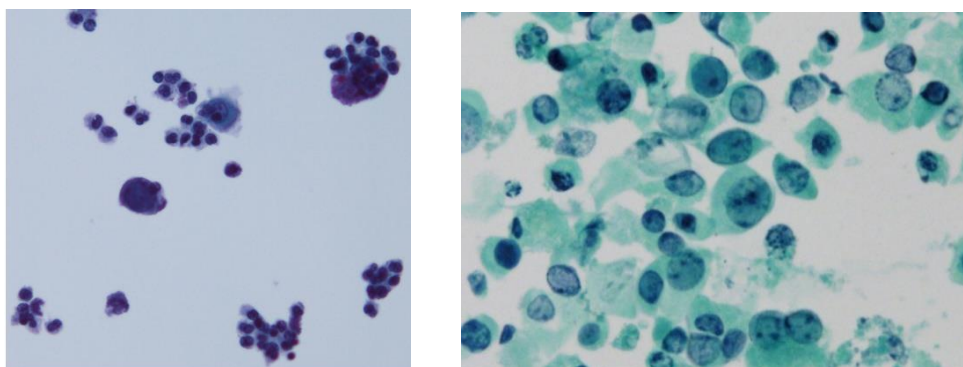


Figure 12: Decoy cells in patients' urine with enlarged nucleus and basophilic intranuclear inclusion, stained with Papanicolaou ((Koh et al., 2012), right; (Nankivell et al., 2015), left).

Polyomavirus-Haufen test

This is a noninvasive method for the purpose of predicting BKPyVAN based on the observation of polyomavirus aggregates (Haufen in German) in urine post renal transplantation. Haufen can be visualized by using negative-staining electron microscopy (**Figure 13**). They develop in damaged renal tubules due to virus infection. After being liberated from infected tubular epithelial cells, BK polyomavirus Haufen streams from the diseased kidneys to the urine. Shedding of urinary BKPyV Haufen is tightly correlated with definitive BKPyV nephropathy, with negative and positive predictive values greater than 95%. Furthermore, quantitative Haufen testing is an effective early diagnosis of BKPyVAN and can be used to monitor intrarenal viral load levels during the course of treatment (Singh et al., 2009, 2015). However, its use is limited by the difficulties of applying electron microscopy to routine clinical practice.

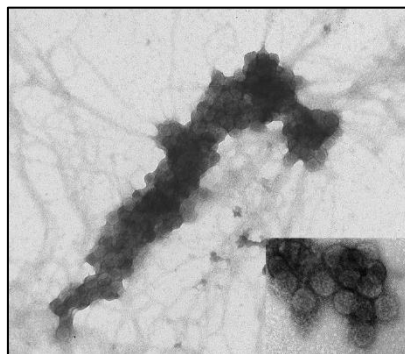


Figure 13: Negative staining electron microscopy of BKPyV aggregates (Haufen) observed in urine of a BKPyVAN patient (Singh et al., 2015) (uranyl acetate stain: x100.000 magnification).

BKPyV DNA detection in urine and blood

Detection of BKPyV DNA in urine (viruria) and blood (viremia) by quantitative PCR (qPCR) currently plays a significant role in the follow-up to kidney transplantation. The Kidney Disease | Improving Global Outcomes (KDIGO) Transplant Work Group recommends that it is necessary to conduct BKPyV screening in kidney recipients by qPCR because of its sensitivity and specificity. The screening should be done monthly for 3-6 months post-transplant, then every quarter until the end of the first year post-transplant (KDIGO Transplant Work Group, 2009). If serum creatinine increases

inexplicably after acute rejection treatment, repeating and augmenting test frequency are advisable (Lamarche et al., 2016). Testing for BKPyV viremia is a noninvasive and cheap method with a window period of 3-6 months prior to viremia and nephropathy. It has a high negative predictive value but very poor positive predictive value for BKPyVAN. It is believed that BKPyV viremia most likely does not directly correlate with the occurrence of BKPyVAN because mathematical modeling suggests that more than 95% of urinary viral DNA comes from urothelial replication and less than 5% from tubular epithelial cells (Funk et al., 2008; Hirsch et al., 2013; Krejci et al., 2018). However, direct evaluation of the origin of decoy cells has shown that most BKPyV viremia reflects virus replication in renal tubules (Ariyasu et al., 2015), and high level viremia $> 10^7$ copies/mL can be used as an early marker for BKPyV viremia, with positive predictive value for BKPyVAN of up to 67% (Randhawa et al., 2004). BKPyV viremia is a crucial diagnostic tool as its positive predictive value is higher than that of viremia. Plasma BKPyV DNA screening should be performed monthly and in patients with prolonged plasma viral loads $> 10^4$ copies/mL, and in the absence of biopsy confirmation, the diagnosis is “presumptive BKPyVAN” (Hirsch et al., 2013).

Histological examination

Definitive BKPyVAN diagnosis requires kidney graft biopsy that should be performed when viremia repeatedly exceeds 10^4 copies/mL to confirm the presence of virus in renal tissue. This test may give false negative results due to sampling error in 10-36.5% of cases, hence it is advisable to collect two biopsy samples, especially try to get medulla tissue where BKPyV primarily replicates (Hirsch et al., 2013). The Banff Working Group on Polyomavirus Nephropathy (PVN) has recently developed “a clinically relevant morphologic classification for definitive Polyomavirus nephropathy”. Disease severity is grouped into three classes (I, II and III) based on polyomavirus replication/load level (pvl) and a Banff ci score (interstitial fibrosis) (**Figure 14**). Polyomavirus nephropathy class 1 can be seen early post grafting. It is the initial stage of the disease when the virus is actively replicating in tissue, but pathology is at an early stage. At the moment of

diagnosis, 33% of patients in this stage have stable graft function. Later, PVN progresses and enters stages 2 and 3 with increased intratubular viral replication, tubular injury and graft scarring that negatively impacts graft function and survival (Nickeleit et al., 2018). Viral antigen is detected by immunohistochemistry staining (IHC) using anti SV40-TAg antibody which cross-reacts with BKPyV TAg and JCPyV TAg, which excludes viral infections caused by Adenovirus, Herpes Simplex Virus or Cytomegalovirus (Nickeleit & Mihatsch, 2006).

Biopsy-Proven PVN ^a Class 1		Biopsy-Proven PVN ^a Class 2		Biopsy-Proven PVN ^a Class 3	
pvl	Banff ci Score	pvl	Banff ci Score	pvl	Banff ci Score
1	0-1	1	2-3	—	—
—	—	2	0-3	—	—
—	—	3	0-1	3	2-3

Figure 14: Histologic classification system of Polyomavirus nephropathy (Nickeleit et al., 2018).

(Upper table) ^aHistologic classes of definitive PVN based on polyomavirus replication/load level (pvl) and Banff ci scores. Banff ci score from 0 to 3 evaluates the extent of cortical fibrosis. The pvl scoring is based on the degree of tubular changes induced by viral infection. A tubule is positive when intranuclear viral inclusion bodies are observed and/or TAg+ cells are detected by IHC. The percentage of positive tubular cross-sections is measured in all available biopsy samples (cores, cortex and medulla). pvl 1 = <1% of all tubules/ducts with viral replication; pvl 2 = 1-10% of all tubules/ducts with viral replication; pvl 3 = >10% of all tubules/ducts with viral replication.

(A-B) Biopsy-proven PVN class 1 (pvl 1, Banff ci ≤1). Seven tubules are positive with SV40-TAg (arrows in A) in the renal cortex, occupying less than 1% of all tubules (cortex and medulla) (pvl 1). No intranuclear viral inclusion bodies observed (B) (Banff ci 0).

(C-D) Biopsy-proven PVN class 2 (pvl 1, Banff ci ≥2 or pvl 2, any Banff ci or pvl 3, Banff ci ≤1). Greater than 10% of all tubules (cortex and medulla) with polyomavirus replication are detected in an SV40-TAg stain (C) (pvl 3). Only minimal fibrosis is seen (arrows in D) (Banff ci 0).

(E-F) Biopsy-proven PVN class 3 (pvl 3, Banff ci ≥2). A few areas with polyomavirus replication are shown in an SV40-TAg stain, making up >10% of all tubules (cortex and medulla) (E) (pvl 3). Interstitial fibrosis spreads out (F) (Banff ci 3).

5.2. Prevention and Prophylaxis

Identification of kidney transplant recipients at high risk of BKPyV reactivation and nephropathy is important to prevent kidney rejection. It needs to be done in a systematic way after transplantation. Screening for BKPyV reactivation should be conducted at least every 3 months during the first 2 years following transplant and then every year until the fifth year posttransplant (Hirsch et al., 2013). Based on the available information, current clinical practices and recommendations, a detailed algorithm of monitoring BKPyV and surveillance is outlined in **Figure 15** (Nickeleit et al., 2018).

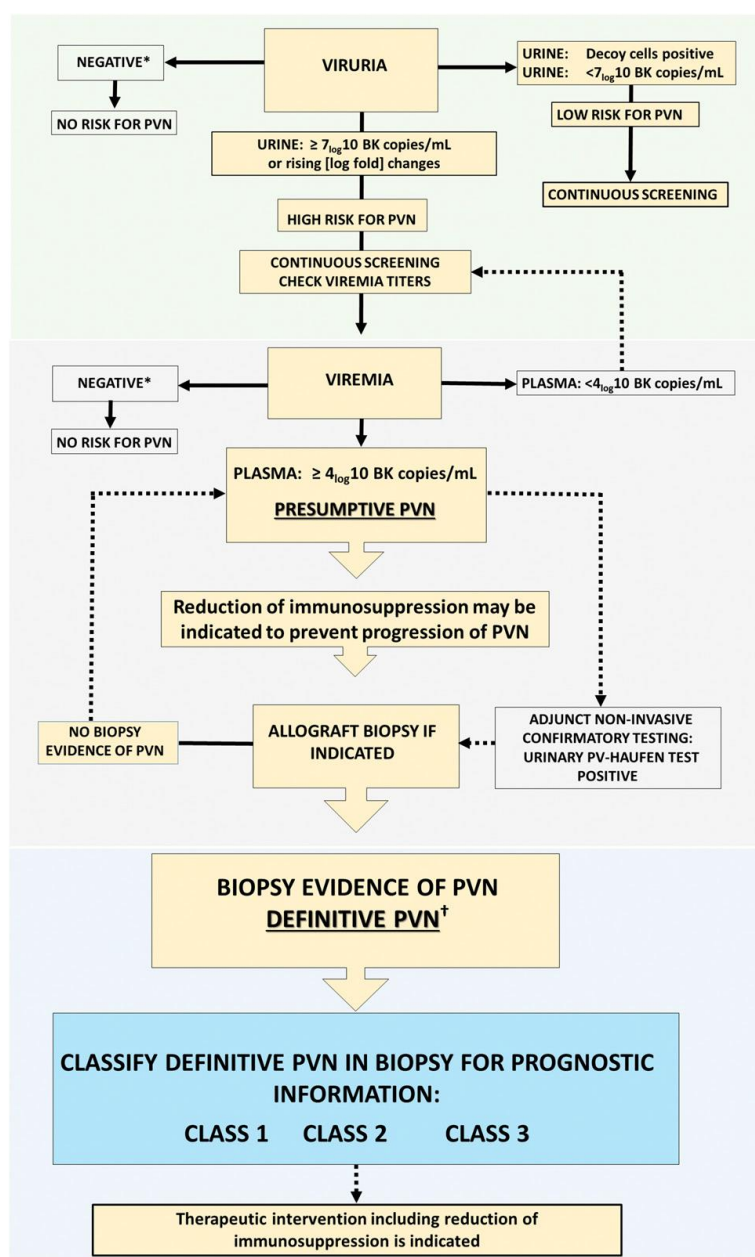


Figure 15: BKPyV screening and patient management after renal transplantation.

5.3. Current therapeutic approaches

In the absence of clinically effective BKPyV-specific antiviral agents, the primary treatment of patients developing BKPyV reactivation and/or BKPyV-associated nephropathy is the reduction of immunosuppression. The objective of this approach is to allow the immune system to respond to viral reactivation. Following the detection of presumptive or definitive BKPyVAN, reducing or discontinuing immunosuppressants should be applied for kidney recipients. Among common immunosuppressive agents used, tacrolimus, cyclosporine (calcineurin inhibitors) and sirolimus (an mTOR inhibitor) trough levels should be less than 6 ng/mL, 150 ng/mL and 6 ng/mL respectively. Similarly, mycophenolate mofetil, a cellular proliferation inhibitor, should not exceed 1000 mg daily dose (Hirsch et al., 2013). Monitoring BKPyV viruria and viremia by qPCR helps to adapt immunosuppressive drugs. Many observational studies have documented that more than 85% of cases succeeded to eliminate viremia (Giraldi et al., 2007; Schaub et al., 2010; Wadei et al., 2006; Wu et al., 2008). Another strategy can be used is to switch from tacrolimus to low-dose cyclosporine or replace calcineurin inhibitor with low-dose sirolimus (Hirsch et al., 2013). All immunosuppression treatment regimens are center-specific.

Regardless of reduction in immunosuppression, there are still patients with sustained high-level BKPyV viremia, and most cases of graft loss following BKPyVAN occur in these patients (Nickeleit et al., 2020). An effective antiviral therapy could have clinical value for these patients, and different antiviral molecules have been used in clinical trials as preventive or curative approaches for BKPyVAN.

Cidofovir is a nucleoside analog that shows good activity for the treatment of cytomegalovirus infection. The action of cidofovir against BKPyV is unclear. Some studies report no renal dysfunction (Araya et al., 2008; Vats et al., 2003), but others report no benefits (Wadei et al., 2006; Wu et al., 2009). Furthermore, cidofovir should be administered with caution in kidney transplant recipients due to its nephrotoxicity (Krejci et al., 2018).

Brincidofovir (CMX-001) is a lipid ester of cidofovir. It has a lower nephrotoxicity but higher anti-BKPyV activity *in vitro* (Rinaldo et al., 2010). Successful outcomes in kidney transplant recipients who receive brincidofovir therapy (Papanicolaou et al., 2015; Reisman et al., 2014).

Leflunomide is an immunosuppressant agent which is approved for rheumatoid arthritis treatment, but it also has antiviral activity. It is able to inhibit BKPyV genome replication and early gene expression in human primary tubular epithelial cells *in vitro* (Liacini et al., 2010). Its positive effect on BKPyV nephropathy was reported in several early studies (Josephson et al., 2006; Nesselhauf et al., 2015; Williams et al., 2005), but this was not confirmed in subsequent trials (Guasch et al., 2010) and adverse side effects, such as hepatic toxicity, hemolysis, and thrombotic microangiopathy have also been reported. A recent systematic review noted that the quality of the available clinical data is too low to draw conclusions on the antiviral efficacy of leflunomide for BKPyVAN and recommended further, well designed clinical trials (Schneidewind et al., 2020).

Fluoroquinolones are antibiotics that target bacterial topoisomerase II and IV. Interestingly, it has an inhibitory function on BKPyV replication on renal proximal tubular epithelial cells (RPTECs) *in vitro* by disturbing viral TAG helicase activity (Sharma et al., 2011). In one clinical study, fluoroquinolones showed effective prevention of BKPyV viruria development early after renal transplantation (Gabardi et al., 2010). In contrast, Knoll et al. reported that levofloxacin, a member of fluoroquinolone family, failed to prevent BKPyV infection posttransplant (Knoll et al., 2014).

Intravenous immunoglobulin (IVIg) has been used as an adjunctive therapy for BKPyV nephropathy as it contains high titers of neutralizing antibodies against BK polyomavirus (Randhawa et al., 2015) and IVIg infusion increases serum neutralizing titers kidney transplant recipients (Velay et al., 2019). Graft functions remain stable in patients administered with IVIg, and several studies have reported positive virological responses when IVIg is used as a salvage therapy for PyVAN (Anyaegbu et al., 2012; Matsumura et al., 2020; Sener et al., 2006; Sharma et al., 2009). More recently, a

retrospective study found a significantly reduced incidence of BKPyV viremia in kidney transplant recipients with low pre-graft anti-BKPyV titers who received IVIG compared to those who did not strongly indicating that IVIG may be effective as a preventive measure against PyVAN (Benotmane et al., 2021).

PART 2: HUMORAL IMMUNE RESPONSE AND ROLES OF B CELLS IN THE RESPONSE AGAINST INFECTIOUS DISEASE

6. Humoral immunity and B lymphocytes

6.1. Discovery of humoral immunity

Humoral immunity is a form of immunity which is mediated by elements found in the humors or body fluids, especially secreted antibodies produced by B cells, that eliminate extracellular pathogens such as bacteria, and can inhibit the cell-to-cell spread of intracellular pathogens like viruses. The function of humoral immunity was first discovered in 1890 by the Germany researcher Emil von Behring (1854-1917) and the Japanese guest researcher Shibasaburo Kitasato (1853-1931) at the Institute for Infectious Diseases in Berlin. They demonstrated that injection of sera from *Clostridium tetani*-infected rabbits helped to protect naïve mice against live tetanus bacilli and tetanus toxin (Behring & Kitasato, 1890). In a single-authored paper published one week later, Behring described the protective activity of immunized serum against diphtheria (Behring, 1890). This is the first evidence for the effective protection of circulating “antitoxins” (now known as “antibodies”) in injected serum. Behring translated his research to human beings who suffered from diphtheria and got positive results with cure rates probably reaching almost 100%, depending on the time of treatment. With standardized techniques developed by Paul Ehrlich, serum was produced in larger quantities and higher qualities in horses for human use in clinical trials. His successful serum therapy of diphtheria and tetanus was honored by the first Nobel Prize in Medicine in 1901 (Kaufmann, 2017).

6.2. Antibodies and their functions

Humoral immunity, or antibody-mediated immunity, is a component of adaptive immunity mediated through the production of antibodies. Antibodies, or soluble immunoglobulins (Ig), are glycoproteins with a Y-shaped Ig monomer (around 150 kDa),

dimer or pentamer. Each Y-shaped structure consists of four polypeptide chains, including two identical heavy (H) chains and two identical light (L) chains (**Figure 16, left**). Five isotypes are defined based on five basic sequences of heavy chain constant regions and named with Greek letters: μ (IgM), δ (IgD), γ (IgG), ϵ (IgE) and α (IgA). Similarly, two major constant sequences are used to classify light chains into κ (kappa) or λ (lambda) chains. In humans, kappa chains make up 60% of light chains compared to only 40% of lambda. The association of heavy and light chains forms two functional regions called Fab which contain the antigen-binding site (**Figure 16, right**). This part is capable of recognizing and binding to a specific epitope, the particular area of the antigen that is recognized by the antibody (Judith A Owen et al., 2013). Antibodies secreted by plasma cells play a key role in the prevention and control of bacterial and/or viral infections in four main ways: 1) binding to pathogens to prevent their entrance into target cells (neutralization); 2) coating pathogens' surface and facilitating their uptake by phagocytic cells (opsonization); 3) activating the complement cascade and 4) activating immune-effector cells (macrophages and NK cells for instance) through antibody-dependent cell-mediated cytotoxic (ADCC) activity (Charles A Janeway et al., 2001; Suzuki et al., 2015). Due to the rearrangement mechanisms between various genes during the development of B lymphocytes, the Fab region has phenomenal genetic diversity, enabling antibodies to recognize an infinite number of antigens (Alberts et al., 2002).

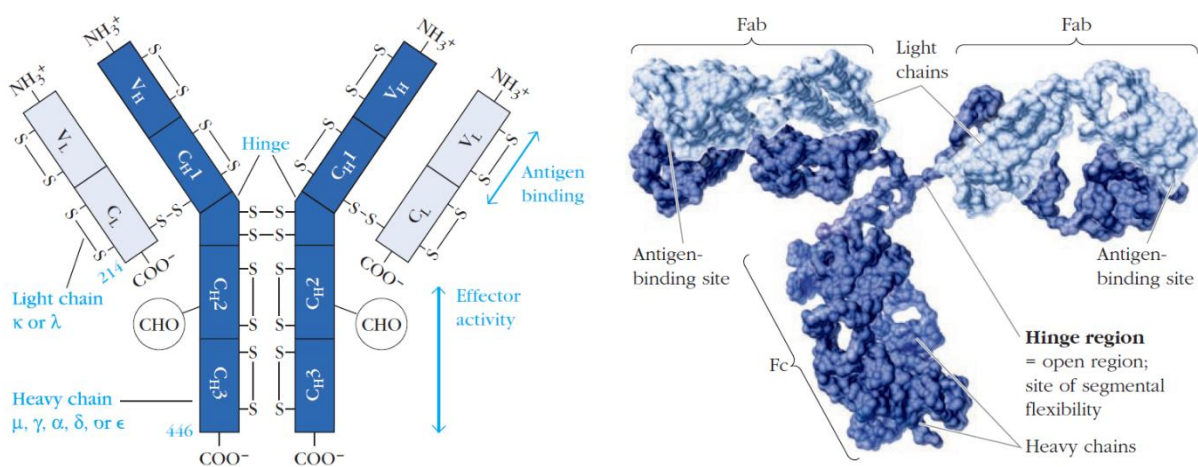


Figure 16: Immunoglobulin structure (Judith A Owen et al., 2013).

The F_C region is made up uniquely by immunoglobulin heavy chains, defining 5 different isotypes with different characteristics.

IgM is the only immunoglobulin to be found in all vertebrate species. This Ig class is always the first antibody produced in a humoral immune response, including viral infections; therefore, it has acute diagnostic value. There are two forms of IgM: dimeric membrane-bound IgM and pentameric soluble/secreted IgM. Although each monomeric IgM structure has low affinity to pathogens, it can be compensated by its multimeric form, allowing IgM to have high avidity and to potentially tolerate mutations in viral antigens. Natural IgM is likely to be more polyreactive with relatively low affinity as it is expressed early in the B cell development process. Adaptive IgM is secreted after exposure to antigens, so it is more specific and cross-reactivity with other antigens is limited. IgM also plays an important role in activating the complement system (Charles A Janeway et al., 2001; Ehrenstein & Notley, 2010; Gong & Ruprecht, 2020; Schroeder & Cavacini, 2010).

IgD exists in circulating and membrane-bound forms. Secreted IgD only makes up approximately 0.25% of total serum immunoglobulins and has a half-life of only 2.8 days. Despite the fact that serum IgD concentrations are increased in patients with chronic infections such as tuberculosis, infectious hepatitis and malaria, the function of circulating IgD has not yet been fully elucidated. It is proposed that IgD plays a regulatory role in enhancing the protective antibody responses of other isotypes and interfering with viral replication. Membrane-bound IgD is co-expressed with IgM on naïve B cells and might regulate B cell fate at certain stages (Schroeder & Cavacini, 2010; Vladutiu, 2000).

IgA is the predominant mucosal antibody and protects the mucosal environment from microbial pathogens by neutralization. IgA can be found at high concentrations at mucosal surfaces or in secretions such as saliva and breast milk. Serum IgA is generally monomeric, while secretory IgA is dimeric or sometimes trimeric and tetrameric (Schroeder & Cavacini, 2010).

IgE is a crucial immunoglobulin for anti-parasite responses and is responsible for allergic reactions. This isotype has the lowest concentration in serum and the shortest half-life as well. IgE binds to receptors on mast cells with extremely high affinity. Antigens that bind to this IgE will stimulate mast cells to release inflammatory mediators, inducing physiological reactions such as coughing, sneezing and vomiting (Schroeder & Cavacini, 2010).

IgG is one of the most abundant immunoglobulins in human serum. IgG can be divided into four subclasses IgG1, IgG2, IgG3 and IgG4 with different functional activities. IgG4 is the only subclass that cannot fix and trigger the complement cascade. Concerning the secondary IgG antibody response, class-switching to IgG1 and IgG3 takes place when T cells interact with antigenic peptides displayed on MHC-class II expressed on the B cell surface. In the absence of T-cell help, IgG2 and IgG4 are induced in response to polysaccharide antigens. Among the five isotypes, IgG is the best opsonin as it contains a tail for Fc receptors on the surface of phagocytes, leading to the activation of phagocytosis. IgG can also cross the placenta to provide passive immunity in the fetus (Charles A Janeway et al., 2001; Schroeder & Cavacini, 2010; Vidarsson et al., 2014).

Given the fact that IgG, IgA and IgE are produced by B cells undergoing somatic hypermutation and class switching, these Ig types become more specific to infectious agents and possesses high affinity.

6. 3. B-cell development: generation, activation and differentiation

B cells and their antibodies have a central role in the humoral immunity which comprises the primary response (activation of naïve lymphocytes) and secondary response (memory lymphocytes). The whole developmental process of B cells can be divided into three important stages: 1) generation of mature B cells, 2) activation of mature B cells, and 3) differentiation of activated B cells into antibody-secreting cells (plasma cells) and memory B cells (Judith A Owen et al., 2013).

B-cell maturation in bone marrow

Mature B cells are generated in the fetal liver before birth and in the bone marrow after birth. The first event of the B cell development process is the differentiation of hematopoietic stem cells in the bone marrow into progenitor B cells (pro-B cells). In contact with bone-marrow stromal cells, pro-B cells proliferate and differentiate to precursor B cells (pre-B cells) which are subsequently stimulated by interleukin-7 (IL-7) leading them to become immature B cells. In the late stage of pro-B cells, heavy-chain rearrangement starts with D_H and J_H genes, followed by the joining of V_H gene to the upstream of D_H - J_H in the early pre-B stage to create the pre-BCR on the surface of B cells (**Figure 17**) (Mak et al., 2014). The engagement of the pre-BCR validates the rearranged V_H segments and leads to a process called allelic exclusion, which is the arrest of rearrangement on the other heavy chain locus (Vettermann & Schlissel, 2010).

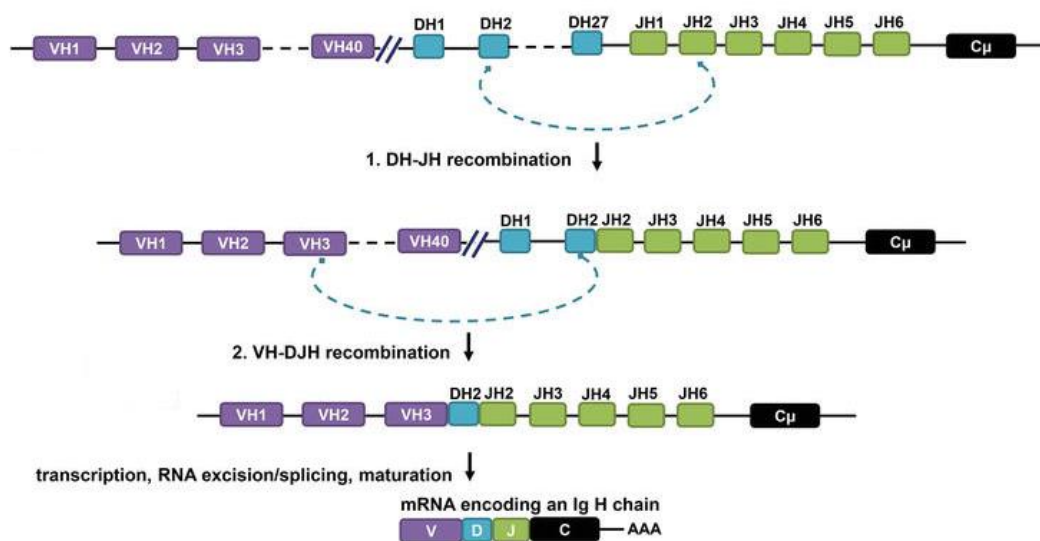


Figure 17: VDJ rearrangement of gene segments (Aribi, 2020). First, one D_H segment joins with one J_H segment by deletion of DNA pattern between them. Second, one V_H segment recombines with rearranged D_H - J_H site by deletion of DNA separating them, resulting in a single exon encoding the entire variable VDJ region. V_H : heavy chain variable genes, D_H : heavy chain diversity genes, J_H : heavy chain joining genes.

After a productive light-chain rearrangement, pre-B cells become immature B cells expressing membrane-bound IgM (mIgM) on the cell surface. Prior to being released from the bone marrow, immature B cells undergo a further light-chain rearrangement

(receptor editing) and apoptosis (negative selection) that eliminates immature B cells recognizing self-antigens. Nonself-reactive immature B cells leave the bone marrow and migrate to the spleen, where they differentiate to transitional type 1 B cells (T1 B cells) and subsequently transitional type 2 B cells (T2 B cells). Some T2 cells turn into follicular mature (FM) B cells by recirculating throughout the lymphoid system. Other T2 B cells migrate to the marginal zone in the spleen and become marginal zone B cells (MZ B cells). Both types of T2 co-express mIgM and mIgD on the surface, and are considered to be mature naïve B cells in the periphery (Mak et al., 2014).

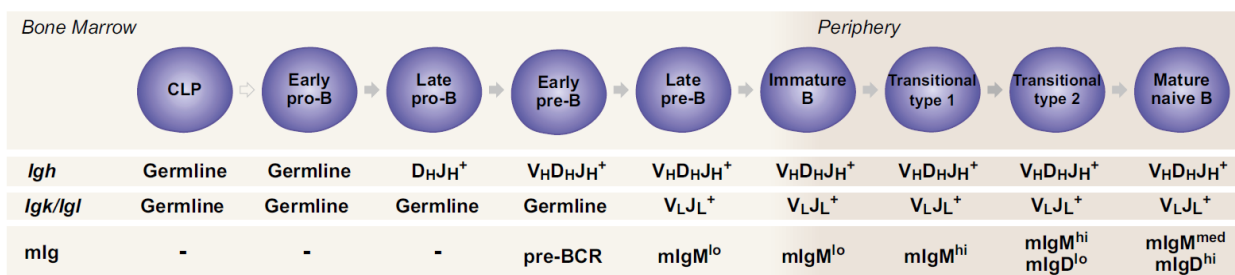


Figure 18: Different stages of B cell development (Mak et al., 2014). From common lymphoid progenitors (CLP) in the bone marrow, they differentiate to become mature naïve B cells in the periphery. At each stage, the status of heavy and light Ig chains is shown, and the expression levels of membrane-bound IgM and IgD (mIgM and mIgD) are indicated (lo: low, med: medium, hi: high). BCR: B-cell receptor.

B-cell activation & differentiation in the spleen

Mature naïve B cells are activated and differentiated via two pathways: T-dependent (Td) or T-independent (Ti) responses (Figure 19). T-independent humoral responses which are the first ‘innate-like’ defense against blood-borne pathogens are mounted by MZ B cells. There are two types of Ti antigens, including Ti-1 and Ti-2 antigens. Ti-1 antigens are polyclonal B-cell activators that activate B cells non-specifically. They act as mitogens that induce mitosis and cell differentiation. In contrast, Ti-2 antigens are generally large polymeric proteins or polysaccharides that activate, proliferate and differentiate B cells by extensively crosslinking the mIg receptor on the B-cell surface. After being stimulated by antigens, MZ B cells develop into extrafollicular plasma cells that secrete IgM. It has been demonstrated that IgM-expressing MZ B cells are

somatically hypermutated (Hendricks et al., 2018), however, the process is not related to antigen-driven clonal expansion in germinal centers (GCs). In general, the immune response to T-independent antigens is weak, does not lead to the formation of memory cells, and displays very low level of class switching which explains the predominance of secreted IgM (Judith A Owen et al., 2013; Mak et al., 2014; Pieper et al., 2013). In T-dependent humoral responses, FM B cells travel between bone marrow and secondary lymphoid organs to seek antigens. Once encountering cognate antigens, B cells bind to follicular T helper (Th) cells which recognize antigen-derived peptides displayed by MHC-II molecules on the B-cell surface. This direct interaction leads to the activation of B cells and the establishment of a specialized structure called germinal center (GC). Activated B cells that do not get involved in the GC reaction become short-lived plasmablasts and eventually short-lived plasma cells expressing low affinity IgM, the so-called extrafollicular response. In the GC, activated B cells proliferate and mature in terms of affinity. The variable regions of immunoglobulins are somatically mutated due to the upregulation of activation-induced cytidine deaminase (AID), resulting in clones of B cells that can bind to antigens with higher affinity. Class switch recombination occurs in parallel to create other types of immunoglobulins including IgG, IgA or IgE. All of these events contribute to the diversity of the antibody repertoire. Ultimately, the GC B cells that have gone through these steps become long-lived plasma cells or memory B cells. They stay either in secondary lymphoid organs or recirculate to the bone marrow (Bhattacharya, 2018; Jones et al., 2020; Pieper et al., 2013). Short-lived IgM-expressing B cells, long-lived plasma cells and memory B cells are very important in the initial time of infection/reinfection to induce a protective immune response.

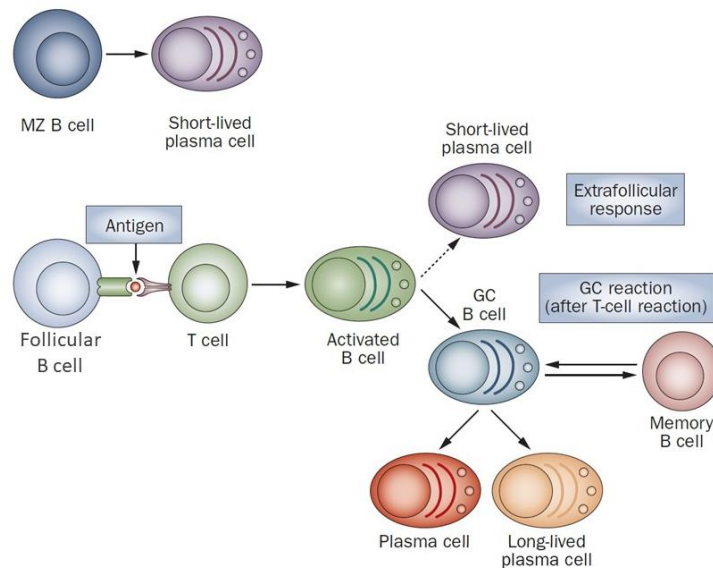


Figure 19: A schematic of B-cell developmental stages in the spleen (Adapted from(Dörner et al., 2009)). **(Upper)** T-independent response of marginal zone (MZ) B cell. **(Lower)** T-dependent response of follicular B cell. GC: Germinal center.

7. Memory B cell response to secondary infection

7.1. Functions of memory B cells

One miraculous ability of our immune system is to remember previous pathogens. Once our body is re-exposed to the same pathogens (reinfection or primary infection following vaccination), we are rapidly and ideally protected. This immunological memory depends, at least in part, on long-lived plasma cells and memory B cells. It is suggested that long-lived plasma cells constitutively secreting pre-existing antibodies with high affinity build the first layer of protection against homologous challenge, whereas memory B cells establish a protective defense against variant pathogens that are capable of avoiding the long-lived plasma response (**Figure 20**) (Akkaya et al., 2020). As soon as memory B cells re-encounter pathogens, they are reactivated and differentiated into antibody-secreting cells in order to mount a rapid and robust specific antibody response. Classically, it has been thought that newly generated high-affinity antibodies are class switched in the GC; however, the existence of unswitched IgM⁺ memory B cells and GC-independent memory B cells has recently been demonstrated (Kurosaki et al., 2015).

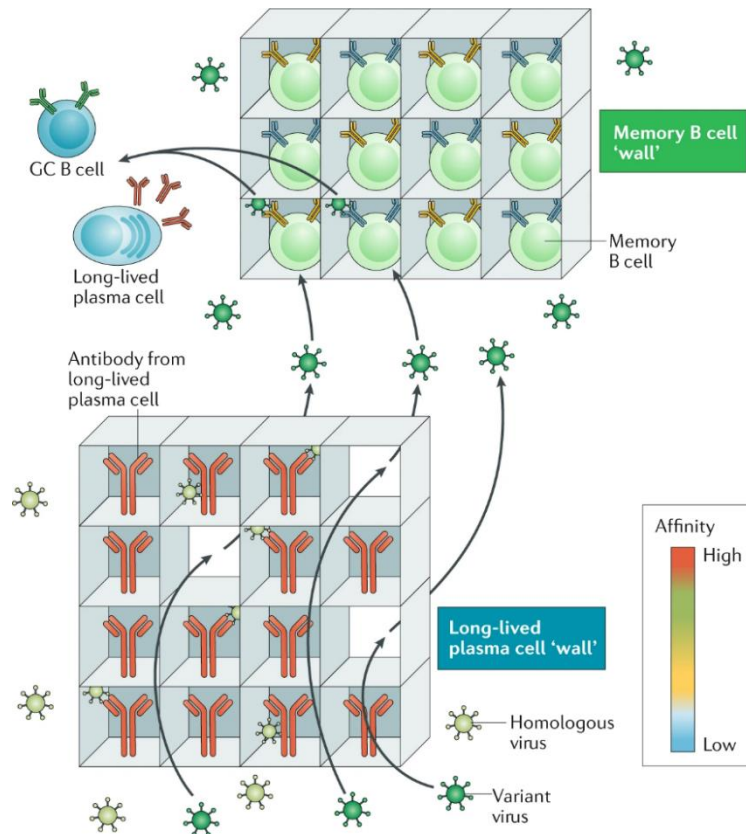


Figure 20: Roles of long-lived plasma cells and memory B cells in the secondary response to pathogens (Akkaya et al., 2020). **(Bottom)** Long-lived plasma cells in the bone marrow response to reinfection of homologous viruses by secreting highly specific and high-affinity antibodies (red). However, variants can evade antibodies from the long-lived plasma cells through holes in this wall and unfortunately bump into a second wall of memory B cells **(Top)**. These cells are less highly selected, so manage to detect a wider range of antigens, including mutated viruses. Memory B cells are activated by variant viruses, followed by differentiation into long-lived plasma cells or re-enter the germinal centers (GCs).

The role of memory B cells in inducing a protective recall humoral response has been proven in various infectious diseases. Using a mouse model infected with West Nile virus, Purtha et al. showed that memory B cell-derived plasma cells, but not long-lived plasma cells, produced antibodies that were able to equivalently neutralize the wild-type virus and the variant virus with a single mutation at the dominant neutralizing epitope. Interestingly, they also found memory B cell clones without additional somatic hypermutations that better recognized the mutant epitope compared to the wild-type (Purtha et al., 2011). Leach et al. obtained similar results in influenza virus-reinfected mice by tracing memory B cells specific to influenza virus haemagglutinin (HA). Mice were first immunized with the H1N1 A/Narita/1/2009 (Narita) strain. They showed that

pre-existing antibodies secreted by long-lived plasma cells are protective for the Narita reinfection, whereas protection from secondary challenge with PR8 infection required memory B cell activation (Leach et al., 2019). One more example of the protective functions of memory B cells was indicated in cytomegalovirus (CMV) infection. Adoptive transfer of memory B cells from CMV-immunized mice into T-cell and B-cell-deficient mice induced a CMV-specific IgG response within 4 to 7 days in the recipients. This supports the idea that effector functions of memory B cells can be activated in the absence of T cells as well as a cell-based therapy to enhance the humoral immunity in immunodeficient hosts (Klenovsek et al., 2007).

7.2. Memory B cell phenotypes and characteristics

In humans, a wide variety of memory B cell subsets have been described. CD27 was identified as one specific marker of memory B cells and has been widely used to distinguish memory and naïve B-cells based on the correlation between high CD27 expression and somatically mutated IgM⁺IgD⁺ B cells (Klein et al., 1998). Nevertheless, it does not mean that all memory B cells express the CD27 marker and *vice versa*, not all CD27⁺ cells are truly memory B cells. Approximately 40% of the B cell pool in peripheral blood express CD27 (Klein et al., 1998). In the blood and bone marrow, there are generally three memory B cell populations including CD27⁺IgM⁺IgD⁺ B cells, CD27⁺IgM⁺IgD⁻ (IgM-only) B cells and class-switched CD27⁺IgM⁻IgD⁻ (IgG⁺ or IgA⁺) B cells. The CD27⁺IgM⁺IgD⁺ B subset occupies a major proportion of the human peripheral B cell compartment. By CDR3 spectratyping analysis and gene expression profiling, Weller et al. demonstrated that blood CD27⁺IgM⁺IgD⁺ B cells correlate with circulating splenic MZ B cells. They bear somatically mutated V genes, so develop a pre-diversified and protective immune repertoire in a T-independent pathway (Weller et al., 2004). The formation of MZ B cells can occur in the absence of the spleen, however, these cells cannot expand in older splenectomized individuals (Weill et al., 2009). In a study of splenectomized children under 2 years old, who were exposed to many antigenic challenges by vaccination, the CD27⁺IgM⁺IgD⁺ memory B repertoire in the spleen did

not exhibit any signs of antigen-driven activation and expansion compared to switched memory B cells. This suggests another somatic diversification pathway distinct from T-dependent and T-independent responses in infants (Weller et al., 2008). The CD27⁺IgM⁺IgD⁺ B cells are phenotypically similar to IgM-only and class-switched B cells, which each account for 10-15% of B lymphocytes (Klein et al., 1998). By tracing tetanus toxoid-specific memory B cells during the steady state, Giesecke et al. noticed that the largest memory B cell reservoir is the spleen, followed by the tonsils, bone marrow and peripheral blood. Furthermore, memory B cells in these compartments share similar phenotypes. Interestingly, the secondary responses to tetanus are not affected in the absence of spleen and tonsils, suggesting a maintenance and reactivation of memory B cells that are organ-independent (Giesecke et al., 2014). A high-throughput VH sequencing of human B cell subsets on paired blood and spleen samples revealed that IgM sequences from shared clones of the MZ and the memory IgG/IgA compartments exhibited a mutation and repertoire profile of IgM-only but not of MZ B cells. The "IgM-only" subpopulation, therefore, represents as the only subset showing a precursor-product relationship with class-switched CD27⁺ memory B cells. This indicates that IgM-only B cells are derived from GC-IgM memory B cells and that IgM memory and MZ B cells are two distinct entities (Bagnara et al., 2015).

Apart from CD27⁺ memory B cells, several studies noted that among B cells lacking CD27 expression, there were IgG⁺ and IgA⁺ B cells, proving the additional existence of memory B subsets that are antigen-experienced but CD27⁻. This subpopulation makes up 1-4% of peripheral B cells, roughly 25% of circulating IgG⁺ memory B cells and are called "atypical" or "tissue-like" memory B cells (Fecteau et al., 2006; Shah et al., 2019; Wei et al., 2007). CD27⁻ memory B cells are characterized by differential expression of CD21 and Fc receptor-like 4 (FCRL4) (other names as IRTA1 or FcRH4), an inhibitory receptor that potentially inhibits BCR signaling. Due to the lack of CD27 expression, atypical memory B cells fail to be stimulated via their BCR but preferentially respond to T-dependent stimulation (Ehrhardt et al., 2005; Shah et al., 2019). This subpopulation of

memory B cells are relatively limited in healthy individuals but increased frequency in systemic lupus erythematosus (Wei et al., 2007), in chronic HCV-infected patients (Oliviero et al., 2015), in patients with malaria (Portugal et al., 2015; Weiss et al., 2009), in HIV-infected patients (Meffre et al., 2016) and in SARS-CoV-2-infected patients (Oliviero et al., 2020).

7.3. Memory B cell localization

Several studies have revealed that memory B cells are widely present in secondary lymphoid tissues in tonsillar mucosal epithelium (Liu et al., 1995), human Payer's patches (Dunn-Walters et al., 1996), and healthy gingiva (Mahanonda et al., 2016). Memory B cells can also be retained and accumulated in draining lymph nodes of skin subsequent to subcutaneous protein vaccination (Fazilleau et al., 2007). Memory B cells can be found recirculating in the blood but in small amounts compared to secondary lymphoid organs. Anti-smallpox long-lived memory B cells are concentrated in the spleen of vaccinated individuals where they comprise 0.24% of all IgG⁺ cells, in contrast to circulating IgG⁺ B cells in blood where they represent only 0.07% (Mamani-Matsuda et al., 2008). Similar results have been demonstrated in mouse models. Either IgM or IgA memory B cells were found in mouse Payer's patches (Lindner et al., 2015). In orally cholera toxin-immunized mice, memory B cells were detectable and isolated eight months post-immunization from various lymphoid tissues including the spleen, mesenteric lymph nodes, Peyer's patches, and intestinal lamina propria (Vajdy & Lycke, 1993). Notably, mice with intranasal influenza virus administration displayed high frequencies of IgG and IgA memory B cells at least five months post-infection in draining lymph nodes and in the lung, a non-secondary lymphoid tissue. The fact that memory B cells are maintained at the sites of infection suggests the existence of tissue-resident memory B cells (Joo et al., 2008; Onodera et al., 2012). Generally, the strategic localization and recirculation between the bone marrow and secondary lymphoid organs of memory B cells help them encounter antigens in the most optimal way.

Concerning CD27⁻ atypical memory B cells, their presence was confirmed in subepithelial locations in lymphoid tissues such as tonsil (Ehrhardt et al., 2005; Wei et al., 2007). These CD27-lacking memory B cells also circulate in the peripheral blood of healthy subjects and in systemic lupus erythematosus patients and they display a comparable level of hypermutation to CD27⁺ unswitched memory B cells (Wei et al., 2007). Increased circulating CD27⁻CD21⁻ atypical memory B cells were reported in rheumatoid arthritis patients (Isnardi et al., 2010), patients with chronic HIV viremia (Moir et al., 2008) as well as malaria-infected patients (Portugal et al., 2015; Weiss et al., 2009). A study in a cohort of pregnant women who were diagnosed with primary cytomegalovirus infection in Belgium revealed that both virus-activated memory B cells and atypical memory B cells were expanded in peripheral blood (Dauby et al., 2014). The increase of IgD⁻CD27⁻ late memory or exhausted memory B cells in peripheral blood was documented in the elderly aged from 75-102 years and were hypothesized to be an age-related manifestation of long-term stimulation or dysregulation of the immune system (Colonna-Romano et al., 2008, 2009).

8. Immune responses to BK polyomavirus

The outcome of BKPyV infection in kidney transplant recipients relies on the efficient deployment of antiviral immune responses. Primary infections are generally controlled by innate responses of non-specific cells, followed by cellular responses involving BKPyV-specific T-cell populations and humoral responses with increasing antibody titers. In this section, innate and adaptive immunity are discussed, with a focus on the antiviral humoral responses and the production of BKPyV-specific antibodies.

8.1. Innate immune response

Viruses that invade the human body have to encounter the first line of protection which is innate immunity. It exerts its defensive functions thanks to soluble molecules including the interferon system and various cell systems such as macrophages, dendritic

cells (DCs), natural killer cells (NKs), polymorphonuclear leukocytes and mast cells (Kariminik et al., 2016). Macrophages and DCs contribute to the defense against BKPyV either directly via endocytosis and destruction of virus particles or indirectly through secretion of interferon or presentation of BKPyV antigens to induce the generation of virus-specific CD8⁺ T cells (Drake et al., 2001; Kariminik et al., 2016). Especially, in kidney transplant recipients, the reduced number of peripheral blood DCs was correlated with a higher risk of BKPyV nephropathy (Womer et al., 2010). Despite the important role of DC activation in priming adaptive immune responses to BKPyV, the VP1 capsid protein of BKPyV is unable to strongly induce DC maturation compared to that of other polyomaviruses (Drake et al., 2000; Gedvilaite et al., 2006).

Another cellular component of innate immunity that plays a crucial role in controlling BKPyV infection in renal recipients is NK cells. Their functions are controlled by a number of activating and inhibitory receptors on the NK cell surface, especially killer cell immunoglobulin-like receptors (KIR) which bind to HLA class I molecules. Trydzenskaya et al. observed that patients with BKPyV carried a significantly small number of activating KIRs, particularly the KIR3DS1 genotype, in comparison with the control group of patients with stable kidney function and no BKPyVAN (Trydzenskaya et al., 2013), and Tonnerre et al. found that donor MICA (major histocompatibility complex (MHC) class I-related chain A) genotype was related to BKPyV reactivation in the graft recipient (Tonnerre et al., 2016). Furthermore, BKPyV 3p' miRNAs have been described to downregulate the expression of UL16-binding protein 3 (ULBP3) which is recognized by the activating NKG2D (natural-killer group 2, member D) receptor on NK cells. As a result, the virus succeeds in escaping NK cell-mediated cytotoxicity (Bauman et al., 2011). Since NKG2D receptors are expressed on many T cell populations as well, it has been proposed that targeting ULBP3 by using miRNAs is a mechanism of BKPyV to escape the elimination of both innate and adaptive immune systems.

Soluble molecules are also involved in viral elimination by either directly targeting the virus like the complement system or indirectly by opsonizing the particle. Human α -

defensin 5 (HD5) was shown to interact directly with BKPyV and promote aggregation of virions, hence reducing binding of the virus to host cells (Dugan et al., 2008). Another study on BKPyV-infected HRPTE cells *in vitro* demonstrated that interferon-gamma (IFN- γ) which is primarily secreted by NK cells was able to inhibit the expression of BKPyV TAg and VP1 in a dose-dependent way (Abend et al., 2007). More recent work has shown that this effect depends on the induction of indoleamine 2'3-dioxygenase in host cells (Fiore et al., 2020). Similarly, RPTECs pre-treated with IFN- β in a dose-dependent manner showed a reduction of both infected cells and viral loads in supernatant, suggesting a protective role of type-1 interferon in BKPyV infection *in vitro* (Manzetti et al., 2020).

8.2. Adaptive immune response

8.2.1. Cellular immunity

Several studies have concentrated on the role of T cells in controlling BKPyV replication and in the maintenance of latency. All three capsid proteins VP1, VP2, VP3 and TAg as well as tAg can be targeted by the cellular response to BKPyV infection, in which the immune response to VP1 and VP3 are significantly stronger and more frequently detected than responses to VP2, TAg and tAg. This suggests that VP1 and VP3 - which are the major capsid components - may be the major target of BKPyV specific T-cell response (Blyth et al., 2011; Fan et al., 2019; Mueller et al., 2011), which in turn implies that virions, and not infected cells, are the main sources of BKPyV antigens processed by antigen presenting cells. Several studies have revealed that in kidney transplant recipients, BKPyV viruria and viremia are controlled better when patients develop virus-specific T cells (Ahlenstiel-Grunow et al., 2020; Leboeuf et al., 2017). CD4⁺ and CD8⁺ T cells specific to BKPyV are detectable in both healthy individuals and kidney transplant patients, however, it has been suggested that the CD4⁺ T cell response is predominant (Fan et al., 2019; Weist et al., 2014). CD4⁺ T cells were reported to directly control BKPyV infection by up-regulating the secretion of proinflammatory cytokines, including IFN- γ

and TNF- α , and by expressing the cytolytic molecule granzyme B (Weist et al., 2014). In the context of kidney transplantation, immunosuppressant drugs which are used to avoid graft rejection might reduce the expression of these cytokines by BKPyV-specific T cells (Weist et al., 2015). Multifunctional BKPyV-specific CD4⁺ T cells can even exert their protective roles in the absence of CD8⁺ T cells in several BKPyV-seropositive but symptomless patients (Weist et al., 2014). The significantly increased number of CD4⁺ T helper cells was observed before and after the clearance phase, whereas cytolytic CD4⁺ T cells were enriched during the clearance phase (Weist et al., 2015). Moreover, CD4⁺ T cells were reported to maintain persistent memory response, suggesting that they may play a role in suppressing BKPyV replication in healthy individuals (Zhou et al., 2007). A study in 42 kidney transplant patients developing active BKPyV reactivation showed that while CD4⁺ T cells were mainly elicited by the viral capsid VP1 protein, CD8⁺ T cells mostly targeted BKPyV TA_g (Binggeli et al., 2007). Furthermore, functional responses of both CD4⁺ and CD8⁺ T cells were impaired in patients with BKPyVAN, and this was correlated with the use of immunosuppression based on tacrolimus rather than cyclosporine (Renner et al., 2013).

It is undoubtable that BKPyV-specific T cells are necessary for the immune response to viral infection, yet it has been suggested that virus-specific T lymphocytes might provoke immunopathogenic phenomena. When BKPyV-specific cytotoxic T cells succeed in controlling viral reactivation and eliminate the virus at an early stage, intragraft inflammation remains low grade with no progression of BKPyV nephropathy. Nevertheless, if the cytotoxic T cells fail to achieve viral clearance, the virus is chronically reactivated causing extensive intragraft inflammation. This may lead to the migration of activated T cells into the inflammatory area, leading to progressive tissue damage, and a cycle of continuous intragraft inflammation, active BKPyV replication and further recruitment of activated cytotoxic T cells, ultimately resulting in nephropathy (Babel et al., 2011). This view of BKPyVAN is supported by observations in the MPyV kidney transplant model showing that the adaptive immune response, and not direct cytopathic effects of virus replication, are involved in nephropathy (Albrecht et al.,

2012) and that allo-specific rather than virus-specific T-cells are responsible for tissue damage (Kim et al., 2017). More recently, a study of the TCR repertoire of T-cells infiltrating kidney biopsies showed that allo-specific T-cell clones were almost 8 times more numerous than virus-specific clones in BKPyVAN biopsies (Zeng et al., 2016), further implicating the T-cell response in the pathology of PyVAN.

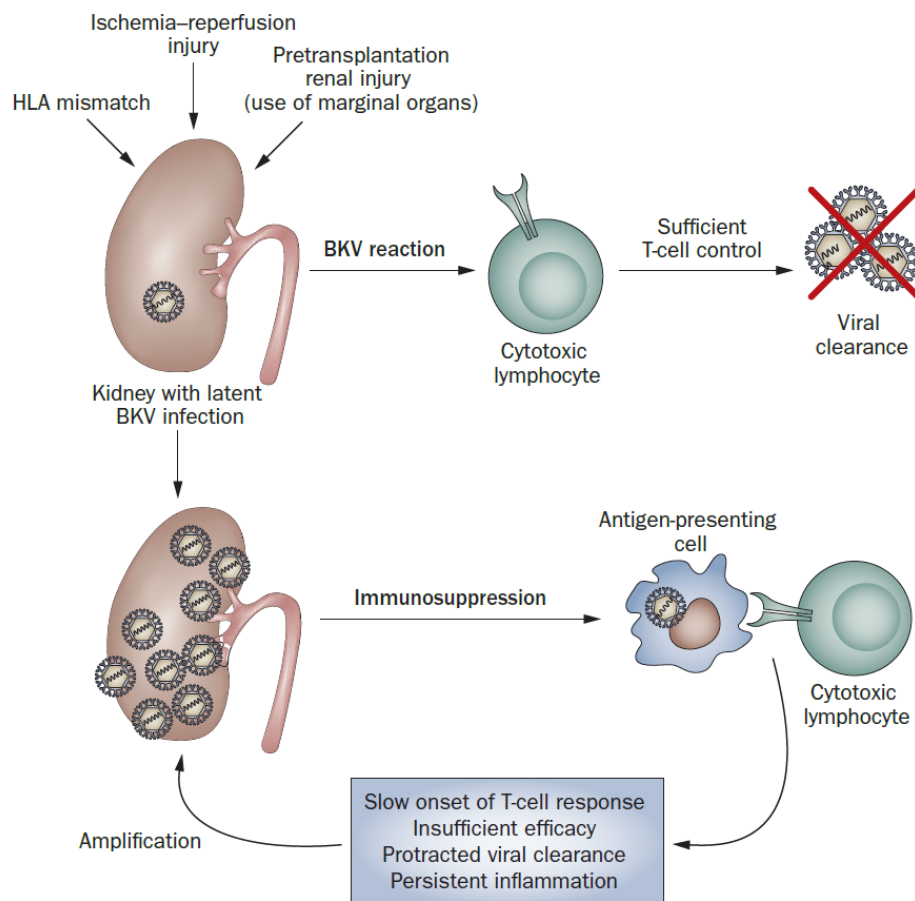


Figure 21: Relationship between T cell response and clinical outcomes of BKPyV infection (Babel et al., 2011). A sufficient BKPyV-specific T cell response can control BK reactivation and viral clearance. On the contrary, insufficient T cell responses against BKPyV lead to prolonged virus clearance and persistent intra-graft inflammation. At this stage, cellular immunity needs to be restored by a reduction in immunosuppression to prevent renal rejection. BKV: BK virus.

8.2.2. Humoral immunity

The first indications that the antiviral humoral response may have a protective effect against BKPyV came from a case report of a six-year-old boy with hyperimmunoglobulin M immunodeficiency, it was announced that massive BKPyV infection caused the

severe renal injury. The young boy died five months post dialysis. The researchers hypothesized that under the impaired humoral immune response conditions, such as the increased level of IgM or IgD, or inadequate immunoglobulin class switching, the patient was more susceptible to opportunistic BKPyV and eventually developed BKPyV-associated renal failure (Rosen et al., 1983). However, in the context of kidney transplantation, the protective function of antibodies in BKPyV infection has been a controversial topic because most kidney graft recipients who develop BKPyVAN are seropositive. Indeed, it has been shown that both BKPyV seronegative and seropositive recipients shared a similar incidence of BKPyV viremia (Bohl et al., 2005). More careful analysis of antibody titers showed that pre-transplant BKPyV antibody levels were lower in recipients who developed viremia compared to those who never developed viremia (Bohl et al., 2008). Similarly, a recent study in Japan found that seropositive donor and seronegative recipient status is related to the early appearance and the high number of decoy cells, which predict severe BKPyV infection (Hisadome et al., 2020). Finally, in a recent prospective longitudinal study in 168 kidney transplant recipients, it was reported that patients with elevated neutralizing titers against the replicating strain had a lower risk of developing viremia at any given time, while patients with no or low neutralizing titers against the infecting BKPyV genotype prior transplant were at high risk of viremia after transplant. These findings have suggested that BKPyV genotype-specific neutralizing antibody titers can be used as a new predictive marker for BKPyV infection before and after transplant (Solis et al., 2018), and indicate that pre-existing antibodies in the graft recipient have some protective value against BKPyV.

With respect to the ability of antibodies to control BKPyVAN once it occurs, data are conflicting. Evaluation of humoral immunity to BKPyV by EIA enzyme immunoassay (EIA) in pediatric kidney recipients showed that IgG level was significantly higher at the time of viral clearance compared to that before viral reactivation or during the early phase of viremia. Peak BKPyV-specific antibody responses coincided with long-term good allograft function, suggesting a protective rather than a pathogenetic role of humoral immunity in the course of BKPyVAN development (Ginevri et al., 2007). Similar

results were reported in adult kidney transplant recipients who recovered from BKPyVAN (Hariharan et al., 2005). In a longitudinal study on 535 plasma samples derived from 107 kidney transplant recipients and collected from 1 week up to 1 year posttransplant, the levels of IgG, IgA and IgM were higher in patients with BKPyV reactivation than those without BKPyV replication. The study also suggested that BKPyV-specific antibody titers can be used as a potential marker to detect viral reactivation after kidney transplantation as low anti-BKPyV IgG and IgA titers coincided with higher peak viruria and greater risk of viremia (Randhawa et al., 2008).

On the other hand, some studies found no evidence for a protective role of BKPyV-specific antibodies during PyVAN. For example, the first research on the interaction between the virus and the humoral response in kidney transplant patients observed a 100-fold increase of BKPyV-specific antibody titers which was correlated with the shedding of the virus in urine among six kidney graft recipients. Nonetheless, these antibodies did not prevent the development of BKPyV nephropathy (Gardner et al., 1984). Similarly, Bohl et al. found that BKPyV-specific antibodies increased over the first posttransplant year and the highest antibody levels were coincident with sustained viremia, indicating that the strong antibody responses were not associated with clearance of the virus (Bohl et al., 2008). Notably, two studies concluded that BKPyV-specific T cell response, but not the humoral response, plays a critical role in resolution of the viral infection in kidney transplant recipients with nephropathy (Chen et al., 2006; Schachtner et al., 2011).

Taken together, the available data shows that humoral or antibody responses provide partial protection against BKPyV nephropathy in kidney recipients after renal transplantation. With respect to clinical practice, evaluation of BKPyV-specific antibody titers has been proposed as a means to identify graft recipients at high risk of BKPyV infection, and as discussed below, interventions to increase recipient anti-BKPyV titers have been suggested as strategies to prevent BKPyVAN or even kidney graft loss.

9. Neutralizing monoclonal antibodies and viral infections

9.1. Introduction

Many viral infections lack effective curative therapies. Moreover, new viruses and their variants never stop emerging, the appearance of SARS-CoV-2 by the end of 2019 for instance, illustrating the need to discover and develop highly potent therapeutic agents for the treatment and prevention of future viral outbreaks, epidemics or even pandemics. Antibodies represent potential candidates in our permanent struggle against viruses. The role of antibodies in host defense against viral infections in both the acute phase and long-term protection was scientifically documented by passive immunization of B-cell-deficient mice, vaccination and by the transfer of maternal antibody immunity in neonates (Sanna & Burton, 2000; Zinkernagel, 2001). For therapeutic purposes, monoclonal antibodies (mAbs) are of interest due to their antigenic specificity (Ahangarzadeh et al., 2020). Reminiscent of the serum therapy invented by Emil Behring and Shibasaburo Kitasato (E. von Behring & Kitasato, 1890), post-exposure rabies serotherapy was the first application of antibody treatment against infectious diseases. With the development of purification techniques, the use of crude sera was gradually replaced by rabies immunoglobulin purified from animal sera. In both therapeutic approaches, patients receive a mix of antibodies, with potential variability in antiviral activity and side-effects. In 1975, the development of the hybridoma method allowed scientists to obtain monoclonal antibodies in large amounts from immunized mice, improving fundamental research and opening up the potential for their clinical application (Köhler & Milstein, 1975).

9.2. Antibody-mediated neutralization

There are several ways for antibodies to contribute to effective protection in viral infections. They can either directly contact viral particles to block virus-host interactions (so-called “neutralization”) or bind to viral antigens on infected cells leading to their elimination through antibody-dependent cellular cytotoxicity (ADCC), antibody-

dependent cellular phagocytosis (ADCP) or the complement-dependent cytotoxic (CDC) pathway (Pelegriin et al., 2015). This section focuses on neutralization of infectivity as it is thought to be the principal defense mechanism of antibodies. Furthermore, the neutralization activity of antibodies is by far the easiest antiviral mechanism study *in vitro* using infectious viral particles (Parren & Burton, 2001) or pseudotypes.

There are many scientific questions related neutralization, for example how and where the neutralizing antibodies (NAbs) bind to a specific virus; whether NAbs cause conformational changes after binding that affect post-attachment steps required for virus entry; whether they persistently inactivate viral proteins; and whether they are most effective against free viral particles or after virion attachment to cells (Klasse, 2014). However, the mechanism of neutralization refers specifically to the early phase of viral life cycle, which is the process of virus entry. The minimum requirement for neutralization is the interaction between antigen-binding sites (paratopes) of antibodies and antibody-binding sites (epitopes) of viral particles, in which epitopes are present on the glycoproteins of enveloped viruses or the protein shell of naked viruses (Klasse & Sattentau, 2002). The paratope-epitope binding can block virus attachment to cellular receptors and may inhibit the fusion machinery for enveloped viruses or penetration into the cytosol for non-enveloped viruses (Corti & Lanzavecchia, 2013). Owing to the highly antigen-specific characteristic of monoclonal antibodies, they can effectively neutralize the virus of interest without disrupting the host's normal microbiota. This outstanding property of mAb is also its weakness due to antigenic variability. Viral entry proteins are capable of varying the antigenic surface with little impact on their binding functions to the host, resulting in escape from the antibody response. In parallel, the humoral immune system also has the ability to produce broadly neutralizing antibodies (bNAbs) that are able to restrict different viral isolates by hitting conserved exposed sites. Despite the presence of bNAbs, challenges will never disappear due to viruses with extremely diverse antigenic variability and the rapid appearance of resistant mutants as observed with influenza virus, hepatitis C virus (HCV) and human immunodeficiency virus (HIV) (Klasse, 2014). Last but not least, only

a minority of virus-specific memory B cells produce NAbs, and only a small proportion of those are bNAbs, since the majority of antibodies are recognize denatured or internal virus proteins (Corti & Lanzavecchia, 2013; Srinivasan et al., 2016).

9.3. Neutralizing antibodies and BKPyV infection

In 2012, Christopher B. Buck's group published their work on the development of BKPyV pseudoviruses (PSV), which are made of the BKPyV structural proteins VP1, VP2, VP3 that form a capsid incorporating a reporter gene instead of the viral genome, and used them for neutralization-based testing of sera. Among 48 sera from healthy adults, they found 94 % and 23% positive for BKPyV genotype I and genotype IV neutralization, respectively. In a longitudinal analysis of 108 sera from kidney transplant recipients, neutralizing titers increased considerably by one year after the time of transplantation (Pastrana et al., 2012). In another study on healthy adults from same group published in 2013, they demonstrated greater than 80% of sera had BKPyV genotype I-specific neutralizing antibodies, around 70% of sera had detectable neutralizing activity against BKPyV genotype II and less than 50% of sera were positive for neutralizing antibodies against genotype III and IV. The finding confirmed that different BKPyV genotypes represent different neutralizing serotypes. Interestingly, they showed that the sera of some subjects neutralized BKPyV subtype Ib1 but not the closely related subtype Ib2, suggesting that Ib1 and Ib2 are possibly distinct serotypes (Pastrana et al., 2013). It should be noted however, that the Ib2 VP1 sequence used in the study carried the E73K mutation in the BC-loop, and did not therefore represent a wild-type genotype Ib2 sequence.

More recently, by *ex vivo* stimulation of single B-cells from the peripheral blood of five healthy donors combined with a high-throughput, functional antibody screen, Lindner et al. succeeded in reconstituting BKPyV-specific neutralizing antibodies, including many IgG and IgM that broadly neutralized all BKPyV genotypes and also the related JC polyomavirus. Cryo-electron microscopy of a broadly neutralizing IgG in complex with

BKPyV VLPs identified a conserved viral epitope at the junction between capsid pentamers (Lindner et al., 2015). This supports the idea that bNAbs target conserved regions on the viral surface rather than hitting the highly variable antigenic regions.

9.4. Methods for obtaining therapeutic antibodies

Since the first success of hybridoma technology to produce mouse monoclonal antibodies for therapeutic purposes, several techniques have been developed to obtain therapeutic antibodies. Compared to humanized, chimeric and murine antibodies, human monoclonal antibody makes up more than 51% of all mAbs in clinical use (Lu et al., 2020). This section will describe three well-known techniques to generate full human monoclonal antibodies, including phage display, transgenic mice and single B cell antibody isolation (Figure 22).

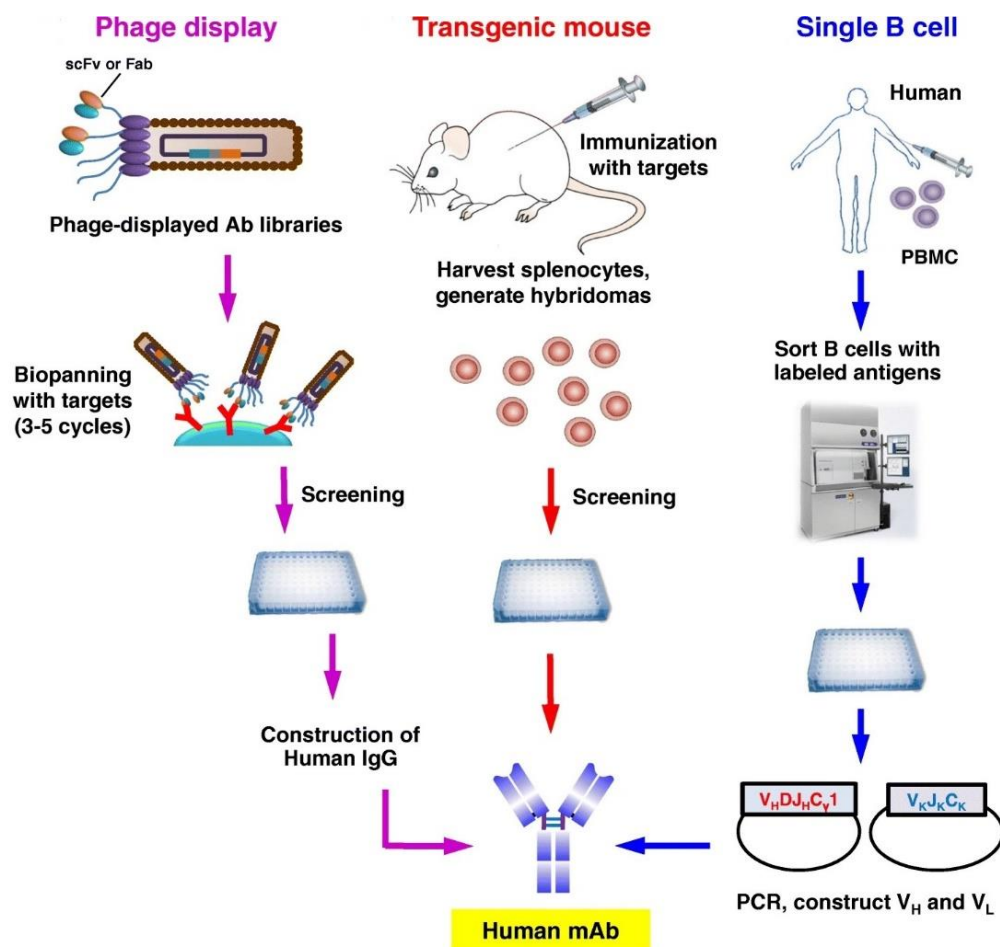


Figure 22: Approaches for the generation of fully human therapeutic antibodies (Lu et al., 2020).

The phage display antibody method was developed by Sir Gregory Paul Winter in 1990 (McCafferty et al., 1990) and he was awarded the 2018 Nobel Prize in Chemistry for his invention (Barderas & Benito-Peña, 2019). Briefly, genes encoding the heavy and light chains of B cells derived from immunized or infected human or animals are cloned as antigen-binding fragments (Fab) or single-chain variable fragment (scFv) fragments and displayed on filamentous bacteriophages to compose a library. By panning the library against the virus of interest, specific antibodies are selected and isolated. Since the selection depends on the binding of purified and well-characterized antigens, this method is not suitable to identify new neutralizing epitopes of viral pathogens (Corti & Lanzavecchia, 2014). Until now, the United States Food and Drug Administration (US FDA) has approved nine human antibody drugs generated by phage display for the treatment of autoimmune diseases and cancer (Lu et al., 2020). Concerning infectious diseases, using libraries constructed from the human IgM⁺ B cell repertoire from individuals receiving seasonal influenza vaccines, it was possible to produce potent neutralizing antibodies that showed a broad activity against diverse influenza subtypes (Throsby et al., 2008). A human IgG antibody 5H/11-BMV-D5 that displayed cross-neutralizing potential against HIV-1 clinical isolates was also generated from a native antibody library (Miller et al., 2005).

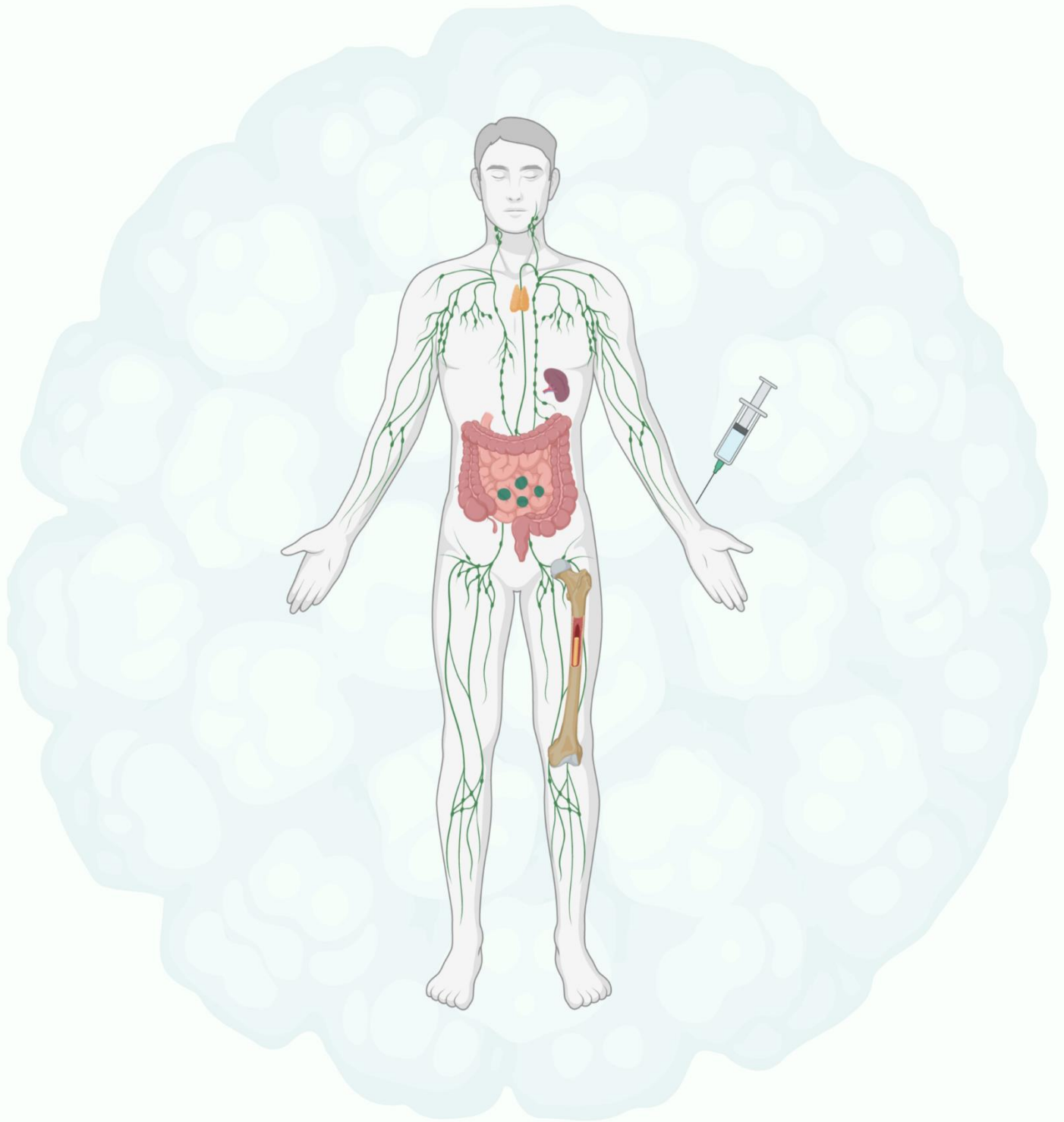
The transgenic mouse technique was first described in 1994 (Green et al., 1994; Lonberg et al., 1994). In general, endogenous immunoglobulin genes of mice were replaced by the human Ig genes of interest, making them able to express fully human antibodies after immunization. In order to select high-affinity antibodies, further selection steps need to be done. HuMab17C7 (or RAB-1) monoclonal antibody produced from transgenic mice by Medarex is a potent neutralizing antibody against rabies virus and has been under clinical development in India (De Benedictis et al., 2016; Sloan et al., 2007; Y. Wang et al., 2011).

Single B cell antibody technology is a remarkable advance in isolating and reconstituting specific antiviral mAbs from naturally infected or immunized patients.

Virus-specific memory B cells are isolated from peripheral blood by fluorescence-activated cell sorting based on specific B cell surface markers at different stages, for instance, CD19 for pan B cells and CD27 for memory B cells. After isolation of single B cells, each pair of heavy and light chain genes are cloned into expression vectors, then transfected into mammalian cell lines to express fully human mAbs. The final steps are high-throughput screening and evaluation of secreted antibodies to select the potent neutralizing clones (Lu et al., 2020). A number of virus-targeting mAbs generated by this approach are in clinical trials, such as human mAb114 against Ebolavirus (Rijal et al., 2019), human MHAA4549A mAb against seasonal influenza A in phase II (Nakamura et al., 2013), or MEDI8897 NAb against respiratory syncytial virus (RSV) in phase II (Gilman et al., 2016; Goodwin et al., 2018).

RESEARCH OBJECTIVES

Encouraging results using IVIG for the prevention and treatment of PyVAN indicate that antibody-based therapy may improve clinical outcomes for patients with pathologies caused by BKPyV. However, IVIG represents a complex mix of human antibodies of which only a small fraction are specific for BKPyV. Monoclonal antibodies against BKPyV could potentially combine the antiviral properties of IVIG in a more potent and better-characterized form, and therefore might represent future therapeutic agents against BKPyV. In order to be effective, such antibodies would need to be active against all four BKPyV genotypes. The central aim of my PhD project was therefore to generate such BKPyV-specific broadly neutralizing monoclonals with therapeutic potential. For this, the initial approach was to perform single B cell sorting, then reconstitute naturally expressed antibodies by cloning and eventually screen secreted antibodies *in vitro* to obtain potent clones. However, from 2019, the experimental approach was modified to increase throughput by using Chromium Single Cell Immune Profiling of 10x Genomics. In doing so, the main objective was always to achieve potent broadly neutralizing antibodies against BKPyV, by generating a much larger dataset of antibody sequences. In addition, the results generated allowed us to explore the BCR repertoire and the gene expression profile of BKPyV-specific B population as well.



RESULTS

The experimental results are presented in three sections:

Part 1 - Preparation of fluorescence labeled BKPyV VLPs, identification of BKPyV-specific B-cells in PBMC, and analysis of BCR repertoires and expression profiles of BKPyV-specific B-cells in kidney transplant recipients.

(manuscript deposited on MedRxiv)

DOI : <https://doi.org/10.1101/2021.02.04.21250913>

Part 2 - Identification of a 41F17-like family of BKPyV-specific bNAbs

Part 3 - Detailed report used for patent application, Projet Innovant n° 4380, SATT OUEST VALORISATION.

We aim to publish all these results in one article. However, as we are in the process of patent application, we cannot publish our antibodies' sequences before the patent is approved. As a result, the preprint describing the BKPyV-specific BCR repertoires in kidney transplant recipients with BKPyV reactivation has been deposited on MedRxiv.

PART 1: MedRXiv preprint

The humoral response to BK polyomavirus in kidney transplant recipients is dominated by IgM clones, expressing a distinct B-cell repertoire from that found in IgG B-cells specific for the same antigen.

Authors: Nguyen Ngoc-Khanh, Gautreau-Rolland Laetitia, Devilder Marie-Claire, Fourgeux Cynthia, Sinha Debajyoti, Poschmann Jeremie, Hourmant Maryvonne, Bressollette-Bodin Céline, Saulquin Xavier, McIlroy Dorian



HOME | ABOUT | SUBMIT | NEWS & NOTES | ALERTS / RSS

 Advanced Search

The humoral response to BK polyomavirus in kidney transplant recipients is dominated by IgM antibodies that use a distinct repertoire compared to IgG against the same antigen

[Comment on this paper](#)

[Previous](#)

[Next](#)

Posted February 09, 2021.

Ngoc-Khanh NGUYEN, Laetitia Gautreau-Rolland, Marie-Claire Devilder, Cynthia Fourgeux, Debajyoti Sinha, Jeremie Poschmann, Maryvonne Hourmant, Céline Bressollette-Bodin, Xavier Saulquin, Dorian McILROY

doi: <https://doi.org/10.1101/2021.02.04.21250913>

This article is a preprint and has not been certified by peer review [what does this mean?]. It reports new medical research that has yet to be evaluated and so should not be used to guide clinical practice.

[Download PDF](#)

[Email](#)

[Author Declarations](#)

[Share](#)

[Supplementary Material](#)

[Citation Tools](#)

[Data/Code](#)

[Tweet](#)

[Like 0](#)

The humoral response to BK polyomavirus in kidney transplant recipients is dominated by IgM antibodies that use a distinct repertoire compared to IgG against the same antigen

Authors: Nguyen Ngoc-Khanh¹, Gautreau-Rolland Laetitia^{2,3}, Devilder Marie-Claire², Fourgeux Cynthia¹, Sinha Debajyoti¹, Poschmann Jeremie¹, Hourmant Maryvonne⁵, Bressollette-Bodin Céline^{1,4,6}, Saulquin Xavier^{*2,3}, McIlroy Dorian^{*1,3}

1. CRTI, UMR 1064 INSERM, Université de Nantes
2. CRCINA, UMR 1232 INSERM, Université de Nantes
3. UFR Sciences et Techniques, Université de Nantes
4. Service du Virologie, CHU Nantes
5. Service de Néphrologie-Immunologie clinique, CHU Nantes
6. UFR Médecine, Université de Nantes

* Corresponding author

1. Abstract

The BK polyomavirus (BKPyV) persists asymptomatically in the kidney and active replication is only seen in immunosuppressed individuals, such as kidney transplant (KTx) recipients, in whom BKPyV reactivation can cause significant morbidity. KTx recipients with BKPyV reactivation mount a robust humoral response, but this often fails to clear the virus. In order to characterize the BKPyV-specific B-cell receptor (BCR) repertoire in KTx recipients, we used fluorescence-labeled BKPyV virus-like particles (VLPs) to sort with BKPyV-specific B-cells, then single-cell RNAseq to obtain paired heavy and light chain antibody sequences, and gene transcriptome data. The BCR repertoire was highly diverse in terms of both V-gene usage and clonotype diversity, with approximately 3% repertoire overlap between patients. The BKPyV-specific response was characterized by the presence of both memory IgG and memory IgM B-cells with extensive somatic hypermutation, which expressed distinct BCR repertoires within the same patient. The gene expression profile of IgG and IgM memory B-cells was highly similar, with only 19 genes, including *CD83*, *CD79A* and *PARP1* showing significant differential expression. These results confirm that the IgM memory B-cells are a significant component of the BKPyV-specific humoral response, and show for the first time that IgG and IgM repertoires directed against the same antigen can have significant differences.

2. Introduction

The BK polyomavirus PyV (BKPyV) is a typical opportunistic pathogen. Following asymptomatic primary infection during childhood, it establishes a latent infection in the kidney which appears to persist throughout life. Approximately 7% of healthy adults excrete BKPyV in the urine (Egli et al., 2009), and this proportion increases during acquired (Sundsford et al., 1994), or iatrogenic (Leung et al., 2001) immunosuppression. Its pathogenic potential is manifested in patients treated with allogeneic hematopoietic stem-cell transplantation (HSCT), in whom BKPyV replication can cause hemorrhagic cystitis (BKPyV-HC), and kidney transplant (KTx) recipients, in whom uncontrolled BKPyV replication can result in polyomavirus nephropathy (PyVAN) and graft loss or dysfunction. PyVAN can only be diagnosed definitively by histology, but it is correlated with DNAemia greater than 10^4 genome copies/mL (Nickeleit et al., 2000), and high-level DNAemia is generally classified as presumptive PyVAN (Hirsch et al., 2019). There is currently no approved antiviral therapy with clinical efficacy against BKPyV, so presumptive or biopsy-confirmed PyVAN is managed by modulation of immunosuppressive therapy, which allows host immune responses to clear the virus (Babel et al., 2011). The virological response rate to this intervention appears to vary between centres, with recent publications reporting clearance of DNAemia in response to modulation of immunosuppression in proportions varying from 30% (Bruminhent et al., 2019; Garofalo et al., 2019) up to more than 75% (Mühlbacher et al., 2020) of PyVAN patients. In the single-centre study with the longest follow-up and the largest cohort, at least 25% of PyVAN patients had DNAemia that persisted for more than one year, despite modulation of immunosuppressive therapy (Bischof et al., 2019). Similarly, the Banff working group on PyVAN, analyzing data from nine transplant centres in Europe and North America, found that PyVAN persisted for more than 24 months in 39 of 149 (26%) patients (Nickeleit et al., 2018). Importantly, recent analysis indicates that persistent PyVAN is associated with an increased risk of graft failure, and that graft loss occurs almost exclusively in patients with persistent PyVAN (Nickeleit et al., 2020).

Several previous studies have shown that the antiviral CTL response plays a key role in BKPyV clearance (Binggeli et al., 2007; Leboeuf et al., 2017; Schachtner et al., 2011), leading to the development of cellular immunotherapy for active BKPyV replication in the context of HSCT (Papadopoulou et al., 2014; Tzannou et al., 2017) and solid organ transplant (Nelson et al., 2020). With respect to the BKPyV-specific humoral response, it has been observed that the incidence of PyVAN is higher in KTx recipients with low ELISA (Bohl et

al., 2008) and neutralizing antibody titres (Solis et al., 2018), and some studies and case reports have indicated that infusion of intravenous immunoglobulin (IVIG) containing BKPyV-specific neutralizing antibodies (Velay et al., 2019), can prevent active BKPyV replication in KTx recipients (Benotmane et al., 2021), and successfully treat PyVAN (Hwang et al., 2018; Matsumura et al., 2020; Piburn & Al-Akash, 2020).

However, several studies have shown that the robust humoral response following BKPyV reactivation does not always coincide with control of virus replication (Bohl et al., 2008; Chen et al., 2006; Schachtner et al., 2011). Persistent BKPyV DNAemia in the face of a strong humoral response appears to be related to the emergence of neutralization escape mutations in the virus capsid (McIlroy et al., 2020; Peretti et al., 2018), which raises the question of whether differences exist in the quality of the BKPyV-specific humoral response that might predispose some KTx recipients to neutralization escape. In particular, KTx recipients who fail to control BKPyV replication despite a strong antibody response could have a narrower BKPyV-specific B-cell receptor (BCR) repertoire, focused mainly on variable capsid regions such as the BC-loop, rather than the conserved epitopes that are recognized by broadly neutralizing antibodies described in healthy blood donors (Lindner et al., 2019).

In the present work we aimed to characterize features of the BKPyV-specific BCR repertoire in KTx recipients who had developed a strong humoral response to the virus. By combining sorting of specific B-cells with fluorescence-labeled BKPyV virus-like particles and single cell RNAseq on the 10x Genomics platform, we were able to analyze both the BCR repertoire and gene expression profile in KTx recipients' circulating BKPyV-specific B-cells.

3. Materials and Methods

Patients and Clinical Samples

Patients included in this study were transplanted in 2011 and 2012, and had previously been included in a prospective observational study, approved by the local ethics committee and declared to the French Commission Nationale de l'Informatique et des Libertés (CNIL, n°1600141). All patients gave informed consent authorizing the use of archived urine and blood samples for research purposes. Anonymized clinical and biological data for these patients were extracted from the hospital databases. The six patients in this study were diagnosed with BKPyV reactivation based on the detection of viruria $>10^7$ copies/mL correlated with an increase in serum neutralizing titre >1 log₁₀. A total of 17 PBMC samples (two to four per patient) were collected at different timepoints (1-12 months) after peak viral load and were cryopreserved in liquid nitrogen.

Cell culture

HEK 293TT cells, purchased from the National Cancer Institute's Developmental Therapeutics Program (Frederick, Maryland, USA), were grown in complete DMEM High Glucose (ThermoFisher) containing 10% FBS (Dutscher), 100 U/mL penicillin, 100 µg/mL streptomycin (Dutscher), 1x Glutamax-I (ThermoFisher) and 250 µg/mL Hygromycin B (Sigma). RS cells (Evercyte, Vienna, Austria), an immortalized human renal tubule epithelial cell line, were maintained in serum-free medium OptiPRO (ThermoFisher) supplemented with 100 U/mL penicillin, 100 µg/mL streptomycin (ThermoFisher) and 1x Glutamax-I (ThermoFisher) in tissue-culture plasticware coated with 50 µg/mL Collagen I (ThermoFisher). Cells were maintained at 37°C in a humidified 5% CO₂ incubator, and passaged at confluence by trypsinization for 10 minutes with 1x TrypLE Express (ThermoFisher).

Plasmids

The BKPyV VP2 and VP3 expression plasmids ph2b (#32109) and ph3b (#32110), as well as the murine polyomavirus (MPyV) VP1 plasmid (#22519) were purchased from Addgene (Cambridge, MA). VP1 expression plasmids encoding BKPyV genotypes Ia, II, III, IVc2 and were kindly provided by Dr Christopher Buck, National Cancer Institute (NCI), Bethesda, MD. The plasmid pEGFP-N1 (Clontech) was used as the reporter gene. Plasmids containing mutated VP1 sequences have been described previously were obtained by site-directed mutagenesis using the NEBase changer kit (New England Biolabs) (McIlroy et al., 2020).

Labeled and non-labeled BKPyV VLP production

BKPyV virus-like particles (VLPs) were prepared following the protocols developed by the Buck lab with slight modifications (Pastrana et al., 2012). Briefly, 1×10^7 HEK 293TT cells were seeded in a 75 cm² flask in DMEM 10% FBS without antibiotics, then transfected using Lipofectamine 2000 reagent (Invitrogen) according to manufacturer's instructions. A total of 36 μ g VP1 plasmid DNA was mixed with 1.5 mL of Opti-MEM I (ThermoFisher). 72 μ L of Lipofectamine 2000 was diluted in 1.5 mL of Opti-MEM I and incubated for 5 min at room temperature prior to mixing with the diluted plasmid DNA. After 20 min at room temperature, 3 mL of DNA-Lipofectamine complexes were added to each flask containing pre-prepared 293TT cells.

Cells were harvested 48h post transfection by trypsinization and washed once in PBS then resuspended in one pellet volume (x μ L) of PBS, then mixed with 0.4x μ L of 25 U/mL type V Neuraminidase (Sigma). After 15 min at 37°C, 0.125x μ L of 10% Triton X-100 (Sigma) was added to lyse cells for 15 min at 37°C. The pH of the lysate was adjusted by addition of 0.075x μ L of 1M ammonium sulphate, or sodium bicarbonate if VLPs were to be fluorescence-labeled before ultracentrifugation, then 1 μ L of 250 U/ μ L Pierce Nuclease (Pierce) was added to degrade free DNA. After 3h at 37°C, lysates were adjusted to 0.8M NaCl, incubated on ice for 10 min and centrifuged at 5000g for 5 min at 4°C. Supernatant was transferred to a new tube and pellet was resuspended in 2 pellet volumes of PBS 0.8M NaCl, then centrifuged. The second supernatant was combined with the first, then pooled supernatant was re-clarified by centrifuging. Cleared lysates containing BKPyV genotype I VLPs were labeled with either Alexa Fluor 555 or Alexa Fluor 647 and lysate containing MPyV VLP was labeled with Alexa Fluor 488 following Alexa Fluor Microscale Protein Labeling kit instructions (ThermoFisher).

Labeled or non-labeled lysate was layered onto an Optiprep 27%/33%/39% gradient (Sigma) prepared in DPBS/0.8M NaCl, then centrifuged at 175 000 g at 4°C overnight in a Sw55TI rotor (Beckman). Tubes were punctured with a 25G syringe needle, and ten fractions of each gradient were collected into 1.5 mL microcentrifuge tubes. 6.5 μ L of each fraction was kept for SDS-PAGE to verify VP1 purity and determine peak fractions for pooling, then PBS 5% bovine serum albumin (BSA) was added to each fraction to get a final concentration of 0.1% BSA as a stabilizing agent. Peak VP1 fractions were pooled, then the VP1 concentration of each VLP stock was quantified by migrating 5 μ L of the stock on SDS-PAGE, then quantifying the VP1 band by densitometry using a standard curve constructed from a series of

4-fold dilutions of bovine serum albumin (BSA) starting at 5 µg/well. VLP morphology was confirmed at the electron microscopy facility at the Université François Rabelais, Tours.

BKPyV Pseudovirus production

BKPyV Pseudovirus (PSV) particles were prepared following the protocols developed by the Buck lab with slight modifications (Pastrana et al., 2012). Briefly, cell preparation and transfection were performed similarly to BKPyV VLP production. However, instead of transfecting only VP1 plasmid, a total of 36 µg plasmid DNA consisting of 16 µg VP1 plasmid, 4 µg ph2b, 8 µg ph3b and 8 µg pEGFP-N1 was transfected into 293TT cells.

48h after transfection, producer cells were collected by trypsinization. The pellet was washed once in cold PBS then resuspended in 800 µL hypotonic lysis buffer containing of 25 mM Sodium Citrate pH 6.0, 1 mM CaCl₂, 1 mM MgCl₂ and 5mM KCl. Cells were subjected to sonication in a Bioruptor Plus device (Diagenode) for 10 minutes at 4°C with 5 cycles of 1 min ON / 1 min OFF. Type V neuraminidase (Sigma) was added to a final concentration of 1 U/mL and incubated for 30 min at 37°C. 100 µL of 1M HEPES buffer pH 7.4 (ThermoFisher) was added to neutralize the pH, then 1 µL of 250 U/µL Pierce Nuclease (Pierce) was added before incubation for 2 hours at 37°C. The lysate was clarified by centrifuging twice at 5000 g for 5 min at 4°C and PSV was purified in an Optiprep gradient as described for VLP production. After ultracentrifugation and fraction collection, 8 µL of each fraction was removed for qPCR and the peak fractions were pooled, aliquoted and stored at -80°C for use in neutralization assays.

For quantification of pEGFP-N1 plasmid, 8 µL of each fraction was mixed with 2 µL of proteinase K buffer containing 100 mM Tris-HCl pH 7.5 (ThermoFisher), 100 mM DTT (Sigma), 25 mM EDTA (Sigma), 1% SDS (Sigma) and 200 µg/ml proteinase K (Qiagen). This solution was incubated at 50°C for 60 min followed by 95°C for 10 min. Proteinase K extracts were diluted 80-fold in milliQ water and 1 µL was used for qPCR using Applied Biosystems 2x SYBR Green Mix (Applied Biosystems). Primers were CMV-F 5'-CGC AAA TGG GCG GTA GGC GTG-3' and pEGFP-N1-R 5'-GTC CAG CTC GAC CAG GAT G-3'. Thermal cycling was initiated with a first denaturation step at 95°C for 10 min, followed by 35 cycles of 95°C for 15 sec and 55°C for 40 sec. Standard curves were constructed using serial dilutions from 10⁷ to 10² copies of the pEGFP-N1 plasmid per tube.

ELISA screening

Nunc MaxiSorp 96-well plates (Sigma) were coated with 50 ng of BKPyV VLPs in 50 μ L PBS at 37°C overnight, then blocked with 5% powdered milk in PBS for 1h. Supernatants of transfected cells were used at 2 μ L per well, and purified antibodies were assayed at 4-fold serial dilutions, starting at 10 μ g/mL in 50 μ L blocking buffer. Antibodies bound to VLPs were detected using goat anti-human IgG horseradish peroxidase-conjugated secondary antibody (Bethyl) diluted 1:5000 in blocking buffer. Washing was performed between each step with PBS 0.05% Tween-20 (Sigma). 50 μ L TMB substrate (BD Biosciences) was added and the reaction was stopped by adding 50 μ L 0.5M H₂SO₄. Absorbance was read at 450 nm in a TECAN Spark reader. The effective concentration 50% (EC50) was calculated using GraphPad Prism software.

Neutralization assays

293TT and RS cells were seeded at a density of 1×10^4 cells/well in flat bottom 96-well plates (BD Falcon) then allowed to attach at 37°C for at least one hour. BKPyV pseudovirus were diluted in the corresponding cell culture medium containing antibiotics, 0.1% BSA and 25 mM HEPES (ThermoFisher) to a concentration of 5×10^6 EGFP-N1 copies/well for RS cells and 2×10^6 EGFP-N1 copies/well for 293TT cells. Each produced antibody was added into PSV wells to make a series of 5-fold antibody dilutions starting at 500 ng/well (that is, 5 μ g/mL). IgG-PSV mix was incubated at 4°C for 1h, then added onto plated 293T or RS cells. Plates were kept in a humidified 5% CO₂ incubator at 37°C for 72h (293TT cells), or 96 hours (RS cells). Cells were washed once in PBS 0.5 mM CaCl₂, 0.5 mM MgCl₂ prior to fixing and staining in PBS 0.5 mM CaCl₂, 0.5 mM MgCl₂, 1% paraformaldehyde (EMS) and 10 μ g/mL Hoechst 33342 (ThermoFisher). The number and percentage of GFP⁺ cells were quantified using a Cellomics ArrayScan VTI HCS Reader (ThermoFisher). Neutralization curves were constructed using GraphPad Prism software.

Cloning, expression and purification of monoclonal antibodies

Monoclonal antibodies to BKPyV were produced as previously described (Devilder et al., 2018). The selected paired variable heavy (vH) and light chain (vL) sequences were sent to Eurofins for gene synthesis. vH and vL sequences were cut from the plasmid backbone by restriction enzymes prior to cloning into expression vectors containing constant regions of heavy chain (C γ 1 of IgG1) and light kappa chain (C κ) or light lambda chain (C λ). Cloned

expression vectors were confirmed by Sanger sequencing, then plasmid Maxipreps were prepared.

Antibodies were first produced on a small scale to check specificity. The day before transfection, 1.5×10^4 HEK 293A cells were seeded in 96-well plates in 200 μ L DMEM supplemented with 1% Glutamax, 10% FBS. 125 ng of vH and 125 ng of vL expression vectors were diluted in 25 μ L of 150 mM NaCl, then mixed with 0.5 μ L transfection reagent jetPEI (Polypus) diluted in 25 μ L of 150 mM NaCl. After 15 min incubation at room temperature, the complex was gently added onto pre-plated 293A cells. 16h post transfection, medium was replaced with serum-free medium Pro293a (Lonza) to avoid serum-IgG contamination. Cells were cultured for 5 days at 37°C in a humidified 5% CO₂ incubator, then supernatants were harvested and centrifuged at 460 g for 5 min to eliminate cells and debris. The presence of antibody in supernatant was confirmed by ELISA using Affinity Purified goat anti-human IgG Fc Fragment (BD Biosciences) to coat plates and goat anti-human IgG horseradish peroxidase-conjugated (BD Biosciences) as secondary antibody.

Antibodies with confirmed VLP binding were scaled up for production and purification. Briefly, the day before transfection, 6×10^6 HEK 293A cells seeded into 175 cm² flasks were transfected with 10 μ g of vH and 10 μ g of vL expression vectors following jetPEI DNA transfection protocol. At 5 days post-transfection, supernatants were harvested and centrifuged at 460 g for 5 min to remove cells, then filtered using a 1.22 μ m filter, then a 0.45 μ m filter prior to purification.

Antibodies were purified using a 1 mL HiTrap rProtein A Fast Flow column (Sigma-Aldrich) on a fast protein liquid chromatography (FPLC) system (Bio-Rad). First, the protein A sepharose column was equilibrated with 20 mM pH 7.2 phosphate buffer. Filtered supernatant containing antibodies was loaded onto the column, then washed with 20 mM pH 7.2 phosphate buffer, and finally eluted with 0.1M pH 3.0 citrate buffer. 500 μ L of each fraction was collected into tubes containing 1M pH 9.0 Tris buffer. Optical density was read at 280 nm on a spectrophotometer (Eppendorf) to determine peak fractions to pool. Pooled fractions were dialyzed in a Slide-A-Lyser cassette (ThermoFisher) with a 3.5K molecular weight cutoff against PBS overnight at 4°C with agitation, then sterilized by filtration at 0.2 μ m. Antibody purity was verified by size-exclusion chromatography using Superdex200 Increase 10/300 GL column (GE Healthcare) following the manufacturer's instructions.

10x Chromium Single-cell RNA sequencing with Immune profiling

B cell enrichment from PBMC

B cells were isolated from frozen PBMCs using human B cell isolation kit II (Miltenyi Biotec) according to the manufacturer's instructions. Briefly, frozen PBMC were thawed, counted and centrifuged then resuspended in 40 μ L 1x PBS pH 7.2 buffer containing 0.5% BSA and 2 mM EDTA (Fluka), then labeled with a cocktail of biotinylated antibodies targeting non-B cells. Non-B cells were subsequently separated magnetically using the AutoMACS Pro Separator with "Deplete" program. Purified untouched B cells were collected and counted prior to labeling with antibodies and BKPyV VLPs.

BKPyV-specific B cell staining and FACS sorting

Enriched B cells from 17 samples were resuspended in 100 μ L of 1x PBS 1% BSA labeling buffer containing the following anti-human antibodies: anti-CD3-BV510 (diluted 1/20) (BD Pharmingen), anti-CD19-BV421 (diluted 1/50) (BD Pharmingen), BKPyV-gI-VLP-AlexaFluor555 (1.34 μ g/mL), BKPyV-gI-VLP-AlexaFluor647 (0.54 μ g/mL) and MPyV-VLP-AlexaFluor488 (1.34 μ g/mL). Patient-specific and timepoint-specific TotalSeq-C oligonucleotide-labeled antibodies (BioLegend) were added into the mix as shown in Table 1, then incubated at 4°C for 30 min. Cells were washed three times in 13 mL of 1x PBS 1% BSA, centrifuged at 300 g for 5 min at 4°C. After the final wash, cells were resuspended in 1 mL of 1x PBS 0.04% BSA. 10 μ L 7-AAD viability staining solution (BD Pharmingen) was added and incubated for 5 min in the dark. The 17 samples were pooled prior to sorting through a BD Aria FACS sorter (Becton-Dickinson). 1×10^5 CD19⁺ B cells were sorted first, followed by BKPyV-specific B cells. The sorted cells were immediately used in the single-cell RNA seq procedure.

Single-cell 5' mRNA and VDJ sequencing

CD19⁺ B cells and BKPyV-specific B cells were loaded onto separate wells of a 10x Chromium A Chip. Subsequent steps were performed using 10x Chromium Single Cell 5' Library & Gel Bead kit; 10x Chromium Single Cell 5' Library Construction kit; 10x Chromium Single Cell 5' Feature Barcode Library kit; 10x Chromium Single Cell V(D)J Enrichment kit, Human B Cell; 10x Chromium Single Cell A Chip kit and 10x Chromium i7 Multiplex kit according to the manufacturer's protocols. Three libraries were prepared for each cell sample: a V(D)J enriched library, a 5' gene expression library and a 5' cell surface protein library. All libraries were quantified and verified using Quantus (Promega) and Caliper LabChip GX

(LifeSciences). Libraries from the same cell sample were pooled at the ratio of 1 V(D)J Enriched : 5 5' Gene Expression : 1 Cell Surface Protein and sequenced using an Illumina NextSeq500 system.

B cell single-cell RNA seq data analysis

TotB and SpecB raw sequencing reads in FASTQ files obtained from Illumina sequencing were aligned with the human reference transcriptome (GRCh38) by the 10x Genomics cellranger count pipeline. Output matrices of filtered features of each B population were loaded separately into R version 3.5.1 using the Read10X function. Barcode matrices containing antibody-based hashtag oligo (HTO) count tables were added into each dataset, followed by a combination of parameters from the TotB and SpecB dataset to create a merged object. HTO counts were normalized by the centered-log ratio (CLR) method, followed by demultiplexing using the Seurat function HTODemux to trace back the cell's origin. In a regular setting, doublets are removed; however, our experiments were designed to obtain double HTO-labeled cells, or doublets. Therefore, singlets and cells with wrong HTO combinations were eliminated from the dataset. Another quality control step was applied to filter out low quality cells which had the number of genes less than 500 and greater than 3000, the number of RNA counts less than 1000 and more than 15000. Cells with the percentage of mitochondrial genes more than 10% were also excluded. The remaining cells were then joined with the single-cell VDJ data to obtain merged B cells with productive pairs of heavy and light chain sequences. The merged B cells were used for further gene expression analysis.

Next, immunoglobulin variable genes were deleted from the dataset. To remove batch effects, the combined dataset was processed into the standard workflow of the Seurat Integration and Label Transfer pipeline (Stuart et al., 2019). The raw RNA counts were normalized in a log scale with a factor of 10.000 by default including the percentages of mitochondrial expression and the number of RNA counts as regression factors. Highly variable genes were identified by running FindVariableFeatures functions with the vst selection method, and the results were used as the input for principal component analysis (PCA). Performing RunPCA function returned 30 principal components (PCs) that were used to generate two-dimensional representations via RunUMAP function. Using the top 15 PCs together with the resolution of 0.1, cells were clustered by computing FindClusters and FindNeighbors functions. Clusters were visualized on a non-linear dimensional reduction plot UMAP.

B cell single-cell VDJ data analysis

Sequencing FASTQ files were submitted to 10x Genomics cellranger vdj pipeline in the presence of the human VDJ reference (GRCh38) to perform sequence assembly and paired clonotype calling. For further analysis, data was extracted from the `all_contig_annotations.json` and `filtered_contig_annotations.xls` output files. Data were rearranged in R and OpenOffice Calc for repertoire analysis using the BRepertoire webtools (Margreitter et al., 2018), IMGT-V-Quest (Brochet et al., 2008) and Immunarch (www.immunarch.com). Firstly, clonotypes were identified in BRepertoire based on heavy chain V and J segment usage, then CDR3 homology initially using a Levenshtein distance of 20. Somatic hypermutations (SHM) were identified in heavy chain V-regions in IMGT-V-Quest, using the cell barcode as the sequence ID, then the number of non-synonymous heavy chain mutations was integrated to the dataframe, so that the proportion of IgM clones and mean number of SHM could be analyzed by clonotype using the `dplyr` package in R. Heavy and light chain V-gene usage, repertoire diversity and repertoire overlap were calculated and visualized using Immunarch, after substituting the clonotype ID numbers generated by BRepertoire for the CDR sequence used by Immunarch for clonotype identification. The Chao1 estimator for repertoire diversity was independently calculated using the `vegan` package in R, in order to determine the repertoire size using the different time points from individuals as independent observations.

4. Results

Production and validation of labeled BKPyV VLPs

To generate VLPs, expression vectors containing VP1 sequences of either BKPyV genotype Ia or murine polyomavirus (MPyV) were transiently transfected into HEK 293TT cells. Cell lysates containing BKPyV were stained with either Alexa Fluor (AF) 555 or AF647, while MPyV lysate was stained with AF488. Labeled VLPs were then purified by ultracentrifugation through an Optiprep gradient and Optiprep was subsequently eliminated by repeated washes with 1x PBS in Amicon filters with a molecular weight cut-off of 100 kDa. Fluorescent VLPs had a homogeneous polyomavirus-like morphology in negative stain electron microscopy (Figure 1A) and SDS-PAGE showed that VLP stocks consisted of a single protein band corresponding to VP1, migrating at approximately 40 kDa for BKPyV and 42 kDa for MPyV (Figure 1B). Finally, no serological cross-reactivity was found between BKPyV VLPs and MPyV VLPs (Figure 1C), confirming that the binding of KTx patient antibodies to BKPyV VLPs to antibodies was specific, and that labeled MPyV VLPs could be used as a marker to eliminate non-BKPyV-specific B cells.

Next, we tested the ability of labeled BKPyV VLPs to target virus-specific memory B cells in different groups, including healthy donors, seronegative and seropositive KTx recipients post-transplant. 10-50 million frozen PBMC were thawed then stained with a cocktail of antibodies against CD3 (BV510), CD14, CD16 (PerCPCy5.5-Dump), CD19 (BV421), CD27 (APC-H7), BKPyV-gI VLP AF555, BKPyV-gI VLP AF647 and MPyV VLP AF488. FACS gating is shown in Figure 1D. Non-B cells ($CD3^+CD14^+CD16^+$) were first removed, then $CD19^+$ B cells were selected, and an analysis gate defined for AF555 and AF647 double-positive B cells. BKPyV-specific B cells were finally identified by a gate that excluded cells binding MPyV VLP. We observed that in 2 healthy donors, the percentage of BKPyV-specific B cells was extremely low, comprising no more than 0.01% of the $CD19^+$ population (Figure 1D, one healthy donor shown: #4637). Similar proportions of BKPyV-specific B cells were detected in 2 BKPyV-seronegative KTx with no evidence of viral reactivation and in 1 seropositive patient with weak BKPyV reactivation (Supplementary Figure 1). In contrast, in 5 PBMC samples from 2 KTx recipients who were seropositive and experienced high BKPyV viremia and viremia, the percentage of BKPyV-specific B cells detected was always greater than 0.1%, at least 10-fold higher compared to the other groups (Figure 1D, patient 3.12). For the first attempt at isolating BKPyV-specific antibodies from patients 3.2 and 3.12, we sorted 14 and 49 single-B cells from which heavy and light-chain antibody sequences were amplified.

We succeeded in reconstituting only 1 antibody from patient 3.2 (7%) and 6 from patient 3.12 (12%). An ELISA assay was conducted to identify antibodies that bind to BKPyV VLPs. Plates were coated with BKPyV-gIa VLPs, and incubated with generated antibodies. Among 7 antibodies tested, only 2 bound specifically to BKPyV VLP gIa (Figure 1E). To test neutralizing capacity, the 2 binders were incubated with BKPyV PSVs of each genotype, then inoculated onto 293TT cells. Only 1 binder specifically neutralized BKPyV PSV gIa (antibody 3.2-1, Figure 1F). These data showed that fluorescent BKPyV VLPs could be used as probes to sort circulating BKPyV-specific B cells.

Sorting of BKPyV-specific B-cells from multiple KTx recipients

In order to obtain a sufficient number of BKPyV-specific B cells, we developed a strategy to process multiple frozen PBMC samples the same day, allowing us to obtain paired heavy and light chain antibody sequences that could then be screened for BKPyV-specific binding and neutralization (Figure 2A). Six KTx patients who had significant increases in neutralizing antibody titres following BKPyV reactivation (Supplementary Figure 2) were selected for this experiment. A total of approximately 270 million frozen PBMCs from 17 samples (at least two independent PBMC samples per patient) were thawed, then B cells were enriched from each sample by magnetic sorting. With a slight modification compared to the first staining strategy, enriched B cells were stained in parallel with antibodies against CD3-BV510, CD19-BV421, AF555 and AF647 labeled BKPyV VLP gIa, and MPyV VLP-AF488, in addition to two oligonucleotide hashtagged antibodies for each sample. These antibody-based oligonucleotide sequences enabled us to associate each cell's RNAseq data to a specific PBMC sample during the demultiplexing analysis step (Supplementary Table 1). After separately processing and staining each PBMC sample, labeled B cells were pooled and FACS sorted. To study the total B cell repertoire, roughly 10^5 CD19⁺ B cells were isolated first (TotB population), then the BKPyV-specific B cells were sorted from the remainder of the sample, yielding approximately 10^4 sorted cells (SpecB population) (Figure 2B). Subsequent to FACS sorting, around 6×10^4 TotB and 10^4 SpecB cells were processed on the Chromium 10x platform in order to generate single-cell cDNA libraries for 1) heavy and light chain BCR sequences 2) 5' gene expression profiles and 3) antibody hashtags identifying the sample. Libraries were pooled for the TotB and the SpecB sample, then sent for Illumina sequencing.

BCR repertoire of BKPyV-specific B-cells

Paired heavy and light chain BCR sequences were obtained for 2105 cells, with a very uneven distribution between patients. More than 1500 antibody sequences were derived from

patient 3.1, while only 13 antibody sequences from patient 3.12 and only 12 from patient 3.3 were obtained. However, at least 50 BKPyV-specific BCR sequences were obtained from each of the other three patients (SpecB, Figure 3A), in addition to several hundred paired heavy and light-chain BCR sequences from circulating CD19⁺ B-cells from the same patients (TotB, Figure 3A). In all four patients with at least 50 BKPyV-specific antibody sequences, most BKPyV-specific B-cells carried Lambda light chains, whereas the total B-cell repertoire from the same patients was dominated by antibodies with Kappa light chains (Figure 3B). Only a minority of BKPyV-specific B-cells expressed IgA or IgG, even though the proportion of class-switched antibodies was higher than that observed in the corresponding total B-cell population for three out of the four patients (Figure 3C). In terms of V-gene usage, all four patients showed a greater than two-fold enrichment of IGVH4-39 in BKPyV-specific B-cells compared to total B-cells from the same patient, and in patients 3.1, 3.4 and 2.6, IGVH4-39 was the dominant heavy chain V-gene, present in at least 20% of BKPyV-specific B-cells (Supplementary Figure 3). In terms of light chain V-gene usage, no single V-gene stood out, although IGLV2-11 showed a greater than two-fold enrichment in three of the four patients.

Clonotype diversity, as measured by the Shannon diversity and the D50 index (Figure 3D-E) was significantly lower in BKPyV-specific B-cells compared to the total B-cell population, whereas the unevenness of the repertoire measured by the Gini coefficient (Figure 3F), was significantly higher. These characteristics are expected for B-cell repertoires biased toward recognition of a given antigen. Sufficient data were available for patients 3.1 and 3.2 to analyze the BKPyV-specific repertoire overlap in independent PBMC samples from the same individual. The BKPyV-specific repertoire overlap found in two samples from patient 3.2 was 51%, while for the three PBMC samples that provided sufficient data from patient 3.1, the average repertoire overlap was 68% (Figure 3G). The availability of repeated samples from these two patients allowed us to calculate the α -diversity of the BKPyV-specific BCR repertoire using the Chao1 estimator. The total number of BKPyV-specific clonotypes was 437 ± 25 in patient 3.1 and 599 ± 99 in patient 3.2. Between patients, repertoire overlap was much lower – approximately 3% (Figure 3H) indicating that each patient's BKPyV-specific BCR repertoire is mostly private, with only a few shared clonotypes between any two individuals. Since pooled cells were used to generate the BCR data in a single experiment, the possibility that errors in demultiplexing (for example, if two B-cells from the same clonotype in the same individual were erroneously assigned to two different patients) may have led to the spurious identification of shared clonotypes was addressed by inspecting the heavy and light chain V-

(D)-J gene usage and CDR3 sequences in putative shared clonotypes (Figure 3I). In some cases, distinct light chain V-genes and/or heavy chain D-genes were used in the BCRs from different individuals, proving that these cells came from distinct clonal lineages. In other cases, despite identical heavy and light chain V-(D)-J gene usage, differences in CDR3 length or the number of heavy-chain non-synonymous SHM suggested a distinct clonal history for cells within the same clonotype assigned to different patients. We therefore concluded that these BKPyV-specific BCRs were indeed generated in distinct individuals, and represented genuine shared, or public clonotypes. Having validated the observed repertoire overlap between individuals, we estimated the size of the population level BKPyV-specific BCR repertoire as approximately 11400 ± 3200 distinct clonotypes.

Next, we investigated the characteristics of IgM and IgG BKPyV-specific antibodies. As expected, the mean number of heavy-chain non-synonymous (NS) SHM was lower in B-cells expressing IgM or IgD compared to class-switched B-cells (Figure 4A). However, there were IgM outliers with very high numbers of SHM, and within clonotypes that contained both IgG and IgM antibodies, there was no difference in the mean number of SHM between IgG and IgM clones (Figure 4B). The relationship between class switching and SHM within clonotypes in BKPyV-specific B-cells was analyzed systematically in patients 3.1 and 3.2 by calculating the mean number of heavy chain SHM and the proportion of class-switched cells for each clonotype (Figure 4C). In both patients, a cluster of expanded IgM clones with low SHM that seemed to indicate a strong primary B-cell response were observed, as well as clonotypes with a progressively higher proportion of class switched B cells and a progressively higher number of SHM (Figure 4C), culminating in a cluster of clonotypes that were almost exclusively IgG, representing IgG memory B-cells (MBG). In addition, both patients also harbored a number of clonotypes with high levels of SHM that were predominantly IgM (upper-left quadrant, Figure 4C), which appeared to be IgM memory B-cells (MBM). These MBM included the dominant clonotype in patient 3.1 (Figure 4C), which had genotype I specific neutralizing activity when tested on 29TT cells and RS cells (Figure 5B).

We then compared V-gene usage in BKPyV-specific MBM and MBG, that is, cells expressing IgM or IgG antibodies with 5 or more NS heavy chain SHM. In both patients 3.1 and 3.2, BKPyV-specific MBM and MBG showed distinct patterns of heavy and light-chain V-gene use (Figure 4D and 4E). In patient 3.1, IGHV1-3, IGHV3-53, and IGHV4-61, and the light chain genes IGKV3-11, IGKV3-20 and IGLV3-21 were more frequent in MBG compared to MBM. A similar pattern was observed in patient 3.2, with IGHV2-5 and IGHV4-61, and

IGKV3-11 and IGLV3-21 found predominantly in MBG. Conversely, IGHV5-51 and IGLV3-1 were preferentially used by BKPyV-specific MBM in both patients 3.1 and 3.2. The heavy-chain IGHV4-39 gene that showed the greatest enrichment in the overall BKPyV-specific BCR repertoire was found in both MBG and MBM. These results indicate affinity matured IgG and IgM antibodies specific for BKPyV use distinct BCR repertoires.

Single-cell RNA seq profiling of BKPyV-specific B-cells

Single-cell RNA datasets of TotB and SpecB were integrated with V(D)J datasets to select only B lymphocytes with paired heavy and light chain sequences. After filtering out low quality and unwanted cells, we obtained and performed single-cell transcriptome profiling on 5450 cells including 3345 from TotB and 2105 from SpecB datasets. Using differential expression-based clustering and UMAP visualization, two distinct clusters were identified. We manually annotated these two clusters based on the expression of *CD27*, a reliable marker of human memory B cells, and IgD isotype (Figure 5A, UMAP). 3297 memory B cells were defined as IgD⁻CD27⁺; whereas, 2153 naive B cells were IgD⁺CD27⁻. Furthermore, the cluster of naive B cells showed high expression of *TCLIA*, *BACH2* as well as *CXCR4* (Figure 5B). *TCLIA* was demonstrated to be mainly expressed in naive B cells, and its expression diminishes proportionally to the maturation stages of B-cell development (Chong & Sciammas, 2011; Horns et al., 2020). Similarly, naive B cells at the early stage in the GC strongly express the transcription factor *BACH2* compared to memory B cells or plasma cells (Palm & Henry, 2019). The chemokine receptor *CXCR4* is upregulated in naive B cells, but downregulated in memory B cells and plays important roles in B-cell localization within the GC (Allen et al., 2004) and in controlling homeostasis of B cell compartments (Nie et al., 2004). Concerning the transcriptional signatures of memory B cells, elevated expression of genes associated with the activation of memory B cells and humoral responses was observed, such as the activation marker *CD86*, and the *EBI3* gene together with the chemokine receptor *CXCR3* (Figure 5B).

Next, we projected BKPyV-specific IgM and IgA/IgG memory B cells, which were defined as having greater than 4 SHM, on UMAP plots (Figure 5C). These cells were mainly found inside the cluster of memory B cells, and did not map to distinct sub-clusters within the memory B-cell population. As the BKPyV-specific antibody response was biased towards IgM⁺ B cells, we hypothesized that there might be specific genes that could distinguish IgM memory B-cells from class-switched memory B-cells. Analysis of differentially expressed genes between BKPyV-specific memory IgM and memory IgA/IgG using the negative binomial distribution test DESeq2 (Love et al., 2014) with a log2 fold change threshold of 0.15

revealed downregulation of 5 genes and upregulation of 14 genes (Figure 5D) in IgM memory B-cells compared to the expression of these genes in IgA/IgG memory B-cells. Among downregulated genes were *CD83*, which is a marker for mature dendritic cells and activated B cells during the GC reaction (Breloer & Fleischer, 2008; Krzyzak et al., 2016) and *IGLC3*, the lambda light chain constant region 3 gene. Among genes that were upregulated, we found *CD79B* which is associated with *CD79A* and membrane-bound immunoglobulin to form a mature BCR complex. Another B cell-involved gene that has a higher expression level in memory IgM subset is *PARP-1*. This gene acts in many important events during B-cell maturation (Yélamos et al., 2020). Overall, although we found various genes that were significantly differentially expressed (p -value less than 0.05), the levels of differential expression were small, indicating that the expression profiles of BKPyV-specific switched and unswitched memory B cells were highly similar.

5. Discussion

In order to study the BCR repertoire of BKPyV-specific B-cells in KTx recipients, we first validated that VLP purified from VP1-transfected 293TT cells had uniform polyomavirus morphology, and that AF555 and AF647 labeled BKPyV VLP could effectively stain susceptible cells (Supplementary Figure 4). Next, we tested whether labeled VLP could be used to specifically sort BKPyV-specific B cells. The frequencies of BKPyV VLP stained B cells exceeded 0.1% only in PBMC of KTx recipients who had experienced active BKPyV replication, and could not be reliably detected in PBMC from healthy donors. In contrast, Lindner et al. reported an average frequency of BKPyV-specific B-cells of 1/500 in three healthy blood donors using an unbiased screen of single B-cell cultures (Lindner et al., 2019). The frequencies of BKPyV specific B-cells that we observed may therefore be an underestimate, possibly due to the stringent FACS gating parameters that we applied.

Initial experiments sorting individual B-cells confirmed that BKPyV specific antibodies could be isolated from B cells that were specifically labeled with BKPyV VLP, although the yield of heavy and light chain sequences obtained was low. In order to increase the throughput of the analysis, we applied sc-RNAseq using the 10x Genomics Chromium platform, which has previously been used to obtain antibodies against influenza, HIV-1 (Setliff et al., 2019) and SARS-CoV2 (Cao et al., 2020; Shiakolas et al., 2020). The main technical obstacle was the requirement for approximately 10^4 purified cells to load the Chromium chip: since the frequency of BKPyV-specific B cells was expected to be in the range 0.1 - 1%, this would require the processing of approximately 10^8 PBMC. Each cryopreserved sample from a KTx recipient contained only 1 to 3×10^7 PBMC, so similar to Cao et al. (Cao et al., 2020) we pooled samples from several patients in order to obtain a sufficient number of purified BKPyV-specific cells. However, we also used hashtag oligonucleotide labeled antibodies to demultiplex sequence data in order to assign each antibody to its PBMC sample. From 10^4 sorted B cells, we obtained 2105 paired heavy and light chain sequences that were associated with a single patient sample, most of which were derived from patient 3.1. However, since at least 50 BKPyV-specific antibody sequences were obtained from three additional patients, it is possible to draw some conclusions concerning the BKPyV-specific BCR repertoire in KTx recipients.

Firstly, BKPyV-specific repertoires in all four patients were dominated by lambda light chain antibodies, with a clear inversion of the ratio of kappa/lambda light chain ratio between

TotB and SpecB repertoires. Secondly, although significantly less diverse than the total B cell repertoires observed in the same patients, BKPyV-specific repertoires were highly varied in all four patients, with many different VH and VL genes contributing to the repertoire. Estimates of the overall clonotype diversity obtained in patients 3.1 and 3.2 indicated that an individual's BKPyV-specific BCR repertoire consists of 400-700 distinct clonotypes. Analyzing each individual's BKPyV-specific BCR repertoire as an independent sample of the γ -diversity led to an estimate of 8000-15000 distinct clonotypes, implying that each individual's BKPyV-specific BCR represents approximately 5-10% of the available population-level repertoire. These estimates of repertoire diversity are based on two patients who controlled BKPyV replication, and may not be representative of patients with prolonged PyVAN, in whom virus neutralization escape occurs. As shown in Supplementary Figure 2, patients 3.3 and 3.4 displayed persistent high level BKPyV replication, and we have previously documented neutralization escape in these two patients (McIlroy et al., 2020; Peretti et al., 2018). Unfortunately, the low number of BKPyV-specific antibody sequences obtained from these two patients did not allow us to compare their BCR repertoires with those observed in patients 3.1 and 3.2, and further work will be required to systematically compare virus-specific BCR repertoires between patients with different virological and clinical outcomes.

Another potential bias in the estimation of repertoire size is the clonotype definition used: as clonotype definition becomes more stringent, the number of distinct clonotypes becomes larger, and the clonotype overlap between individuals becomes smaller. An extreme example of this is found in the clonotype definition in the 10x Genomics Loupe VDJ browser, which only classes antibodies as the same clonotype if they share identical heavy and light chain V- and J- gene usage, and share identical heavy and light chain CDR3 sequences. By this definition, even antibodies differing by a single CDR3 somatic hypermutation are classed as distinct clonotypes. On the other hand, using a less stringent clonotype definition introduces the risk of clustering unrelated antibodies together, in which case repertoire diversity would be underestimated. Some previous studies have used the Hamming distance as a clustering metric to group closely related antibody sequences (Jiang et al., 2013; Shlemov et al., 2017) and this has been shown to accurately define clonotypes within an individual's BCR repertoire (Gupta et al., 2017). However, in the present work, we defined clonotypes on the basis of heavy chain CDR3 nucleotide sequence using the Levenshtein distance, which can account for insertions and deletions, rather than the Hamming distance, which cannot. The reasoning behind this choice was to enable us to group antibodies with the same specificities into clonotypes, even if

they were expressed by B cells with distinct clonal histories, in which case CDR3 length could differ. Furthermore, because only heavy chain sequences contributed to the clonotype definition, we were able to use light chain sequences as an independent verification of clonotype validity. Within individuals, antibodies defined as the same clonotype based on the heavy-chain sequences also shared the same light chain V- and J- gene usage and CDR3 sequence, and as shown in Figure 3I when shared clonotypes were found between individuals, light chain CDR3 sequences were generally also very similar. These observations suggest that our strategy for clonotype definition was valid, although we cannot rule out the possibility that some clonotypes (for example clonotype 544, Figure 3) may have placed two distinct antibodies within the same cluster. Another concern is whether all the antibody sequences in the SpecB dataset were in fact specific for BKPyV, particularly since only two of seven antibodies expressed from sorted B-cells were BKPyV-specific in preliminary experiments (Figure 1E). Significantly, six of the initially screened antibodies came from cells sorted from patient 3.12, from whom we only obtained 13 antibody sequences in the scRNAseq experiment. It therefore seems likely that BKPyV-specific B-cells were relatively infrequent in this patient, which could explain the low ratio of BKPyV-specific B-cells observed in our initial experiments. On the other hand, all 10 of the antibodies that we expressed from the SpecB dataset bound specifically to BKPyV VLP, even when the antibody clonotype was represented by only two or three cells (Figure 5). We therefore have confidence that clonotypes observed at least twice in the SpecB dataset are indeed BKPyV-specific.

The third reproducible feature of the BKPyV-specific BCR repertoire was the predominance of IgM antibodies, which confirms previous observations in healthy donors (Lindner et al., 2019). MBM have also been described in the context of humoral responses to Gram negative bacteria (Rollenske et al., 2018), *Plasmodium falciparum* (Tan et al., 2018; Yilmaz et al., 2014) and more recently, SARS-CoV2 (Newell et al., 2020). In mice, MBM persist longer than MBG (Pape et al., 2011). If the same were true in humans, this might explain the contribution of MBM to the BKPyV-specific BCR repertoire in KTx recipients. Primary BKPyV infection occurs during childhood, and although the virus persists in the kidney, serum antibodies wane over time, indicating that the humoral response is not persistently stimulated. The KTx recipients studied here were all more than 50 years old, so over the decades that separated primary BKPyV infection from the superinfection after KTx, MBM may have become progressively more frequent compared to MBG, leading to the dominance of MBM that we observed in the SpecB dataset. However, virus-specific MBM were observed to be

short lived in Yellow-Fever vaccine recipients, and in two convalescent patients recovering from an acute flavivirus infection (Wec et al., 2020). It is therefore not clear whether the relative longevity of MBM compared to MBG observed in the mouse is recapitulated in humans.

Another important feature observed in BKPyV-specific MBM, is that they expressed a distinct BCR repertoire compared to that found in BKPyV-specific MBG. Repertoire differences between MBM and MBG are well documented in circulating B-cell subsets (Bagnara et al., 2015; Wu et al., 2010), but to the best of our knowledge, the present work is the first time that IgM and IgG repertoires have been compared in antibodies specific for the same antigen. Antibody responses dominated by IgM are characteristic of T-independent antigens (Allman et al., 2019), and indeed, the humoral response to mouse polyomavirus is T-independent (Guay et al., 2009; Szomolanyi-Tsuda & Welsh, 1996). Polyomavirus capsids are rigid structures presenting multiple copies of the same epitope in an ordered array, which is similar to the structural properties of the TI-2 antigens. However, this property alone cannot explain why distinct B-cell clones directed against the BKPyV capsid differentiate towards either MBG or MBM. One explanation for this observation could be that IgM and IgG antibodies recognize distinct epitopes on the capsid. In this regard it is tempting to speculate that 5-fold and 6-fold symmetry in the distribution of certain epitopes on polyomavirus capsids may favour IgM antibodies. If this is the case, then one would expect that IgM will make a significant contribution to the B-cell memory repertoire specific for other non-enveloped viruses with icosahedral capsids. Structural studies will be required to test this hypothesis. Alternatively, the distinct repertoires observed in BKPyV-specific MBM and MBG could reflect the different processes of B-cell activation and differentiation occurring in different clonal lineages, with B-cells that respond to BKPyV capsids in an extrafollicular activation process differentiating into MBM, while those clones that enter germinal centres give rise to MBG lineages. The lower expression of *CD83* that was seen in the MBM subset is consistent with this model, as is the observation that many BKPyV-specific IgM clonotypes had little SHM, even though the expression profile of these cells placed them in the memory B-cell population. As a consequence, the MBM repertoire would be more diverse and more extensive than that found in MBG, but perhaps less effective in the antiviral response in terms of specificity or neutralization potency.

In addition to repertoire differences, we also studied the gene expression profiles of BKPyV-specific MBM from MBG. Both types of cells were found predominantly within the memory B-cell cluster defined on the UMAP plot, and did not appear to define specific sub-clusters within the memory B-cell population (Figure 5A). Accordingly, differences in gene expression between BKPyV-specific MBM from MBG were minor, concerning only a handful of genes. Interestingly, the expression of *PARP-1* was found to be slightly increased in the MBM subset. Affinity maturation of antibodies is characterized as somatic hypermutation and class-switch recombination which require AID. However, AID activity is restricted in the presence of PARP-1 at Ig loci due to its mutagenic repair function, leading to a decrease of the number of somatic hypermutations (Paddock et al., 2010; Tepper et al., 2019). This can be an explanation for the lower mean number of non-synonymous SHM in the MBM subset compared to that in the MBG subset in our dataset, even though they were both activated memory B cells. Furthermore, *PARP-1*-deficient mice stimulated by T cell-independent antigens expressed predominantly IgG1 and IgG2b antibodies (Ambrose et al., 2009; Galindo-Campos et al., 2019; Robert et al., 2009). Similarly, inhibition of *PARP-1* enhanced the abundance of class-switched immunoglobulins (Shockett & Stavnezer, 1993). These findings suggest the involvement of *PARP-1* in suppressing class-switching in MBM. Further investigations are required to confirm this hypothesis.

Acknowledgments

Funding: This research was funded by grants from the Agence de la Biomedecine (AO Recherche et Greffe 2017) the Fondation Centaure (PAC10, 2017), and the Agence Nationale de la Recherche (Project ANR-17-CE17-0003). Recruitment of Nantes patients into a prospective cohort was made possible by funding from the CHU Nantes (AO Interne CHU Nantes 2011).

Acknowledgments: The authors would like to thank Chris Buck for advice in setting up VLP and PSV purification protocols, Jacques LePendou and Antoine Touzé for discussions at several stages of this work, and Antoine Touzé for help with electron microscopy.

Conflicts of Interest: The authors declare no conflict of interest. The funders had no role in the design of the study; in the collection, analyses, or interpretation of data; in the writing of the manuscript, or in the decision to publish the results.

Figure Legends

Figure 1. Fluorescence-labeled VLP characterization and isolation of BKPyV-specific B cells

(A) Negative stain electron microscopy of fluorescent VLPs. Bar = 0.5 μm . (B) Denatured labeled BKPyV VLP and MPyV VLP on SDS-PAGE protein gel. (C) IgG ELISA binding of serum from KTx recipient 3.1 and a seronegative KTx recipient to BKPyV and MPyV VLPs. (D) Binding of fluorescence-labeled BKPyV VLPs to B cells from healthy donors (upper panels) and seropositive KTx recipient with BKPyV reactivation (lower panels). From total PBMC, $\text{CD3}^+\text{CD14}^+\text{CD16}^+$ cells were gated out, then CD19^+ B cells were identified. A gate of AF555 and AF647 double-positive B cells were set and finally MPyV VLP⁺ cells were excluded. (E) Genotype I specific BKPyV binding and (F) neutralization of antibody 3.2-1.

Figure 2. Experimental strategy for the analysis of BKPyV-specific B cell repertoire from multiple donors

(A) Strategy of the scRNA seq experiment and (B) FACS profile of pooled BKPyV-specific B cells.

Figure 3. Features of BKPyV-specific BCR repertoire

(A) Number of cells with paired heavy and light chain antibody sequences obtained per patient from sorted BKPyV-specific (SpecB) and total (TotB) B cells. (B) Proportion of cells expressing Kappa light chain antibodies in SpecB and TotB datasets. (C) Proportion of cells expressing class-switched antibodies in SpecB and TotB datasets. (D-F) Shannon diversity, D50 index and Gini coefficient of clonotype distributions observed in SpecB and TotB datasets. Paired data represent cells from the same patient. (G) Venn diagram of B cell repertoire overlap in SpecB cells observed in independent PBMC samples from patients 3.1 and 3.2. Numbers represent the number clonotypes observed in each sector of the graph, independent of the number of cells per clonotype. (H) B cell repertoire overlap in SpecB cells between patients. The percentage overlap is calculated as the number of shared clonotypes divided by the number of clonotypes in the smaller dataset. (I) Sequence characteristics of selected “public” clonotypes.

Figure 4. BKPyV-specific repertoire includes IgM memory B-cells with a BCR repertoire distinct from that found in IgG memory B-cells

(A) Number of heavy chain non-synonymous (NS) mutations in BKPyV-specific B cell repertoire as a function of antibody isotype. (B) Number of heavy chain NS mutations in class switched and IgM antibodies of the same clonotype. Two representative clonotypes are shown. (C) Mean number of heavy chain NS mutations per clonotype plotted as a function of the proportion of IgG/IgA cells within the clonotype. Bubble size is proportional to the number of cells within the clonotype, but the sizes are not normalized between patients. (D, E) Heavy and light chain V-gene usage in SpecB IgG and IgM antibodies with at least 5 heavy chain NS mutations in patient 3.1 (D) and patient 3.2 (E).

Figure 5. Specificity of selected antibodies in the SpecB dataset

(A) Binding properties of selected antibodies from the SpecB data set. Heatmap indicates ELISA OD450 values normalized to positive control binding to immobilized anti-IgG Fc antibody. (B) Neutralization properties of antibody 152 IgM in 293TT cells (upper panels) and RS cells (lower panels).

Figure 6. B cell clustering and differentially expressed gene analysis

(A) TotB and SpecB were merged, then clustered based on differential expression of genes (UMAP). The expression of CD27 marker and IgD are shown in feature plots (right, upper panels) and in violin plots (right, lower panels). (B) Expression levels of specific genes in naive and memory B clusters are displayed in feature plots (6 upper panels) and violin plots (6 lower panels). (C) IgM and IgA/IgG memory B cells with more than 4 SHM are projected on the clustering UMAP. (D) Volcano plot shows upregulated genes (right, red dots) and downregulated genes (left, red dots) in activated IgM memory B cells in comparison with activated IgA/IgG memory B cells. The p -value cut-off is 0.05.

References

- Allen, C. D. C., Ansel, K. M., Low, C., Lesley, R., Tamamura, H., Fujii, N., & Cyster, J. G. (2004). Germinal center dark and light zone organization is mediated by CXCR4 and CXCR5. *Nature Immunology*, 5(9), 943–952. <https://doi.org/10.1038/ni1100>
- Allman, D., Wilmore, J. R., & Gaudette, B. T. (2019). The continuing story of T-cell independent antibodies. *Immunological Reviews*, 288(1), 128–135. <https://doi.org/10.1111/imr.12754>
- Ambrose, H. E., Willimott, S., Beswick, R. W., Dantzer, F., de Murcia, J. M., Yelamos, J., & Wagner, S. D. (2009). Poly(ADP-ribose) polymerase-1 (Parp-1)-deficient mice demonstrate abnormal antibody responses. *Immunology*, 127(2), 178–186. <https://doi.org/10.1111/j.1365-2567.2008.02921.x>
- Babel, N., Volk, H.-D., & Reinke, P. (2011). BK polyomavirus infection and nephropathy: The virus-immune system interplay. *Nature Reviews. Nephrology*, 7(7), 399–406. <https://doi.org/10.1038/nrneph.2011.59>
- Bagnara, D., Squillario, M., Kipling, D., Mora, T., Walczak, A. M., Da Silva, L., Weller, S., Dunn-Walters, D. K., Weill, J.-C., & Reynaud, C.-A. (2015). A Reassessment of IgM Memory Subsets in Humans. *Journal of Immunology (Baltimore, Md.: 1950)*, 195(8), 3716–3724. <https://doi.org/10.4049/jimmunol.1500753>
- Benotmane, I., Solis, M., Velay, A., Cognard, N., Olagne, J., Gautier Vargas, G., Perrin, P., Marx, D., Soulier, E., Gallais, F., Moulin, B., Fafi-Kremer, S., & Caillard, S. (2021). Intravenous immunoglobulin as a preventive strategy against BK virus viremia and BKV-associated nephropathy in kidney transplant recipients—Results from a proof-of-concept study. *American Journal of Transplantation: Official Journal of the American Society of Transplantation and the American Society of Transplant Surgeons*, 21(1), 329–337. <https://doi.org/10.1111/ajt.16233>
- Binggeli, S., Egli, A., Schaub, S., Binet, I., Mayr, M., Steiger, J., & Hirsch, H. H. (2007). Polyomavirus BK-specific cellular immune response to VP1 and large T-antigen in kidney transplant recipients. *American Journal of Transplantation: Official Journal of the American Society of Transplantation and the American Society of Transplant Surgeons*, 7(5), 1131–1139. <https://doi.org/10.1111/j.1600-6143.2007.01754.x>
- Bischof, N., Hirsch, H. H., Wehmeier, C., Amico, P., Dickenmann, M., Hirt-Minkowski, P., Steiger, J., Menter, T., Helmut, H., & Schaub, S. (2019). Reducing calcineurin inhibitor first for treating BK polyomavirus replication after kidney transplantation: Long-term outcomes. *Nephrology, Dialysis, Transplantation: Official Publication of the European Dialysis and Transplant Association - European Renal Association*, 34(7), 1240–1250. <https://doi.org/10.1093/ndt/gfy346>
- Bohl, D. L., Brennan, D. C., Ryschkewitsch, C., Gaudreault-Keener, M., Major, E. O., & Storch, G. A. (2008). BK virus antibody titers and intensity of infections after renal transplantation. *Journal of Clinical Virology: The Official Publication of the Pan American Society for Clinical Virology*, 43(2), 184–189. <https://doi.org/10.1016/j.jcv.2008.06.009>
- Breloer, M., & Fleischer, B. (2008). CD83 regulates lymphocyte maturation, activation and homeostasis. *Trends in Immunology*, 29(4), 186–194. <https://doi.org/10.1016/j.it.2008.01.009>

- Brochet, X., Lefranc, M.-P., & Giudicelli, V. (2008). IMGT/V-QUEST: The highly customized and integrated system for IG and TR standardized V-J and V-D-J sequence analysis. *Nucleic Acids Research*, *36*(Web Server), W503–W508. <https://doi.org/10.1093/nar/gkn316>
- Bruminhent, J., Srisala, S., Klinmalai, C., Pinsai, S., Watcharananan, S. P., Kantachuvesiri, S., Hongeng, S., & Apiwattanakul, N. (2019). BK Polyomavirus-specific T cell immune responses in kidney transplant recipients diagnosed with BK Polyomavirus-associated nephropathy. *BMC Infectious Diseases*, *19*(1), 974. <https://doi.org/10.1186/s12879-019-4615-x>
- Cao, Y., Su, B., Guo, X., Sun, W., Deng, Y., Bao, L., Zhu, Q., Zhang, X., Zheng, Y., Geng, C., Chai, X., He, R., Li, X., Lv, Q., Zhu, H., Deng, W., Xu, Y., Wang, Y., Qiao, L., ... Xie, X. S. (2020). Potent Neutralizing Antibodies against SARS-CoV-2 Identified by High-Throughput Single-Cell Sequencing of Convalescent Patients' B Cells. *Cell*, *182*(1), 73-84.e16. <https://doi.org/10.1016/j.cell.2020.05.025>
- Chen, Y., Trofe, J., Gordon, J., Du Pasquier, R. A., Roy-Chaudhury, P., Kuroda, M. J., Woodle, E. S., Khalili, K., & Koralknik, I. J. (2006). Interplay of Cellular and Humoral Immune Responses against BK Virus in Kidney Transplant Recipients with Polyomavirus Nephropathy. *Journal of Virology*, *80*(7), 3495–3505. <https://doi.org/10.1128/JVI.80.7.3495-3505.2006>
- Chong, A. S., & Sciammas, R. (2011). Matchmaking the B-Cell Signature of Tolerance to Regulatory B Cells. *American Journal of Transplantation*, *11*(12), 2555–2560. <https://doi.org/10.1111/j.1600-6143.2011.03773.x>
- Devilder, M.-C., Moyon, M., Saulquin, X., & Gautreau-Rolland, L. (2018). Generation of Discriminative Human Monoclonal Antibodies from Rare Antigen-specific B Cells Circulating in Blood. *Journal of Visualized Experiments*, *132*, 56508. <https://doi.org/10.3791/56508>
- Egli, A., Infanti, L., Dumoulin, A., Buser, A., Samaridis, J., Stebler, C., Gosert, R., & Hirsch, H. H. (2009). Prevalence of Polyomavirus BK and JC Infection and Replication in 400 Healthy Blood Donors. *The Journal of Infectious Diseases*, *199*(6), 837–846. <https://doi.org/10.1086/597126>
- Galindo-Campos, M. A., Bedora-Faure, M., Farrés, J., Lescale, C., Moreno-Lama, L., Martínez, C., Martín-Caballero, J., Ampurdanés, C., Aparicio, P., Dantzer, F., Cerutti, A., Deriano, L., & Yélamos, J. (2019). Coordinated signals from the DNA repair enzymes PARP-1 and PARP-2 promotes B-cell development and function. *Cell Death & Differentiation*, *26*(12), 2667–2681. <https://doi.org/10.1038/s41418-019-0326-5>
- Garofalo, M., Pisani, F., Lai, Q., Montali, F., Nudo, F., Gaeta, A., Russo, G., Natilli, A., Poli, L., Martinelli, C., Binda, B., & Pretagostini, R. (2019). Viremia Negativization After BK Virus Infection in Kidney Transplantation: A National Bicentric Study. *Transplantation Proceedings*, *51*(9), 2936–2938. <https://doi.org/10.1016/j.transproceed.2019.04.091>
- Guay, H. M., Mishra, R., Garcea, R. L., Welsh, R. M., & Szomolanyi-Tsuda, E. (2009). Generation of protective T cell-independent antiviral antibody responses in SCID mice reconstituted with follicular or marginal zone B cells. *Journal of Immunology (Baltimore, Md.: 1950)*, *183*(1), 518–523. <https://doi.org/10.4049/jimmunol.0900068>
- Gupta, N. T., Adams, K. D., Briggs, A. W., Timberlake, S. C., Vigneault, F., & Kleinstein, S. H. (2017). Hierarchical Clustering Can Identify B Cell Clones with High Confidence in

- Ig Repertoire Sequencing Data. *Journal of Immunology (Baltimore, Md.: 1950)*, 198(6), 2489–2499. <https://doi.org/10.4049/jimmunol.1601850>
- Hirsch, H. H., Randhawa, P. S., & AST Infectious Diseases Community of Practice. (2019). BK polyomavirus in solid organ transplantation—Guidelines from the American Society of Transplantation Infectious Diseases Community of Practice. *Clinical Transplantation*, 33(9), e13528. <https://doi.org/10.1111/ctr.13528>
- Horns, F., Dekker, C. L., & Quake, S. R. (2020). Memory B Cell Activation, Broad Anti-influenza Antibodies, and Bystander Activation Revealed by Single-Cell Transcriptomics. *Cell Reports*, 30(3), 905–913.e6. <https://doi.org/10.1016/j.celrep.2019.12.063>
- Hwang, S. D., Lee, J. H., Lee, S. W., Kim, J. K., Kim, M.-J., & Song, J. H. (2018). High-Dose Intravenous Immunoglobulin Treatment of Polyomavirus Nephropathy Developing After T Cell-Mediated Rejection Treatment: A Case Report. *Transplantation Proceedings*, 50(8), 2575–2578. <https://doi.org/10.1016/j.transproceed.2018.01.021>
- Jiang, N., He, J., Weinstein, J. A., Penland, L., Sasaki, S., He, X.-S., Dekker, C. L., Zheng, N.-Y., Huang, M., Sullivan, M., Wilson, P. C., Greenberg, H. B., Davis, M. M., Fisher, D. S., & Quake, S. R. (2013). Lineage Structure of the Human Antibody Repertoire in Response to Influenza Vaccination. *Science Translational Medicine*, 5(171), 171ra19–171ra19. <https://doi.org/10.1126/scitranslmed.3004794>
- Krzyzak, L., Seitz, C., Urbat, A., Hutzler, S., Ostalecki, C., Gläsner, J., Hiergeist, A., Gessner, A., Winkler, T. H., Steinkasserer, A., & Nitschke, L. (2016). CD83 Modulates B Cell Activation and Germinal Center Responses. *Journal of Immunology (Baltimore, Md.: 1950)*, 196(9), 3581–3594. <https://doi.org/10.4049/jimmunol.1502163>
- Leboeuf, C., Wilk, S., Achermann, R., Binet, I., Golshayan, D., Hadaya, K., Hirzel, C., Hoffmann, M., Huynh-Do, U., Koller, M. T., Manuel, O., Mueller, N. J., Mueller, T. F., Schaub, S., van Delden, C., Weissbach, F. H., Hirsch, H. H., & Swiss Transplant Cohort Study. (2017). BK Polyomavirus-Specific 9mer CD8 T Cell Responses Correlate With Clearance of BK Viremia in Kidney Transplant Recipients: First Report From the Swiss Transplant Cohort Study. *American Journal of Transplantation: Official Journal of the American Society of Transplantation and the American Society of Transplant Surgeons*, 17(10), 2591–2600. <https://doi.org/10.1111/ajt.14282>
- Leung, A. Y. H., Suen, C. K. M., Lie, A. K. W., Liang, R. H. S., Yuen, K. Y., & Kwong, Y. L. (2001). Quantification of polyoma BK viruria in hemorrhagic cystitis complicating bone marrow transplantation. *Blood*, 98(6), 1971–1978. <https://doi.org/10.1182/blood.V98.6.1971>
- Lindner, J. M., Cornacchione, V., Sathe, A., Be, C., Srinivas, H., Riquet, E., Leber, X.-C., Hein, A., Wrobel, M. B., Scharenberg, M., Pietzonka, T., Wiesmann, C., Abend, J., & Traggiai, E. (2019). Human Memory B Cells Harbor Diverse Cross-Neutralizing Antibodies against BK and JC Polyomaviruses. *Immunity*, 50(3), 668–676.e5. <https://doi.org/10.1016/j.immuni.2019.02.003>
- Love, M. I., Huber, W., & Anders, S. (2014). Moderated estimation of fold change and dispersion for RNA-seq data with DESeq2. *Genome Biology*, 15(12), 550. <https://doi.org/10.1186/s13059-014-0550-8>
- Margreitter, C., Lu, H.-C., Townsend, C., Stewart, A., Dunn-Walters, D. K., & Fraternali, F. (2018). BRepertoire: A user-friendly web server for analysing antibody repertoire data. *Nucleic Acids Research*, 46(W1), W264–W270. <https://doi.org/10.1093/nar/gky276>

- Matsumura, S., Kato, T., Taniguchi, A., Kawamura, M., Nakazawa, S., Namba-Hamano, T., Abe, T., Nonomura, N., & Imamura, R. (2020). Clinical Efficacy of Intravenous Immunoglobulin for BK Polyomavirus-Associated Nephropathy After Living Kidney Transplantation. *Therapeutics and Clinical Risk Management*, *16*, 947–952. <https://doi.org/10.2147/TCRM.S273388>
- McIlroy, D., Hönemann, M., Nguyen, N.-K., Barbier, P., Peltier, C., Rodallec, A., Halary, F., Przyrowski, E., Liebert, U., Hourmant, M., & Bressollette-Bodin, C. (2020). Persistent BK Polyomavirus Viruria Is Associated with Accumulation of VP1 Mutations and Neutralization Escape. *Viruses*, *12*(8), 824. <https://doi.org/10.3390/v12080824>
- Mühlbacher, T., Beck, R., Nadalin, S., Heyne, N., & Guthoff, M. (2020). Low-dose cidofovir and conversion to mTOR-based immunosuppression in polyomavirus-associated nephropathy. *Transplant Infectious Disease: An Official Journal of the Transplantation Society*, *22*(2), e13228. <https://doi.org/10.1111/tid.13228>
- Nelson, A. S., Heyenbruch, D., Rubinstein, J. D., Sabulski, A., Jodele, S., Thomas, S., Lutzko, C., Zhu, X., Leemhuis, T., Cancelas, J. A., Keller, M., Bollard, C. M., Hanley, P. J., Davies, S. M., & Grimley, M. S. (2020). Virus-specific T-cell therapy to treat BK polyomavirus infection in bone marrow and solid organ transplant recipients. *Blood Advances*, *4*(22), 5745–5754. <https://doi.org/10.1182/bloodadvances.2020003073>
- Newell, K. L., Clemmer, D. C., Cox, J. B., Kayode, Y. I., Zoccoli-Rodriguez, V., Taylor, H. E., Endy, T. P., Wilmore, J. R., & Winslow, G. (2020). Switched and unswitched memory B cells detected during SARS-CoV-2 convalescence correlate with limited symptom duration. *MedRxiv: The Preprint Server for Health Sciences*. <https://doi.org/10.1101/2020.09.04.20187724>
- Nickeleit, V., Klimkait, T., Binet, I. F., Dalquen, P., Del Zenero, V., Thiel, G., Mihatsch, M. J., & Hirsch, H. H. (2000). Testing for polyomavirus type BK DNA in plasma to identify renal-allograft recipients with viral nephropathy. *The New England Journal of Medicine*, *342*(18), 1309–1315. <https://doi.org/10.1056/NEJM200005043421802>
- Nickeleit, Volker, Singh, H. K., Dadhania, D., Cornea, V., El-Husseini, A., Castellanos, A., Davis, V. G., Waid, T., & Seshan, S. V. (2020). The 2018 Banff Working Group classification of definitive polyomavirus nephropathy: A multicenter validation study in the modern era. *American Journal of Transplantation*, *ajt.16189*. <https://doi.org/10.1111/ajt.16189>
- Nickeleit, Volker, Singh, H. K., Randhawa, P., Drachenberg, C. B., Bhatnagar, R., Bracamonte, E., Chang, A., Chon, W. J., Dadhania, D., Davis, V. G., Hopfer, H., Mihatsch, M. J., Papadimitriou, J. C., Schaub, S., Stokes, M. B., Tungekar, M. F., Seshan, S. V., & Banff Working Group on Polyomavirus Nephropathy. (2018). The Banff Working Group Classification of Definitive Polyomavirus Nephropathy: Morphologic Definitions and Clinical Correlations. *Journal of the American Society of Nephrology: JASN*, *29*(2), 680–693. <https://doi.org/10.1681/ASN.2017050477>
- Nie, Y., Waite, J., Brewer, F., Sunshine, M.-J., Littman, D. R., & Zou, Y.-R. (2004). The role of CXCR4 in maintaining peripheral B cell compartments and humoral immunity. *The Journal of Experimental Medicine*, *200*(9), 1145–1156. <https://doi.org/10.1084/jem.20041185>
- Paddock, M. N., Buelow, B. D., Takeda, S., & Scharenberg, A. M. (2010). The BRCT domain of PARP-1 is required for immunoglobulin gene conversion. *PLoS Biology*, *8*(7), e1000428. <https://doi.org/10.1371/journal.pbio.1000428>

- Palm, A.-K. E., & Henry, C. (2019). Remembrance of Things Past: Long-Term B Cell Memory After Infection and Vaccination. *Frontiers in Immunology*, 10. <https://doi.org/10.3389/fimmu.2019.01787>
- Papadopoulou, A., Gerdemann, U., Katari, U. L., Tzannou, I., Liu, H., Martinez, C., Leung, K., Carrum, G., Gee, A. P., Vera, J. F., Krance, R. A., Brenner, M. K., Rooney, C. M., Heslop, H. E., & Leen, A. M. (2014). Activity of broad-spectrum T cells as treatment for AdV, EBV, CMV, BKV, and HHV6 infections after HSCT. *Science Translational Medicine*, 6(242), 242ra83. <https://doi.org/10.1126/scitranslmed.3008825>
- Pape, K. A., Taylor, J. J., Maul, R. W., Gearhart, P. J., & Jenkins, M. K. (2011). Different B Cell Populations Mediate Early and Late Memory During an Endogenous Immune Response. *Science*, 331(6021), 1203–1207. <https://doi.org/10.1126/science.1201730>
- Pastrana, D. V., Brennan, D. C., Cuburu, N., Storch, G. A., Viscidi, R. P., Randhawa, P. S., & Buck, C. B. (2012). Neutralization serotyping of BK polyomavirus infection in kidney transplant recipients. *PLoS Pathogens*, 8(4), e1002650. <https://doi.org/10.1371/journal.ppat.1002650>
- Peretti, A., Geoghegan, E. M., Pastrana, D. V., Smola, S., Feld, P., Sauter, M., Lohse, S., Ramesh, M., Lim, E. S., Wang, D., Borgogna, C., FitzGerald, P. C., Bliskovsky, V., Starrett, G. J., Law, E. K., Harris, R. S., Killian, J. K., Zhu, J., Pineda, M., ... Buck, C. B. (2018). Characterization of BK Polyomaviruses from Kidney Transplant Recipients Suggests a Role for APOBEC3 in Driving In-Host Virus Evolution. *Cell Host & Microbe*, 23(5), 628–635.e7. <https://doi.org/10.1016/j.chom.2018.04.005>
- Piburn, K. H., & Al-Akash, S. (2020). Use of intravenous immunoglobulin in a highly sensitized pediatric renal transplant recipient with severe BK DNAemia and rising DSA. *Pediatric Transplantation*, 24(1), e13600. <https://doi.org/10.1111/petr.13600>
- Robert, I., Dantzer, F., & Reina-San-Martin, B. (2009). Parp1 facilitates alternative NHEJ, whereas Parp2 suppresses IgH/c-myc translocations during immunoglobulin class switch recombination. *The Journal of Experimental Medicine*, 206(5), 1047–1056. <https://doi.org/10.1084/jem.20082468>
- Rollenske, T., Szijarto, V., Lukasiewicz, J., Guachalla, L. M., Stojkovic, K., Hartl, K., Stulik, L., Kocher, S., Lasitschka, F., Al-Saeedi, M., Schröder-Braunstein, J., von Frankenberg, M., Gaebelein, G., Hoffmann, P., Klein, S., Heeg, K., Nagy, E., Nagy, G., & Wardemann, H. (2018). Cross-specificity of protective human antibodies against *Klebsiella pneumoniae* LPS O-antigen. *Nature Immunology*, 19(6), 617–624. <https://doi.org/10.1038/s41590-018-0106-2>
- Schachtner, T., Müller, K., Stein, M., Diezemann, C., Sefrin, A., Babel, N., & Reinke, P. (2011). BK virus-specific immunity kinetics: A predictor of recovery from polyomavirus BK-associated nephropathy. *American Journal of Transplantation: Official Journal of the American Society of Transplantation and the American Society of Transplant Surgeons*, 11(11), 2443–2452. <https://doi.org/10.1111/j.1600-6143.2011.03693.x>
- Setliff, I., Shiakolas, A. R., Pilewski, K. A., Murji, A. A., Mapengo, R. E., Janowska, K., Richardson, S., Oosthuysen, C., Raju, N., Ronsard, L., Kanekiyo, M., Qin, J. S., Kramer, K. J., Greenplate, A. R., McDonnell, W. J., Graham, B. S., Connors, M., Lingwood, D., Acharya, P., ... Georgiev, I. S. (2019). High-Throughput Mapping of B Cell Receptor Sequences to Antigen Specificity. *Cell*, 179(7), 1636–1646.e15. <https://doi.org/10.1016/j.cell.2019.11.003>

- Shiakolas, A. R., Kramer, K. J., Wrapp, D., Richardson, S. I., Schäfer, A., Wall, S., Wang, N., Janowska, K., Pilewski, K. A., Venkat, R., Parks, R., Manamela, N. P., Raju, N., Fechter, E. F., Holt, C. M., Suryadevara, N., Chen, R. E., Martinez, D. R., Nargi, R. S., ... Georgiev, I. S. (2020). Cross-reactive coronavirus antibodies with diverse epitope specificities and extra-neutralization functions. *BioRxiv: The Preprint Server for Biology*. <https://doi.org/10.1101/2020.12.20.414748>
- Shlemov, A., Bankevich, S., Bzikadze, A., Turchaninova, M. A., Safonova, Y., & Pevzner, P. A. (2017). Reconstructing Antibody Repertoires from Error-Prone Immunosequencing Reads. *Journal of Immunology (Baltimore, Md.: 1950)*, *199*(9), 3369–3380. <https://doi.org/10.4049/jimmunol.1700485>
- Shockett, P., & Stavnezer, J. (1993). Inhibitors of poly(ADP-ribose) polymerase increase antibody class switching. *The Journal of Immunology*, *151*(12), 6962–6976.
- Solis, M., Velay, A., Porcher, R., Domingo-Calap, P., Soulier, E., Joly, M., Meddeb, M., Kack-Kack, W., Moulin, B., Bahram, S., Stoll-Keller, F., Barth, H., Caillard, S., & Fafi-Kremer, S. (2018). Neutralizing Antibody-Mediated Response and Risk of BK Virus-Associated Nephropathy. *Journal of the American Society of Nephrology: JASN*, *29*(1), 326–334. <https://doi.org/10.1681/ASN.2017050532>
- Stuart, T., Butler, A., Hoffman, P., Hafemeister, C., Papalexi, E., Mauck, W. M., Hao, Y., Stoeckius, M., Smibert, P., & Satija, R. (2019). Comprehensive Integration of Single-Cell Data. *Cell*, *177*(7), 1888–1902.e21. <https://doi.org/10.1016/j.cell.2019.05.031>
- Sundsford, A., Flaegstad, T., Flø, R., Spein, A. R., Pedersen, M., Permin, H., Julsrud, J., & Traavik, T. (1994). BK and JC viruses in human immunodeficiency virus type 1-infected persons: Prevalence, excretion, viremia, and viral regulatory regions. *The Journal of Infectious Diseases*, *169*(3), 485–490. <https://doi.org/10.1093/infdis/169.3.485>
- Szomolanyi-Tsuda, E., & Welsh, R. M. (1996). T cell-independent antibody-mediated clearance of polyoma virus in T cell-deficient mice. *The Journal of Experimental Medicine*, *183*(2), 403–411. <https://doi.org/10.1084/jem.183.2.403>
- Tan, J., Sack, B. K., Oyen, D., Zenklusen, I., Piccoli, L., Barbieri, S., Foglierini, M., Fregni, C. S., Marcandalli, J., Jongo, S., Abdulla, S., Perez, L., Corradin, G., Varani, L., Sallusto, F., Sim, B. K. L., Hoffman, S. L., Kappe, S. H. I., Daubenberger, C., ... Lanzavecchia, A. (2018). A public antibody lineage that potently inhibits malaria infection through dual binding to the circumsporozoite protein. *Nature Medicine*, *24*(4), 401–407. <https://doi.org/10.1038/nm.4513>
- Tepper, S., Mortusewicz, O., Czlonka, E., Bello, A., Schmidt, A., Jeschke, J., Fischbach, A., Pfeil, I., Petersen-Mahrt, S. K., Mangerich, A., Helleday, T., Leonhardt, H., & Jungnickel, B. (2019). Restriction of AID activity and somatic hypermutation by PARP-1. *Nucleic Acids Research*, *47*(14), 7418–7429. <https://doi.org/10.1093/nar/gkz466>
- Tzannou, I., Papadopoulou, A., Naik, S., Leung, K., Martinez, C. A., Ramos, C. A., Carrum, G., Sasa, G., Lulla, P., Watanabe, A., Kuvalekar, M., Gee, A. P., Wu, M.-F., Liu, H., Grilley, B. J., Krance, R. A., Gottschalk, S., Brenner, M. K., Rooney, C. M., ... Omer, B. (2017). Off-the-Shelf Virus-Specific T Cells to Treat BK Virus, Human Herpesvirus 6, Cytomegalovirus, Epstein-Barr Virus, and Adenovirus Infections After Allogeneic Hematopoietic Stem-Cell Transplantation. *Journal of Clinical Oncology: Official Journal of the American Society of Clinical Oncology*, *35*(31), 3547–3557. <https://doi.org/10.1200/JCO.2017.73.0655>

- Velay, A., Solis, M., Benotmane, I., Gantner, P., Soulier, E., Moulin, B., Caillard, S., & Fafi-Kremer, S. (2019). Intravenous Immunoglobulin Administration Significantly Increases BKPyV Genotype-Specific Neutralizing Antibody Titers in Kidney Transplant Recipients. *Antimicrobial Agents and Chemotherapy*, 63(8). <https://doi.org/10.1128/AAC.00393-19>
- Wec, A. Z., Haslwanter, D., Abdiche, Y. N., Shehata, L., Pedreño-Lopez, N., Moyer, C. L., Bornholdt, Z. A., Lilov, A., Nett, J. H., Jangra, R. K., Brown, M., Watkins, D. I., Ahlm, C., Forsell, M. N., Rey, F. A., Barba-Spaeth, G., Chandran, K., & Walker, L. M. (2020). Longitudinal dynamics of the human B cell response to the yellow fever 17D vaccine. *Proceedings of the National Academy of Sciences of the United States of America*, 117(12), 6675–6685. <https://doi.org/10.1073/pnas.1921388117>
- Wu, Y.-C., Kipling, D., Leong, H. S., Martin, V., Ademokun, A. A., & Dunn-Walters, D. K. (2010). High-throughput immunoglobulin repertoire analysis distinguishes between human IgM memory and switched memory B-cell populations. *Blood*, 116(7), 1070–1078. <https://doi.org/10.1182/blood-2010-03-275859>
- Yélamos, J., Moreno-Lama, L., Jimeno, J., & Ali, S. O. (2020). Immunomodulatory Roles of PARP-1 and PARP-2: Impact on PARP-Centered Cancer Therapies. *Cancers*, 12(2). <https://doi.org/10.3390/cancers12020392>
- Yilmaz, B., Portugal, S., Tran, T. M., Gozzelino, R., Ramos, S., Gomes, J., Regalado, A., Cowan, P. J., d'Apice, A. J. F., Chong, A. S., Doumbo, O. K., Traore, B., Crompton, P. D., Silveira, H., & Soares, M. P. (2014). Gut microbiota elicits a protective immune response against malaria transmission. *Cell*, 159(6), 1277–1289. <https://doi.org/10.1016/j.cell.2014.10.053>

Figure 1: Fluorescence-labeled VLP characterization and isolation of BKPyV-specific B cells

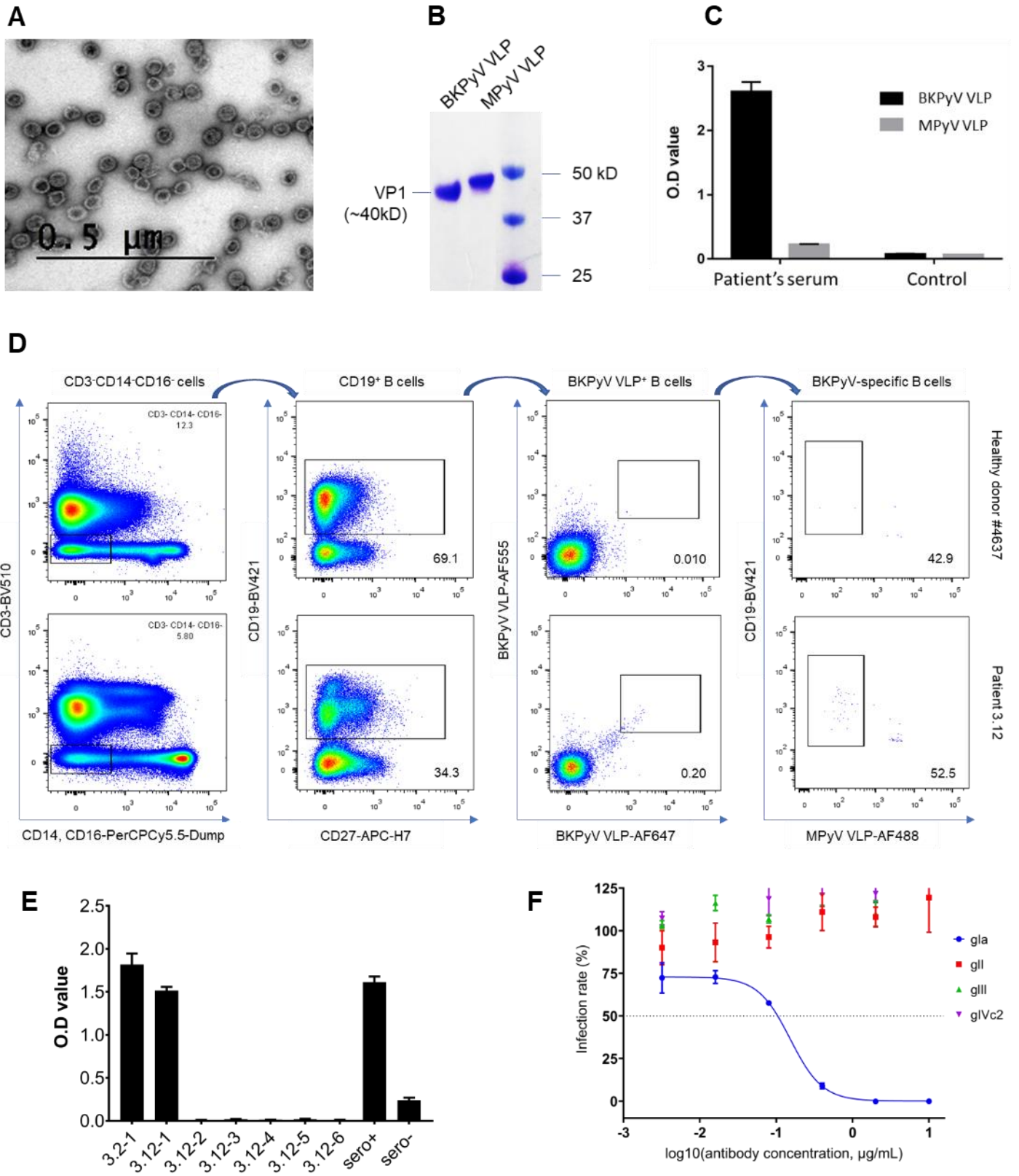


Figure 2: Experimental strategy for the analysis of BKPvV-specific B cell repertoire from multiple donors

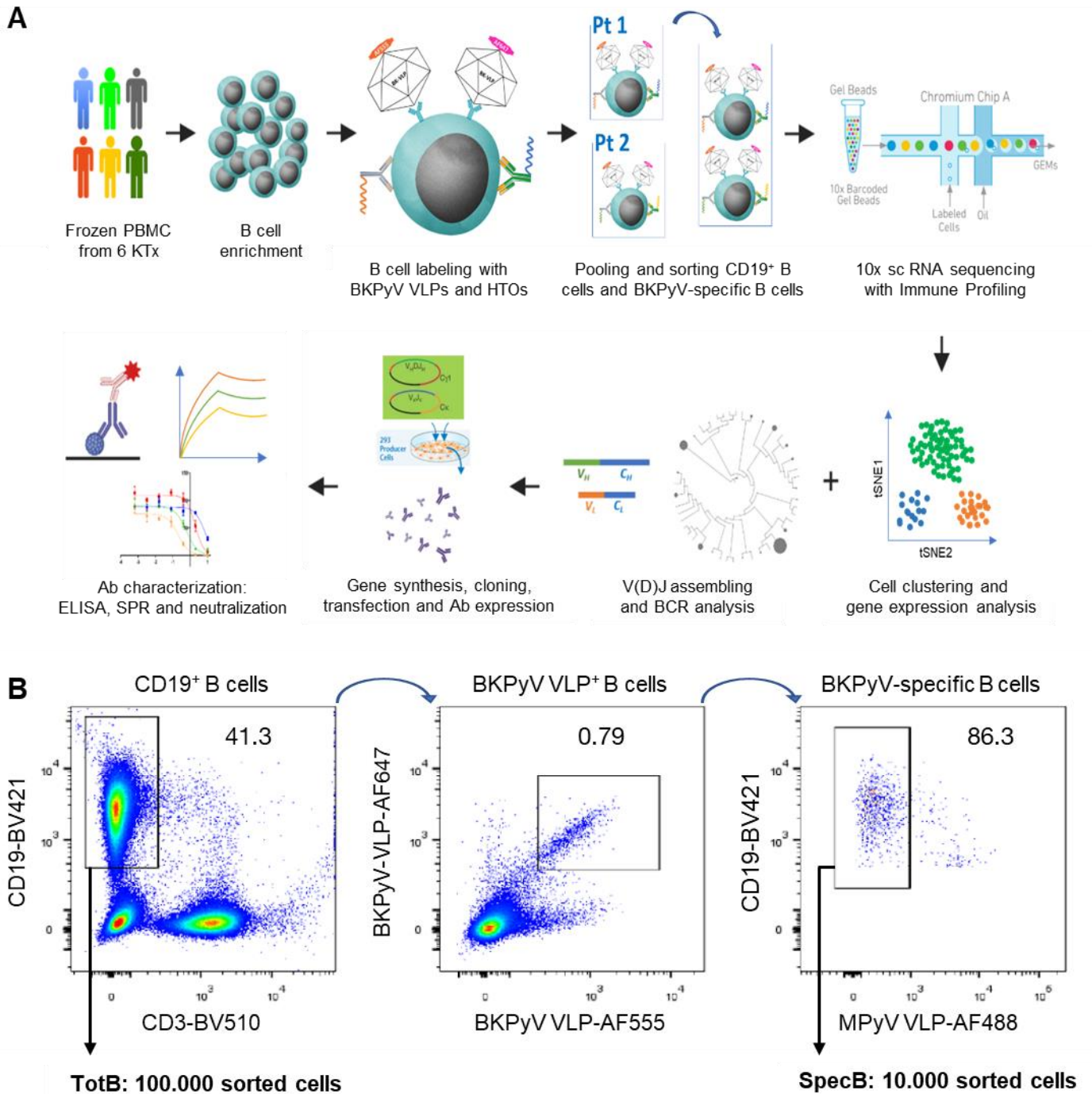


Figure 3: Features of BKPyV-specific BCR repertoire

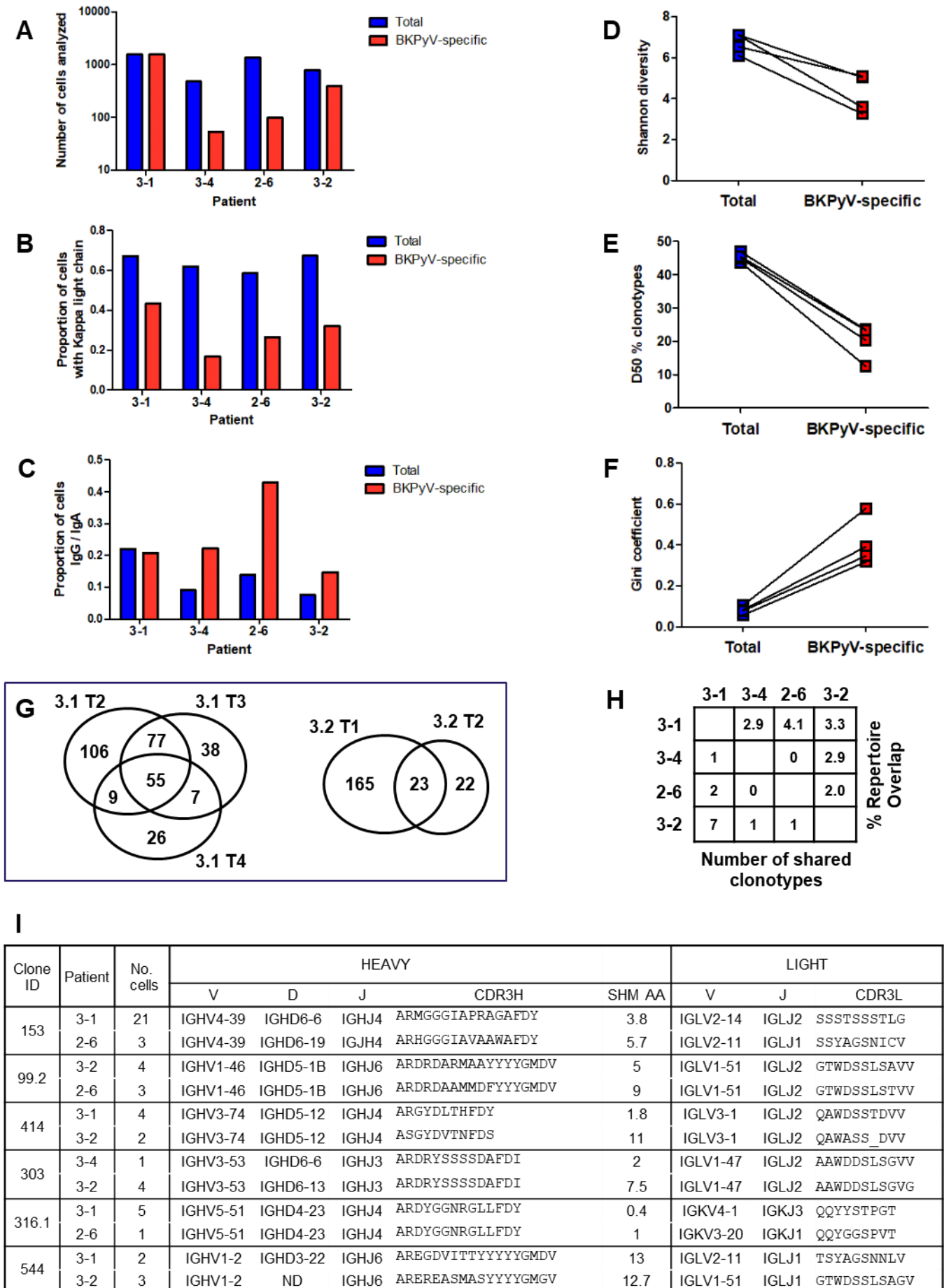


Figure 4. BkPyV-specific repertoire includes IgM memory B-cells with a BCR repertoire distinct from that found in IgG memory B-cells

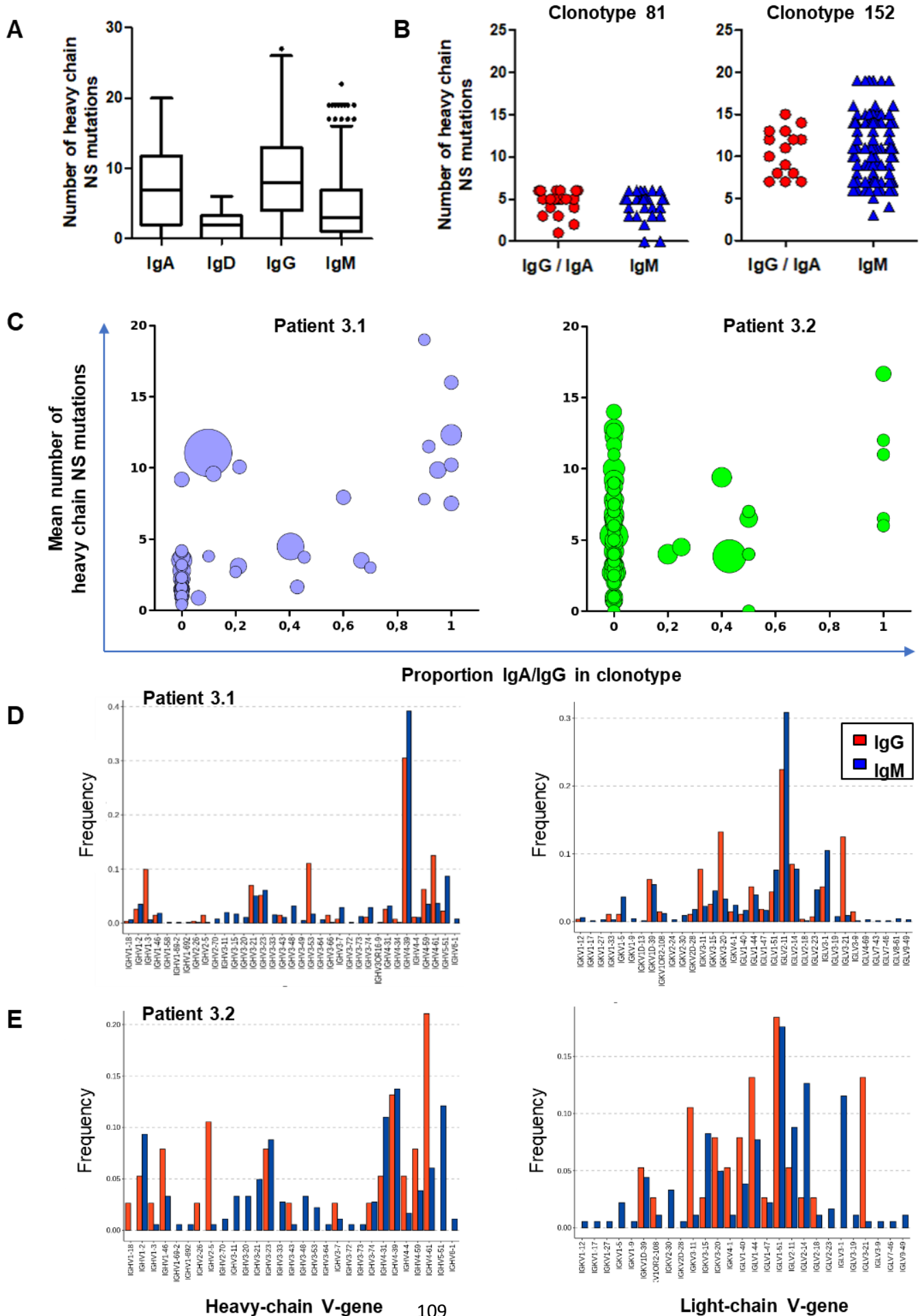


Figure 5. Specificity of selected antibodies in the SpecB dataset

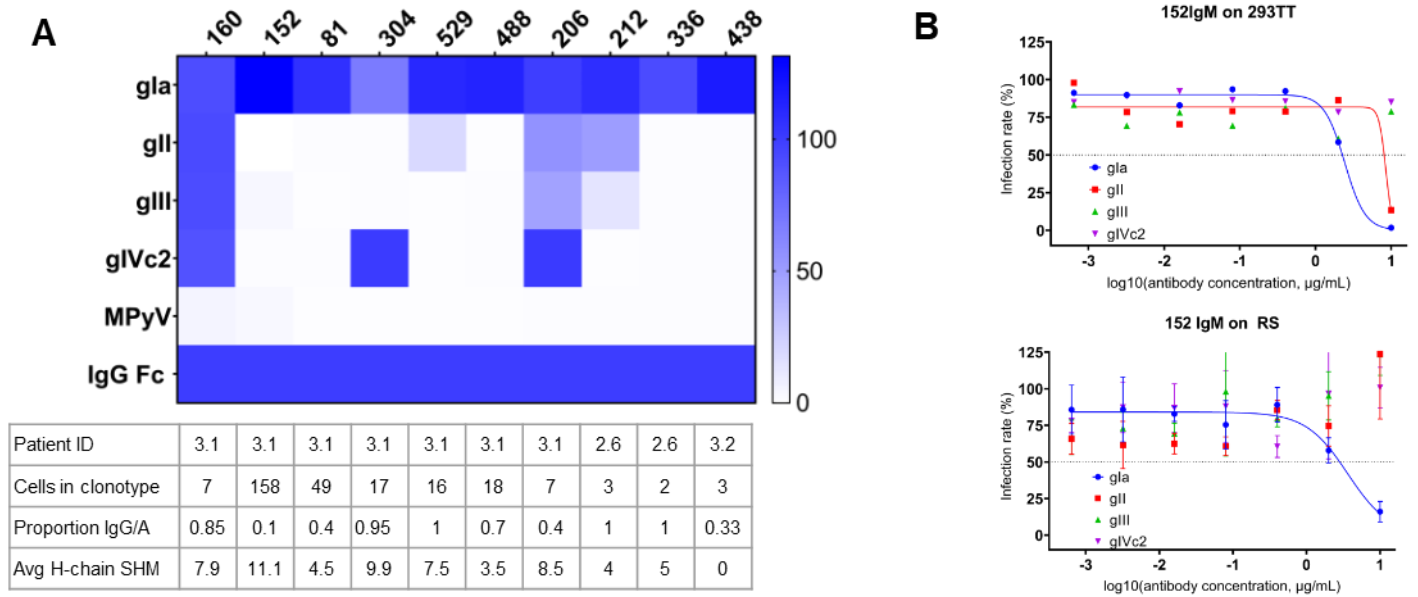
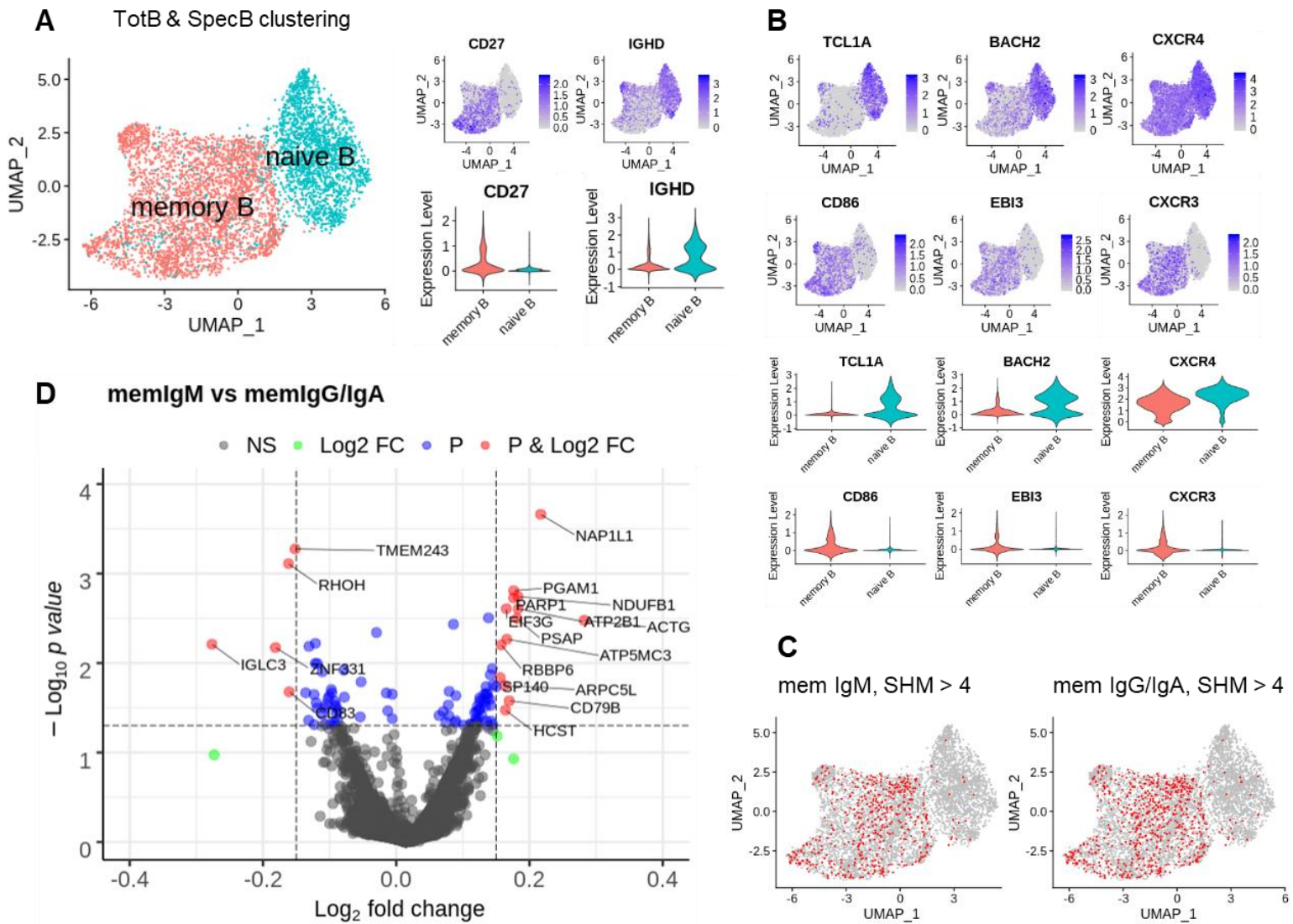


Figure 6: B cell clustering and differentially expressed gene analysis



Supplementary Table 1:

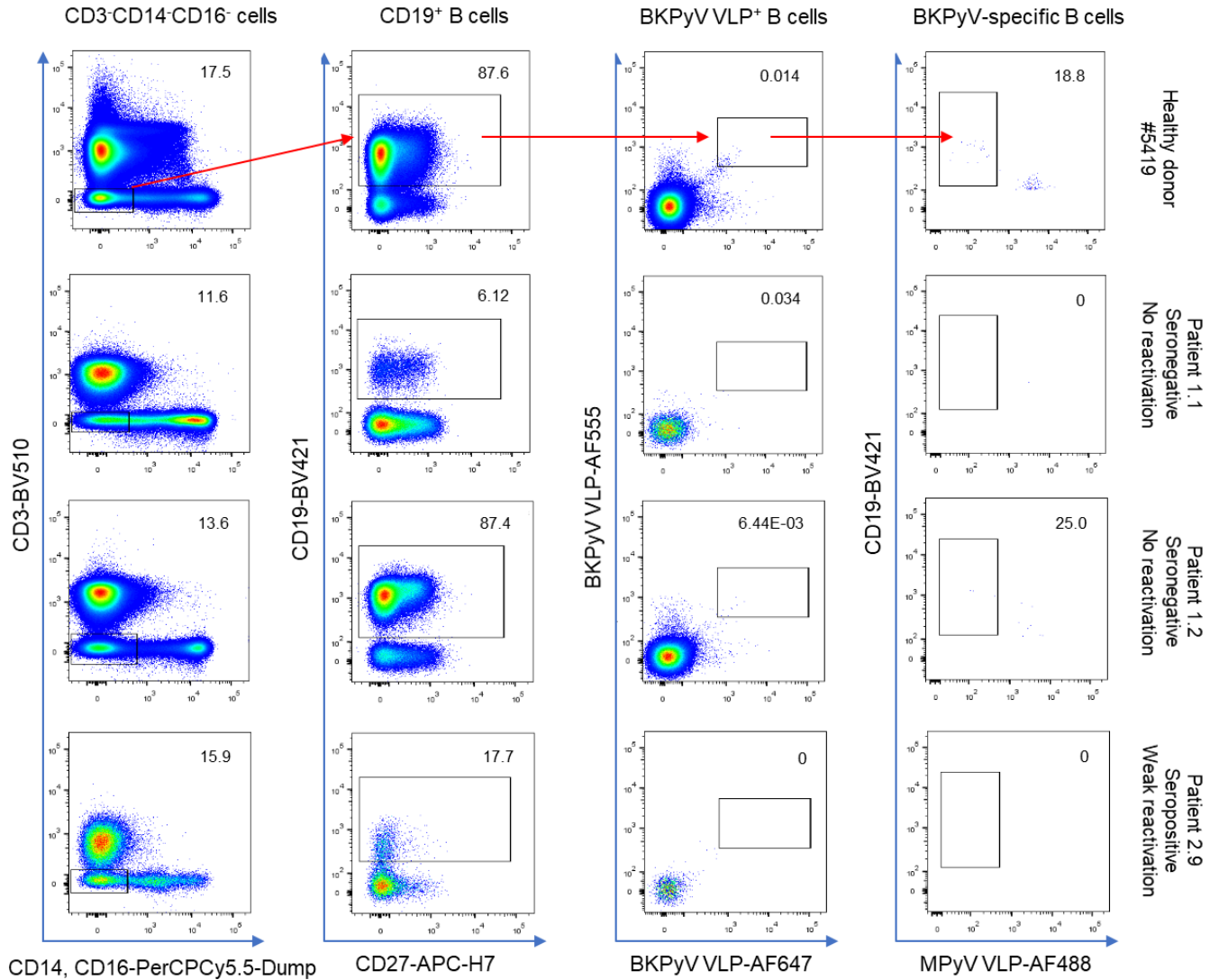
Combinatorial sample barcoding

Patient	Patient-specific antibodies	Timepoint-specific antibodies			
		Timepoint 1	Timepoint 2	Timepoint 3	Timepoint 4
2.6	Hashtag 1	anti-CD11a	anti-CD18	anti-CD45	
3.1	Hashtag 2	anti-CD11a	anti-CD18	anti-CD45	anti-CD20
3.12	anti-HLA-ABC	anti-CD11a	anti-CD18		
3.2	anti-HLA-DR	anti-CD11a	anti-CD18		
3.3	Hashtag 4	anti-CD11a	anti-CD18	anti-CD45	
3.4	Hashtag 5	anti-CD11a	anti-CD18	anti-CD45	

** Barcoded antibodies against human surface antigens with TotalSeq C oligonucleotides, specifically compatible with the Single Cell 5' workflow of 10X Genomics.*

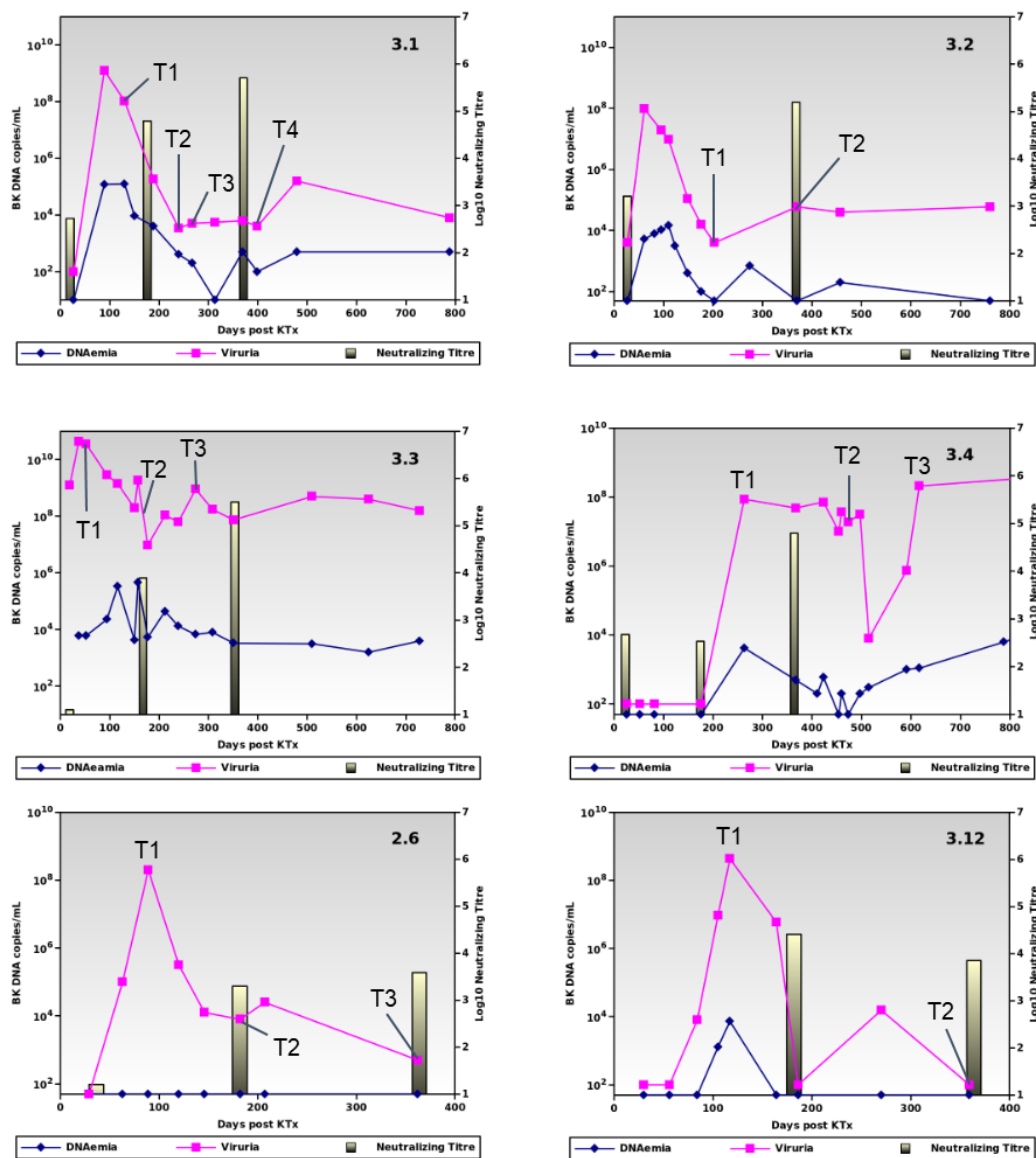
Supplementary Figure 1:

Binding of fluorescence-labeled BKPyV VLPs to B cells from healthy donor, seronegative KTx, seropositive KTx



Supplementary Figure 2

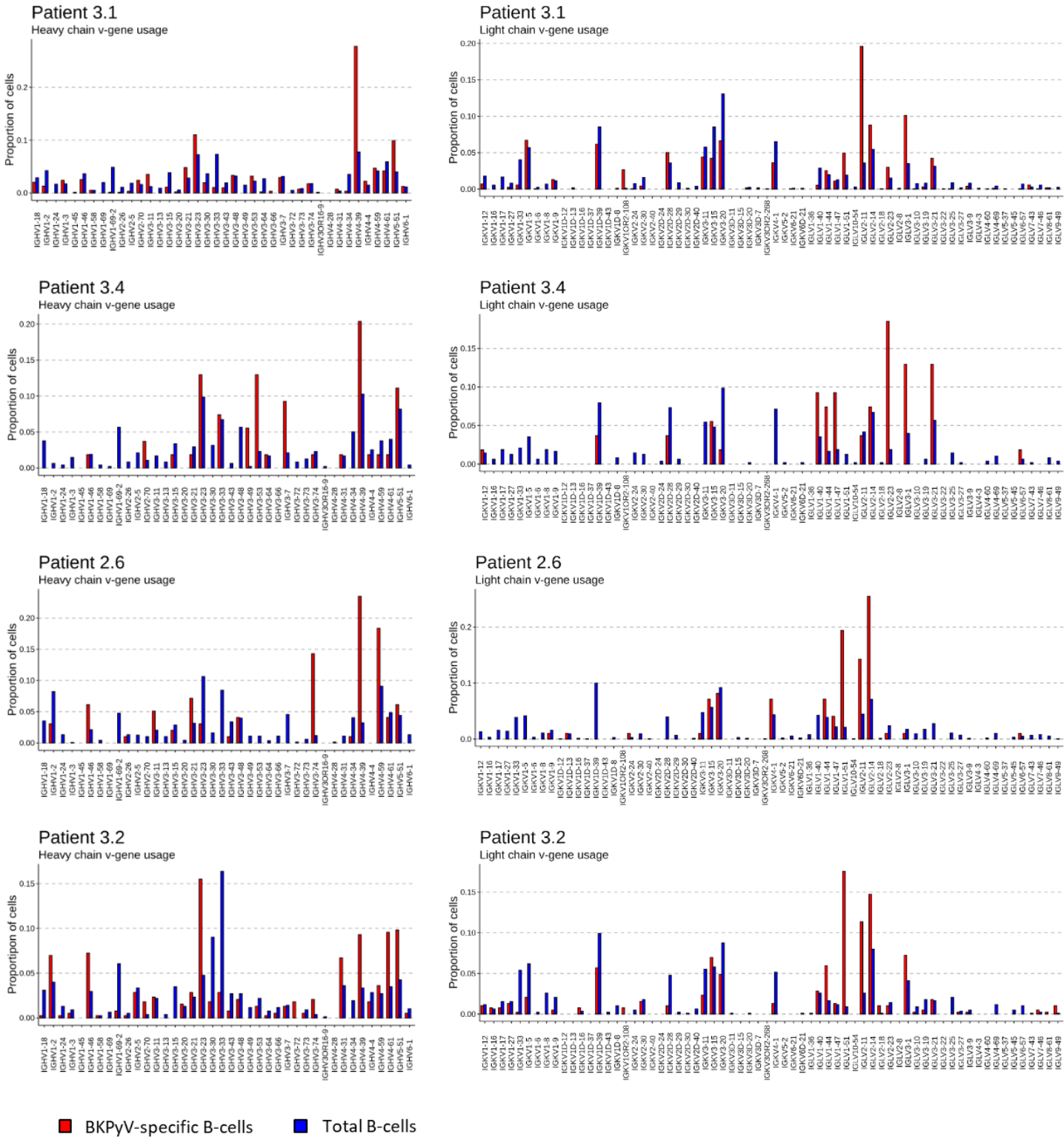
Viral load, neutralizing antibody titres, and summary clinical data of patients selected for scRNA seq experiment



Patient	Sex	Age at KTx	KTx date	BKPyV genotype
3.1	F	67	05/08/11	Ib2
3.2	M	62	11/02/12	Ib2
3.3	M	61	14/10/11	IV
3.4	M	64	10/12/11	Ib2
2.6	F	55	07/07/11	Ib1
3.12	M	59	19/7/11	Ib2

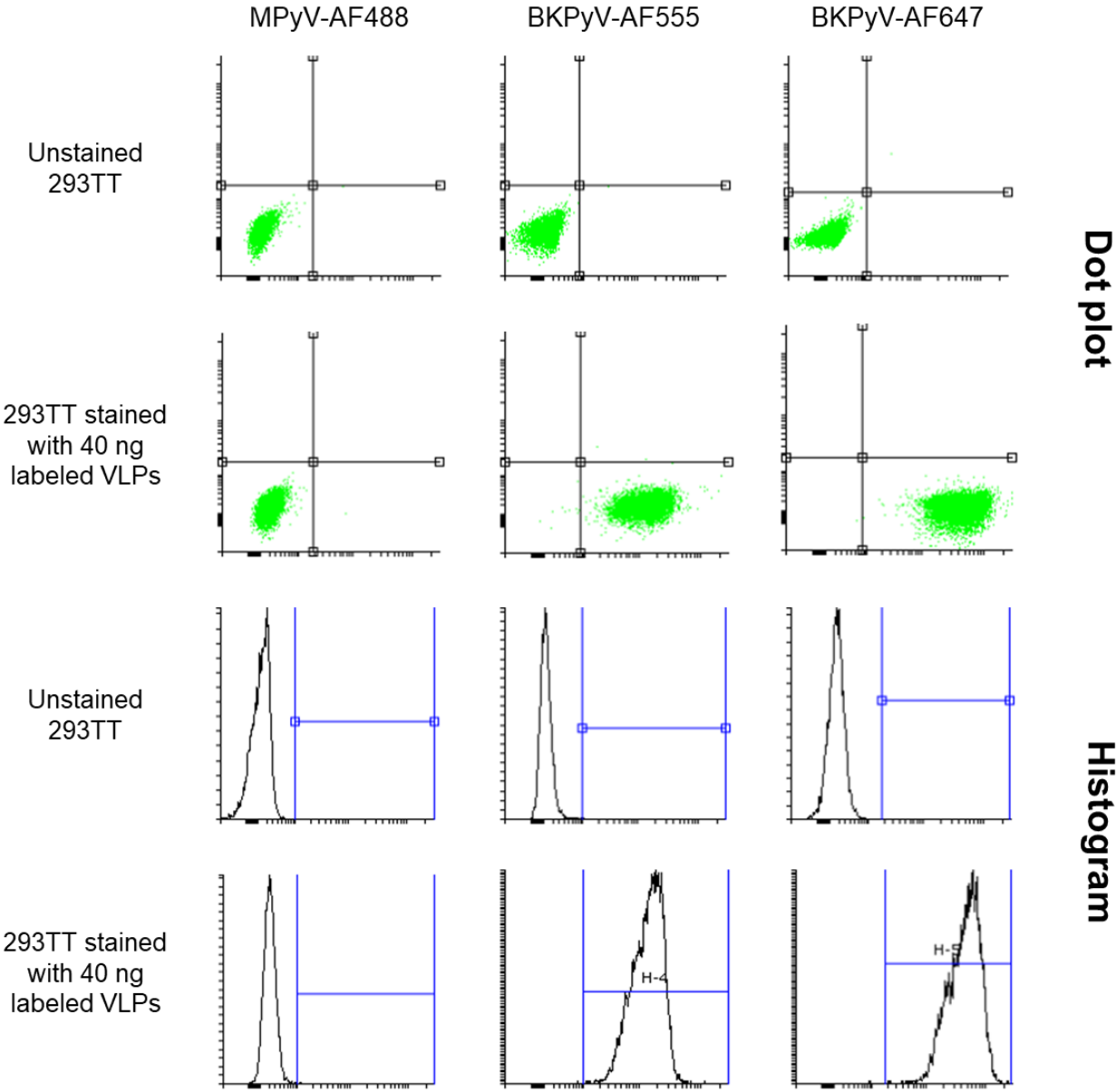
Supplementary Figure 3:

Heavy and light chain v-gene usage in total and BKPyV-specific B-cells



Supplementary Figure 4:

Binding of fluorescence-labeled BKPyV VLPs to susceptible 293TT cells



PART 2: Identification of a 41F17-like family of BKPyV-specific bNAbs

Identification of a "41F17-like" family of broadly neutralizing antibodies

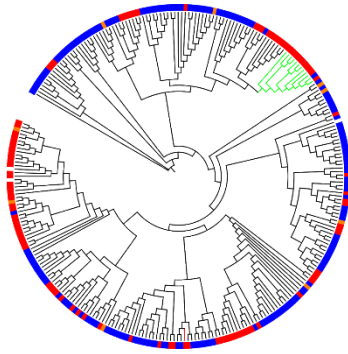
Broadly neutralizing BKPyV-specific monoclonal antibodies, including the high-affinity clones 41F17 and 27O24, have previously been isolated from the PBMC of a healthy adult donor (Lindner et al., 2019). Since four of the KTx recipients we studied had successfully suppressed BKPyV replication, we investigated whether their BCR repertoire included antibodies with similar broadly neutralizing properties. In order to identify antibodies in our dataset with similar heavy and light chain sequences to the previously described 41F17 and 27O24 monoclonals (Lindner et al., 2019), antibodies with fewer than 5 heavy chain somatic hypermutations were excluded, then the heavy and light chain CDR3 amino-acid sequences were concatenated and aligned in UGene (Okonechnikov et al., 2012) using a two-step procedure, first with Clustal Omega, then with Muscle to align conserved C-terminal sequences. Aligned sequences were clustered as a phylogenetic tree by Neighbour-Joining. Antibodies with κ and λ light chains were analyzed separately, and trees were visualized using iTOL 5.7 (<https://itol.embl.de/>) (Letunic & Bork, 2019).

Although we did not detect a close sequence neighbor to the 27O24 antibody (**red branch, Figure 23A, Figure 24**), we were able to identify a cluster of kappa light chain IgG antibodies (**green clade, Figure 23A, Figure 24**) that shared a CDR3 sequence motif with the 41F17 antibody (**Figure 23B**). When cloned and expressed, antibodies from clonotypes 120, 160 and 198 specifically bound all four genotypes of BKPyV (**Figure 23C**), a property that they shared with the 41F17 antibody, and which was found in only one of nine other antibodies from the dataset that were tested (**Figure 25A**). Clonotypes 120, 160 and 198 had identical heavy and light chain V-gene usage (IGHV4-39 / IGKV3-11), which differed from that found in 41F17 (IGHV4-31 / IGKV3-11). As described in the previous section, the IGKV3-11 gene was used preferentially by MBG, and indeed

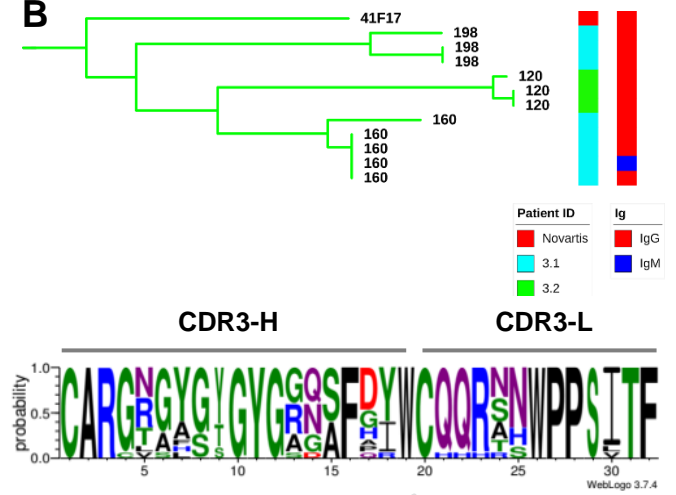
clonotypes 120, 160 and 198 were characterized by a proportion of >85% IgG within the clonotype, so despite the dominance of IgM in the overall BKPyV-specific repertoire, this cluster of broadly neutralizing antibodies was predominantly IgG.

Binding avidity to VLPs measured by surface plasmon resonance was in the sub-nanomolar range, with clonotypes 120 and 160 binding to all four BKPyV genotypes with an avidity similar to that observed for the 41F17 antibody (**Figure 23D**). In terms of neutralization, like the 41F17 antibody, clonotypes 120 and 160 neutralized all four BKPyV genotypes when assayed in 293TT cells (**Figure 23F, upper panels**), whereas only clonotype 120 and the 41F17 monoclonal were broadly neutralizing in immortalized renal tubular epithelial cells (**Figure 23F, lower panels**) with inhibitory concentrations (IC₅₀) in the sub-nanomolar range (**Figure 23F, table**). Concerning antibody 198, by incubating BKPyV PSVs with supernatants containing antibodies secreted by transfected cells at a 96-well plate scale, we demonstrated that this antibody was also able to broadly neutralize BKPyV in RS cells (**Figure 23E**). However, due to an unknown technical issue when scaling up to 175 cm² flasks, the yield was always less than 10 µg/mL. As a result, we have not so far been able to produce purified 198 for further analysis, including binding avidity measurement and neutralization assay.

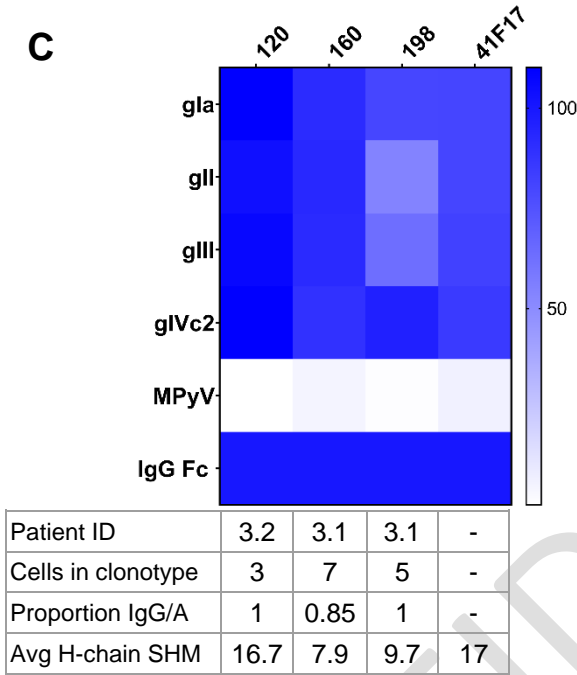
A



B



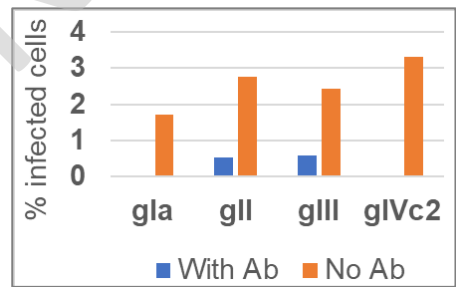
C



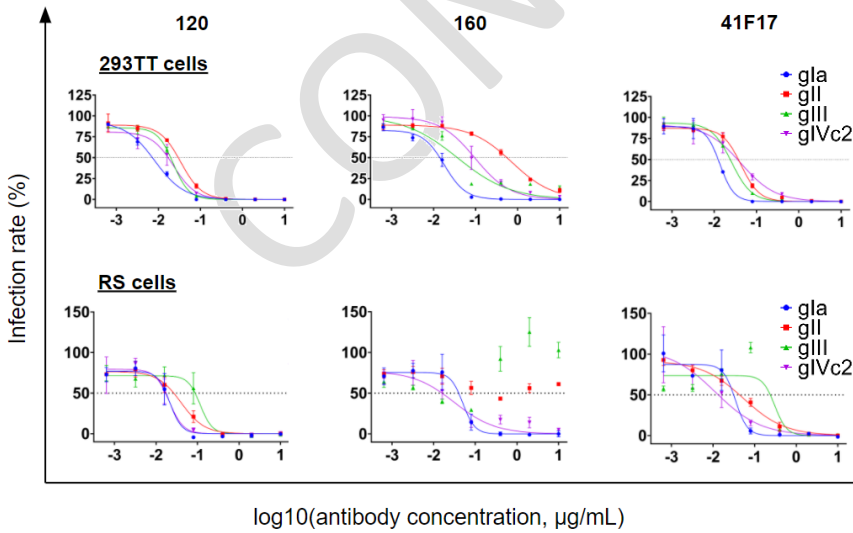
D

	Binding avidity (nM)			
	gl	gll	glll	gIV
120	0.11	0.16	0.21	0.86
160	0.23	0.28	0.17	0.27
198	NA	NA	NA	NA
41F17	0.34	0.15	0.23	3.8

E



F



	IC50 (nM)					
	RS cells			293TT cells		
	120	160	41F17	120	160	41F17
gla	0.14	0.33	0.23	0.05	0.12	0.09
gll	0.27	NA	0.36	0.23	4.86	0.29
glll	0.77	NA	2.03	0.15	0.25	0.17
gIVc2	0.14	0.21	0.08	0.15	0.64	0.28

Figure 23: CDR3 sequence clustering BkPyV-specific IgG and definition of a 41F17-like family of BNAb. (A) NJ cladogram of Kappa light chain SpecB antibodies with at least 5 heavy chain NS mutations, constructed using concatenated heavy and light chain CDR3 amino acid sequences. The 41F17-like cluster is shown in green, and the single red branch shows the 27O24 antibody. (B) Phylogram of antibodies in the 41F17-like cluster, associated with patient ID and antibody isotype, and consensus CDR3 amino acid sequence. (C) Binding properties of 41F17-like antibodies. Heatmap indicates ELISA OD450 values normalized to positive control binding to immobilized anti-IgG Fc antibody. (D) Binding avidity to VLPs measured by SPR. (E) Neutralization properties of antibody 198 in RS cells using antibody-containing supernatant. (F) Neutralization properties of 41F17-like antibodies in RS cells (upper panels), 293TT cells (lower panels) and corresponding IC50 values (table).

CONFIDENTIAL

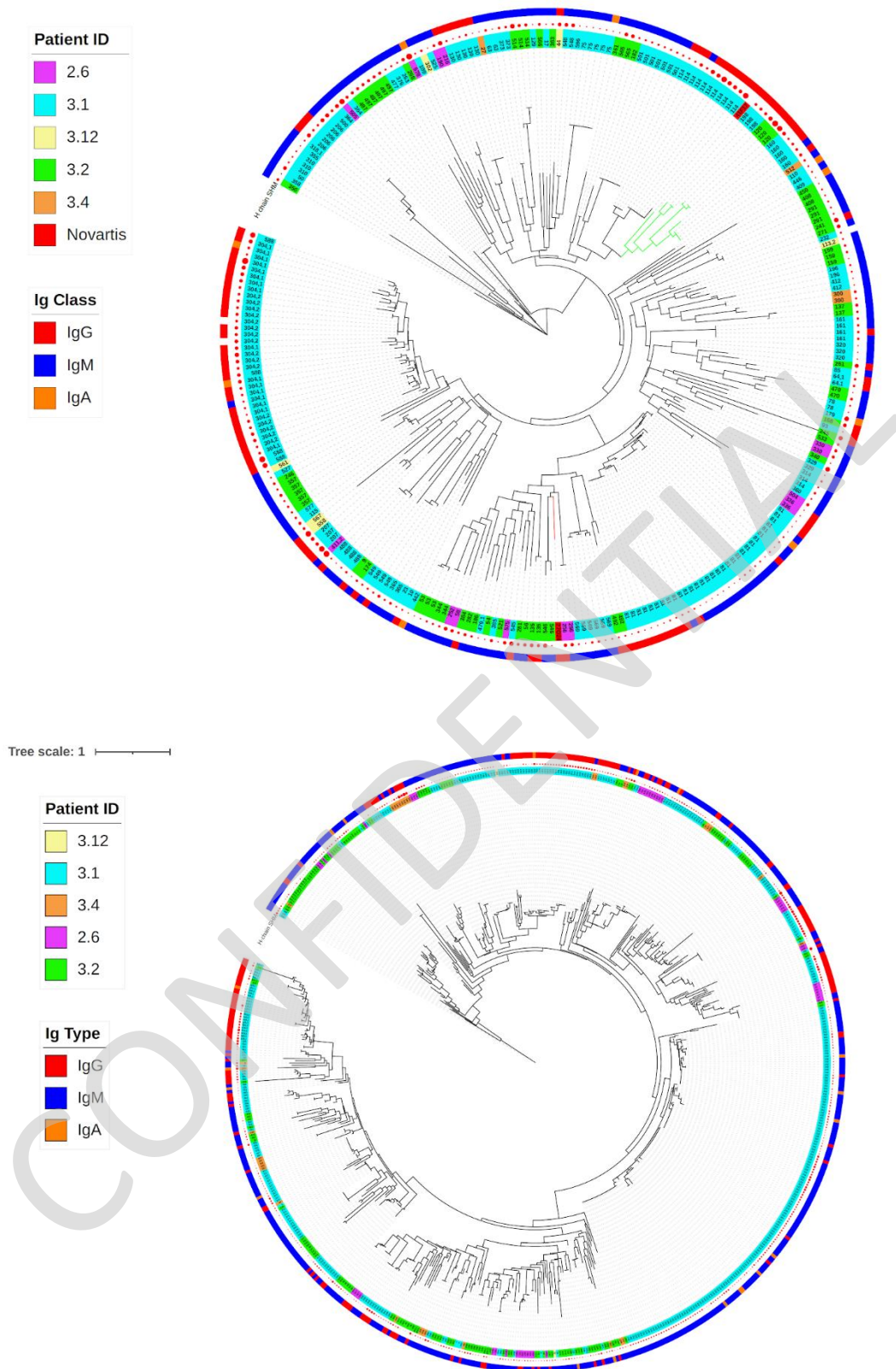


Figure 24: Phylogram of Kappa (upper panel) and Lambda (lower panel) light chain SpecB antibodies. Antibodies with at least 5 heavy chain NS mutations, constructed using concatenated heavy and light chain CDR3 amino acid sequences. Clonotype and patient ID are shown in the first ring, then red circles are proportional to the number of heavy chain NS mutations. The outer ring shows antibody isotype.

Expression & characterization of non-41F17-like antibodies

Apart from the antibody cluster containing 41F17, we also tested nine other candidates that were picked from the SpecB dataset, representing both dominant and minor clones, and clonotypes dominated by either class-switched or IgM antibodies. Five of them (antibodies 152, 81, 488, 336, 438) bound specifically to BKPyV gI VLP, three (antibodies 304, 529, 212) bound to two genotypes, and one (antibody 206) bound to all four genotypes (**Figure 25A**). Preliminary testing of their neutralization properties in 293TT cells using supernatants of transfected cells, showed that the five antibodies that specifically bound to BKPyV gI VLP also specifically neutralized BKPyV gI PSV (**Figure 25B**). The other purified antibodies had diverse neutralizing profiles (**Figure 25D**). Clonotype 206 neutralized gI and gIV PSV, with approximately 100-fold weaker neutralization of gII and gIII; clonotypes 212 and 529 showed preferential neutralization of gI PSV compared to other genotypes; clonotype 304, although derived from a patient with gI BKPyV infection, showed preferential neutralization of gIV PSV. Antibody 152 is the dominant memory IgM clonotype found in patient 3.1. We therefore expressed and tested this antibody as IgM isotype. Similar to IgG 152 (**Figure 25B**), IgM 152 was only able to neutralize BKPyV gI PSV on 293TT cells, and expression as IgM rather than IgG did not appear to enhance its neutralizing potency (**Figure 25C**).

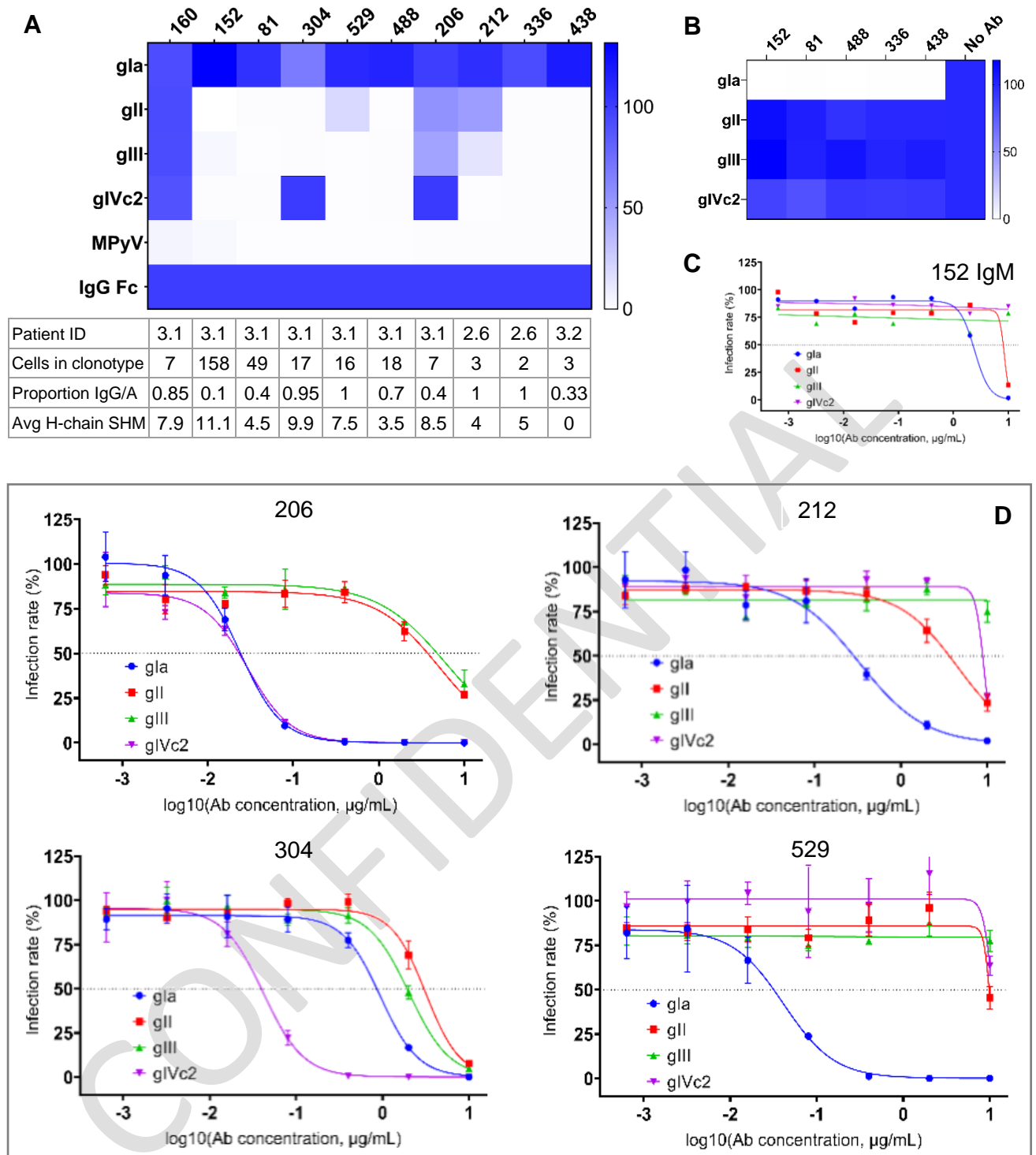


Figure 25: Neutralization properties of non-41F17-like antibodies on 293TT cells.

(A) Binding properties of selected antibodies from the SpecB data set. Heatmap indicates ELISA OD450 values normalized to positive control binding to immobilized anti-IgG Fc antibody. (B) Heatmap indicates percentages of infected cells in the presence of antibodies normalized to positive control without antibodies. Neutralization properties of purified antibody 152 in form of IgM (C) and different purified antibodies (D).

Alanine scanning mutants were introduced into the glb2 wild-type VP1 sequence by site-directed mutagenesis using the Q5 Site-directed mutagenesis kit from New England Biolabs, then mutant VLPs were used to identify sites on the capsid involved in antibody binding (**Figure 26**). Binding of clonotypes 152, 488, 212, 336, 438 and antibody 3.2-1 to genotype I VLP was abrogated by mutations in selected BC-loop amino acids (D60A, E73A, S77A, E82A) that arise frequently in KTx recipients with prolonged BKPyV replication (McIlroy et al., 2020). Binding of clonotypes 120 and 160 was only reduced by the E326A mutation, and no single mutant was found to prevent the binding of clones 81, 529, 206, 198 nor the 41F17 antibody. Titering different concentrations of selected antibodies did not reveal any additional amino-acid residues essential for binding (**Figure 27**).

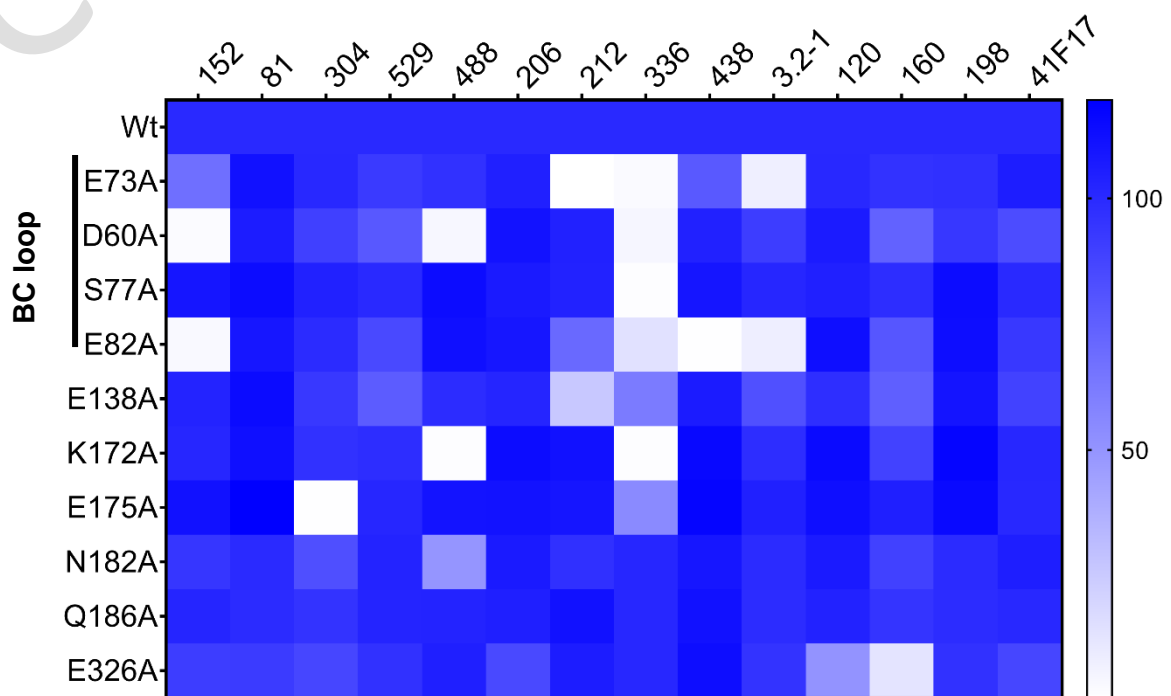


Figure 26: Identification of critical binding residues on the virus capsid by alanine scanning. Binding to different mutant VLPs was measured by ELISA for each monoclonal antibody, as indicated. OD450nm values observed for each mutant were normalized to the value observed for wild-type genotype I VLPs, and visualized as a heatmap.

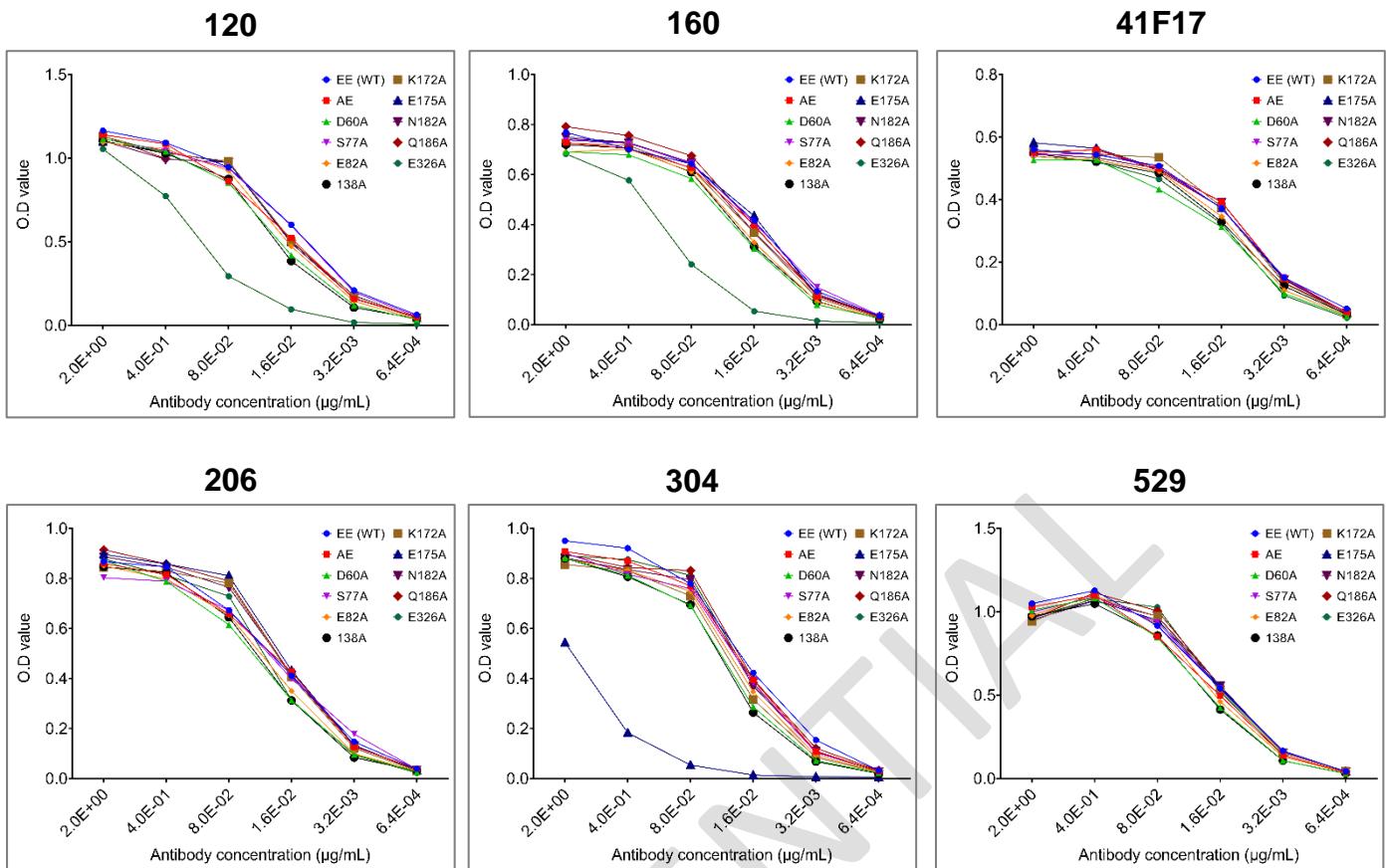


Figure 27: Titration of antibody binding to wild-type and mutant gl BKPv VLP.

Overall, five of the six gl-specific antibodies (152, 488, 336, 438 and 3.2-1) and one of the bi-specific antibodies (212) bound to epitopes that included the BC-loop, confirming the antigenicity of this region of VP1. Binding of antibodies 120 and 160 was weakened by mutation to the E326 residue, which makes up part of the epitope recognized by the 41F17 monoclonal (Lindner et al., 2019). This is consistent with the identification of clonotypes 120 and 160 as “41F17-like” antibodies. No information was found concerning the binding sites of antibodies 81, 529, 206 and 198. However, since the BC-loop was not exhaustively mutated (in particular the K69A mutant was not generated) it is possible that the gl-specific antibody 81 might also make contacts with some BC-loop residues. Furthermore, the D60, Q186 and E326 side chains contribute to the 41F17 epitope (Lindner et al., 2019), but their mutation did not significantly impact binding of the 41F17 antibody to gl VLPs. This shows that a single mutation may not be sufficient to abrogate binding to high-affinity antibodies in an ELISA assay, and either

short deletions or the generation of a limited number of double-mutants may be required to increase the sensitivity of the technique.

In conclusion, we succeeded in isolating and reconstituting BKPyV-specific antibodies from frozen PBMC of kidney transplant patients with high titers of neutralizing antibodies. Among several broadly neutralizing antibodies, clonotype 120 represents a potent monoclonal due to its broad neutralizing activity, which was slightly superior to that observed for the 41F17 antibody. The sequences of antibody 120 together with 160 and 198 are being submitted to the SATT Ouest Valorisation to be patented. The detailed report for patent application is described in part 3 of this section.

CONFIDENTIAL

Human monoclonal antibodies neutralizing the BK polyomavirus

Introduction

The BK polyomavirus (BKPyV) is a small double-stranded DNA virus with a non-enveloped icosahedral capsid, first described in 1971. Four genotypes of BKPyV exist, that are characterized by sequence variation in the major capsid protein VP1, and correspond to distinct neutralizing virus serotypes [1,2]. Genotype I is the most prevalent BKPyV genotype worldwide, followed by genotype IV, while genotypes II and III are rare throughout the world [3]. In structural terms, the virus capsid is composed of 72 pentamers of the major capsid protein VP1, and each pentamer is associated with one copy of either VP2 or VP3, which are the minor capsid proteins. The circular double-stranded DNA genome is packaged inside the capsid in a condensed form associated with histones from the host cell. Importantly, the exterior of the virus particle is composed entirely of the VP1 protein, and virus like particles (VLP) composed of VP1 are structurally and antigenically identical to infectious virus particles [4].

BKPyV is a typical opportunistic virus, which provokes overt pathology almost exclusively in the context of immunosuppression. It is estimated that 80% of the adult population is latently infected with BKPyV. After kidney transplantation (KTx), reactivation of BKPyV from sites of persistent infection (mainly kidney epithelial cells) frequently occurs, leading to virus detection in urine [5]. Overall, 1-10% of KTx patients develop a BK polyomavirus-associated nephropathy (PyVAN), which emerged as an important cause of kidney allograft failure in the late 1990s [6], and remains an important cause of kidney transplant dysfunction [7]. In addition, BKPyV is also responsible for hemorrhagic cystitis (BKPyV-HC), which arises as a complication after 5% to 25% of allogeneic hematopoietic cell transplantations (HCT) [8]. BKPyV has also been associated, less frequently, with pneumonitis, retinitis, and meningoencephalitis in immunocompromised individuals [9].

To date, there is no specific antiviral molecule licensed for the treatment of these infections, as polyomaviruses lack their own polymerase and are entirely dependent on host machinery for their replication. For this reason, the clinical management of PyVAN relies on modification or dose reduction of immunosuppressive therapy, with the aim of inducing host

antiviral immune responses that may then control viral replication. This strategy is applied in the case of histologically confirmed PyVAN (curative treatment), as well as in cases of “presumptive PyVAN”, defined by a high viruria and DNAemia [3]. In BKPyV-HC, symptoms can persist for several weeks in patients with high plasma DNAemia [10], and their resolution is thought to depend on the reconstitution of the BK-specific immune response that follows successful engraftment [11]. In both clinical situations, patients would benefit from effective antiviral therapy.

The incidence of PyVAN is higher in KTx recipients with low neutralizing antibody titres [12], and some studies and case reports have indicated that infusion of intravenous immunoglobulin (IVIG), containing BKPyV-specific neutralizing antibodies [13], can prevent active BKPyV replication in KTx recipients [14], and successfully treat PyVAN [15–17]. Therefore, the existing data indicates that antibody-based therapies may be effective against BKPyV. However, IVIG is a blood product that contains a complex mix of antibody specificities, and although rare, acute antibody-mediated rejection after infusion of IVIG containing donor-specific antibodies has been reported in the literature [18].

Neutralizing monoclonal antibodies could combine the antiviral potency of IVIG in a better characterized product with lower risk of off-target effects. Broadly neutralizing antibodies, capable of inhibiting all four BKPyV genotypes would be good potential candidates for therapeutics for the treatment of PyVAN and/or BKPyV-HC. In the present disclosure, we describe the isolation and characterization of such broadly neutralizing human monoclonal antibodies.

Methods

Labeled and non-labeled BKPyV VLP production

BKPyV virus-liked particles (VLPs) were prepared in HEK 293TT cells (National Cancer Institute (NCI), USA) following the procedure of Pastrana et al. [19] using expression plasmids coding for the major capsid protein of BKPyV genotypes I, II, III and IV (Sequence numbers 1, 2, 3, 4, Table 1) provided by Dr C. Buck (NCI, Bethesda, USA). Mouse polyomavirus (MPyV) VLPs were prepared using an expression plasmid carrying the sequence of MPyV VLP1 (Sequence number 5, Table 1). VP1 protein content of purified VLPs was validated by SDS-PAGE.

For measurements of antibody binding by ELISA and surface plasmon resonance,

unlabeled VLPs were used. For the specific labeling of B-cells carrying antibodies specific for BKPyV, genotype I VLPs were covalently labeled with Alexa Fluor 555 (AF555) or Alexa Fluor 647 (AF647).

Patient Samples

Cryopreserved peripheral blood mononuclear cells (PBMC) from six adult kidney transplant patients were used for the isolation of BKPyV-specific B-cells. These patients were included in a prospective observational study at the CHU Hotel Dieu Hospital, Nantes, approved by the local ethics committee and declared to the French Commission Nationale de l'Informatique et des Libertés (CNIL, n°1600141). All patients gave informed consent authorizing the use of archived urine and blood samples for research purposes.

All of six patients in this study were diagnosed with BKPyV reactivation based on the detection of viruria $>10^7$ copies/mL and viremia $>10^3$ copies/mL, and had a documented increase in serum neutralizing titer of more than 1 log₁₀, indicating that the humoral response had been mobilized in these patients.

Isolation of BKPyV-specific B cells and antibody sequencing

PBMC were thawed, B-cells were enriched using the human B cell isolation kit II (Miltenyi Biotech) according to the manufacturer's instructions, then labeled with the following anti-human antibodies: anti-CD3-BV510 (Becton-Dickinson), anti-CD19-BV421 (Becton-Dickinson), BKPyV-gI-VLP-AF555, BKPyV-gI-VLP-AF647, and Hashtag-oligonucleotide antibodies (BioLegend). CD19⁺AF555⁺AF647⁺ B-cells were sorted using a BD Aria cell sorter, then either processed as single sorted cells, or loaded directly onto a 10x Genomics Chromium A Chip. CDNA banks were prepared using the 10X Genomics Chromium Single Cell 5' Library & Gel Bead kit; 10x Chromium Single Cell 5' Library Construction kit; 10x Chromium Single Cell 5' Feature Barcode Library kit; 10x Chromium Single Cell V(D)J Enrichment kit, Human B Cell; 10x Chromium Single Cell A Chip kit and 10x Chromium i7 Multiplex kit according to the manufacturer's protocols. Three libraries were prepared separately, including V(D)J enriched library, 5' gene expression library and 5' cell surface protein library. Libraries were quantified and verified using the Quantus instrument (Promega) then pooled and sequenced using NextSeq500 system. Data were analyzed using the 10x Genomics VDJ browser, then the Immunarch package in R (<https://immunarch.com/>).

Cloning, expression and purification of monoclonal antibodies

The selected paired immunoglobulin variable heavy (vH) and light chain (vL) sequences

were sent to Eurofins Genomics for gene synthesis, then cloned into expression vectors containing constant regions of heavy chain (C γ 1 of IgG1) and light kappa chain (C κ) or light lambda chain (C λ). Cloned expression vectors were confirmed by Sanger sequencing, then plasmid DNA was transfected into HEK 293A cells (Thermo Fisher). After initial screening for BKPyV specificity, confirmed antibodies were scaled up for production and purification. Briefly, the day before transfection, 6×10^6 HEK 293A cells were seeded into 75 cm² flasks containing 25 mL DMEM supplemented with 1% Glutamax and 10% FBS. The following day, 10 μ g of vH and 10 μ g of vL expression vectors were diluted in 500 μ L of 150 mM NaCl, then mixed with 40 μ L of transfection reagent jetPEI (Polyplus) diluted in 450 μ L of 150 mM NaCl. After 15 min incubation at room temperature, the complex was gently added onto pre-plated 293A cells. 16h post transfection, medium was replaced with serum-free Pro293a medium (Lonza Bioscience) and cultured for 5 days at 37°C in a humidified 5% CO₂ incubator, and antibodies.

Antibodies were purified using a 1 mL HiTrap rProtein A Fast Flow column (Sigma-Aldrich) on a fast protein liquid chromatography (FPLC) system (Bio-Rad) at 4°, and antibody purity was controlled by size-exclusion chromatography using Superdex200 Increase 10/300 GL column (GE Healthcare) following the manufacturer's instructions. Purified, filter-sterilized antibodies were used in the following analyses.

ELISA screening

Nunc MaxiSorp 96-well plates (Sigma) were coated with 50 ng of BKPyV VLPs in 50 μ L PBS at 37°C overnight, then blocked with 5% powdered milk in PBS buffer for 1h. Purified antibodies were assayed at 4-fold serial dilutions, starting at 10 μ g/mL in 50 μ L blocking buffer. Antibodies bound to VLPs were detected using goat anti-human IgG horseradish peroxidase-conjugated secondary antibody (Bethyl) diluted 1:5000 in blocking buffer, with washes in PBS 0.05% Tween-20 between each step. 50 μ L TMB substrate was added and the reaction was stopped by adding 50 μ L 0.5M H₂SO₄. Absorbance was read at 450 nm in a TECAN plate reader. The effective concentration 50% (EC₅₀) was calculated using GraphPad Prism software.

Neutralization assays

Pseudovirus BKPyV (PSV) particles for different BKPyV genotypes were prepared following the procedure of Pastrana et al. [16] using expression plasmids coding for the major capsid protein of BKPyV genotypes I, II, III and IV (Seq 1, 2, 3, 4, Table 1) provided by Dr C.

Buck (NCI, Bethesda, USA), the ph2b and ph3b plasmids (Addgene) coding for the minor capsid proteins VP2 and VP3, and the pEGFP-N1 plasmid (Clontech) as a reporter gene. Purified PSV were quantified by qPCR specific for the packaged pEGFP-N1 plasmid, and expressed as number of plasmid copies per μL .

For neutralization assays, 293TT and RS (Evercyte, Vienna) cells were seeded in flat bottom 96-well plates (BD Falcon) then allowed to attach at 37°C for at least one hour. In parallel, BKPyV PSV were prepared at a dose of 5×10^6 EGFP-N1 copies/well for RS cells and 2×10^6 EGFP-N1 copies/well for 293TT cells. Each antibody was added to PSV in serial 5-fold dilutions starting at $5 \mu\text{g}/\text{mL}$. IgG-PSV mixes were incubated at 4°C for 1h, then added onto plated 293T or RS cells. Plates were kept in a humidified 5% CO_2 incubator at 37°C for 72h (293TT cells), or 96 hours (RS cells), then fixed and counterstained with $10 \mu\text{g}/\text{mL}$ Hoechst 33342 before quantifying the number and percentage of GFP^+ cells using a Cellomics ArrayScan VTI HCS Reader (Thermo Scientific). Neutralization curves were constructed by normalizing to the percentage of GFP^+ cells observed in the absence of antibody, and IC50 values for neutralization were calculated using GraphPad Prism software.

Monoclonal antibody binding avidity measurement

The binding strength and kinetics of produced BKPyV-specific antibodies to each BKPyV VLP genotype were assessed using surface plasmon resonance (SPR). Briefly, anti-IgG antibody diluted to $20 \mu\text{g}/\text{mL}$ in sodium acetate buffer pH 5.0 was immobilized to a CM5 sensor chip (GE Healthcare) until the SPR signal reached 10.000 response units (RUs) using a Biacore T200 (GE Healthcare). BKPyV-specific monoclonal antibodies were then captured at 50 nM concentration. Different BKPyV VLPs including genotype Ia, II, III and IVc2 were injected with a series of 3-fold dilutions from 6 nM to 500 nM. Kinetic parameters and avidity were determined by non-linear regression analysis using Biacore Evaluation software.

Results

Sequences of antigens and antibodies

Table 1. BKPyV VP1 sequences

Sequence number	Designation	Sequence
1	BKPyV VP1 genotype I	MAPTKRKGECPGAAPKKPKPEPVQVPKLLIKGGVEVLEVKTGVDVAITEVECF LNPEMGDPDENLRGFSKLKLSAENDFSSDSPERKMLPCYSTARIPLPNLNED LTCGNLLMWEAVTVQTEVIGITSMNLNHAGSQKVHEHGGGKPIQGSNFHFF AVGGDPLEMQGVLNMYRTKYPDGTITPKNPTAQSQVMNTDHKAYLDKNNAY PVECWVPDPSRNENTRYFGTFTGGENVPPVLHVNTNTATTVLLDEQGVGPLC KADSLYVSAADICGLFTNSSGTQQWRGLARYFKIRLRKRSVKNPYPISFLL SDLINRRTQRVDGQPMYGMESQVEEVRVFDGTERLPGDPDMIRYIDKQGQL QTKML
2	BKPyV VP1 genotype II	MAPTKRKGECPGAAPKKPKPEPVQVPKLLIKGGVEVLEVKTGVDVAITEVECF LNPEMGDPDNDLRGYSKLKTAENAFSDSDPKKMLPCYSTARIPLPNLNED LTCGNLLMWEAVTVKTEVIGITSMNLNHAGSQKVHENGGGKPVQGSNFHFF AVGGDPLEMQGVLNMYRTKYPQGTITPKNPTAQSQVMNTDHKAYLDKNNAY PVECWIPDPSRNENTRYFGTYTGGENVPPVLHVNTNTATTVLLDEQGVGPLC KADSLYVSAADICGLFTNSSGTQQWRGLARYFKIRLRKRSVKNPYPISFLL SDLINRRTQKVDGQPMYGMESQVEEVRVFDGTEQLPGDPDMIRYIDRQGQL QTKMV
3	BKPyV VP1 genotype III	MAPTKRKGECPGAAPKKPKPEPVQVPKLLIKGGVEVLEVKTGVDVAITEVECF LNPEMGDPDDHLRGYSQHLTAENAFSDSDPKKMLPCYSTARIPLPNLNED LTCGNLLMWEAVTVKTEVIGITSMNLNHAGSQKVHENGGGKPVQGSNFHFF AVGGDPLEMQGVLNMYRTKYPQGTITPKNPTAQSQVMNTDHKAYLDKNNAY PVECWIPDPSKNENTRYFGTYTGGENVPPVLHVNTNTATTVLLDEQGVGPLC KADSLYVSAADICGLFTNSSGTQQWRGLARYFKIRLRKRSVKNPYPISFLL SDLINRRTQKVDGQPMYGMESQVEEVRVFDGTEQLPGDPDMIRYIDRQGQL QTKMV
4	BKPyV VP1 genotype IV	MAPTKRKGECPGAAPKKPKPEPVQVPKLLIKGGVEVLEVKTGVDVAITEVECF LNPEMGDPDNDLRGYSRLRTAETAFAFSDSDPDRKMLPCYSTARIPLPNLNED LTCGNLLMWEAVTVKTEVIGITSMNLNHAGSQKVHENGGGKPIQGSNFHFF AVGGDPLEMQGVLNMYRTKYPEGTVTPKNPTAQSQVMNTDHKAYLDKNNAY PVECWIPDPSKNENTRYFGTYTGGENVPPVLHVNTNTATTVLLDEQGVGPLC KADSLYVSAADICGLFTNSSGTQQWRGLPRYFKIRLRKRSVKNPYPISFLL SDLINRRTQRVDGQPMYGMESQVEEVRVFDGTEQLPGDPDMIRYIDRQGQL QTKMV
5	MPyV VP1	MAPKRKSGVSKCETKCTKACPRPAPVPKLLIKGGMEVLDLVTGPDSVTEIE AFLNPRMGQPPTPESLTEGGQYYGWSRGINLATSDETDSPENNTLPTWSMA KLQLPMLNEDLTCDTLQMWAEVSVKTEVVGSGSLLDVHGFNKPTDVTNTKG ISTPVEGSQYHVFVAVGGEPLDLQGLVTDARTKYKEEGVVTIKTITKKDMVN KDQVLNPI SKAKLDKGMYPVEIWHPPAKNENTRYFGNYTGGTTTTPPVLQ FTNTLTTLVLLDENGVGPLCKGEGLYLSCVDIMGWRVTRNYDVHHRGLPRY FKITLRKRWVKNPYPMASLISSLFNNMLPQVQGPMEGENTQVEEVRVYDG TEPVPDPDMTRYVDRFGKTKTVFPGN

Table 2 BKPyV-specific antibody sequences

BK160-1		
Sequence number	Designation	Sequence
6	HCDR1 (IMGT)	GGSISSYY
7	HCDR2 (IMGT)	IYYSGST
8	HCDR3 (IMGT)	ARGRYGGYGGQSFY
9	VH	QRQLQESGPGVPQSETLSLTCTVSGGSISTSSYYWGWIRQPPGKGLELIG TIYYSGSTYYNPSLKSRTISVDTSKNQFSLKLRVTAADTAVYYCARGRG YGGYGGQSFYWGQGLTVTVSS
10	Heavy Chain	QRQLQESGPGVPQSETLSLTCTVSGGSISTSSYYWGWIRQPPGKGLELIG TIYYSGSTYYNPSLKSRTISVDTSKNQFSLKLRVTAADTAVYYCARGRG YGGYGGQSFYWGQGLTVTVSSASTKGPSVFLAPSSKSTSGGTAALGCLV KDYFPEPVTVSWNSGALTSVHTFPAVLQSSGLYSLSSVTVPSSSLGTQT YICNVNHKPSNTKVDKKEPKSCDKTHTCPPCPAPELLGGPSVFLFPPKPK DTLMI SRTPEVTCVVVDVSHEDPEVKFNWYVDGVEVHNAKTKPREEQYNST YRVVSVLTVLHQDWLNGKEYKCKVSNKALPAPIEKTISKAKGQPREPQVY LPPSRDELTKNQVSLTCLVKGFYPSDIAVEWESNGQPENNYKTTTPVLDSD GSFFLYSKLTVDKSRWQQGNVFCFSVMHEALHNHYTQKLSLSLSPGK*
11	DNA VH	CAGCGGCAGCTGCAGGAGTCGGGCCAGGACCGGTGCAGCCTTCGGAGACC CTGTCCCTCACCTGCACGTCTCTGGTGGCTCCATCAGCACTAGTAGTTAC TACTGGGGCTGGATCCGCCAGCCCCAGGGAAGGGGCTGGAGTTGATTGGG ACTATTTATTATAGTGGGAGCACCTACTACAACCCGTCCTCAAGAGTCGA GTCACCATTTCCGTAGACACGTCCAAGAACCAGTTCTCCCTGAAGCTGAGA TCTGTGACCGCCGCAGACACGGCTGTATATTACTGTGCGAGAGGACGTGGA TATGGTGGCTACGGGGCCAATCCTTTGACTACTGGGGCCAGGGAACCCTG GTCACCCTCTCCTCA
12	DNA Heavy Chain	CAGCGGCAGCTGCAGGAGTCGGGCCAGGACCGGTGCAGCCTTCGGAGACC CTGTCCCTCACCTGCACGTCTCTGGTGGCTCCATCAGCACTAGTAGTTAC TACTGGGGCTGGATCCGCCAGCCCCAGGGAAGGGGCTGGAGTTGATTGGG ACTATTTATTATAGTGGGAGCACCTACTACAACCCGTCCTCAAGAGTCGA GTCACCATTTCCGTAGACACGTCCAAGAACCAGTTCTCCCTGAAGCTGAGA TCTGTGACCGCCGCAGACACGGCTGTATATTACTGTGCGAGAGGACGTGGA TATGGTGGCTACGGGGCCAATCCTTTGACTACTGGGGCCAGGGAACCCTG GTCACCCTCTCCTCAGCCTCGACCAAGGGCCCATCGGTCTTCCCCCTGGCA CCCTCCTCCAAGAGCACCTCTGGGGGCACAGCGGCCCTGGGCTGCCTGGTC AAGGACTACTTCCCCGAACCTGTGACGGTCTCGTGGAACTCAGGCGCCCTG ACCAGCGGCGTGACACCTTCCCGGCTGTCTACAGTCTCAGGACTCTAC TCCCTCAGCAGCGTGGTGACCGTGCCCTCCAGCAGCTTGGGCACCCAGACC TACATCTGCAACGTGAATCACAAGCCAGCAACACCAAGGTGGACAAGAAA GTTGAGCCAAATCTTGTGACAAAACCTCACACATGCCACCCGTGCCAGCA CCTGAACTCCTGGGGGGACCGTCAGTCTTCCCTCTTCCCCCAAACCCAAG GACACCTCATGATCTCCCGGACCCCTGAGGTACATGCGTGGTGGTGGAC GTGAGCCACGAAGACCCCTGAGGTCAAGTTCAACTGGTACGTGGACGGCGTG GAGGTGCATAATGCCAAGACAAAGCCGCGGGAGGAGCAGTACAACAGCACG TACCGTGTGGTCAGCGTCTCACCCTTGCACCAAGGCTGACCTGATGGC AAGGAGTACAAGTGAAGGTCTCCAACAAGCCCTCCAGCCCCCAATCGAG AAAACCATCTCCAAGCCAAAGGGCAGCCCCGAGAACCACAGGTGTACACC CTGCCCCATCCCGGATGAGCTGACCAAGAACCAGGTGAGCCTGACCTGC CTGGTCAAAGGCTTCTATCCAGCGACATCGCCGTGGAGTGGGAGAGCAAT GGGCAGCCGGAGAACAACCTACAAGACCACGCCTCCCGTGTGGACTCCGAC GGCTCCTTCTCCTCTACAGCAAGCTCACCGTGGACAAGAGCAGGTGGCAG

		CAGGGGAACGTCTTCTCATGCTCCGTGATGCATGAGGCTCTGCACAACCAC TACACGCAGAAGAGCCTCTCCCTGTCTCCGGGTAAATGA
13	LCDR1 (IMGT)	QSVSSS
14	LCDR2 (IMGT)	DAS
15	LCDR3 (IMGT)	QQRSNWPPSIT
16	VL	EIVLTQSPASLSLSPGERATLSCRASQSVSSSLAWYQQKPGRAPRLLIYDA SNRASGIPARFSGSGSGTDFTLTISSLEPEDFAVYYCQQRSNWPPSITFGQ GTRLVIK
17	Light Chain	EIVLTQSPASLSLSPGERATLSCRASQSVSSSLAWYQQKPGRAPRLLIYDA SNRASGIPARFSGSGSGTDFTLTISSLEPEDFAVYYCQQRSNWPPSITFGQ GTRLVIKRTVAAPSVFIFPPSDEQLKSGTASVVCLLNNFYPREAKVQWKVD NALQSGNSQESVTEQDSKDYSLSTLTLSKADYEKHKVYACEVTHQGLS SPVTKSFNRGEC*
18	DNA VL	GAAATTGTGTTGACACAGTCTCCAGCCTCCCTGTCTTTGTCTCCAGGGGAA AGAGCCACCTCTCCTGCAGGGCCAGTCAGAGTGTTAGCAGCTCCTTAGCC TGGTACCAACAGAAACCTGGCCGGGCTCCCAGGCTCCTCATCTATGATGCA TCCAACAGGGCCTCTGGCATCCCAGCCAGGTTAGTGGCAGTGGGTCTGGG ACAGACTTCACTCTCACCATCAGCAGCCTAGAGCCTGAAGATTTTGCAGTT TATTACTGTCAGCAGCGTAGCAACTGGCCTCCCTCGATCACCTTCGGCCAA GGGACACGACTGGTGATTAAC
19	DNA Light Chain	GAAATTGTGTTGACACAGTCTCCAGCCTCCCTGTCTTTGTCTCCAGGGGAA AGAGCCACCTCTCCTGCAGGGCCAGTCAGAGTGTTAGCAGCTCCTTAGCC TGGTACCAACAGAAACCTGGCCGGGCTCCCAGGCTCCTCATCTATGATGCA TCCAACAGGGCCTCTGGCATCCCAGCCAGGTTAGTGGCAGTGGGTCTGGG ACAGACTTCACTCTCACCATCAGCAGCCTAGAGCCTGAAGATTTTGCAGTT TATTACTGTCAGCAGCGTAGCAACTGGCCTCCCTCGATCACCTTCGGCCAA GGGACACGACTGGTGATTAACCGTACGGTGGCTGCACCATCTGTCTTCAT CTTCCC GCCATCTGATGAGCAGTTGAAATCTGGAAGTGCCTCTGTTGTGTG CCTGCTGAATAACTTCTATCCCAGAGAGGCCAAAGTACAGTGGAAAGGTGGA TAACGCCCTCCAATCGGGTAACCTCCAGGAGAGTGTACAGAGCAGGACAG CAAGGACAGCACCTACAGCCTCAGCAGCACCTGACGCTGAGCAAAGCAGA CTACGAGAAACAAAAGTCTACGCCTGCGAAGTACCCATCAGGGCCTGAG CTCGCCCGTCAAAAAGAGCTTCAACAGGGGAGAGTGTTAG

BK206		
Sequence number	Designation	Sequence
20	HCDR1 (IMGT)	GGSISSGSYY
21	HCDR2 (IMGT)	IHYSGST
22	HCDR3 (IMGT)	ARQRVGRNYDILTGYL
23	VH	QLQLQESGPGPLVKPPETLSLTCTVSGGSISSGSYYWGWIRQPPGKGLEWIG SIHYSGSTYYSPSLKSRVTISVDTSKNQFSLKVYSVTAADTAVYYCARQRV GRNYDILTGYLFGQGLTVTVSS
24	Heavy Chain	QLQLQESGPGPLVKPPETLSLTCTVSGGSISSGSYYWGWIRQPPGKGLEWIG SIHYSGSTYYSPSLKSRVTISVDTSKNQFSLKVYSVTAADTAVYYCARQRV GRNYDILTGYLFGQGLTVTVSSASTKGPSVFLAPSSKSTSGGTAALGCLV KDYFPEPVTVSWNSGALTSVHTFPAVLQSSGLYSLSSVTVPSSSLGTQT YICNVNHKPSNTKVDKKEPKSCDKTHTCPPCPAPELLGGPSVFLFPPKPK DTLMI SRTPEVTCVVVDVSHEDPEVKFNWYVDGVEVHNAKTKPREEQYNST YRVVSVLTVLHQDWLNGKEYKCKVSNKALPAPIEKTISKAKGQPREPQVY TLPSSRDELTKNQVSLTCLVKGFYPSDIAVEWESNGQPENNYKTTTPVLDSD GSFFLYSKLTVDKSRWQQGNV FSCSV MHEALHNHYTQKLSLSLSPGK*
25	DNA VH	CAACTGCAGCTGCAGGAGTCGGGCCAGGACTGGTGAAGCCTCCGGAGACC CTGTCCCTCACCTGCACGTCTCTGGTGGCTCCATCAGCAGTGGAAGTTAC TACTGGGGCTGGATCCGCCAGCCCCAGGGAAGGGGCTTGAGTGGATTGGG AGTATCCATTACAGTGGGAGCACCTACTACAGCCCGTCCCTCAAGAGTCGA GTCACCATATCCGTAGACACGTCCAAGAACCAGTTCTCCCTGAAGGTGTAC TCTGTGACCGCCGACACACGGCTGTGTATTACTGTGCGAGACAGCGTGTG GGCGGAATTACGATATTTTGACTGGTTATCTCTTTGGCCAGGGAACCCTG GTCACCGTCTCCTCA
26	DNA Heavy Chain	CAACTGCAGCTGCAGGAGTCGGGCCAGGACTGGTGAAGCCTCCGGAGACC CTGTCCCTCACCTGCACGTCTCTGGTGGCTCCATCAGCAGTGGAAGTTAC TACTGGGGCTGGATCCGCCAGCCCCAGGGAAGGGGCTTGAGTGGATTGGG AGTATCCATTACAGTGGGAGCACCTACTACAGCCCGTCCCTCAAGAGTCGA GTCACCATATCCGTAGACACGTCCAAGAACCAGTTCTCCCTGAAGGTGTAC TCTGTGACCGCCGACACACGGCTGTGTATTACTGTGCGAGACAGCGTGTG GGCGGAATTACGATATTTTGACTGGTTATCTCTTTGGCCAGGGAACCCTG GTCACCGTCTCCTCAGCCTCGACCAAGGGCCCATCGGTCTTCCCCCTGGCA CCCTCCTCCAAGAGCACCTCTGGGGGCACAGCGGCCCTGGGCTGCCTGGTC AAGGACTACTTCCCCGAACCTGTGACGGTCTCGTGGAACCTCAGGCGCCCTG ACCAGCGGCGTGACACCTTCCCGGCTGTCTACAGTCTCAGGACTCTAC TCCCTCAGCAGCGTGGTGACCGTGCCCTCCAGCAGCTTGGGCACCCAGACC TACATCTGCAACGTGAATCACAAGCCCAGCAACACCAAGGTGGACAAGAAA GTTGAGCCCAAATCTTGTGACAAAACACACATGCCACCGTGCCAGCA CCTGAACTCCTGGGGGACCGTCAGTCTTCCTCTTCCCCCAAACCCAAG GACACCCTCATGATCTCCCGGACCCCTGAGGTACATGCGTGGTGGTGGAC GTGAGCCACGAAGACCCTGAGGTCAAGTTCAACTGGTACGTGGACGGCGTG GAGGTGCATAATGCCAAGACAAAGCCGCGGGGAGGAGCAGTACAACAGCACG TACCGTGTGGTCAGCGTCTCACCCTCCTGCACCAGGACTGGCTGAATGGC AAGGAGTACAAGTGCAAGGTCTCCAACAAGCCCTCCAGCCCCCATCGAG AAAACCATCTCAAAGCCAAAGGGCAGCCCCGAGAACCACAGGTGTACACC CTGCCCCATCCCGGATGAGCTGACCAAGAACCAGGTGACCGTGTACCTGC CTGGTCAAAGGCTTCTATCCCAGCGACATCGCCGTGGAGTGGGAGGCAAT GGGCAGCCGGAGAACAACACAAGACCACGCCTCCCGTGTGACTCCGAC GGCTCCTTCTTCTTACAGCAAGCTCACCCTGGACAAGAGCAGGTGGCAG CAGGGGAACGTCTTCTCATGCTCCGTGATGCATGAGGCTCTGCACAACCAC TACACGCAGAAGAGCCTCTCCCTGTCTCCGGGTAATGA

27	LCDR1 (IMGT)	QSLLRNGYNY
28	LCDR2 (IMGT)	LGS
29	LCDR3 (IMGT)	MQALRTPHT
30	VL	DIVMTQSPLSLPVTPEGEPASISCRSSQSLLRNGYNYLDWYLQKPRQSPQL LIYLGSNRASGVPDRFSGSGSGTDFTLKISRVEAEDVGVYYCMQALRTPHT FGQGTKLEIK
31	Light Chain	DIVMTQSPLSLPVTPEGEPASISCRSSQSLLRNGYNYLDWYLQKPRQSPQL LIYLGSNRASGVPDRFSGSGSGTDFTLKISRVEAEDVGVYYCMQALRTPHT FGQGTKLEIKRTVAAPSVFIFPPSDEQLKSGTASVVCLLNNFYPREAKVQW KVDNALQSGNSQESVTEQDSKSTYLSSTLTLSKADYEKHKVYACEVTHQ GLSSPVTKSFNRGEC*
32	DNA VL	GATATTGTGATGACTCAGTCTCCACTCTCCCTGCCCGTCACCCCTGGAGAG CCGGCCTCCATTTCCCTGCAGGTCTAGTCAGAGCCTCCTGCATAGAAATGGA TACAACATTTGGATTGGTACCTGCAGAAGCCACGGCAGTCTCCACAGCTC CTGATCTATTTGGGTTCTAATCGGGCCTCCGGGGTCCCTGACAGGTTTCAGT GGCAGTGGATCAGGCACAGATTTTACACTGAAAATCAGCAGAGTGGAGGCT GAGGATGTTGGGGTTTATTACTGCATGCAAGCTCTACGAACTCCTCATACT TTTGGCCAGGGGACCAAGCTGGAGATCAAAC
33	DNA Light Chain	GATATTGTGATGACTCAGTCTCCACTCTCCCTGCCCGTCACCCCTGGAGAG CCGGCCTCCATTTCCCTGCAGGTCTAGTCAGAGCCTCCTGCATAGAAATGGA TACAACATTTGGATTGGTACCTGCAGAAGCCACGGCAGTCTCCACAGCTC CTGATCTATTTGGGTTCTAATCGGGCCTCCGGGGTCCCTGACAGGTTTCAGT GGCAGTGGATCAGGCACAGATTTTACACTGAAAATCAGCAGAGTGGAGGCT GAGGATGTTGGGGTTTATTACTGCATGCAAGCTCTACGAACTCCTCATACT TTTGGCCAGGGGACCAAGCTGGAGATCAAACCGTACGGTGGCTGCACCATC TGTCTTCATCTTCCCGCCATCTGATGAGCAGTTGAAATCTGGAAGTGCCTC TGTGTGTGCTGCTGAATAACTTCTATCCCAGAGAGGCCAAAGTACAGTG GAAGGTGGATAACGCCCTCCAATCGGGTAACTCCCAGGAGAGTGTACACAGA GCAGGACAGCAAGGACAGCACCTACAGCCTCAGCAGCACCTGACGCTGAG CAAAGCAGACTACGAGAAACACAAAGTCTACGCCTGCGAAGTCAACCATCA GGCCTGAGCTCGCCCGTCACAAAGAGCTTCAACAGGGGAGAGTGTTAG

BK120		
Sequence number	Designation	Sequence
34	HCDR1 (IMGT)	GGSVSTNSYY
35	HCDR2 (IMGT)	IYYNGKT
36	HCDR3 (IMGT)	ARGTAAGTGYGAGSFGY
37	VH	QVQLQESGPGLVKPSSETLSLTCIVSGGSVSTNSYYWSWIRQPPGKGLECVG YIYYNGKTNYNPSLKGKRVMSLDTSRNQFSLKLTSVTAADTAVYYCARGTA AGTGYGAGSFGYWGQGSGLVTVSS
38	Heavy Chain	QVQLQESGPGLVKPSSETLSLTCIVSGGSVSTNSYYWSWIRQPPGKGLECVG YIYYNGKTNYNPSLKGKRVMSLDTSRNQFSLKLTSVTAADTAVYYCARGTA AGTGYGAGSFGYWGQGSGLVTVSSASTKGPSVFLAPSSKSTSGGTAALGCL VKDYFPEPVTVSWNSGALTSVHTFPAVLQSSGLYSLSSVTVPPSSSLGTQ TYICNVNHKPSNTKVDKKEPKSCDKHTHTCPPAPPELLGGPSVFLFPPKQ KDTLMI SRTPEVTCVVDVSHEDPEVKFNWYVDGVEVHNAKTKPREEQYNS TYRVVSVLTVLHQDWLNGKEYKCKVSNKALPAPIEKTI SKAKGQPREPQVY TLPPSRDELTKNQVSLTCLVKGFYPSDIAVEWESNGQPENNYKTTTPVLDLDS DGSFFLYSKLTVDKSRWQQGNVFCFSVMHEALHNHYTQKSLSLSPGK*
39	DNA VH	CAGGTGCAGCTGCAGGAGTCGGGCCAGGACTGGTGAAGCCTTCGGAGACC CTGTCCCTCACCTGCATTGTCTCTGGTGGCTCCGTCAGCACTAATAGTTAC TATTGGAGCTGGATCCGTCAGCCCCAGGGAAGGGACTGGAGTGTGTTGGC TATATCTATTACAATGGGAAAACCAACTACAATCCCTCCCTCAAGGGCCGA GTCTCCATGTCACTAGACACGTCCAGGAACCAGTTCTCCCTGAAGCTGACG TCTGTTACCGCTGCGGACACGGCCGTTTATTACTGTGCGAGAGGCACGGCG GCCGGTACGGGCTATGGTGCAGGGGAGTTTTGGCTACTGGGGCCAGGGATCC CTGGTCACCGTCTCCTCA
40	DNA Heavy Chain	CAGGTGCAGCTGCAGGAGTCGGGCCAGGACTGGTGAAGCCTTCGGAGACC CTGTCCCTCACCTGCATTGTCTCTGGTGGCTCCGTCAGCACTAATAGTTAC TATTGGAGCTGGATCCGTCAGCCCCAGGGAAGGGACTGGAGTGTGTTGGC TATATCTATTACAATGGGAAAACCAACTACAATCCCTCCCTCAAGGGCCGA GTCTCCATGTCACTAGACACGTCCAGGAACCAGTTCTCCCTGAAGCTGACG TCTGTTACCGCTGCGGACACGGCCGTTTATTACTGTGCGAGAGGCACGGCG GCCGGTACGGGCTATGGTGCAGGGGAGTTTTGGCTACTGGGGCCAGGGATCC CTGGTCACCGTCTCCTCAGCCTCGACCAAGGGCCCATCGGTCTTCCCCCTG GCACCTCCTCCAAGAGCACCTCTGGGGGCACAGCGGCCCTGGGCTGCCTG GTCAAGGACTACTTCCCCGAACCTGTGACGGTCTCGTGGAACCTCAGGCGCC CTGACCAGCGGCTGCACACCTTCCCGGCTGTCTACAGTCTCAGGACTC TACTCCCTCAGCAGCGTGGTGACCGTGCCCTCCAGCAGCTTGGGCACCCAG ACCTACATCTGCAACGTGAATCACAAGCCCAGCAACACCAAGGTGGACAAG AAAGTTGAGCCCAAATCTTGTGACAAAACCTCACACATGCCACCGTGCCCA GCACCTGAACCTCCTGGGGGACCGTCAGTCTTCTCTTCCCCCAAACCC AAGGACACCCTCATGATCTCCCGGACCCCTGAGGTACATGCGTGGTGGTG GACGTGAGCCACGAAGACCCTGAGGTCAAGTTCAACTGGTACGTGGACGGC GTGGAGGTGCATAATGCCAAGACAAAGCCGCGGGAGGAGCAGTACAACAGC ACGTACCGTGTGGTCAGCGTCTCACCCTCCTGCACCAGGACTGGCTGAAT GGCAAGGAGTACAAGTGAAGGTCTCCAACAAGCCCTCCAGCCCCATC GAGAAAACCATCTCCAAAGCCAAAGGGCAGCCCCGAGAACACACAGGTGTAC ACCTGCCCCCATCCCGGATGAGCTGACCAAGAAGCAGGTGACCGTGAAC TGCTGGTCAAAGGCTTCTATCCCAGCGACATCGCCGTGGAGTGGGAGAGC AATGGGCAGCCGGAGAACAACCTACAAGACCACGCCTCCCGTGCTGGACTCC GACGGCTCCTTCTTCTTACAGCAAGCTCACCCTGGACAAGAGCAGGTGG CAGCAGGGGAACGTCTTCTCATGCTCCGTGATGCATGAGGCTCTGCACAAC CACTACACGCAGAAGAGCCTCTCCCTGTCTCCGGTAAATGA

41	LCDR1 (IMGT)	QSVSID
42	LCDR2 (IMGT)	DTS
43	LCDR3 (IMGT)	QQRAHWPPSIT
44	VL	EIVLTQSPATLSLSPGERAILSSCRASQSVSIDLAWYQQKPGQAPRLLIYDT SNRATGVPARFSGSGSGTDFTLTISLGPEDFAVYYCQQRAHWPPSITFGQ GTRLEIK
45	Light Chain	EIVLTQSPATLSLSPGERAILSSCRASQSVSIDLAWYQQKPGQAPRLLIYDT SNRATGVPARFSGSGSGTDFTLTISLGPEDFAVYYCQQRAHWPPSITFGQ GTRLEIKRTVAAPSVFIFPPSDEQLKSGTASVVCLLNNFYPREAKVQWKVD NALQSGNSQESVTEQDSKDYSLSTLTLSKADYEKHKVYACEVTHQGLS SPVTKSFNRGEC*
46	DNA VL	GAAATTGTGTTGACACAGTCTCCAGCCACCCTGTCTTTGTCTCCAGGGGAA AGAGCCATCCTCTCCTGCAGGGCCAGTCAGAGTGTTAGCATCGACTTAGCC TGGTACCAACAGAAACCTGGCCAGGCTCCCAGGCTCCTCATCTATGATACA TCCAACAGGGCCACTGGCGTCCCAGCCAGGTTTCAGTGGCAGTGGGTCTGGG ACAGACTTCACTCTCACCATCAGCAGCCTGGGGCCTGAAGATTTTGCAGTT TATTACTGTCAGCAGCGTGCCCACTGGCCTCCCTCGATCACCTTCGGCCAA GGGACACGACTGGAGATTAAC
47	DNA Light Chain	GAAATTGTGTTGACACAGTCTCCAGCCACCCTGTCTTTGTCTCCAGGGGAA AGAGCCATCCTCTCCTGCAGGGCCAGTCAGAGTGTTAGCATCGACTTAGCC TGGTACCAACAGAAACCTGGCCAGGCTCCCAGGCTCCTCATCTATGATACA TCCAACAGGGCCACTGGCGTCCCAGCCAGGTTTCAGTGGCAGTGGGTCTGGG ACAGACTTCACTCTCACCATCAGCAGCCTGGGGCCTGAAGATTTTGCAGTT TATTACTGTCAGCAGCGTGCCCACTGGCCTCCCTCGATCACCTTCGGCCAA GGGACACGACTGGAGATTAACCGTACGGTGGCTGCACCATCTGTCTTCAT CTTCCC GCCATCTGATGAGCAGTTGAAATCTGGAAGTGCCTCTGTTGTGTG CCTGCTGAATAACTTCTATCCCAGAGAGGCCAAAGTACAGTGGAAAGGTGGA TAACGCCCTCCAATCGGGTAACTCCCAGGAGAGTGTACAGAGCAGGACAG CAAGGACAGCACCTACAGCCTCAGCAGCACCTGACGCTGAGCAAAGCAGA CTACGAGAAACACAAAGTCTACGCCTGCGAAGTACCCATCAGGGCCTGAG CTCGCCCGTACAAAAGAGCTTCAACAGGGGAGAGTGTTAG

BK198		
Sequence number	Designation	Sequence
48	HCDR1 (IMGT)	GGSISSSSYS
49	HCDR2 (IMGT)	IYYSGNT
50	HCDR3 (IMGT)	ARGNGYSYGYGRNAFHI
51	VH	QMQLQESGPGPLVKPSETLSLTCTVSGGSISSSSYSWDWVRQPPGKGLEWIG TIYYSGNTYYNPSLKGRVTISVDPSKNQFSLKLSSVTAADTAVFYCARGNG YSYGYGRNAFHIWGQGTMTVTVSS
52	Heavy Chain	QMQLQESGPGPLVKPSETLSLTCTVSGGSISSSSYSWDWVRQPPGKGLEWIG TIYYSGNTYYNPSLKGRVTISVDPSKNQFSLKLSSVTAADTAVFYCARGNG YSYGYGRNAFHIWGQGTMTVTVSSASTKGPSVFLAPSSKSTSGGTAALGCL VKDYFPEPVTVSWNSGALTSVHTFPAVLQSSGLYLSVTVVPSSSLGTQ TYICNVNHKPSNTKVDKKEPKSCDKHTHTCPPELLEGGPSVFLFPPKP KDTLMI SRTPEVTCVVVDVSHEDPEVKFNWYVDGVEVHNAKTKPREEQYNS TYRVVSVLTVLHQDWLNGKEYKCKVSNKALPAPIEKTI SKAKGQPREPQVY TLPSSRDELTKNQVSLTCLVKGFYPSDIAVEWESNGQPENNYKTTTPVLDSD DGSFFLYSKLTVDKSRWQQGNVFCFSVMHEALHNHYTQKSLSLSPGK*
53	DNA VH	CAGATGCAGCTGCAGGAGTCGGGCCAGGACTGGTGAAGCCTTCGGAGACC CTGTCCCTCACCTGCACGTCTCTGGTGGCTCCATCAGCAGTAGTAGTTAC TCTGGGACTGGGTCCGCCAGCCCCAGGGAAGGGGCTGGAGTGGATTGGG ACTATCTATTATAGTGGGAATACCTACTACAACCCGTCTCTCAAGGGTCTGA GTCACCATATCAGTAGACCCGTCCAAGAACCAGTTCTCCCTGAAGCTGAGC TCTGTGACCGCCGCGGACACGGCTGTGTTTTACTGTGCGAGAGGAAATGGA TACAGCTATGGTTACGGGCGGAATGCTTTTTCATATCTGGGGCCAAGGGACA ATGGTCACCGTCTCTTCAG
54	DNA Heavy Chain	CAGATGCAGCTGCAGGAGTCGGGCCAGGACTGGTGAAGCCTTCGGAGACC CTGTCCCTCACCTGCACGTCTCTGGTGGCTCCATCAGCAGTAGTAGTTAC TCTGGGACTGGGTCCGCCAGCCCCAGGGAAGGGGCTGGAGTGGATTGGG ACTATCTATTATAGTGGGAATACCTACTACAACCCGTCTCTCAAGGGTCTGA GTCACCATATCAGTAGACCCGTCCAAGAACCAGTTCTCCCTGAAGCTGAGC TCTGTGACCGCCGCGGACACGGCTGTGTTTTACTGTGCGAGAGGAAATGGA TACAGCTATGGTTACGGGCGGAATGCTTTTTCATATCTGGGGCCAAGGGACA ATGGTCACCGTCTCTTCAGCCTCGACCAAGGGCCCATCGGTCTTCCCCCTG GCACCTCCTCCAAGAGCACCTCTGGGGGCACAGCGGCCCTGGGCTGCCTG GTCAAGGACTACTTCCCCGAACCTGTGACGGTCTCGTGGAACTCAGGCGCC CTGACCAGCGCGTGCACACCTTCCCGGCTGTCTACAGTCTCAGGACTC TACTCCCTCAGCAGCGTGGTGACCGTGCCCTCCAGCAGCTTGGGCACCCAG ACCTACATCTGCAACGTGAATCACAAGCCCAGCAACACCAAGGTGGACAAG AAAGTTGAGCCCAAATCTTGTGACAAAACCTCACACATGCCACCGTGCCCA GCACCTGAACCTCCTGGGGGACCGTCAGTCTTCTCTTCCCCCAAACCC AAGGACACCTCATGATCTCCCGGACCCCTGAGGTACATGCGTGGTGGTG GACGTGAGCCACGAAGACCCCTGAGGTCAAGTTCAACTGGTACGTGGACGGC GTGGAGGTGCATAATGCCAAGACAAAGCCGCGGGAGGAGCAGTACAACAGC ACGTACCGTGTGGTCAGCGTCTCACCCTCCTGCACCAGGACTGGCTGAAT GGCAAGGAGTACAAGTGAAGGTCTCCAACAAGCCCTCCCAGCCCCATC GAGAAAACCATCTCCAAGCCAAAGGGCAGCCCCGAGAACACACAGGTGTAC ACCTGCCCCCATCCCGGATGAGCTGACCAAGAAGCAGGTGACCGTGAAC TGCTGGTCAAAGGCTTCTATCCCAGCGACATCGCCGTGGAGTGGGAGAGC AATGGGCAGCCGGAACAACCTACAAGACCACGCCTCCCGTGTGGACTCC GACGGCTCCTTCTCTCTACAGCAAGCTCACCCTGGACAAGAGCAGGTGG CAGCAGGGGAACGTCTTCTCATGCTCCGTGATGCATGAGGCTCTGCACAAC CACTACACGCAGAAGAGCCTCTCCCTGTCTCCGGTAAATGA

55	LCDR1 (IMGT)	QSVSSY
56	LCDR2 (IMGT)	DAS
57	LCDR3 (IMGT)	QQRNNWPPIT
58	VL	EIVLTQSPATLSLSPGERATLSCRASQSVSSYLAWYQQKPGQAPRLLIYDASNRATGIPARFSGSGSGTDFTLTISGLEPEDFAVYYCQQRNNWPPITFGQGTRLEIK
59	Light Chain	EIVLTQSPATLSLSPGERATLSCRASQSVSSYLAWYQQKPGQAPRLLIYDASNRATGIPARFSGSGSGTDFTLTISGLEPEDFAVYYCQQRNNWPPITFGQGTRLEIKRTVAAPSVFIFPPSDEQLKSGTASVVCLLNNFYPREAKVQWKVDNALQSGNSQESVTEQDSKSTYLSSTLTLSKADYEKHKVYACEVTHQGLSSPVTKSFNRGEC*
60	DNA VL	GAAATTGTGTTGACACAGTCTCCAGCCACCCTGTCTTTGTCTCCAGGGGAAAGAGCCACCCTCTCCTGCAGGGCCAGTCAGAGTGTTAGCAGCTACTTAGCC TGGTACCAACAGAAACCTGGCCAGGCTCCCAGGCTCCTCATCTATGATGCA TCCAACAGGGCCACTGGCATCCCAGCCAGGTTTCAGTGGCAGTGGGTCTGGG ACAGACTTCACTCTCACCATCAGCGGCCTAGAGCCTGAAGATTTTGCAGTT TATTACTGTCAGCAGCGTAACAACCTGGCCTCCGATCACCTTCGGCCAAGGG ACACGACTGGAGATTAAAC
61	DNA Light Chain	GAAATTGTGTTGACACAGTCTCCAGCCACCCTGTCTTTGTCTCCAGGGGAAAGAGCCACCCTCTCCTGCAGGGCCAGTCAGAGTGTTAGCAGCTACTTAGCC TGGTACCAACAGAAACCTGGCCAGGCTCCCAGGCTCCTCATCTATGATGCA TCCAACAGGGCCACTGGCATCCCAGCCAGGTTTCAGTGGCAGTGGGTCTGGG ACAGACTTCACTCTCACCATCAGCGGCCTAGAGCCTGAAGATTTTGCAGTT TATTACTGTCAGCAGCGTAACAACCTGGCCTCCGATCACCTTCGGCCAAGGG ACACGACTGGAGATTAAACCGTACGGTGGCTGCACCATCTGTCTTCATCTT CCCGCCATCTGATGAGCAGTTGAAATCTGGAAGTGCCTCTGTTGTGTGCCT GCTGAATAACTTCTATCCCAGAGAGGCCAAAGTACAGTGAAGGTGGATAA CGCCCTCCAATCGGGTAACTCCCAGGAGAGTGTACAGAGCAGGACAGCAA GGACAGCACCTACAGCCTCAGCAGCACCTGACGCTGAGCAAAGCAGACTA CGAGAAACACAAAGTCTACGCCTGCGAAGTCAACCATCAGGGCCTGAGCTC GCCGTCAAAAGAGCTTCAACAGGGGAGAGTGTTAG

Specificity and neutralizing properties of antibodies

Table 3 Binding properties of antibodies

		BK160-1	BK206	BK120	BK198	Control MAb
ELISA OD450	BKPyV gI	0.566	0.768	0.809	0.507	0.017
	BKPyV gII	0.566	0.431	0.760	0.342	0.016
	BKPyV gIII	0.545	0.367	0.786	0.399	0.017
	BKPyV gIV	0.504	0.784	0.806	0.609	0.011
	MPyV	0.000	0.008	0.008	0.012	0.015
SPR Binding avidity (M)	BKPyV gI	2.3×10^{-10}	2.0×10^{-10}	1.1×10^{-10}		NT
	BKPyV gII	2.8×10^{-10}	2.2×10^{-9}	1.6×10^{-10}		NT
	BKPyV gIII	1.7×10^{-10}	3.1×10^{-9}	2.1×10^{-10}		NT
	BKPyV gIV	2.7×10^{-10}	2.5×10^{-10}	8.6×10^{-10}		NT

OD450 values > 0.1 indicate antibody binding to the coated antigen.

NT – Not tested

An irrelevant anti-HLA-A2 human monoclonal antibody (Control MAb) does not bind to BKPyV VLPs, or MPyV VLPs, whereas the J1 antibody shows specific binding to BKPyV genotype I VLPs.

Antibodies BK160-1, BK206, BK120 and BK198 bind to all four BKPyV genotypes. This binding is specific, since the antibodies do not bind to MPyV VLPs.

Binding avidity of the BK160-1, BK206, BK120 and BK198 antibodies to BKPyV VLPs was in the range 1×10^{-10} to 3×10^{-9} M.

BK198 data pending

Figure 1 Neutralizing properties of antibodies in 293TT cells

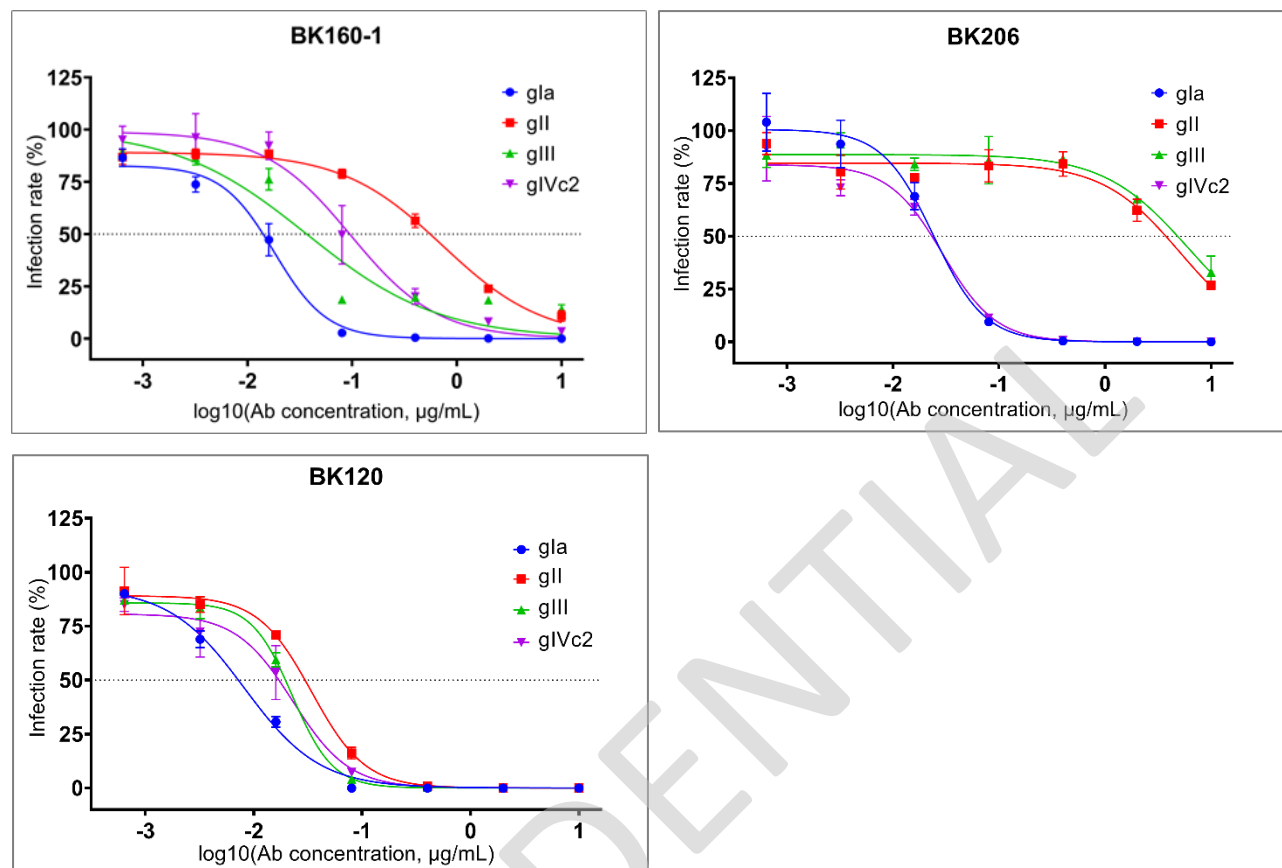


Table 4 Neutralizing titre of antibodies in 293TT cells

		BK160-1	BK206	BK120	BK198
PSV Neutralizing IC50 (nM) in 293TT cells	BKPyV gI	0.12	0.16	0.05	NA
	BKPyV gII	4.86	34.01	0.23	NA
	BKPyV gIII	0.25	40.78	0.15	NA
	BKPyV gIV	0.64	0.19	0.15	NA

Antibodies BK160-1, BK120 and BK198 neutralize infectious entry of all four BKPyV genotypes into 293TT cells, whereas antibody BK206 efficiently neutralizes genotype I and genotype IV BKPyV PSV.

Antibodies BK160-1, BK206, and BK198 (to be confirmed) are therefore broadly neutralizing in 293TT cells, with neutralizing IC50 <1nM for all genotypes for antibody BK120.

BK198 data pending

Figure 2 Neutralizing properties of antibodies in RS cells

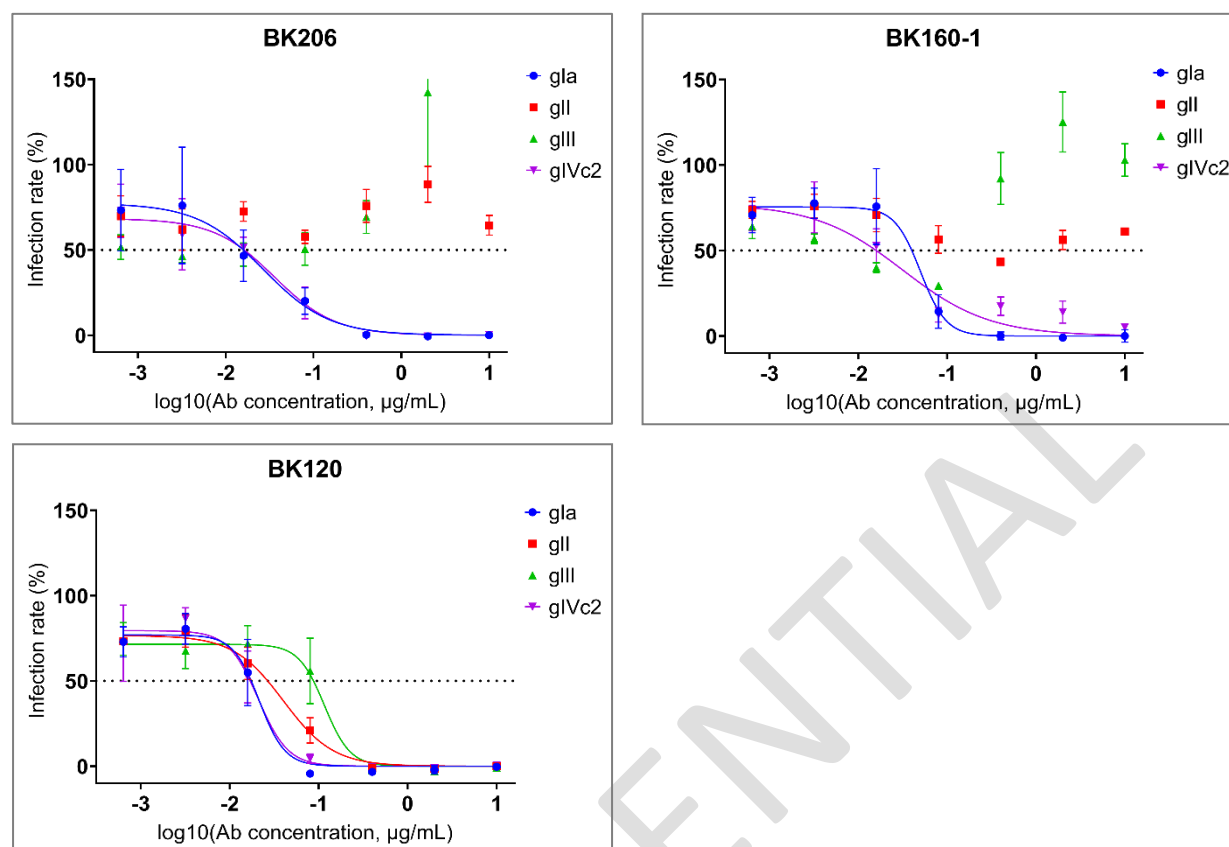


Table 5 Neutralizing titre of antibodies in RS cells

		BK160-1	BK206	BK120	BK198
PSV Neutralizing IC50 (nM) in RS cells	BKPyV gI	0.33	0.18	0.14	NA
	BKPyV gII	-	-	0.27	NA
	BKPyV gIII	-	-	0.77	NA
	BKPyV gIV	0.21	0.24	0.14	NA

Antibodies BK160-1 and BK206 neutralize infectious entry of all genotype I and genotype IV BKPyV PSV into RS cells, whereas antibody BK120 neutralizes infectious entry of all four BKPyV genotypes into RS cells.

Antibodies BK160-1 and BK206 therefore neutralize the two most frequent BKPyV genotypes, while antibody BK120 is broadly neutralizing in RS cells, which are immortalized human renal epithelial cells, with neutralizing IC50 <1nM for all genotypes.

Results pending for BK198

Bibliography

1. Knowles, W.A.; Gibson, P.E.; Gardner, S.D. Serological typing scheme for BK-like isolates of human polyomavirus. *J. Med. Virol.* **1989**, *28*, 118–123.
2. Pastrana, D.V.; Ray, U.; Magaldi, T.G.; Schowalter, R.M.; Çuburu, N.; Buck, C.B. BK polyomavirus genotypes represent distinct serotypes with distinct entry tropism. *J. Virol.* **2013**, *87*, 10105–10113, doi:10.1128/JVI.01189-13.
3. Zhong, S.; Randhawa, P.S.; Ikegaya, H.; Chen, Q.; Zheng, H.-Y.; Suzuki, M.; Takeuchi, T.; Shibuya, A.; Kitamura, T.; Yogo, Y. Distribution patterns of BK polyomavirus (BKV) subtypes and subgroups in American, European and Asian populations suggest co-migration of BKV and the human race. *J. Gen. Virol.* **2009**, *90*, 144–152, doi:10.1099/vir.0.83611-0.
4. Hurdiss, D.L.; Frank, M.; Snowden, J.S.; Macdonald, A.; Ranson, N.A. The Structure of an Infectious Human Polyomavirus and Its Interactions with Cellular Receptors. *Structure* **2018**, *26*, 839-847.e3, doi:10.1016/j.str.2018.03.019.
5. Bressollette-Bodin, C.; Coste-Burel, M.; Hourmant, M.; Sebille, V.; Andre-Garnier, E.; Imbert-Marcille, B.M. A prospective longitudinal study of BK virus infection in 104 renal transplant recipients. *Am. J. Transplant.* **2005**, *5*, 1926–1933, doi:10.1111/j.1600-6143.2005.00934.x.
6. Nickeleit, V.; Klimkait, T.; Binet, I.F.; Dalquen, P.; Del Zenero, V.; Thiel, G.; Mihatsch, M.J.; Hirsch, H.H. Testing for polyomavirus type BK DNA in plasma to identify renal-allograft recipients with viral nephropathy. *N. Engl. J. Med.* **2000**, *342*, 1309–1315, doi:10.1056/NEJM200005043421802.
7. Hirsch, H.H.; Randhawa, P.; AST Infectious Diseases Community of Practice BK polyomavirus in solid organ transplantation. *Am. J. Transplant.* **2013**, *13 Suppl 4*, 179–188, doi:10.1111/ajt.12110.
8. Cesaro, S.; Dalianis, T.; Hanssen Rinaldo, C.; Koskenvuo, M.; Pegoraro, A.; Einsele, H.; Cordonnier, C.; Hirsch, H.H.; ECIL-6 Group ECIL guidelines for the prevention, diagnosis and treatment of BK polyomavirus-associated haemorrhagic cystitis in haematopoietic stem cell transplant recipients. *J Antimicrob Chemother* **2018**, *73*, 12–21, doi:10.1093/jac/dkx324.
9. Reploeg, M.D.; Storch, G.A.; Clifford, D.B. Bk virus: a clinical review. *Clin Infect Dis* **2001**, *33*, 191–202, doi:10.1086/321813.
10. Imlay, H.; Xie, H.; Leisenring, W.M.; Duke, E.R.; Kimball, L.E.; Huang, M.-L.; Pergam, S.A.; Hill, J.A.; Jerome, K.R.; Milano, F.; et al. Presentation of BK polyomavirus-associated hemorrhagic cystitis after allogeneic hematopoietic cell transplantation. *Blood Adv* **2020**, *4*, 617–628, doi:10.1182/bloodadvances.2019000802.
11. Espada, E.; Cheng, M.P.; Kim, H.T.; Woolley, A.E.; Avigan, J.I.; Forcade, E.; Soares, M.V.D.; Lacerda, J.F.; Nikiforow, S.; Gooptu, M.; et al. BK virus-specific T-cell immune reconstitution after allogeneic hematopoietic cell transplantation. *Blood Adv* **2020**, *4*,

- 1881–1893, doi:10.1182/bloodadvances.2019001120.
12. Solis, M.; Velay, A.; Porcher, R.; Domingo-Calap, P.; Soulier, E.; Joly, M.; Meddeb, M.; Kack-Kack, W.; Moulin, B.; Bahram, S.; et al. Neutralizing Antibody-Mediated Response and Risk of BK Virus-Associated Nephropathy. *J. Am. Soc. Nephrol.* **2018**, *29*, 326–334, doi:10.1681/ASN.2017050532.
 13. Velay, A.; Solis, M.; Benotmane, I.; Gantner, P.; Soulier, E.; Moulin, B.; Caillard, S.; Fafi-Kremer, S. Intravenous Immunoglobulin Administration Significantly Increases BKPyV Genotype-Specific Neutralizing Antibody Titers in Kidney Transplant Recipients. *Antimicrob Agents Chemother* **2019**, *63*, doi:10.1128/AAC.00393-19.
 14. Benotmane, I.; Solis, M.; Velay, A.; Cognard, N.; Olagne, J.; Gautier Vargas, G.; Perrin, P.; Marx, D.; Soulier, E.; Gallais, F.; et al. Intravenous immunoglobulin as a preventive strategy against BK virus viremia and BKV-associated nephropathy in kidney transplant recipients-Results from a proof-of-concept study. *Am J Transplant* **2020**, doi:10.1111/ajt.16233.
 15. Matsumura, S.; Kato, T.; Taniguchi, A.; Kawamura, M.; Nakazawa, S.; Namba-Hamano, T.; Abe, T.; Nonomura, N.; Imamura, R. Clinical Efficacy of Intravenous Immunoglobulin for BK Polyomavirus-Associated Nephropathy After Living Kidney Transplantation. *Ther Clin Risk Manag* **2020**, *16*, 947–952, doi:10.2147/TCRM.S273388.
 16. Piburn, K.H.; Al-Akash, S. Use of intravenous immunoglobulin in a highly sensitized pediatric renal transplant recipient with severe BK DNAemia and rising DSA. *Pediatr Transplant* **2020**, *24*, e13600, doi:10.1111/petr.13600.
 17. Hwang, S.D.; Lee, J.H.; Lee, S.W.; Kim, J.K.; Kim, M.-J.; Song, J.H. High-Dose Intravenous Immunoglobulin Treatment of Polyomavirus Nephropathy Developing After T Cell-Mediated Rejection Treatment: A Case Report. *Transplant Proc* **2018**, *50*, 2575–2578, doi:10.1016/j.transproceed.2018.01.021.
 18. Mainra, R.; Xu, Q.; Chibbar, R.; Hassan, A.; Shoker, A. Severe antibody-mediated rejection following IVIG infusion in a kidney transplant recipient with BK-virus nephropathy. *Transpl Immunol* **2013**, *28*, 145–147, doi:10.1016/j.trim.2013.05.004.
 19. Pastrana, D.V.; Brennan, D.C.; Cuburu, N.; Storch, G.A.; Viscidi, R.P.; Randhawa, P.S.; Buck, C.B. Neutralization serotyping of BK polyomavirus infection in kidney transplant recipients. *PLoS Pathog.* **2012**, *8*, e1002650, doi:10.1371/journal.ppat.1002650.

DISCUSSION



DISCUSSION

The main objective of the project was to isolate and generate BkPyV-specific monoclonal antibodies from PBMC of kidney transplant recipients who had generated high antibody titres in response to BkPyV reactivation after KTx. By performing 10x Chromium single-cell RNA seq with Immune Profiling, we successfully identified a 41F17-like cluster of neutralizing antibodies generated in two patients who had successfully suppressed BkPyV replication. Antibody expression and characterization in vitro confirmed the antiviral activities of 41F17-like broadly neutralizing antibodies on 293TT and RS cells. In addition, this high throughput technique also allowed us to further investigate the BCR repertoires in kidney transplant recipients.

In this section, I will discuss:

- 1) some technical aspects of the project,
- 2) IgM memory B-cells in BkPyV-specific humoral response in kidney transplant recipients,
- 3) 41F17-like broadly neutralizing antibodies.

PART 1: Technical aspects

The technique of sorting specific B-cells using labeled antigen in combination with the high throughput 10x Genomics single-cell RNA seq platform to obtain paired heavy and light chain antibody sequences has been increasingly used (Cox et al., 2016; Seydoux et al., 2020; Williams et al., 2017; Zhou et al., 2020) over the last five years. It is a powerful technique that requires 5000 to 10000 cells loaded into the 10x Chromium system to obtain sufficient information for the subsequent bioinformatic analysis step. This was our principal obstacle because of the very small number of BKPyV-specific B-cells that we observed in each patient's PBMC sample in the preliminary test. In order to get enough cells, we had to pool several PBMC samples from multiple patients. A similar approach was recently used by Cao et al. to generate a large dataset of SARS-CoV2-specific BCR (Cao et al., 2020). The pooling was successful because approximately 10000 BKPyV-specific B cells, according to the cell sorter count, were isolated and were passed through the 10x Chromium system. We did not recount the number of B cells after FACS sorting to confirm as it risked losing a lot of cells. After Illumina sequencing and the bioinformatic quality control step, we were able to obtain more than 2000 antibody sequences. This number was lower than the recovery rate proposed by 10x Genomics (~6000 cells recovered from ~10500 cells loaded) but many more higher than the number of BKPyV-specific antibodies screened by Lindner et al. (Lindner et al., 2019). However, our Illumina sequencing did not reach sequence saturation, so many cells were eliminated because the number of reads-per-cell was too low. For further experiments, we suggest increasing sequence depth, which in turn increases the number of reads, leading to increase of transcript numbers per cell and eventually fewer cells will be eliminated.

Pooling many samples raised the question about how to assign each individual cell to a particular starting sample. The main innovation that we introduced here was to couple VDJ sequencing to sample identification using hashtag oligo-coupled antibodies, to link each cell to a specific sample. Since the VDJ sequence starts at the 5' end of

immunoglobulin mRNA, we needed to use the 10x Chromium Single Cell 5' Library kit to produce full-length antibody transcripts and to construct a 5' cDNA library for gene expression analysis. In order to integrate cell hashtagging, we used TotalSeq-C oligo-conjugated antibodies which contain a capture sequence that is compatible with the Template Switch Oligo (TSO) on the Single Cell 5' Gel Bead oligos. However, at the time we carried out the experiment, only 5 TotalSeq-C Hashtag antibodies were commercially available, which was not enough to demultiplex the 15-20 PBMC samples that we planned to pool together. This was why we used other TotalSeq-C labelled pan-leukocyte or pan-B cell antibodies for sample hashtagging. We also realized that combinations of different oligo-tagged antibodies could be used to indicate 1) patient ID and 2) time point. To the best of our knowledge, this dual hashtagging has not been used in any other publication.

Owing to the combinations of the TotalSeq-C Hashtag and the other TotalSeq-C antibodies, we encountered some issues of demultiplexing. First, the cut-off values of normalized read count numbers showed a lot of variability. It might be due to 1) different antibodies targeting different surface markers or 2) different numbers of BkPyV-specific B cells in each sample. Second, instead of retaining singlets (a single barcode on each single cell) according to the "Demultiplexing with hashtag oligos" workflow of Seurat (Stoeckius et al., 2018), we eliminated singlets and stored doublets (double barcodes on each single cell). In this situation, two cells which were encapsidated in the same droplet were rejected due to the detection of more than two barcodes. In addition, B cells containing wrong combinations (two timepoint-specific antibodies detected in the same cell, for instance) were also removed from the dataset. Finally, due to the highly selected quality control step together with the integration of cells presenting in both VDJ and transcriptome datasets, the number of cells used for clustering and differential expression analysis in the combined SpecB and TotB datasets reduced dramatically, from a total of 9526 cells to 5450 cells.

Since we had not measured the percentage of BK-specific B-cells in the samples before conducting the single-cell RNA seq experiment, there was no guarantee that an adequate sample size from each patient would be obtained. In fact, the dataset was dominated by antibody sequences from patient 3.1, and a sufficient dataset for extensive repertoire analysis was obtained from only two patients. Ideally, it would be important to measure the proportion of specific B-cells in each PBMC sample by flow cytometry before running a single-cell RNA seq experiment. By doing so, it would be possible to adjust the number of PBMC used to obtain a roughly equivalent number of antibody sequences from each sample.

During the planning for the single-cell RNA seq experiment, we had discussed the possibility of using genotype IV labelled VLP in order to sort B-cells expressing gI-gIV cross-reactive antibodies. However, the first sorting results showed a really low number of specific B cells (less than 50) might be obtained from each vial of frozen PBMC, and the addition of BKPyV gIV screening might lead to a vanishingly low number of sorted cells. As a consequence, we decided that it would be better to use only gI VLPs since 5 out of the 6 patients had gI BKPyV infection. One solution to this problem would be to adapt the LIBRA-seq protocol (Setliff et al., 2019). LIBRA-seq stands for Linking B-cell Receptor to Antigen Specificity through Sequencing. This technique entails tagging the antigen used for sorting with a hashtag oligonucleotide. In this way, it might be possible to use gI VLPs for sorting, and add gIV hashtag-coupled VLPs during the labelling step so that cross-reactive antibodies could be directly identified in the BCR sequence dataset. As a result of doing this, we might be able to identify potentially broadly neutralizing antibodies. However, protocols for adding oligonucleotide tags to VLPs have not been published, and would need to be set up and validated. If this could be set up, then the technique could be used to search for rare broadly reactive mAbs for example, against JCPyV and BKPyV, or other more antigenically variable viruses.

The other technical issue we were faced with was the production of antibodies. Co-transfection of expression vectors containing heavy and light chain sequences into 293A

cells seeded in 96-well plates provided us a yield of approximately 1 µg/mL, which was sufficient to perform an ELISA and neutralization screening. However, when we scaled the production up to 175 cm² flasks, we sometimes did not get expected yield, or even almost nothing. After preparing new MaxiPreps of heavy and light chain vectors, the problem was resolved, suggesting that plasmid quality was an issue, especially for large-scale transfections. However, this solution was not effective in the case of antibody 198, one of our 41F17-like antibodies. There is no real answer for the production issue of 198, but one possibility to solve this problem would be to express codon optimized antibodies.

PART 2: IgM memory B-cells in BKPyV-specific humoral response in kidney transplant recipients

IgM memory B-cells have been described to play a crucial role in multiple infectious diseases (Gibney et al., 2012; Skountzou et al., 2014; Throsby et al., 2008). In patients with COVID-19, depletion of IgM memory B cells has been observed and correlated with higher mortality and superimposed infections (Lenti et al., 2020). Interestingly, Shen et al. have recently demonstrated that the IgM isotype of C7G6, a neutralizing monoclonal antibody against influenza virus, exhibited more potent and broader antiviral activity compared to the IgG1 counterpart *in vitro* and excellent protection against distinct strains of influenza virus in mice and ferrets (Shen et al., 2019). In the case of BKPyV-infection in kidney transplant recipients, our data showed that the BKPyV-specific repertoire was dominated by IgM memory B cells rather than IgG/IgA memory B cells. It is intriguing that although all the antibodies recognize the same antigen (BKPyV-gI-VLP), the IgM- and switched-memory B cells expressed distinct BCR repertoires. We hypothesize that BKPyV-specific IgG and IgM might not share the same epitopes on the BKPyV capsid. Further structural studies will be required to determine the epitope binding recognized by the dominant IgG and IgM antibodies specific to BKPyV. Moreover, in a prospective study in whether kidney or kidney/pancreas transplant patients, Hariharan et al. revealed higher levels of BKPyV-specific IgM than IgG in the early onset of BKPyV nephritis, and IgM titre was considerably increased in stabilizing BKPyV nephritis stage. However, the clearance of BKPyV viremia was correlated with higher IgG antibody (Hariharan et al., 2005). In contrast, the predominance of IgM over IgG in the BKPyV-specific repertoire in kidney recipients with control of BKPyV viruria suggests that IgM, together with IgG, plays an important role in the humoral response against BKPyV infection.

Memory B cells are known to develop from naïve B cells that enter the follicle and take part in the GC reaction. Inside the GC, SHM and class-switching take place, together with selection to generate high-affinity switched memory B cells (Akkaya et al., 2020). Apart from the classical pathway, naïve B cells can also enter the follicle and differentiate into memory B cells without the GC reaction, which subsequently generates mostly IgM memory B cells with low SHM and no affinity selection (Gibney et al., 2012). In our dataset, although we were able to detect BKPyV-specific IgM antibodies with high SHM, most IgM-expressing B-cell clonotypes had generally low SHM compared to activated and switched B cells. This suggests that after encountering BKPyV, naïve B cells differentiate in either the GC-dependent or GC-independent pathway. Since many BKPyV-specific memory B-cells from healthy blood donors also expressed IgM antibodies (Lindner et al., 2019), this suggests that the importance of the GC-independent pathway in the humoral response against BKPyV is not related to the immunological context of kidney transplant recipients, but rather may reflect the characteristics of the initial B-cell response to primary infection.

The GC-independent origin of BKPyV-specific IgM memory B cells is supported by analyzing differentially expressed genes between non-switched and switched memory B cells of the BKPyV-specific repertoire. We saw that the expression of *PARP-1* was higher in the IgM memory subset than in IgG/IgA memory subset. It has been demonstrated that PARP-1 inhibits the activity of AID due to its mutagenic repair functions (Paddock et al., 2010; Tepper et al., 2019). Higher frequencies of class-switched antibodies have been observed in *PARP-1*-deficient mic (Ambrose et al., 2007; Galindo-Campos et al., 2019; Robert et al., 2009). These findings suggest that the expression of *PARP-1* in B cells might lead both to a bias towards IgM memory B response and to low SHM. Furthermore, we also found lower expression of *CD83* in the activated IgM⁺ B cells compared to IgG/IgA⁺ B cells. The expression of CD83 has been identified as a marker of light zone B cells in the germinal center (Victoria et al., 2012). In the light zone, a selection process takes place with the aid of follicular DCs and follicular T helper cells in order to retain B cells with high BCR affinity (Krzyzak et al.,

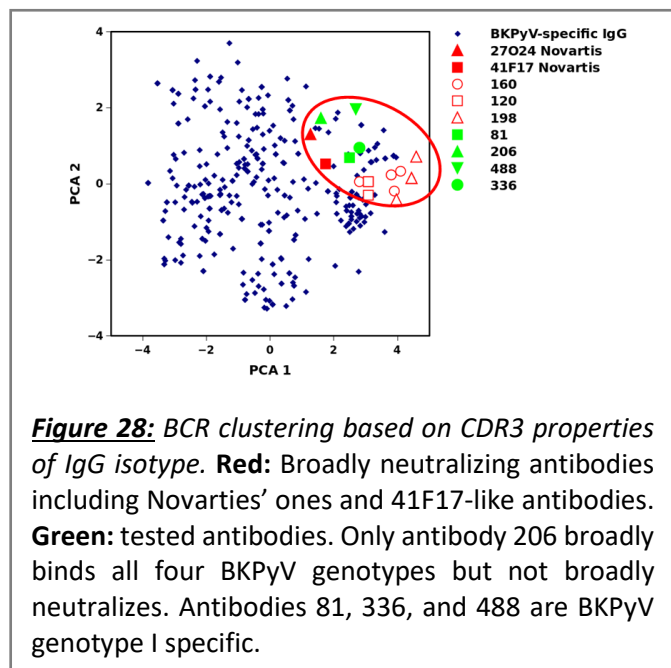
2016). Lower expression of *CD83* suggests that a portion of BKPyV-specific IgM memory B cells containing SHM did not go through events in the GC, including clonal selection. All these findings raise the question about the quality of the memory IgM repertoire versus the memory IgG/IgA repertoire in the response against BKPyV infection. This can be addressed by expressing representatives of each IgM and IgG/IgA clonotype then characterizing them *in vitro*.

Despite of the hypotheses proposed to explain the domination of IgM memory B cells in the BKPyV-specific repertoire, it is unclear how a naïve B cell that binds to BKPyV carries out its differentiation towards whether IgG or IgM memory B cells, nor which factors/genes drive this orientation. We suggest to follow up the transcriptomic dataset with a diffusion pseudotime analysis, also called single-cell trajectory analysis using the Monocle package (Qiu et al., 2017; Trapnell et al., 2014). In general, the algorithm of diffusion pseudotime will order a set of individual cells along one or more trajectories where they show unceasing changes in the transcriptome (Haghverdi et al., 2016). By that, we will hopefully be able to obtain information about which genes drive the developmental paths of naïve B cells to BKPyV-specific IgM or IgG B cells.

PART 3: 41F17-like broadly neutralizing antibodies

Using concatenated heavy and light CDR3 sequences to build phylogenetic trees, we discovered a 41F17-like cluster of broadly neutralizing antibodies. However, this approach only allowed us to identify the “nearest neighbours” to an antibody with known specificity (41F17). Larger clusters of antibodies binding to the same epitope could not be identified. This is probably because the Neighbour-Joining algorithm 1) only counts the number of differences between sequences without taking into account structural or biochemical features and 2) assumes that all antibody sequences are related in a tree-like structure, so it will have a tendency to join groups of antibodies together even if they don’t bind the same epitope. The advantage of this approach is that it is simple to do, and calculations are not intensive, so it can be run on a personal computer. However, more sophisticated clustering techniques will be required to map BCR sequences in the BKPyV-specific repertoire onto the epitopes that antibodies bind to.

Apart from sequence homology, the other approach that we used was PCA clustering on amino acid properties. Briefly, heavy and light chain CDR3 sequences were separately submitted to BRepertoire webserver to calculate the 10 Kidera factors that represent the physico-chemical properties of the CDR3 amino acid side-chains (Margreitter et al., 2018). The calculated results of heavy and light chain CDR3 length and Kidera factors of IgG lambda and kappa chains were taken together to create a PCA plot. In the PCA plot, two broadly neutralizing antibodies

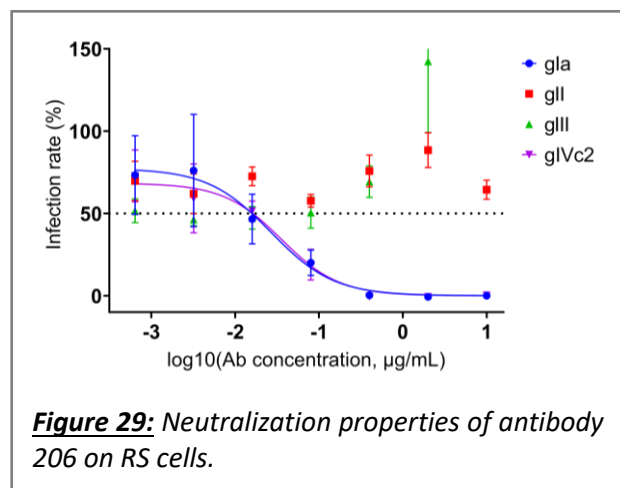


identified by Lindner et al. (Lindner et al., 2019), 41F17 and 27O24, seemed to be in the

same cluster (**Figure 28, red circle**). We hypothesized that antibodies in that cluster would share similar neutralization properties. We therefore tested several antibodies in the cluster in the PCA plot, and it turned out that they did not neutralize all four BKPyV genotypes (**Figure 28, green shapes**). We concluded that clustering based on CDR3 chemical properties failed to identify a cluster of neutralizing antibodies. Although different approaches were tested and we succeeded in identifying a cluster of broadly neutralizing antibodies by sequence homology, it will be difficult for us to progress alone on this topic. It will therefore require collaboration with specialists in the field of antibody bioinformatics to explore all possible information from our VDJ dataset.

After the bioinformatic analysis step, we expressed and characterized the selected antibodies *in vitro*. Neutralization assay was performed in two different cell lines including 293TT, an immortalized human embryonic kidney cell line, and RS, an immortalized renal proximal tubular epithelial cell line. However, the neutralization results were not entirely equivalent between these cell lines. There were antibodies that broadly neutralized when tested on 293TT, but partially neutralized when tested on RS. The first possible explanation is that 293TT are more sensitive to neutralization, which is supported by the neutralization profile of antibody 206.

This antibody had weaker binding to BKPyV VLP gII and gIII, leading to weak neutralization of these genotypes in 293TT cells, and no neutralization of



BKPyV PSV gII and gIII in RS cells (**Figure 29**). Furthermore, HEK 293TT are derived from HEK 293 cell line (Buck et al., 2004) which has been demonstrated to associate with neuronal phenotypes, and which cannot be considered as typical kidney cells (Shaw et al., 2002). In addition, the MM strain of BKPyV was isolated in the brain tumor and the urine of a patient with Wiskott-Aldrich syndrome (Takemoto & Mullarkey, 1973; Yang

& Wu, 1979), suggesting that BKPyV have the ability to infect both brain and kidney cells. 293TT cells may be a model for extra-renal BKPyV infection, whereas RS cells are more closely related to the natural infection site of BKPyV in humans. The second hypothesis is that entry mechanisms BKPyV into 293TT and RS cells possibly are not the same. BKPyV entry into 293TT cells might involve different epitopes from those that are involved in entry into RS cells. This effect could differ between genotypes, hence antibody 160 can block BKPyV gII and gIII entry into 293TT cells, but not RS cells.

Concerning the binding epitopes of the 41F17-like antibodies, the similarity of heavy and light chain CDR3 sequences suggests that the three antibodies 120, 160 and 198 bind to the same epitope as the 41F17 monoclonal. This hypothesis is supported by the effect of the E364A mutant observed in the alanine scanning experiment. Although we failed to produce antibody 198, both antibody 160 and 120 displayed a similar binding curve when E364 was mutated to alanine (**Figure 27**). In order to determine whether antibodies recognize overlapping epitopes, several techniques can be used such as SPR or BLI. These techniques provide clear results for monomeric or trimeric antigens with a limited number of binding sites per molecule. However, in the context of BKPyV which is a large multimeric antigen, it may be difficult to interpret the result. Another possibility would be to perform a competitive binding ELISA in which one antibody is biotinylated. However, definitive identification of epitopes recognized by monoclonal antibodies requires structural studies. In the case of antibody binding to quaternary epitopes on virus capsids, this will require cryo-EM analysis of VLP-Fab complexes.

41F17-like antibodies were only detected in patients with control of BKPyV replication but not in patients with prolonged viremia/viremia. However, we did not obtain enough heavy and light chain sequences in patients with prolonged viremia/viremia to test whether there is any correlation between the presence of 41F17-like antibodies and control of virus replication in patients. As we have demonstrated the feasibility of our approach, it would be possible to run further experiments with PBMC pooled from, for example, 4 donors for each 10x Chromium well. It might be feasible to run two sorts on

the same day and process samples from 8 patients per day. If this is done 3 times, a dataset for n=12 patients per group would be obtained. Sequencing costs could be limited by pooling cDNA libraries only for the VDJ and hashtag sequencing, which would allow multiple samples to be analyzed in a single Illumina run. It would, therefore, be possible to test whether 41F17-like antibodies are only expressed by patients who control BKPyV reactivation.

Finally, apart from the phylogenetic tree of CDR3 heavy and kappa light chains, we also constructed another tree with the CDR3 heavy and lambda light chains. We have found

a branch of the tree in which the Novartis' patented antibody P8D11 (Patent number: US 10,654,914 B2) and the other one 16J14 (Lindner et al., 2019) were clustered together with our clonotypes 86 and 293 (Figure 30). Clonotype 86 is an IgM isotype with 14 non-synonymous mutations in the CDR3, whereas clonotype 293 is IgA antibody

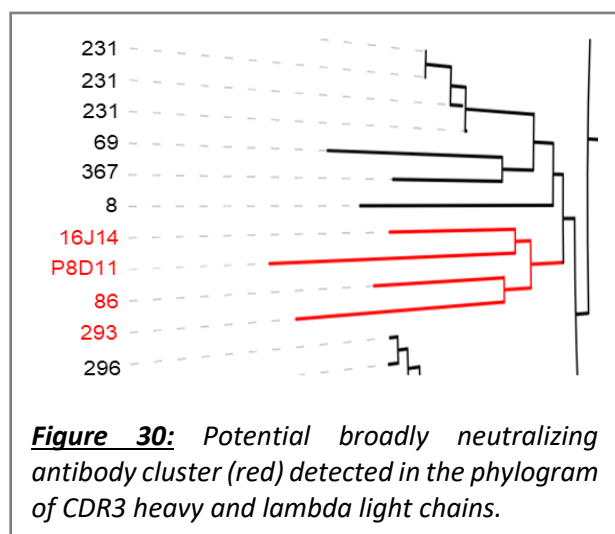


Figure 30: Potential broadly neutralizing antibody cluster (red) detected in the phylogram of CDR3 heavy and lambda light chains.

containing 20 somatic mutations. The protective effect against viral infections via neutralization of serum IgA has been demonstrated in various infectious diseases such as HIV (Lizeng et al., 2004) , SARS-CoV-2 (Sterlin et al., 2021; Wang et al., 2021) and rotavirus (Patel et al., 2013). Thus, the hypermutated BKPyV-specific IgA antibody represents a potent neutralizing antibody that is currently being generated and tested *in vitro*.

In conclusion, in response to the main objective of the project, we generated several broadly neutralizing antibodies against BKPyV infection *in vitro*. Among them, antibody 120 showed its strong antiviral activity, comparable to, or indeed slightly more potent than the neutralizing properties of 41F17. There is currently one BKPyV-specific monoclonal antibody in clinical trials which is MAU 868, licensed from Novartis by

Amplify Pharmaceuticals. According to the latest update on clinicaltrials.gov on January 29, 2021, the monoclonal is in phase 2 of clinical trial. In addition, recent results with IVIG (Benotmane et al., 2021) indicate that infusion of antibodies can indeed prevent PyVAN. Our antibody 120, therefore, will be a potential monoclonal candidate for further clinical development, alone or in combination with other monoclonals and is the subject of a pending patent application.

REFERENCES

REFERENCES

- Abend, J. R., Joseph, A. E., Das, D., Campbell-Cecen, D. B., & Imperiale, M. J. (2009). A truncated T antigen expressed from an alternatively spliced BK virus early mRNA. *The Journal of General Virology*, *90*(Pt 5), 1238–1245. <https://doi.org/10.1099/vir.0.009159-0>
- Abend, J. R., Low, J. A., & Imperiale, M. J. (2007). Inhibitory Effect of Gamma Interferon on BK Virus Gene Expression and Replication. *Journal of Virology*, *81*(1), 272–279. <https://doi.org/10.1128/JVI.01571-06>
- Ahangarzadeh, S., Payandeh, Z., Arezumand, R., Shahzamani, K., Yarian, F., & Alibakhshi, A. (2020). An update on antiviral antibody-based biopharmaceuticals. *International Immunopharmacology*, *86*, 106760. <https://doi.org/10.1016/j.intimp.2020.106760>
- Ahlenstiel-Grunow, T., Sester, M., Sester, U., Hirsch, H. H., & Pape, L. (2020). BK Polyomavirus-specific T Cells as a Diagnostic and Prognostic Marker for BK Polyomavirus Infections After Pediatric Kidney Transplantation. *Transplantation*, *104*(11), 2393–2402. <https://doi.org/10.1097/TP.0000000000003133>
- Akkaya, M., Kwak, K., & Pierce, S. K. (2020). B cell memory: Building two walls of protection against pathogens. *Nature Reviews Immunology*, *20*(4), 229–238. <https://doi.org/10.1038/s41577-019-0244-2>
- Alberts, B., Johnson, A., Lewis, J., Raff, M., Roberts, K., & Walter, P. (2002). The Generation of Antibody Diversity. *Molecular Biology of the Cell*. 4th Edition. <https://www.ncbi.nlm.nih.gov/books/NBK26860/>
- Albrecht, J. A., Dong, Y., Wang, J., Breeden, C., Farris, A. B., Lukacher, A. E., & Newell, K. A. (2012). Adaptive immunity rather than viral cytopathology mediates polyomavirus-associated nephropathy in mice. *American Journal of Transplantation: Official Journal of the American Society of Transplantation and the American Society of Transplant Surgeons*, *12*(6), 1419–1428. <https://doi.org/10.1111/j.1600-6143.2012.04005.x>
- Ambalathingal, G. R., Francis, R. S., Smyth, M. J., Smith, C., & Khanna, R. (2017). BK Polyomavirus: Clinical Aspects, Immune Regulation, and Emerging Therapies. *Clinical Microbiology Reviews*, *30*(2), 503–528. <https://doi.org/10.1128/CMR.00074-16>
- Ambrose, H. E., Papadopoulou, V., Beswick, R. W., & Wagner, S. D. (2007). Poly-(ADP-ribose) polymerase-1 (Parp-1) binds in a sequence-specific manner at the Bcl-6 locus and contributes to the regulation of Bcl-6 transcription. *Oncogene*, *26*(42), 6244–6252. <https://doi.org/10.1038/sj.onc.1210434>
- An, P., Sáenz Robles, M. T., & Pipas, J. M. (2012). Large T Antigens of Polyomaviruses: Amazing Molecular Machines. *Annual Review of Microbiology*, *66*(1), 213–236. <https://doi.org/10.1146/annurev-micro-092611-150154>
- Andrews, C. A., Shah, K. V., Daniel, R. W., Hirsch, M. S., & Rubin, R. H. (1988). A Serological Investigation of BK Virus and JC Virus Infections in Recipients of Renal Allografts. *Journal of Infectious Diseases*, *158*(1), 176–181. <https://doi.org/10.1093/infdis/158.1.176>
- Anyaegbu, E. I., Almond, P. S., Milligan, T., Allen, W. R., Gharaybeh, S., & Al-Akash, S. I. (2012). Intravenous immunoglobulin therapy in the treatment of BK viremia and nephropathy in pediatric renal transplant recipients. *Pediatric Transplantation*, *16*(1), E19–24. <https://doi.org/10.1111/j.1399-3046.2010.01384.x>
- Araya, C. E., Lew, J. F., Fennell, R. S., Neiberger, R. E., & Dharnidharka, V. R. (2008). Intermediate dose cidofovir does not cause additive nephrotoxicity in BK virus allograft nephropathy. *Pediatric Transplantation*, *12*(7), 790–795. <https://doi.org/10.1111/j.1399-3046.2008.00937.x>

- Aribi, M. (2020). Immunogenetic Aspect of B-Cell Antigen Receptor Diversity Generation. In M. Aribi (Ed.), *Normal and Malignant B-Cell*. IntechOpen. <https://doi.org/10.5772/intechopen.90637>
- Ariyasu, S., Yanai, H., Sato, M., Shinno, Y., Taniguchi, K., Yamadori, I., Miki, Y., Sato, Y., Yoshino, T., & Takahashi, K. (2015). Simultaneous immunostaining with anti-S100P and anti-SV40 antibodies revealed the origin of BK virus-infected decoy cells in voided urine samples. *Cytopathology: Official Journal of the British Society for Clinical Cytology*, *26*(4), 250–255. <https://doi.org/10.1111/cyt.12213>
- Babel, N., Volk, H.-D., & Reinke, P. (2011). BK polyomavirus infection and nephropathy: The virus-immune system interplay. *Nature Reviews. Nephrology*, *7*(7), 399–406. <https://doi.org/10.1038/nrneph.2011.59>
- Bagnara, D., Squillario, M., Kipling, D., Mora, T., Walczak, A. M., Da Silva, L., Weller, S., Dunn-Walters, D. K., Weill, J.-C., & Reynaud, C.-A. (2015). A Reassessment of IgM Memory Subsets in Humans. *Journal of Immunology (Baltimore, Md.: 1950)*, *195*(8), 3716–3724. <https://doi.org/10.4049/jimmunol.1500753>
- Barderas, R., & Benito-Peña, E. (2019). The 2018 Nobel Prize in Chemistry: Phage display of peptides and antibodies. *Analytical and Bioanalytical Chemistry*, *411*(12), 2475–2479. <https://doi.org/10.1007/s00216-019-01714-4>
- Bauman, Y., Nachmani, D., Vitenshtein, A., Tsukerman, P., Drayman, N., Stern-Ginossar, N., Lankry, D., Gruda, R., & Mandelboim, O. (2011). An Identical miRNA of the Human JC and BK Polyoma Viruses Targets the Stress-Induced Ligand ULBP3 to Escape Immune Elimination. *Cell Host & Microbe*, *9*(2), 93–102. <https://doi.org/10.1016/j.chom.2011.01.008>
- Behring, E. V. (1890). *Untersuchungen über das Zustandekommen der Diphtherie-Immunität bei Thieren* [Application/xml]. *50*, 1145–1148. <https://doi.org/10.17192/EB2013.0165>
- Behring, E. von, & Kitasato, S. (1890). Ueber das Zustandekommen der Diphtherie-Immunität und der Tetanus-Immunität bei Thieren. *DMW - Deutsche Medizinische Wochenschrift*, *16*(49), 1113–1114. <https://doi.org/10.1055/s-0029-1207589>
- Bennett, S. M., Broekema, N. M., & Imperiale, M. J. (2012). BK polyomavirus: Emerging pathogen. *Microbes and Infection*, *14*(9), 672–683. <https://doi.org/10.1016/j.micinf.2012.02.002>
- Bennett, S. M., Jiang, M., & Imperiale, M. J. (2013). Role of cell-type-specific endoplasmic reticulum-associated degradation in polyomavirus trafficking. *Journal of Virology*, *87*(16), 8843–8852. <https://doi.org/10.1128/JVI.00664-13>
- Bennett, S. M., Zhao, L., Bosard, C., & Imperiale, M. J. (2015). Role of a nuclear localization signal on the minor capsid Proteins VP2 and VP3 in BKPyV nuclear entry. *Virology*, *474*, 110–116. <https://doi.org/10.1016/j.virol.2014.10.013>
- Benotmane, I., Solis, M., Velay, A., Cognard, N., Olagne, J., Gautier Vargas, G., Perrin, P., Marx, D., Soulier, E., Gallais, F., Moulin, B., Fafi-Kremer, S., & Caillard, S. (2021). Intravenous immunoglobulin as a preventive strategy against BK virus viremia and BKV-associated nephropathy in kidney transplant recipients-Results from a proof-of-concept study. *American Journal of Transplantation: Official Journal of the American Society of Transplantation and the American Society of Transplant Surgeons*, *21*(1), 329–337. <https://doi.org/10.1111/ajt.16233>
- Bethge, T., Hachemi, H. A., Manzetti, J., Gosert, R., Schaffner, W., & Hirsch, H. H. (2015). Sp1 Sites in the Noncoding Control Region of BK Polyomavirus Are Key Regulators of

- Bidirectional Viral Early and Late Gene Expression. *Journal of Virology*, 89(6), 3396–3411. <https://doi.org/10.1128/JVI.03625-14>
- Bhattacharya, M. (2018). Understanding B Lymphocyte Development: A Long Way to Go. *Lymphocytes*. <https://doi.org/10.5772/intechopen.79663>
- Binggeli, S., Egli, A., Schaub, S., Binet, I., Mayr, M., Steiger, J., & Hirsch, H. H. (2007). Polyomavirus BK-specific cellular immune response to VP1 and large T-antigen in kidney transplant recipients. *American Journal of Transplantation: Official Journal of the American Society of Transplantation and the American Society of Transplant Surgeons*, 7(5), 1131–1139. <https://doi.org/10.1111/j.1600-6143.2007.01754.x>
- Blyth, E., Clancy, L., Simms, R., Gaundar, S., O'Connell, P., Micklethwaite, K., & Gottlieb, D. J. (2011). BK virus-specific T cells for use in cellular therapy show specificity to multiple antigens and polyfunctional cytokine responses. *Transplantation*, 92(10), 1077–1084. <https://doi.org/10.1097/TP.0b013e31823328c0>
- Bofill-Mas, S., Formiga-Cruz, M., Clemente-Casares, P., Calafell, F., & Girones, R. (2001). Potential transmission of human polyomaviruses through the gastrointestinal tract after exposure to virions or viral DNA. *Journal of Virology*, 75(21), 10290–10299. <https://doi.org/10.1128/JVI.75.21.10290-10299.2001>
- Bofill-Mas, S., Pina, S., & Girones, R. (2000). Documenting the epidemiologic patterns of polyomaviruses in human populations by studying their presence in urban sewage. *Applied and Environmental Microbiology*, 66(1), 238–245. <https://doi.org/10.1128/aem.66.1.238-245.2000>
- Bohl, D. L., Brennan, D. C., Ryschkewitsch, C., Gaudreault-Keener, M., Major, E. O., & Storch, G. A. (2008). BK virus antibody titers and intensity of infections after renal transplantation. *Journal of Clinical Virology: The Official Publication of the Pan American Society for Clinical Virology*, 43(2), 184–189. <https://doi.org/10.1016/j.jcv.2008.06.009>
- Bohl, D. L., Storch, G. A., Ryschkewitsch, C., Gaudreault-Keener, M., Schnitzler, M. A., Major, E. O., & Brennan, D. C. (2005). Donor origin of BK virus in renal transplantation and role of HLA C7 in susceptibility to sustained BK viremia. *American Journal of Transplantation: Official Journal of the American Society of Transplantation and the American Society of Transplant Surgeons*, 5(9), 2213–2221. <https://doi.org/10.1111/j.1600-6143.2005.01000.x>
- Broekema, N. M., & Imperiale, M. J. (2013). MiRNA regulation of BK polyomavirus replication during early infection. *Proceedings of the National Academy of Sciences*, 110(20), 8200–8205. <https://doi.org/10.1073/pnas.1301907110>
- Buck, C. B., Pastrana, D. V., Lowy, D. R., & Schiller, J. T. (2004). Efficient Intracellular Assembly of Papillomaviral Vectors. *Journal of Virology*, 78(2), 751–757. <https://doi.org/10.1128/JVI.78.2.751-757.2004>
- Burke, J. M., Bass, C. R., Kincaid, R. P., Ulug, E. T., & Sullivan, C. S. (2018). The Murine Polyomavirus MicroRNA Locus Is Required To Promote Viruria during the Acute Phase of Infection. *Journal of Virology*, 92(16). <https://doi.org/10.1128/JVI.02131-17>
- Calvignac-Spencer, S., Feltkamp, M. C. W., Daugherty, M. D., Moens, U., Ramqvist, T., Johne, R., Ehlers, B., & Polyomaviridae Study Group of the International Committee on Taxonomy of Viruses. (2016). A taxonomy update for the family Polyomaviridae. *Archives of Virology*, 161(6), 1739–1750. <https://doi.org/10.1007/s00705-016-2794-y>
- Cao, Y., Su, B., Guo, X., Sun, W., Deng, Y., Bao, L., Zhu, Q., Zhang, X., Zheng, Y., Geng, C., Chai, X., He, R., Li, X., Lv, Q., Zhu, H., Deng, W., Xu, Y., Wang, Y., Qiao, L., ... Xie, X. S. (2020).

- Potent Neutralizing Antibodies against SARS-CoV-2 Identified by High-Throughput Single-Cell Sequencing of Convalescent Patients' B Cells. *Cell*, 182(1), 73-84.e16. <https://doi.org/10.1016/j.cell.2020.05.025>
- Charles A Janeway, J., Travers, P., Walport, M., & Shlomchik, M. J. (2001). The Humoral Immune Response. *Immunobiology: The Immune System in Health and Disease. 5th Edition*. <https://www.ncbi.nlm.nih.gov/books/NBK10752/>
- Chatterjee, M., Weyandt, T. B., & Frisque, R. J. (2000). Identification of archetype and rearranged forms of BK virus in leukocytes from healthy individuals. *Journal of Medical Virology*, 60(3), 353–362.
- Chen, Y., Trofe, J., Gordon, J., Du Pasquier, R. A., Roy-Chaudhury, P., Kuroda, M. J., Woodle, E. S., Khalili, K., & Koralnik, I. J. (2006). Interplay of Cellular and Humoral Immune Responses against BK Virus in Kidney Transplant Recipients with Polyomavirus Nephropathy. *Journal of Virology*, 80(7), 3495–3505. <https://doi.org/10.1128/JVI.80.7.3495-3505.2006>
- Cheungpasitporn, W., Thongprayoon, C., Craici, I. M., Sharma, K., Chesdachai, S., Khoury, N. J., & Ettore, A. S. (2018). Reactivation of BK polyomavirus during pregnancy, vertical transmission, and clinical significance: A meta-analysis. *Journal of Clinical Virology*, 102, 56–62. <https://doi.org/10.1016/j.jcv.2018.02.015>
- Chromy, L. R., Oltman, A., Estes, P. A., & Garcea, R. L. (2006). Chaperone-Mediated In Vitro Disassembly of Polyoma- and Papillomaviruses. *Journal of Virology*, 80(10), 5086–5091. <https://doi.org/10.1128/JVI.80.10.5086-5091.2006>
- Coleman, D. V., Gardner, S. D., Mulholland, C., Fridiksdottir, V., Porter, A. A., Lilford, R., & Valdimarsson, H. (1983). Human polyomavirus in pregnancy. A model for the study of defence mechanisms to virus reactivation. *Clinical and Experimental Immunology*, 53(2), 289–296.
- Colonna-Romano, G., Bulati, M., Aquino, A., Pellicanò, M., Vitello, S., Lio, D., Candore, G., & Caruso, C. (2009). A double-negative (IgD–CD27–) B cell population is increased in the peripheral blood of elderly people. *Mechanisms of Ageing and Development*, 130(10), 681–690. <https://doi.org/10.1016/j.mad.2009.08.003>
- Colonna-Romano, G., Bulati, M., Aquino, A., Vitello, S., Lio, D., Candore, G., & Caruso, C. (2008). B Cell Immunosenescence in the Elderly and in Centenarians. *Rejuvenation Research*, 11(2), 433–439. <https://doi.org/10.1089/rej.2008.0664>
- Corti, D., & Lanzavecchia, A. (2013). Broadly neutralizing antiviral antibodies. *Annual Review of Immunology*, 31, 705–742. <https://doi.org/10.1146/annurev-immunol-032712-095916>
- Corti, D., & Lanzavecchia, A. (2014). Efficient Methods To Isolate Human Monoclonal Antibodies from Memory B Cells and Plasma Cells. *Microbiology Spectrum*, 2(5). <https://doi.org/10.1128/microbiolspec.AID-0018-2014>
- Cosio, F. G., Amer, H., Grande, J. P., Larson, T. S., Stegall, M. D., & Griffin, M. D. (2007). Comparison of Low Versus High Tacrolimus Levels in Kidney Transplantation: Assessment of Efficacy by Protocol Biopsies. *Transplantation*, 83(4), 411–416. <https://doi.org/10.1097/01.tp.0000251807.72246.7d>
- Cowan, K., Tegtmeyer, P., & Anthony, D. D. (1973). Relationship of replication and transcription of Simian Virus 40 DNA. *Proceedings of the National Academy of Sciences of the United States of America*, 70(7), 1927–1930. <https://doi.org/10.1073/pnas.70.7.1927>
- Cox, K. S., Tang, A., Chen, Z., Horton, M. S., Yan, H., Wang, X.-M., Dubey, S. A., DiStefano, D. J., Ettenger, A., Fong, R. H., Doranz, B. J., Casimiro, D. R., & Vora, K. A. (2016). Rapid isolation

- of dengue-neutralizing antibodies from single cell-sorted human antigen-specific memory B-cell cultures. *MAbs*, 8(1), 129–140. <https://doi.org/10.1080/19420862.2015.1109757>
- Cubitt, C. L. (2006). Molecular Genetics of the BK Virus. In N. Ahsan (Ed.), *Polyomaviruses and Human Diseases* (Vol. 577, pp. 85–95). Springer New York. https://doi.org/10.1007/0-387-32957-9_6
- Dauby, N., Kummert, C., Lecomte, S., Liesnard, C., Delforge, M.-L., Donner, C., & Marchant, A. (2014). Primary Human Cytomegalovirus Infection Induces the Expansion of Virus-Specific Activated and Atypical Memory B Cells. *The Journal of Infectious Diseases*, 210(8), 1275–1285. <https://doi.org/10.1093/infdis/jiu255>
- De Benedictis, P., Minola, A., Rota Nodari, E., Aiello, R., Zecchin, B., Salomoni, A., Foglierini, M., Agatic, G., Vanzetta, F., Lavenir, R., Lepelletier, A., Bentley, E., Weiss, R., Cattoli, G., Capua, I., Sallusto, F., Wright, E., Lanzavecchia, A., Bourhy, H., & Corti, D. (2016). Development of broad-spectrum human monoclonal antibodies for rabies post-exposure prophylaxis. *EMBO Molecular Medicine*, 8(4), 407–421. <https://doi.org/10.15252/emmm.201505986>
- De Gascun, C. F., & Carr, M. J. (2013). Human polyomavirus reactivation: Disease pathogenesis and treatment approaches. *Clinical & Developmental Immunology*, 2013, 373579. <https://doi.org/10.1155/2013/373579>
- de Silva, L. M., Bale, P., de Courcy, J., Brown, D., & Knowles, W. (1995). Renal failure due to BK virus infection in an immunodeficient child. *Journal of Medical Virology*, 45(2), 192–196. <https://doi.org/10.1002/jmv.1890450214>
- Dean, D. A., Li, P. P., Lee, L. M., & Kasamatsu, H. (1995). Essential role of the Vp2 and Vp3 DNA-binding domain in simian virus 40 morphogenesis. *Journal of Virology*, 69(2), 1115–1121. <https://doi.org/10.1128/JVI.69.2.1115-1121.1995>
- Dolei, A., Pietropaolo, V., Gomes, E., Di Taranto, C., Ziccheddu, M., Spanu, M. A., Lavorino, C., Manca, M., & Degener, A. M. (2000). Polyomavirus persistence in lymphocytes: Prevalence in lymphocytes from blood donors and healthy personnel of a blood transfusion centre. *Journal of General Virology*, 81(8), 1967–1973. <https://doi.org/10.1099/0022-1317-81-8-1967>
- Dörner, T., Radbruch, A., & Burmester, G. R. (2009). B-cell-directed therapies for autoimmune disease. *Nature Reviews Rheumatology*, 5(8), 433–441. <https://doi.org/10.1038/nrrheum.2009.141>
- Drachenberg, C. B., Papadimitriou, J. C., Wali, R., Cubitt, C. L., & Ramos, E. (2003). BK polyoma virus allograft nephropathy: Ultrastructural features from viral cell entry to lysis. *American Journal of Transplantation: Official Journal of the American Society of Transplantation and the American Society of Transplant Surgeons*, 3(11), 1383–1392. <https://doi.org/10.1046/j.1600-6135.2003.00237.x>
- Drake, D. R., Moser, J. M., Hadley, A., Altman, J. D., Maliszewski, C., Butz, E., & Lukacher, A. E. (2000). Polyomavirus-infected dendritic cells induce antiviral CD8(+) T lymphocytes. *Journal of Virology*, 74(9), 4093–4101. <https://doi.org/10.1128/jvi.74.9.4093-4101.2000>
- Drake, Donald R., Shawver, M. L., Hadley, A., Butz, E., Maliszewski, C., & Lukacher, A. E. (2001). Induction of Polyomavirus-Specific CD8+T Lymphocytes by Distinct Dendritic Cell Subpopulations. *Journal of Virology*, 75(1), 544–547. <https://doi.org/10.1128/JVI.75.1.544-547.2001>

- Dugan, A. S., Eash, S., & Atwood, W. J. (2005). An N-linked glycoprotein with alpha(2,3)-linked sialic acid is a receptor for BK virus. *Journal of Virology*, *79*(22), 14442–14445. <https://doi.org/10.1128/JVI.79.22.14442-14445.2005>
- Dugan, A. S., Gasparovic, M. L., Tsomaia, N., Mierke, D. F., O’Hara, B. A., Manley, K., & Atwood, W. J. (2007). Identification of Amino Acid Residues in BK Virus VP1 That Are Critical for Viability and Growth. *Journal of Virology*, *81*(21), 11798–11808. <https://doi.org/10.1128/JVI.01316-07>
- Dugan, A. S., Maginnis, M. S., Jordan, J. A., Gasparovic, M. L., Manley, K., Page, R., Williams, G., Porter, E., O’Hara, B. A., & Atwood, W. J. (2008). Human α -Defensins Inhibit BK Virus Infection by Aggregating Virions and Blocking Binding to Host Cells. *The Journal of Biological Chemistry*, *283*(45), 31125–31132. <https://doi.org/10.1074/jbc.M805902200>
- Dunn-Walters, D. K., Isaacson, P. G., & Spencer, J. (1996). Sequence analysis of rearranged IgVH genes from microdissected human Peyer’s patch marginal zone B cells. *Immunology*, *88*(4), 618–624.
- Eash, S., Manley, K., Gasparovic, M., Querbes, W., & Atwood, W. J. (2006). The human polyomaviruses. *Cellular and Molecular Life Sciences CMLS*, *63*(7–8), 865–876. <https://doi.org/10.1007/s00018-005-5454-z>
- Eash, Sylvia, & Atwood, W. J. (2005). Involvement of cytoskeletal components in BK virus infectious entry. *Journal of Virology*, *79*(18), 11734–11741. <https://doi.org/10.1128/JVI.79.18.11734-11741.2005>
- Eash, Sylvia, Querbes, W., & Atwood, W. J. (2004). Infection of vero cells by BK virus is dependent on caveolae. *Journal of Virology*, *78*(21), 11583–11590. <https://doi.org/10.1128/JVI.78.21.11583-11590.2004>
- Egli, A., Infanti, L., Dumoulin, A., Buser, A., Samaridis, J., Stebler, C., Gosert, R., & Hirsch, H. H. (2009). Prevalence of Polyomavirus BK and JC Infection and Replication in 400 Healthy Blood Donors. *The Journal of Infectious Diseases*, *199*(6), 837–846. <https://doi.org/10.1086/597126>
- Ehrenstein, M. R., & Notley, C. A. (2010). The importance of natural IgM: Scavenger, protector and regulator. *Nature Reviews Immunology*, *10*(11), 778–786. <https://doi.org/10.1038/nri2849>
- Ehrhardt, G. R. A., Hsu, J. T., Gartland, L., Leu, C.-M., Zhang, S., Davis, R. S., & Cooper, M. D. (2005). Expression of the immunoregulatory molecule FcRH4 defines a distinctive tissue-based population of memory B cells. *The Journal of Experimental Medicine*, *202*(6), 783–791. <https://doi.org/10.1084/jem.20050879>
- Erickson, K. D., Bouchet-Marquis, C., Heiser, K., Szomolanyi-Tsuda, E., Mishra, R., Lamothe, B., Hoenger, A., & Garcea, R. L. (2012). Virion assembly factories in the nucleus of polyomavirus-infected cells. *PLoS Pathogens*, *8*(4), e1002630. <https://doi.org/10.1371/journal.ppat.1002630>
- Evans, G. L., Caller, L. G., Foster, V., & Crump, C. M. (2015). Anion homeostasis is important for non-lytic release of BK polyomavirus from infected cells. *Open Biology*, *5*(8). <https://doi.org/10.1098/rsob.150041>
- Fan, Y., Bai, H., Qian, Y., Sun, Z., & Shi, B. (2019). CD4+ T Cell Immune Response to VP1 and VP3 in BK Virus Infected Recipients of Renal Transplantation. *Surgical Infections*, *20*(3), 236–243. <https://doi.org/10.1089/sur.2018.116>

- Fauquet, C. M., & Mayo, M. A. (2001). The 7 th ICTV Report. *Archives of Virology*, 146(1), 189–194. <https://doi.org/10.1007/s007050170203>
- Fazilleau, N., Eisenbraun, M. D., Malherbe, L., Ebright, J. N., Pogue-Caley, R. R., McHeyzer-Williams, L. J., & McHeyzer-Williams, M. G. (2007). Lymphoid reservoirs of antigen-specific memory T helper cells. *Nature Immunology*, 8(7), 753–761. <https://doi.org/10.1038/ni1472>
- Fecteau, J. F., Côté, G., & Néron, S. (2006). A new memory CD27-IgG+ B cell population in peripheral blood expressing VH genes with low frequency of somatic mutation. *Journal of Immunology (Baltimore, Md.: 1950)*, 177(6), 3728–3736. <https://doi.org/10.4049/jimmunol.177.6.3728>
- Fiore, T., Martin, E., Descamps, V., Brochot, E., Morel, V., Handala, L., Dakroub, F., Castelain, S., Duverlie, G., Helle, F., & François, C. (2020). Indoleamine 2,3-Dioxygenase Is Involved in Interferon Gamma's Anti-BKPyV Activity in Renal Cells. *Viruses*, 12(8). <https://doi.org/10.3390/v12080865>
- Funk, G. A., Gosert, R., Comoli, P., Ginevri, F., & Hirsch, H. H. (2008). Polyomavirus BK replication dynamics in vivo and in silico to predict cytopathology and viral clearance in kidney transplants. *American Journal of Transplantation: Official Journal of the American Society of Transplantation and the American Society of Transplant Surgeons*, 8(11), 2368–2377. <https://doi.org/10.1111/j.1600-6143.2008.02402.x>
- Gabardi, S., Waikar, S. S., Martin, S., Roberts, K., Chen, J., Borgi, L., Sheashaa, H., Dyer, C., Malek, S. K., Tullius, S. G., Vadivel, N., Grafals, M., Abdi, R., Najafian, N., Milford, E., & Chandraker, A. (2010). Evaluation of fluoroquinolones for the prevention of BK viremia after renal transplantation. *Clinical Journal of the American Society of Nephrology: CJASN*, 5(7), 1298–1304. <https://doi.org/10.2215/CJN.08261109>
- Galindo-Campos, M. A., Bedora-Faure, M., Farrés, J., Lescale, C., Moreno-Lama, L., Martínez, C., Martín-Caballero, J., Ampurdanés, C., Aparicio, P., Dantzer, F., Cerutti, A., Deriano, L., & Yélamos, J. (2019). Coordinated signals from the DNA repair enzymes PARP-1 and PARP-2 promotes B-cell development and function. *Cell Death & Differentiation*, 26(12), 2667–2681. <https://doi.org/10.1038/s41418-019-0326-5>
- Garcea, R. L., Salunke, D. M., & Caspar, D. L. D. (1987). Site-directed mutation affecting polyomavirus capsid self-assembly in vitro. *Nature*, 329(6134), 86–87. <https://doi.org/10.1038/329086a0>
- Gardner, S. D. (1973). Prevalence in England of Antibody to Human Polyomavirus (B.K.). *BMJ*, 1(5845), 77–78. <https://doi.org/10.1136/bmj.1.5845.77>
- Gardner, S. D., MacKenzie, E. F., Smith, C., & Porter, A. A. (1984). Prospective study of the human polyomaviruses BK and JC and cytomegalovirus in renal transplant recipients. *Journal of Clinical Pathology*, 37(5), 578–586.
- Gardner, Sylvia D., Field, Anne M., Coleman, Dulcie V., & Hulme, B. (1971). New human papovavirus (B.K.) isolated from urine after renal transplantation. *The Lancet*, 297(7712), 1253–1257. [https://doi.org/10.1016/S0140-6736\(71\)91776-4](https://doi.org/10.1016/S0140-6736(71)91776-4)
- Gedvilaite, A., Dorn, D. C., Sasnauskas, K., Pecher, G., Bulavaite, A., Lawatscheck, R., Staniulis, J., Dalianis, T., Ramqvist, T., Schönrich, G., Raftery, M. J., & Ulrich, R. (2006). Virus-like particles derived from major capsid protein VP1 of different polyomaviruses differ in their ability to induce maturation in human dendritic cells. *Virology*, 354(2), 252–260. <https://doi.org/10.1016/j.virol.2006.07.007>

- Gibney, K. B., Edupuganti, S., Panella, A. J., Kosoy, O. I., Delorey, M. J., Lanciotti, R. S., Mulligan, M. J., Fischer, M., & Staples, J. E. (2012). Detection of Anti-Yellow Fever Virus Immunoglobulin M Antibodies at 3–4 Years Following Yellow Fever Vaccination. *The American Journal of Tropical Medicine and Hygiene*, *87*(6), 1112–1115. <https://doi.org/10.4269/ajtmh.2012.12-0182>
- Giesecke, C., Frölich, D., Reiter, K., Mei, H. E., Wirries, I., Kuhly, R., Killig, M., Glatzer, T., Stölzel, K., Perka, C., Lipsky, P. E., & Dörner, T. (2014). Tissue Distribution and Dependence of Responsiveness of Human Antigen-Specific Memory B Cells. *The Journal of Immunology*, *192*(7), 3091–3100. <https://doi.org/10.4049/jimmunol.1302783>
- Gillock, E. T., Rottinghaus, S., Chang, D., Cai, X., Smiley, S. A., An, K., & Consigli, R. A. (1997). Polyomavirus major capsid protein VP1 is capable of packaging cellular DNA when expressed in the baculovirus system. *Journal of Virology*, *71*(4), 2857–2865. <https://doi.org/10.1128/JVI.71.4.2857-2865.1997>
- Gilman, M. S. A., Castellanos, C. A., Chen, M., Ngwuta, J. O., Goodwin, E., Moin, S. M., Mas, V., Melero, J. A., Wright, P. F., Graham, B. S., McLellan, J. S., & Walker, L. M. (2016). Rapid profiling of RSV antibody repertoires from the memory B cells of naturally infected adult donors. *Science Immunology*, *1*(6). <https://doi.org/10.1126/sciimmunol.aaj1879>
- Ginevri, F., Azzi, A., Hirsch, H. H., Basso, S., Fontana, I., Cioni, M., Bodaghi, S., Salotti, V., Rinieri, A., Botti, G., Perfumo, F., Locatelli, F., & Comoli, P. (2007). Prospective monitoring of polyomavirus BK replication and impact of pre-emptive intervention in pediatric kidney recipients. *American Journal of Transplantation: Official Journal of the American Society of Transplantation and the American Society of Transplant Surgeons*, *7*(12), 2727–2735. <https://doi.org/10.1111/j.1600-6143.2007.01984.x>
- Giraldi, C., Noto, A., Tenuta, R., Greco, F., Perugini, D., Dodaro, S., Spadafora, M., Lo Bianco, A. M., Savino, O., Papalia, T., Greco, R., & Bonofiglio, R. (2007). Prospective study of BKV nephropathy in 117 renal transplant recipients. *The New Microbiologica*, *30*(2), 127–130.
- Gong, S., & Ruprecht, R. M. (2020). Immunoglobulin M: An Ancient Antiviral Weapon – Rediscovered. *Frontiers in Immunology*, *11*. <https://doi.org/10.3389/fimmu.2020.01943>
- Goodwin, E., Gilman, M. S. A., Wrapp, D., Chen, M., Ngwuta, J. O., Moin, S. M., Bai, P., Sivasubramanian, A., Connor, R. I., Wright, P. F., Graham, B. S., McLellan, J. S., & Walker, L. M. (2018). Infants Infected with Respiratory Syncytial Virus Generate Potent Neutralizing Antibodies that Lack Somatic Hypermutation. *Immunity*, *48*(2), 339–349.e5. <https://doi.org/10.1016/j.immuni.2018.01.005>
- Gosert, R., Rinaldo, C. H., Funk, G. A., Egli, A., Ramos, E., Drachenberg, C. B., & Hirsch, H. H. (2008). Polyomavirus BK with rearranged noncoding control region emerge in vivo in renal transplant patients and increase viral replication and cytopathology. *Journal of Experimental Medicine*, *205*(4), 841–852. <https://doi.org/10.1084/jem.20072097>
- Goudsmit, J., Dillen, P. W., van Strien, A., & van der Noordaa, J. (1982). The role of BK virus in acute respiratory tract disease and the presence of BKV DNA in tonsils. *Journal of Medical Virology*, *10*(2), 91–99. <https://doi.org/10.1002/jmv.1890100203>
- Green, L. L., Hardy, M. C., Maynard-Currie, C. E., Tsuda, H., Louie, D. M., Mendez, M. J., Abderrahim, H., Noguchi, M., Smith, D. H., Zeng, Y., David, N. E., Sasai, H., Garza, D., Brenner, D. G., Hales, J. F., McGuinness, R. P., Capon, D. J., Klapholz, S., & Jakobovits, A. (1994). Antigen-specific human monoclonal antibodies from mice engineered with human Ig heavy and light chain YACs. *Nature Genetics*, *7*(1), 13–21. <https://doi.org/10.1038/ng0594-13>

- Gross, L. (1953). A Filterable Agent, Recovered from Ak Leukemic Extracts, Causing Salivary Gland Carcinomas in C3H Mice. *Experimental Biology and Medicine*, 83(2), 414–421. <https://doi.org/10.3181/00379727-83-20376>
- Guasch, A., Roy-Chaudhury, P., Woodle, E. S., Fitzsimmons, W., Holman, J., First, M. R., & FK778 BK Nephropathy Study Group. (2010). Assessment of efficacy and safety of FK778 in comparison with standard care in renal transplant recipients with untreated BK nephropathy. *Transplantation*, 90(8), 891–897. <https://doi.org/10.1097/TP.0b013e3181f2c94b>
- Haghverdi, L., Büttner, M., Wolf, F. A., Buettner, F., & Theis, F. J. (2016). Diffusion pseudotime robustly reconstructs lineage branching. *Nature Methods*, 13(10), 845–848. <https://doi.org/10.1038/nmeth.3971>
- Handala, L., Blanchard, E., Raynal, P.-I., Roingeard, P., Morel, V., Descamps, V., Castelain, S., Francois, C., Duverlie, G., Brochot, E., & Helle, F. (2020). BK Polyomavirus Hijacks Extracellular Vesicles for En Bloc Transmission. *Journal of Virology*, 94(6). <https://doi.org/10.1128/JVI.01834-19>
- Hariharan, S., Cohen, E. P., Vasudev, B., Orentas, R., Viscidi, R. P., Kakela, J., & DuChateau, B. (2005). BK virus-specific antibodies and BKV DNA in renal transplant recipients with BKV nephritis. *American Journal of Transplantation: Official Journal of the American Society of Transplantation and the American Society of Transplant Surgeons*, 5(11), 2719–2724. <https://doi.org/10.1111/j.1600-6143.2005.01080.x>
- Harris, K F, Christensen, J. B., & Imperiale, M. J. (1996). BK virus large T antigen: Interactions with the retinoblastoma family of tumor suppressor proteins and effects on cellular growth control. *Journal of Virology*, 70(4), 2378–2386. <https://doi.org/10.1128/JVI.70.4.2378-2386.1996>
- Harris, Kimya F., Christensen, J. B., Radany, E. H., & Imperiale, M. J. (1998). Novel Mechanisms of E2F Induction by BK Virus Large-T Antigen: Requirement of Both the pRb-Binding and the J Domains. *Molecular and Cellular Biology*, 18(3), 1746–1756. <https://doi.org/10.1128/MCB.18.3.1746>
- Haynes, J. I., Chang, D., & Consigli, R. A. (1993). Mutations in the putative calcium-binding domain of polyomavirus VP1 affect capsid assembly. *Journal of Virology*, 67(5), 2486–2495. <https://doi.org/10.1128/JVI.67.5.2486-2495.1993>
- Helle, F., Brochot, E., Handala, L., Martin, E., Castelain, S., Francois, C., & Duverlie, G. (2017). Biology of the BKPyV: An Update. *Viruses*, 9(11), 327. <https://doi.org/10.3390/v9110327>
- Hendricks, J., Bos, N. A., & Kroese, F. G. M. (2018). Heterogeneity of Memory Marginal Zone B Cells. *Critical Reviews in Immunology*, 38(2), 145–158. <https://doi.org/10.1615/CritRevImmunol.2018024985>
- Henriksen, S., Mittelholzer, C., Gosert, R., Hirsch, H. H., & Rinaldo, C. H. (2015). Human BK Polyomavirus Plasmid pBKV (34-2) (Dunlop) Contains Mutations Not Found in the Originally Published Sequences. *Genome Announcements*, 3(2). <https://doi.org/10.1128/genomeA.00046-15>
- Heritage, J., Chesters, P. M., & McCance, D. J. (1981). The persistence of papovavirus BK DNA sequences in normal human renal tissue. *Journal of Medical Virology*, 8(2), 143–150. <https://doi.org/10.1002/jmv.1890080208>
- Hirsch, H. H., Randhawa, P., & the AST Infectious Diseases Community of Practice. (2013). BK Polyomavirus in Solid Organ Transplantation: BK Polyomavirus in Solid Organ

- Transplantation. *American Journal of Transplantation*, 13(s4), 179–188. <https://doi.org/10.1111/ajt.12110>
- Hirsch, H. H., & Snydman, D. R. (2005). BK Virus: Opportunity Makes a Pathogen. *Clinical Infectious Diseases*, 41(3), 354–360. <https://doi.org/10.1086/431488>
- Hirsch, Hans H., Brennan, D. C., Drachenberg, C. B., Ginevri, F., Gordon, J., Limaye, A. P., Mihatsch, M. J., Nickleit, V., Ramos, E., Randhawa, P., Shapiro, R., Steiger, J., Suthanthiran, M., & Trofe, J. (2005). Polyomavirus-Associated Nephropathy in Renal Transplantation: Interdisciplinary Analyses and Recommendations: *Transplantation*, 79(10), 1277–1286. <https://doi.org/10.1097/01.TP.0000156165.83160.09>
- Hirsch, Hans H., Knowles, W., Dickenmann, M., Passweg, J., Klimkait, T., Mihatsch, M. J., & Steiger, J. (2002). Prospective Study of Polyomavirus Type BK Replication and Nephropathy in Renal-Transplant Recipients. *New England Journal of Medicine*, 347(7), 488–496. <https://doi.org/10.1056/NEJMoa020439>
- Hirsch, Hans H., & Steiger, J. (2003). Polyomavirus BK. *The Lancet. Infectious Diseases*, 3(10), 611–623. [https://doi.org/10.1016/s1473-3099\(03\)00770-9](https://doi.org/10.1016/s1473-3099(03)00770-9)
- Hisadome, Y., Noguchi, H., Nakafusa, Y., Sakihama, K., Mei, T., Kaku, K., Okabe, Y., Masutani, K., Ohara, Y., Ikeda, K., Oda, Y., & Nakamura, M. (2020). Association of Pretransplant BK Polyomavirus Antibody Status with BK Polyomavirus Infection After Kidney Transplantation: A Prospective Cohort Pilot Study of 47 Transplant Recipients. *Transplantation Proceedings*, 52(6), 1762–1768. <https://doi.org/10.1016/j.transproceed.2020.01.164>
- Hurdiss, D. L., Morgan, E. L., Thompson, R. F., Prescott, E. L., Panou, M. M., Macdonald, A., & Ranson, N. A. (2016). New Structural Insights into the Genome and Minor Capsid Proteins of BK Polyomavirus using Cryo-Electron Microscopy. *Structure*, 24(4), 528–536. <https://doi.org/10.1016/j.str.2016.02.008>
- Isnardi, I., Ng, Y.-S., Menard, L., Meyers, G., Saadoun, D., Srdanovic, I., Samuels, J., Berman, J., Buckner, J. H., Cunningham-Rundles, C., & Meffre, E. (2010). Complement receptor 2/CD21– human naive B cells contain mostly autoreactive unresponsive clones. *Blood*, 115(24), 5026–5036. <https://doi.org/10.1182/blood-2009-09-243071>
- Jamboti, J. S. (2016). BK virus nephropathy in renal transplant recipients. *Nephrology (Carlton, Vic.)*, 21(8), 647–654. <https://doi.org/10.1111/nep.12728>
- Jiang, M., Abend, J. R., Tsai, B., & Imperiale, M. J. (2009). Early Events during BK Virus Entry and Disassembly. *Journal of Virology*, 83(3), 1350–1358. <https://doi.org/10.1128/JVI.02169-08>
- Jin, L., Gibson, P. E., Booth, J. C., & Clewley, J. P. (1993). Genomic typing of BK virus in clinical specimens by direct sequencing of polymerase chain reaction products. *Journal of Medical Virology*, 41(1), 11–17. <https://doi.org/10.1002/jmv.1890410104>
- Jin, L., Gibson, P. E., Knowles, W. A., & Clewley, J. P. (1993). BK virus antigenic variants: Sequence analysis within the capsid VP1 epitope. *Journal of Medical Virology*, 39(1), 50–56. <https://doi.org/10.1002/jmv.1890390110>
- Johannessen, M., Myhre, M. R., Dragset, M., Tümmler, C., & Moens, U. (2008). Phosphorylation of human polyomavirus BK agnoprotein at Ser-11 is mediated by PKC and has an important regulative function. *Virology*, 379(1), 97–109. <https://doi.org/10.1016/j.virol.2008.06.007>

- Johannessen, M., Walquist, M., Gerits, N., Dragset, M., Spang, A., & Moens, U. (2011). BKV Agnoprotein Interacts with α -Soluble N-Ethylmaleimide-Sensitive Fusion Attachment Protein, and Negatively Influences Transport of VSVG-EGFP. *PLOS ONE*, 6(9), e24489. <https://doi.org/10.1371/journal.pone.0024489>
- Jones, K., Savulescu, A. F., Brombacher, F., & Hadebe, S. (2020). Immunoglobulin M in Health and Diseases: How Far Have We Come and What Next? *Frontiers in Immunology*, 11. <https://doi.org/10.3389/fimmu.2020.595535>
- Joo, H. M., He, Y., & Sangster, M. Y. (2008). Broad dispersion and lung localization of virus-specific memory B cells induced by influenza pneumonia. *Proceedings of the National Academy of Sciences of the United States of America*, 105(9), 3485–3490. <https://doi.org/10.1073/pnas.0800003105>
- Josephson, M. A., Gillen, D., Javaid, B., Kadambi, P., Meehan, S., Foster, P., Harland, R., Thistlethwaite, R. J., Garfinkel, M., Atwood, W., Jordan, J., Sadhu, M., Millis, M. J., & Williams, J. (2006). Treatment of Renal Allograft Polyoma BK Virus Infection with Leflunomide: *Transplantation*, 81(5), 704–710. <https://doi.org/10.1097/01.tp.0000181149.76113.50>
- Judith A Owen, Jenni Punt, & Sharon A Stranford. (2013). *Kuby Immunology* (7th edition). Susan Winslow.
- Kariminik, A., Yaghobi, R., & Dabiri, S. (2016). Innate Immunity and BK Virus: Prospective Strategies. *Viral Immunology*, 29(2), 74–82. <https://doi.org/10.1089/vim.2015.0099>
- Kaufmann, S. H. E. (2017). Remembering Emil von Behring: From Tetanus Treatment to Antibody Cooperation with Phagocytes. *MBio*, 8(1). <https://doi.org/10.1128/mBio.00117-17>
- Kean, J. M., Rao, S., Wang, M., & Garcea, R. L. (2009). Seroepidemiology of Human Polyomaviruses. *PLoS Pathogens*, 5(3), e1000363. <https://doi.org/10.1371/journal.ppat.1000363>
- Kidney Disease: Improving Global Outcomes (KDIGO) Transplant Work Group. (2009). KDIGO clinical practice guideline for the care of kidney transplant recipients. *American Journal of Transplantation: Official Journal of the American Society of Transplantation and the American Society of Transplant Surgeons*, 9 Suppl 3, S1-155. <https://doi.org/10.1111/j.1600-6143.2009.02834.x>
- Kim, M. H., Lee, Y. H., Seo, J.-W., Moon, H., Kim, J. S., Kim, Y. G., Jeong, K.-H., Moon, J.-Y., Lee, T. W., Ihm, C.-G., Kim, C.-D., Park, J. B., Chung, B. H., Kim, Y.-H., & Lee, S.-H. (2017). Urinary exosomal viral microRNA as a marker of BK virus nephropathy in kidney transplant recipients. *PLOS ONE*, 12(12), e0190068. <https://doi.org/10.1371/journal.pone.0190068>
- Kim, S. C., Wang, J., Dong, Y., Mathews, D. V., Albrecht, J. A., Breeden, C. P., Farris, A. B., Lukacher, A. E., Ford, M. L., Newell, K. A., & Adams, A. B. (2017). Alloimmunity But Not Viral Immunity Promotes Allograft Loss in a Mouse Model of Polyomavirus-Associated Allograft Injury. *Transplantation Direct*, 3(6), e161. <https://doi.org/10.1097/TXD.0000000000000677>
- Klasse, P. J. (2014). Neutralization of Virus Infectivity by Antibodies: Old Problems in New Perspectives. *Advances in Biology*, 2014. <https://doi.org/10.1155/2014/157895>
- Klasse, P. J., & Sattentau, Q. J. (2002). Occupancy and mechanism in antibody-mediated neutralization of animal viruses. *The Journal of General Virology*, 83(Pt 9), 2091–2108. <https://doi.org/10.1099/0022-1317-83-9-2091>

- Klein, U., Rajewsky, K., & Küppers, R. (1998). Human immunoglobulin (Ig)M+IgD+ peripheral blood B cells expressing the CD27 cell surface antigen carry somatically mutated variable region genes: CD27 as a general marker for somatically mutated (memory) B cells. *The Journal of Experimental Medicine*, 188(9), 1679–1689. <https://doi.org/10.1084/jem.188.9.1679>
- Klenovsek, K., Weisel, F., Schneider, A., Appelt, U., Jonjic, S., Messerle, M., Bradel-Tretheway, B., Winkler, T. H., & Mach, M. (2007). Protection from CMV infection in immunodeficient hosts by adoptive transfer of memory B cells. *Blood*, 110(9), 3472–3479. <https://doi.org/10.1182/blood-2007-06-095414>
- Knoll, G. A., Humar, A., Fergusson, D., Johnston, O., House, A. A., Kim, S. J., Ramsay, T., Chassé, M., Pang, X., Zaltzman, J., Cockfield, S., Cantarovich, M., Karpinski, M., Lebel, L., & Gill, J. S. (2014). Levofloxacin for BK Virus Prophylaxis Following Kidney Transplantation: A Randomized Clinical Trial. *JAMA*, 312(20), 2106. <https://doi.org/10.1001/jama.2014.14721>
- Knowles, W. A., Gibson, P. E., & Gardner, S. D. (1989). Serological typing scheme for BK-like isolates of human polyomavirus. *Journal of Medical Virology*, 28(2), 118–123. <https://doi.org/10.1002/jmv.1890280212>
- Koh, M. J., Lim, B. J., Noh, S., Kim, Y. H., & Jeong, H. J. (2012). Urinary decoy cell grading and its clinical implications. *Korean Journal of Pathology*, 46(3), 233–236. <https://doi.org/10.4132/KoreanJPathol.2012.46.3.233>
- Köhler, G., & Milstein, C. (1975). Continuous cultures of fused cells secreting antibody of predefined specificity. *Nature*, 256(5517), 495–497. <https://doi.org/10.1038/256495a0>
- Krejci, K., Tichy, T., Bednarikova, J., Zamboch, K., & Zadrazil, J. (2018). BK virus-induced renal allograft nephropathy. *Biomedical Papers of the Medical Faculty of the University Palacky, Olomouc, Czechoslovakia*, 162(3), 165–177. <https://doi.org/10.5507/bp.2018.018>
- Krzyzak, L., Seitz, C., Urvat, A., Hutzler, S., Ostalecki, C., Gläsner, J., Hiergeist, A., Gessner, A., Winkler, T. H., Steinkasserer, A., & Nitschke, L. (2016). CD83 Modulates B Cell Activation and Germinal Center Responses. *Journal of Immunology (Baltimore, Md.: 1950)*, 196(9), 3581–3594. <https://doi.org/10.4049/jimmunol.1502163>
- Kurosaki, T., Kometani, K., & Ise, W. (2015). Memory B cells. *Nature Reviews Immunology*, 15(3), 149–159. <https://doi.org/10.1038/nri3802>
- Lamarche, C., Orio, J., Collette, S., Senécal, L., Hébert, M.-J., Renoult, É., Tibbles, L. A., & Delisle, J.-S. (2016). BK Polyomavirus and the Transplanted Kidney: Immunopathology and Therapeutic Approaches. *Transplantation*, 100(11), 2276–2287. <https://doi.org/10.1097/TP.0000000000001333>
- Leach, S., Shinnakasu, R., Adachi, Y., Momota, M., Makino-Okamura, C., Yamamoto, T., Ishii, K. J., Fukuyama, H., Takahashi, Y., & Kurosaki, T. (2019). Requirement for memory B-cell activation in protection from heterologous influenza virus reinfection. *International Immunology*, 31(12), 771–779. <https://doi.org/10.1093/intimm/dxz049>
- Leboeuf, C., Wilk, S., Achermann, R., Binet, I., Golshayan, D., Hadaya, K., Hirzel, C., Hoffmann, M., Huynh-Do, U., Koller, M. T., Manuel, O., Mueller, N. J., Mueller, T. F., Schaub, S., van Delden, C., Weissbach, F. H., Hirsch, H. H., & Swiss Transplant Cohort Study. (2017). BK Polyomavirus-Specific 9mer CD8 T Cell Responses Correlate With Clearance of BK Viremia in Kidney Transplant Recipients: First Report From the Swiss Transplant Cohort Study. *American Journal of Transplantation: Official Journal of the American Society of*

- Transplantation and the American Society of Transplant Surgeons*, 17(10), 2591–2600. <https://doi.org/10.1111/ajt.14282>
- Lenti, M. V., Aronico, N., Pellegrino, I., Boveri, E., Giuffrida, P., Borrelli de Andreis, F., Morbini, P., Vanelli, L., Pasini, A., Ubezio, C., Melazzini, F., Rascaroli, A., Antoci, V., Merli, S., Di Terlizzi, F., Sabatini, U., Cambiè, G., Tenore, A., Picone, C., ... Di Sabatino, A. (2020). Depletion of circulating IgM memory B cells predicts unfavourable outcome in COVID-19. *Scientific Reports*, 10(1), 20836. <https://doi.org/10.1038/s41598-020-77945-8>
- Letunic, I., & Bork, P. (2019). Interactive Tree Of Life (iTOL) v4: Recent updates and new developments. *Nucleic Acids Research*, 47(W1), W256–W259. <https://doi.org/10.1093/nar/gkz239>
- Leuenberger, D., Andresen, P. A., Gosert, R., Binggeli, S., Ström, E. H., Bodaghi, S., Rinaldo, C. H., & Hirsch, H. H. (2007). Human Polyomavirus Type 1 (BK Virus) Agnoprotein Is Abundantly Expressed but Immunologically Ignored. *Clinical and Vaccine Immunology*, 14(8), 959–968. <https://doi.org/10.1128/CVI.00123-07>
- Li, J. Y. Z., McNicholas, K., Yong, T. Y., Rao, N., Coates, P. T. H., Higgins, G. D., Carroll, R. P., Woodman, R. J., Michael, M. Z., & Gleadle, J. M. (2014). BK Virus Encoded MicroRNAs Are Present in Blood of Renal Transplant Recipients With BK Viral Nephropathy: BK Virus MicroRNAs in Renal Transplant Recipients. *American Journal of Transplantation*, 14(5), 1183–1190. <https://doi.org/10.1111/ajt.12694>
- Liacini, A., Seamone, M. E., Muruve, D. A., & Tibbles, L. A. (2010). Anti-BK virus mechanisms of sirolimus and leflunomide alone and in combination: Toward a new therapy for BK virus infection. *Transplantation*, 90(12), 1450–1457. <https://doi.org/10.1097/TP.0b013e3182007be2>
- Lindner, C., Thomsen, I., Wahl, B., Ugur, M., Sethi, M. K., Friedrichsen, M., Smoczek, A., Ott, S., Baumann, U., Suerbaum, S., Schreiber, S., Bleich, A., Gaboriau-Routhiau, V., Cerf-Bensussan, N., Hazanov, H., Mehr, R., Boysen, P., Rosenstiel, P., & Pabst, O. (2015). Diversification of memory B cells drives the continuous adaptation of secretory antibodies to gut microbiota. *Nature Immunology*, 16(8), 880–888. <https://doi.org/10.1038/ni.3213>
- Lindner, J. M., Cornacchione, V., Sathe, A., Be, C., Srinivas, H., Riquet, E., Leber, X.-C., Hein, A., Wrobel, M. B., Scharenberg, M., Pietzonka, T., Wiesmann, C., Abend, J., & Traggiai, E. (2019). Human Memory B Cells Harbor Diverse Cross-Neutralizing Antibodies against BK and JC Polyomaviruses. *Immunity*, 50(3), 668–676.e5. <https://doi.org/10.1016/j.immuni.2019.02.003>
- Lindstrom, D. M., & Dulbecco, R. (1972). Strand orientation of simian virus 40 transcription in productively infected cells. *Proceedings of the National Academy of Sciences of the United States of America*, 69(6), 1517–1520. <https://doi.org/10.1073/pnas.69.6.1517>
- Liu, Y. J., Barthélémy, C., de Bouteiller, O., Arpin, C., Durand, I., & Banchereau, J. (1995). Memory B cells from human tonsils colonize mucosal epithelium and directly present antigen to T cells by rapid up-regulation of B7-1 and B7-2. *Immunity*, 2(3), 239–248. [https://doi.org/10.1016/1074-7613\(95\)90048-9](https://doi.org/10.1016/1074-7613(95)90048-9)
- Lizeng, Q., Nilsson, C., Sourial, S., Andersson, S., Larsen, O., Aaby, P., Ehnlund, M., & Björling, E. (2004). Potent Neutralizing Serum Immunoglobulin A (IgA) in Human Immunodeficiency Virus Type 2-Exposed IgG-Seronegative Individuals. *Journal of Virology*, 78(13), 7016–7022. <https://doi.org/10.1128/JVI.78.13.7016-7022.2004>

- Lonberg, N., Taylor, L. D., Harding, F. A., Trounstein, M., Higgins, K. M., Schramm, S. R., Kuo, C. C., Mashayekh, R., Wymore, K., & McCabe, J. G. (1994). Antigen-specific human antibodies from mice comprising four distinct genetic modifications. *Nature*, *368*(6474), 856–859. <https://doi.org/10.1038/368856a0>
- Lonergan, R. M., Carr, M. J., De Gascun, C. F., Costelloe, L. F., Waters, A., Coughlan, S., Duggan, M., Doyle, K., Jordan, S., Hutchinson, M. W., Hall, W. W., & Tubridy, N. J. (2009). Reactivation of BK polyomavirus in patients with multiple sclerosis receiving natalizumab therapy. *Journal of Neurovirology*, *15*(5–6), 351–359. <https://doi.org/10.3109/13550280903131923>
- Low, J. A., Magnuson, B., Tsai, B., & Imperiale, M. J. (2006). Identification of gangliosides GD1b and GT1b as receptors for BK virus. *Journal of Virology*, *80*(3), 1361–1366. <https://doi.org/10.1128/JVI.80.3.1361-1366.2006>
- Low, J., Humes, H. D., Szczypka, M., & Imperiale, M. (2004). BKV and SV40 infection of human kidney tubular epithelial cells in vitro. *Virology*, *323*(2), 182–188. <https://doi.org/10.1016/j.virol.2004.03.027>
- Lu, R.-M., Hwang, Y.-C., Liu, I.-J., Lee, C.-C., Tsai, H.-Z., Li, H.-J., & Wu, H.-C. (2020). Development of therapeutic antibodies for the treatment of diseases. *Journal of Biomedical Science*, *27*(1), 1. <https://doi.org/10.1186/s12929-019-0592-z>
- Luo, C., Bueno, M., Kant, J., & Randhawa, P. (2008). Biologic diversity of polyomavirus BK genomic sequences: Implications for molecular diagnostic laboratories. *Journal of Medical Virology*, *80*(10), 1850–1857. <https://doi.org/10.1002/jmv.21281>
- Mahanonda, R., Champaiboon, C., Subbalekha, K., Sa-Ard-lam, N., Rattanathammatada, W., Thawanaphong, S., Rerkyen, P., Yoshimura, F., Nagano, K., Lang, N. P., & Pichyangkul, S. (2016). Human Memory B Cells in Healthy Gingiva, Gingivitis, and Periodontitis. *The Journal of Immunology*, *197*(3), 715–725. <https://doi.org/10.4049/jimmunol.1600540>
- Mak, T. W., Saunders, M. E., & Jett, B. D. (Eds.). (2014). Chapter 5—B Cell Development, Activation and Effector Functions. In *Primer to the Immune Response (Second Edition)* (pp. 111–142). Academic Cell. <https://doi.org/10.1016/B978-0-12-385245-8.00005-4>
- Mamani-Matsuda, M., Cosma, A., Weller, S., Faili, A., Staib, C., Garçon, L., Hermine, O., Beyne-Rauzy, O., Fieschi, C., Pers, J.-O., Arakelyan, N., Varet, B., Sauvanet, A., Berger, A., Paye, F., Andrieu, J.-M., Michel, M., Godeau, B., Buffet, P., ... Weill, J.-C. (2008). The human spleen is a major reservoir for long-lived vaccinia virus-specific memory B cells. *Blood*, *111*(9), 4653–4659. <https://doi.org/10.1182/blood-2007-11-123844>
- Manzetti, J., Weissbach, F. H., Graf, F. E., Unterstab, G., Wernli, M., Hopfer, H., Drachenberg, C. B., Rinaldo, C. H., & Hirsch, H. H. (2020). BK Polyomavirus Evades Innate Immune Sensing by Disrupting the Mitochondrial Network and Promotes Mitophagy. *iScience*, *23*(7), 101257. <https://doi.org/10.1016/j.isci.2020.101257>
- Margreitter, C., Lu, H.-C., Townsend, C., Stewart, A., Dunn-Walters, D. K., & Fraternali, F. (2018). BRepertoire: A user-friendly web server for analysing antibody repertoire data. *Nucleic Acids Research*, *46*(W1), W264–W270. <https://doi.org/10.1093/nar/gky276>
- Markowitz, R. B., Thompson, H. C., Mueller, J. F., Cohen, J. A., & Dynan, W. S. (1993). Incidence of BK virus and JC virus viraemia in human immunodeficiency virus-infected and -uninfected subjects. *The Journal of Infectious Diseases*, *167*(1), 13–20. <https://doi.org/10.1093/infdis/167.1.13>
- Martelli, F., Wu, Z., Delbue, S., Weissbach, F., Giulioli, M., Ferrante, P., Hirsch, H., & Gianecchini, S. (2018). BK Polyomavirus MicroRNA Levels in Exosomes Are Modulated

- by Non-Coding Control Region Activity and Down-Regulate Viral Replication When Delivered to Non-Infected Cells Prior to Infection. *Viruses*, 10(9), 466. <https://doi.org/10.3390/v10090466>
- Matsumura, S., Kato, T., Taniguchi, A., Kawamura, M., Nakazawa, S., Namba-Hamano, T., Abe, T., Nonomura, N., & Imamura, R. (2020). Clinical Efficacy of Intravenous Immunoglobulin for BK Polyomavirus-Associated Nephropathy After Living Kidney Transplantation. *Therapeutics and Clinical Risk Management*, 16, 947–952. <https://doi.org/10.2147/TCRM.S273388>
- McCafferty, J., Griffiths, A. D., Winter, G., & Chiswell, D. J. (1990). Phage antibodies: Filamentous phage displaying antibody variable domains. *Nature*, 348(6301), 552–554. <https://doi.org/10.1038/348552a0>
- McClure, G. B., Gardner, J. S., Williams, J. T., Copeland, C. M., Sylvester, S. K., Garcea, R. L., Meinerz, N. M., Groome, L. J., & Vanchiere, J. A. (2012). Dynamics of pregnancy-associated polyomavirus urinary excretion: A prospective longitudinal study. *Journal of Medical Virology*, 84(8), 1312–1322. <https://doi.org/10.1002/jmv.23320>
- McIlroy, D., Hönemann, M., Nguyen, N.-K., Barbier, P., Peltier, C., Rodallec, A., Halary, F., Przyrowski, E., Liebert, U., Hourmant, M., & Bressollette-Bodin, C. (2020). Persistent BK Polyomavirus Viruria Is Associated with Accumulation of VP1 Mutations and Neutralization Escape. *Viruses*, 12(8), 824. <https://doi.org/10.3390/v12080824>
- Meffre, E., Louie, A., Bannock, J., Kim, L. J. Y., Ho, J., Frear, C. C., Kardava, L., Wang, W., Buckner, C. M., Wang, Y., Fankuchen, O. R., Gittens, K. R., Chun, T.-W., Li, Y., Fauci, A. S., & Moir, S. (2016). Maturational characteristics of HIV-specific antibodies in viremic individuals. *JCI Insight*, 1(3). <https://doi.org/10.1172/jci.insight.84610>
- Melnick, J. L. (1962). Papova Virus Group. *Science*, 135(3509), 1128–1130. <https://doi.org/10.1126/science.135.3509.1128>
- Meneguzzi, G., Pignatti, P. F., Barbanti-Brodano, G., & Milanese, G. (1978). Minichromosome from BK virus as a template for transcription in vitro. *Proceedings of the National Academy of Sciences*, 75(3), 1126–1130. <https://doi.org/10.1073/pnas.75.3.1126>
- Mengel, M. (2017). BK Virus Nephropathy Revisited. *American Journal of Transplantation*, 17(8), 1972–1973. <https://doi.org/10.1111/ajt.14358>
- Michon, C. (2018). *Optimisation d'une méthode de PCR quantitative en temps réel pour la détection de tous les génotypes de BK polyomavirus humain*. Université de Poitiers.
- Miller, M. D., Gelezianas, R., Bianchi, E., Lennard, S., Hrin, R., Zhang, H., Lu, M., An, Z., Ingallinella, P., Finotto, M., Mattu, M., Finnefrock, A. C., Bramhill, D., Cook, J., Eckert, D. M., Hampton, R., Patel, M., Jarantow, S., Joyce, J., ... Pessi, A. (2005). A human monoclonal antibody neutralizes diverse HIV-1 isolates by binding a critical gp41 epitope. *Proceedings of the National Academy of Sciences of the United States of America*, 102(41), 14759–14764. <https://doi.org/10.1073/pnas.0506927102>
- Moens, U., Calvignac-Spencer, S., Lauber, C., Ramqvist, T., Feltkamp, M. C. W., Daugherty, M. D., Verschoor, E. J., Ehlers, B., & ICTV Report Consortium. (2017). ICTV Virus Taxonomy Profile: Polyomaviridae. *Journal of General Virology*, 98(6), 1159–1160. <https://doi.org/10.1099/jgv.0.000839>
- Moens, U., Johansen, T., Johnsen, J. I., Seternes, O. M., & Traavik, T. (1995). Noncoding control region of naturally occurring BK virus variants: Sequence comparison and functional analysis. *Virus Genes*, 10(3), 261–275. <https://doi.org/10.1007/BF01701816>

- Moens, U., & Rekvig, O. P. (2001). Molecular Biology of BK Virus and Clinical and Basic Aspects of BK Virus Renal Infection. In K. Khalili & G. L. Stoner (Eds.), *Human Polyomaviruses* (pp. 359–408). John Wiley & Sons, Inc. <https://doi.org/10.1002/0471221945.ch14>
- Moir, S., Ho, J., Malaspina, A., Wang, W., DiPoto, A. C., O’Shea, M. A., Roby, G., Kottlilil, S., Arthos, J., Proschan, M. A., Chun, T.-W., & Fauci, A. S. (2008). Evidence for HIV-associated B cell exhaustion in a dysfunctional memory B cell compartment in HIV-infected viremic individuals. *Journal of Experimental Medicine*, *205*(8), 1797–1805. <https://doi.org/10.1084/jem.20072683>
- Monini, P., Rotola, A., de Lellis, L., Corallini, A., Secchiero, P., Albin, A., Benelli, R., Parravicini, C., Barbanti-Brodano, G., & Cassai, E. (1996). Latent BK virus infection and Kaposi’s sarcoma pathogenesis. *International Journal of Cancer*, *66*(6), 717–722. [https://doi.org/10.1002/\(SICI\)1097-0215\(19960611\)66:6<717::AID-IJC1>3.0.CO;2-2](https://doi.org/10.1002/(SICI)1097-0215(19960611)66:6<717::AID-IJC1>3.0.CO;2-2)
- Moriyama, T., Marquez, J. P., Wakatsuki, T., & Sorokin, A. (2007). Caveolar endocytosis is critical for BK virus infection of human renal proximal tubular epithelial cells. *Journal of Virology*, *81*(16), 8552–8562. <https://doi.org/10.1128/JVI.00924-07>
- Moriyama, T., & Sorokin, A. (2008a). Intracellular trafficking pathway of BK Virus in human renal proximal tubular epithelial cells. *Virology*, *371*(2), 336–349. <https://doi.org/10.1016/j.virol.2007.09.030>
- Moriyama, T., & Sorokin, A. (2008b). Repression of BK Virus Infection of Human Renal Proximal Tubular Epithelial Cells by Pravastatin: *Transplantation*, *85*(9), 1311–1317. <https://doi.org/10.1097/TP.0b013e31816c4ec5>
- Mueller, K., Schachtner, T., Sattler, A., Meier, S., Friedrich, P., Trydzenskaya, H., Hinrichs, C., Trappe, R., Thiel, A., Reinke, P., & Babel, N. (2011). BK-VP3 as a new target of cellular immunity in BK virus infection. *Transplantation*, *91*(1), 100–107. <https://doi.org/10.1097/tp.0b013e3181fe1335>
- Nakamura, G., Chai, N., Park, S., Chiang, N., Lin, Z., Chiu, H., Fong, R., Yan, D., Kim, J., Zhang, J., Lee, W. P., Estevez, A., Coons, M., Xu, M., Lupardus, P., Balazs, M., & Swem, L. R. (2013). An in vivo human-plasmablast enrichment technique allows rapid identification of therapeutic influenza A antibodies. *Cell Host & Microbe*, *14*(1), 93–103. <https://doi.org/10.1016/j.chom.2013.06.004>
- Nakanishi, A., Itoh, N., Li, P. P., Handa, H., Liddington, R. C., & Kasamatsu, H. (2007). Minor Capsid Proteins of Simian Virus 40 Are Dispensable for Nucleocapsid Assembly and Cell Entry but Are Required for Nuclear Entry of the Viral Genome. *Journal of Virology*, *81*(8), 3778–3785. <https://doi.org/10.1128/JVI.02664-06>
- Nankivell, B. J., Renthawa, J., Jeffreys, N., Kable, K., O’Connell, P. J., Chapman, J. R., Wong, G., & Sharma, R. N. (2015). Clinical Utility of Urinary Cytology to Detect BK Viral Nephropathy: *Transplantation*, *99*(8), 1715–1722. <https://doi.org/10.1097/TP.0000000000000642>
- Nesselhauf, N., Strutt, J., & Bastani, B. (2015). Evaluation of leflunomide for the treatment of BK viremia and biopsy proven BK nephropathy; a single center experience. *Journal of Nephrology*, *5*(1), 34–37. <https://doi.org/10.15171/jnp.2016.06>
- Neu, U., Allen, S. A., Blaum, B. S., Liu, Y., Frank, M., Palma, A. S., Ströh, L. J., Feizi, T., Peters, T., Atwood, W. J., & Stehle, T. (2013). A Structure-Guided Mutation in the Major Capsid Protein Retargets BK Polyomavirus. *PLoS Pathogens*, *9*(10), e1003688. <https://doi.org/10.1371/journal.ppat.1003688>

- Nickeleit, V., & Mihatsch, M. J. (2006). Polyomavirus nephropathy in native kidneys and renal allografts: An update on an escalating threat. *Transplant International*, *19*(12), 960–973. <https://doi.org/10.1111/j.1432-2277.2006.00360.x>
- Nickeleit, V., Singh, H. K., Dadhania, D., Cornea, V., El-Husseini, A., Castellanos, A., Davis, V. G., Waid, T., & Seshan, S. V. (2020). The 2018 Banff Working Group classification of definitive polyomavirus nephropathy: A multicenter validation study in the modern era. *American Journal of Transplantation*, *ajt.16189*. <https://doi.org/10.1111/ajt.16189>
- Nickeleit, V., Singh, H. K., Randhawa, P., Drachenberg, C. B., Bhatnagar, R., Bracamonte, E., Chang, A., Chon, W. J., Dadhania, D., Davis, V. G., Hopfer, H., Mihatsch, M. J., Papadimitriou, J. C., Schaub, S., Stokes, M. B., Tungekar, M. F., Seshan, S. V., & Banff Working Group on Polyomavirus Nephropathy. (2018). The Banff Working Group Classification of Definitive Polyomavirus Nephropathy: Morphologic Definitions and Clinical Correlations. *Journal of the American Society of Nephrology: JASN*, *29*(2), 680–693. <https://doi.org/10.1681/ASN.2017050477>
- Nilsson, J., Miyazaki, N., Xing, L., Wu, B., Hammar, L., Li, T. C., Takeda, N., Miyamura, T., & Cheng, R. H. (2005). Structure and Assembly of a T=1 Virus-Like Particle in BK Polyomavirus. *Journal of Virology*, *79*(9), 5337–5345. <https://doi.org/10.1128/JVI.79.9.5337-5345.2005>
- Nishimoto, Y., Takasaka, T., Hasegawa, M., Zheng, H.-Y., Chen, Q., Sugimoto, C., Kitamura, T., & Yogo, Y. (2006). Evolution of BK Virus Based on Complete Genome Data. *Journal of Molecular Evolution*, *63*(3), 341–352. <https://doi.org/10.1007/s00239-005-0092-5>
- Nishimoto, Y., Zheng, H.-Y., Zhong, S., Ikegaya, H., Chen, Q., Sugimoto, C., Kitamura, T., & Yogo, Y. (2007). An Asian Origin for Subtype IV BK Virus Based on Phylogenetic Analysis. *Journal of Molecular Evolution*, *65*(1), 103–111. <https://doi.org/10.1007/s00239-006-0269-6>
- O’Hara, S. D., Stehle, T., & Garcea, R. (2014). Glycan receptors of the Polyomaviridae: Structure, function, and pathogenesis. *Current Opinion in Virology*, *7*, 73–78. <https://doi.org/10.1016/j.coviro.2014.05.004>
- Okonechnikov, K., Golosova, O., & Fursov, M. (2012). Unipro UGENE: A unified bioinformatics toolkit. *Bioinformatics*, *28*(8), 1166–1167. <https://doi.org/10.1093/bioinformatics/bts091>
- Oliviero, B., Mantovani, S., Ludovisi, S., Varchetta, S., Mele, D., Paolucci, S., Baldanti, F., & Mondelli, M. U. (2015). Skewed B cells in chronic hepatitis C virus infection maintain their ability to respond to virus-induced activation. *Journal of Viral Hepatitis*, *22*(4), 391–398. <https://doi.org/10.1111/jvh.12336>
- Oliviero, Barbara, Varchetta, S., Mele, D., Mantovani, S., Cerino, A., Perotti, C. G., Ludovisi, S., & Mondelli, M. U. (2020). Expansion of atypical memory B cells is a prominent feature of COVID-19. *Cellular & Molecular Immunology*, *17*(10), 1101–1103. <https://doi.org/10.1038/s41423-020-00542-2>
- Onodera, T., Takahashi, Y., Yokoi, Y., Ato, M., Kodama, Y., Hachimura, S., Kurosaki, T., & Kobayashi, K. (2012). Memory B cells in the lung participate in protective humoral immune responses to pulmonary influenza virus reinfection. *Proceedings of the National Academy of Sciences*, *109*(7), 2485–2490. <https://doi.org/10.1073/pnas.1115369109>
- Paddock, M. N., Buelow, B. D., Takeda, S., & Scharenberg, A. M. (2010). The BRCT domain of PARP-1 is required for immunoglobulin gene conversion. *PLoS Biology*, *8*(7), e1000428. <https://doi.org/10.1371/journal.pbio.1000428>

- Padgett, Billie L., Zurhein, Gabriele M., Walker, Duard L., Eckroade, Robert J., & Dessel, Bert H. (1971). Cultivation of papova-like virus from human brain with progressive multifocal leucoencephalopathy. *The Lancet*, 297(7712), 1257–1260. [https://doi.org/10.1016/S0140-6736\(71\)91777-6](https://doi.org/10.1016/S0140-6736(71)91777-6)
- Panou, M.-M., Prescott, E., Hurdiss, D., Swinscoe, G., Hollinshead, M., Caller, L., Morgan, E., Carlisle, L., Müller, M., Antoni, M., Kealy, D., Ranson, N., Crump, C., & Macdonald, A. (2018). Agnoprotein Is an Essential Egress Factor during BK Polyomavirus Infection. *International Journal of Molecular Sciences*, 19(3), 902. <https://doi.org/10.3390/ijms19030902>
- Papanicolaou, G. A., Lee, Y. J., Young, J. W., Seshan, S. V., Boruchov, A. M., Chittick, G., Momméja-Marin, H., & Glezerman, I. G. (2015). Brincidofovir for Polyomavirus-Associated Nephropathy After Allogeneic Hematopoietic Stem Cell Transplantation. *American Journal of Kidney Diseases*, 65(5), 780–784. <https://doi.org/10.1053/j.ajkd.2014.11.020>
- Parren, P. W., & Burton, D. R. (2001). The antiviral activity of antibodies in vitro and in vivo. *Advances in Immunology*, 77, 195–262. [https://doi.org/10.1016/s0065-2776\(01\)77018-6](https://doi.org/10.1016/s0065-2776(01)77018-6)
- Pastrana, D. V., Brennan, D. C., Cuburu, N., Storch, G. A., Viscidi, R. P., Randhawa, P. S., & Buck, C. B. (2012). Neutralization serotyping of BK polyomavirus infection in kidney transplant recipients. *PLoS Pathogens*, 8(4), e1002650. <https://doi.org/10.1371/journal.ppat.1002650>
- Pastrana, D. V., Ray, U., Magaldi, T. G., Schowalter, R. M., Çuburu, N., & Buck, C. B. (2013). BK polyomavirus genotypes represent distinct serotypes with distinct entry tropism. *Journal of Virology*, 87(18), 10105–10113. <https://doi.org/10.1128/JVI.01189-13>
- Patel, M., Glass, R. I., Jiang, B., Santosham, M., Lopman, B., & Parashar, U. (2013). A Systematic Review of Anti-Rotavirus Serum IgA Antibody Titer as a Potential Correlate of Rotavirus Vaccine Efficacy. *The Journal of Infectious Diseases*, 208(2), 284–294. <https://doi.org/10.1093/infdis/jit166>
- Pelegrin, M., Naranjo-Gomez, M., & Piechaczyk, M. (2015). Antiviral Monoclonal Antibodies: Can They Be More Than Simple Neutralizing Agents? *Trends in Microbiology*, 23(10), 653–665. <https://doi.org/10.1016/j.tim.2015.07.005>
- Pelkmans, L., & Helenius, A. (2003). Insider information: What viruses tell us about endocytosis. *Current Opinion in Cell Biology*, 15(4), 414–422. [https://doi.org/10.1016/S0955-0674\(03\)00081-4](https://doi.org/10.1016/S0955-0674(03)00081-4)
- Pho, M. T., Ashok, A., & Atwood, W. J. (2000). JC Virus Enters Human Glial Cells by Clathrin-Dependent Receptor-Mediated Endocytosis. *Journal of Virology*, 74(5), 2288–2292. <https://doi.org/10.1128/JVI.74.5.2288-2292.2000>
- Pieper, K., Grimbacher, B., & Eibel, H. (2013). B-cell biology and development. *The Journal of Allergy and Clinical Immunology*, 131(4), 959–971. <https://doi.org/10.1016/j.jaci.2013.01.046>
- Pietro Paolo, V., Di Taranto, C., Degener, A. M., Jin, L., Sinibaldi, L., Baiocchini, A., Melis, M., & Orsi, N. (1998). Transplacental transmission of human polyomavirus BK. *Journal of Medical Virology*, 56(4), 372–376. [https://doi.org/10.1002/\(sici\)1096-9071\(199812\)56:4<372::aid-jmv14>3.0.co;2-4](https://doi.org/10.1002/(sici)1096-9071(199812)56:4<372::aid-jmv14>3.0.co;2-4)
- Portugal, S., Tipton, C. M., Sohn, H., Kone, Y., Wang, J., Li, S., Skinner, J., Virtaneva, K., Sturdevant, D. E., Porcella, S. F., Doumbo, O. K., Doumbo, S., Kayentao, K., Ongoiba, A.,

- Traore, B., Sanz, I., Pierce, S. K., & Crompton, P. D. (2015). Malaria-associated atypical memory B cells exhibit markedly reduced B cell receptor signaling and effector function. *ELife*, 4, e07218. <https://doi.org/10.7554/eLife.07218>
- Purtha, W. E., Tedder, T. F., Johnson, S., Bhattacharya, D., & Diamond, M. S. (2011). Memory B cells, but not long-lived plasma cells, possess antigen specificities for viral escape mutants. *The Journal of Experimental Medicine*, 208(13), 2599–2606. <https://doi.org/10.1084/jem.20110740>
- Qiu, X., Mao, Q., Tang, Y., Wang, L., Chawla, R., Pliner, H. A., & Trapnell, C. (2017). Reversed graph embedding resolves complex single-cell trajectories. *Nature Methods*, 14(10), 979–982. <https://doi.org/10.1038/nmeth.4402>
- Randhawa, P., Bohl, D., Brennan, D., Ruppert, K., Ramaswami, B., Storch, G., March, J., Shapiro, R., & Viscidi, R. (2008). Longitudinal Analysis of Levels of Immunoglobulins against BK Virus Capsid Proteins in Kidney Transplant Recipients. *Clinical and Vaccine Immunology*, 15(10), 1564–1571. <https://doi.org/10.1128/CVI.00206-08>
- Randhawa, P., Pastrana, D. V., Zeng, G., Huang, Y., Shapiro, R., Sood, P., Puttarajappa, C., Berger, M., Hariharan, S., & Buck, C. B. (2015). Commercially available immunoglobulins contain virus neutralizing antibodies against all major genotypes of polyomavirus BK. *American Journal of Transplantation: Official Journal of the American Society of Transplantation and the American Society of Transplant Surgeons*, 15(4), 1014–1020. <https://doi.org/10.1111/ajt.13083>
- Randhawa, Parmjeet, Ho, A., Shapiro, R., Vats, A., Swalsky, P., Finkelstein, S., Uhrmacher, J., & Weck, K. (2004). Correlates of quantitative measurement of BK polyomavirus (BKV) DNA with clinical course of BKV infection in renal transplant patients. *Journal of Clinical Microbiology*, 42(3), 1176–1180. <https://doi.org/10.1128/jcm.42.3.1176-1180.2004>
- Rayment, I., Baker, T. S., Caspar, D. L. D., & Murakami, W. T. (1982). Polyoma virus capsid structure at 22.5 Å resolution. *Nature*, 295(5845), 110–115. <https://doi.org/10.1038/295110a0>
- Reisman, L., Habib, S., McClure, G. B., Latiolais, L. S., & Vanchiere, J. A. (2014). Treatment of BK virus-associated nephropathy with CMX001 after kidney transplantation in a young child. *Pediatric Transplantation*, 18(7), E227–E231. <https://doi.org/10.1111/petr.12340>
- Renner, F. C., Dietrich, H., Bulut, N., Celik, D., Freitag, E., Gaertner, N., Karoui, S., Mark, J., Raatz, C., Weimer, R., & Feustel, A. (2013). The Risk of Polyomavirus-Associated Graft Nephropathy Is Increased by a Combined Suppression of CD8 and CD4 Cell-Dependent Immune Effects. *Transplantation Proceedings*, 45(4), 1608–1610. <https://doi.org/10.1016/j.transproceed.2013.01.026>
- Rijal, P., Elias, S. C., Machado, S. R., Xiao, J., Schimanski, L., O'Dowd, V., Baker, T., Barry, E., Mendelsohn, S. C., Cherry, C. J., Jin, J., Labbé, G. M., Donnellan, F. R., Rampling, T., Dowall, S., Rayner, E., Findlay-Wilson, S., Carroll, M., Guo, J., ... Townsend, A. R. (2019). Therapeutic Monoclonal Antibodies for Ebola Virus Infection Derived from Vaccinated Humans. *Cell Reports*, 27(1), 172–186.e7. <https://doi.org/10.1016/j.celrep.2019.03.020>
- Rinaldo, C. H., Gosert, R., Bernhoff, E., Finstad, S., & Hirsch, H. H. (2010). 1-O-Hexadecyloxypropyl Cidofovir (CMX001) Effectively Inhibits Polyomavirus BK Replication in Primary Human Renal Tubular Epithelial Cells. *Antimicrobial Agents and Chemotherapy*, 54(11), 4714–4722. <https://doi.org/10.1128/AAC.00974-10>

- Rinaldo, C. H., Traavik, T., & Hey, A. (1998). The Agnogene of the Human Polyomavirus BK Is Expressed. *Journal of Virology*, *72*(7), 6233–6236. <https://doi.org/10.1128/JVI.72.7.6233-6236.1998>
- Robert, I., Dantzer, F., & Reina-San-Martin, B. (2009). Parp1 facilitates alternative NHEJ, whereas Parp2 suppresses IgH/c-myc translocations during immunoglobulin class switch recombination. *The Journal of Experimental Medicine*, *206*(5), 1047–1056. <https://doi.org/10.1084/jem.20082468>
- Rosen, S., Harmon, W., Krensky, A. M., Edelson, P. J., Padgett, B. L., Grinnell, B. W., Rubino, M. J., & Walker, D. L. (1983). Tubulo-interstitial nephritis associated with polyomavirus (BK type) infection. *The New England Journal of Medicine*, *308*(20), 1192–1196. <https://doi.org/10.1056/NEJM198305193082004>
- Rubinstein, R., Schoonakker, B. C., & Harley, E. H. (1991). Recurring theme of changes in the transcriptional control region of BK virus during adaptation to cell culture. *Journal of Virology*, *65*(3), 1600.
- Sahli, R., Freund, R., Dubensky, T., Garcea, R., Bronson, R., & Benjamin, T. (1993). Defect in Entry and Altered Pathogenicity of a Polyoma Virus Mutant Blocked in VP2 Myristylation. *Virology*, *192*(1), 142–153. <https://doi.org/10.1006/viro.1993.1016>
- Salunke, D. M., Caspar, D. L. D., & Garcea, R. L. (1986). Self-assembly of purified polyomavirus capsid protein VP1. *Cell*, *46*(6), 895–904. [https://doi.org/10.1016/0092-8674\(86\)90071-1](https://doi.org/10.1016/0092-8674(86)90071-1)
- Sanna, P. P., & Burton, D. R. (2000). Role of antibodies in controlling viral disease: Lessons from experiments of nature and gene knockouts. *Journal of Virology*, *74*(21), 9813–9817. <https://doi.org/10.1128/jvi.74.21.9813-9817.2000>
- Schachtner, T., Müller, K., Stein, M., Diezemann, C., Sefrin, A., Babel, N., & Reinke, P. (2011). BK virus-specific immunity kinetics: A predictor of recovery from polyomavirus BK-associated nephropathy. *American Journal of Transplantation: Official Journal of the American Society of Transplantation and the American Society of Transplant Surgeons*, *11*(11), 2443–2452. <https://doi.org/10.1111/j.1600-6143.2011.03693.x>
- Schaub, S., Hirsch, H. H., Dickenmann, M., Steiger, J., Mihatsch, M. J., Hopfer, H., & Mayr, M. (2010). Reducing immunosuppression preserves allograft function in presumptive and definitive polyomavirus-associated nephropathy. *American Journal of Transplantation: Official Journal of the American Society of Transplantation and the American Society of Transplant Surgeons*, *10*(12), 2615–2623. <https://doi.org/10.1111/j.1600-6143.2010.03310.x>
- Schneidewind, L., Neumann, T., Dräger, D. L., Kranz, J., & Hakenberg, O. W. (2020). Leflunomide in the treatment of BK polyomavirus associated nephropathy in kidney transplanted patients—A systematic review. *Transplantation Reviews (Orlando, Fla.)*, *34*(4), 100565. <https://doi.org/10.1016/j.trre.2020.100565>
- Schroeder, H. W., & Cavacini, L. (2010). Structure and Function of Immunoglobulins. *The Journal of Allergy and Clinical Immunology*, *125*(2 0 2), S41–S52. <https://doi.org/10.1016/j.jaci.2009.09.046>
- Sener, A., House, A. A., Jevnikar, A. M., Boudville, N., McAlister, V. C., Muirhead, N., Rehman, F., & Luke, P. P. W. (2006). Intravenous immunoglobulin as a treatment for BK virus associated nephropathy: One-year follow-up of renal allograft recipients. *Transplantation*, *81*(1), 117–120. <https://doi.org/10.1097/01.tp.0000181096.14257.c2>

- Setliff, I., Shiakolas, A. R., Pilewski, K. A., Murji, A. A., Mapengo, R. E., Janowska, K., Richardson, S., Oosthuysen, C., Raju, N., Ronsard, L., Kanekiyo, M., Qin, J. S., Kramer, K. J., Greenplate, A. R., McDonnell, W. J., Graham, B. S., Connors, M., Lingwood, D., Acharya, P., ... Georgiev, I. S. (2019). High-Throughput Mapping of B Cell Receptor Sequences to Antigen Specificity. *Cell*, *179*(7), 1636-1646.e15. <https://doi.org/10.1016/j.cell.2019.11.003>
- Seydoux, E., Homad, L. J., MacCamy, A. J., Parks, K. R., Hurlburt, N. K., Jennewein, M. F., Akins, N. R., Stuart, A. B., Wan, Y.-H., Feng, J., Whaley, R. E., Singh, S., Boeckh, M., Cohen, K. W., McElrath, M. J., Englund, J. A., Chu, H. Y., Pancera, M., McGuire, A. T., & Stamatatos, L. (2020). Analysis of a SARS-CoV-2-Infected Individual Reveals Development of Potent Neutralizing Antibodies with Limited Somatic Mutation. *Immunity*, *53*(1), 98-105.e5. <https://doi.org/10.1016/j.immuni.2020.06.001>
- Shah, H. B., Smith, K., Wren, J. D., Webb, C. F., Ballard, J. D., Bourn, R. L., James, J. A., & Lang, M. L. (2019). Insights From Analysis of Human Antigen-Specific Memory B Cell Repertoires. *Frontiers in Immunology*, *9*. <https://doi.org/10.3389/fimmu.2018.03064>
- Shah, K. V., Daniel, R. W., & Warszawski, R. M. (1973). High Prevalence of Antibodies to BK Virus, an SV40-related Papovavirus, in Residents of Maryland. *Journal of Infectious Diseases*, *128*(6), 784-787. <https://doi.org/10.1093/infdis/128.6.784>
- Sharma, A. P., Moussa, M., Casier, S., Rehman, F., Filler, G., & Grimmer, J. (2009). Intravenous immunoglobulin as rescue therapy for BK virus nephropathy. *Pediatric Transplantation*, *13*(1), 123-129. <https://doi.org/10.1111/j.1399-3046.2008.00958.x>
- Sharma, B. N., Li, R., Bernhoff, E., Gutteberg, T. J., & Rinaldo, C. H. (2011). Fluoroquinolones inhibit human polyomavirus BK (BKV) replication in primary human kidney cells. *Antiviral Research*, *92*(1), 115-123. <https://doi.org/10.1016/j.antiviral.2011.07.012>
- Sharma, R., & Zachariah, M. (2020). BK Virus Nephropathy: Prevalence, Impact and Management Strategies. *International Journal of Nephrology and Renovascular Disease*, *13*, 187-192. <https://doi.org/10.2147/IJNRD.S236556>
- Shaw, G., Morse, S., Ararat, M., & Graham, F. L. (2002). Preferential transformation of human neuronal cells by human adenoviruses and the origin of HEK 293 cells. *FASEB Journal: Official Publication of the Federation of American Societies for Experimental Biology*, *16*(8), 869-871. <https://doi.org/10.1096/fj.01-0995fje>
- Shen, C., Zhang, M., Chen, Y., Zhang, L., Wang, G., Chen, J., Chen, S., Li, Z., Wei, F., Chen, J., Yang, K., Guo, S., Wang, Y., Zheng, Q., Yu, H., Luo, W., Zhang, J., Chen, H., Chen, Y., & Xia, N. (2019). An IgM antibody targeting the receptor binding site of influenza B blocks viral infection with great breadth and potency. *Theranostics*, *9*(1), 210-231. <https://doi.org/10.7150/thno.28434>
- Singh, H. K., Donna Thompson, B., & Nিকেleit, V. (2009). Viral Haufen are Urinary Biomarkers of Polyomavirus Nephropathy: New Diagnostic Strategies Utilizing Negative Staining Electron Microscopy. *Ultrastructural Pathology*, *33*(5), 222-235. <https://doi.org/10.3109/01913120903241081>
- Singh, H. K., Reisner, H., Derebail, V. K., Kozlowski, T., & Nিকেleit, V. (2015). Polyomavirus nephropathy: Quantitative urinary polyomavirus-Haufen testing accurately predicts the degree of intrarenal viral disease. *Transplantation*, *99*(3), 609-615. <https://doi.org/10.1097/TP.0000000000000367>
- Skountzou, I., Satyabhama, L., Stavropoulou, A., Ashraf, Z., Esser, E. S., Vassilieva, E., Koutsonanos, D., Compans, R., & Jacob, J. (2014). Influenza Virus-Specific Neutralizing

- IgM Antibodies Persist for a Lifetime. *Clinical and Vaccine Immunology : CVI*, 21(11), 1481–1489. <https://doi.org/10.1128/CVI.00374-14>
- Sloan, S. E., Hanlon, C., Weldon, W., Niezgodna, M., Blanton, J., Self, J., Rowley, K. J., Mandell, R. B., Babcock, G. J., Thomas, W. D., Rupprecht, C. E., & Ambrosino, D. M. (2007). Identification and characterization of a human monoclonal antibody that potently neutralizes a broad panel of rabies virus isolates. *Vaccine*, 25(15), 2800–2810. <https://doi.org/10.1016/j.vaccine.2006.12.031>
- Solis, M., Velay, A., Porcher, R., Domingo-Calap, P., Soulier, E., Joly, M., Meddeb, M., Kack-Kack, W., Moulin, B., Bahram, S., Stoll-Keller, F., Barth, H., Caillard, S., & Fafi-Kremer, S. (2018). Neutralizing Antibody–Mediated Response and Risk of BK Virus–Associated Nephropathy. *Journal of the American Society of Nephrology : JASN*, 29(1), 326–334. <https://doi.org/10.1681/ASN.2017050532>
- Srinivasan, S., Ghosh, M., Maity, S., & Varadarajan, R. (2016, January 8). *Broadly neutralizing antibodies for therapy of viral infections*. Antibody Technology Journal; Dove Press. <https://doi.org/10.2147/ANTI.S92190>
- Stacy, T., Chamberlain, M., & Cole, C. N. (1989). Simian virus 40 host range/helper function mutations cause multiple defects in viral late gene expression. *Journal of Virology*, 63(12), 5208–5215. <https://doi.org/10.1128/JVI.63.12.5208-5215.1989>
- Stehle, T., Yan, Y., Benjamin, T. L., & Harrison, S. C. (1994). Structure of murine polyomavirus complexed with an oligosaccharide receptor fragment. *Nature*, 369(6476), 160–163. <https://doi.org/10.1038/369160a0>
- Sterlin, D., Mathian, A., Miyara, M., Mohr, A., Anna, F., Claër, L., Quentric, P., Fadlallah, J., Devilliers, H., Ghillani, P., Gunn, C., Hockett, R., Mudumba, S., Guihot, A., Luyt, C.-E., Mayaux, J., Beurton, A., Fourati, S., Bruel, T., ... Gorochov, G. (2021). IgA dominates the early neutralizing antibody response to SARS-CoV-2. *Science Translational Medicine*, 13(577). <https://doi.org/10.1126/scitranslmed.abd2223>
- Stoeckius, M., Zheng, S., Houck-Loomis, B., Hao, S., Yeung, B. Z., Mauck, W. M., Smibert, P., & Satija, R. (2018). Cell Hashing with barcoded antibodies enables multiplexing and doublet detection for single cell genomics. *Genome Biology*, 19(1), 224. <https://doi.org/10.1186/s13059-018-1603-1>
- Sullivan, C. S., Grundhoff, A. T., Tevethia, S., Pipas, J. M., & Ganem, D. (2005). SV40-encoded microRNAs regulate viral gene expression and reduce susceptibility to cytotoxic T cells. *Nature*, 435(7042), 682–686. <https://doi.org/10.1038/nature03576>
- Sundsford, A., Osei, A., Rosenqvist, H., Van Ghelue, M., Silsand, Y., Haga, H. J., Rekvig, O. P., & Moens, U. (1999). BK and JC viruses in patients with systemic lupus erythematosus: Prevalent and persistent BK viremia, sequence stability of the viral regulatory regions, and nondetectable viremia. *The Journal of Infectious Diseases*, 180(1), 1–9. <https://doi.org/10.1086/314830>
- Sundsford, A., Spein, A. R., Lucht, E., Flaegstad, T., Seternes, O. M., & Traavik, T. (1994). Detection of BK virus DNA in nasopharyngeal aspirates from children with respiratory infections but not in saliva from immunodeficient and immunocompetent adult patients. *Journal of Clinical Microbiology*, 32(5), 1390–1394. <https://doi.org/10.1128/JCM.32.5.1390-1394.1994>
- Suwelack, B., Malyar, V., Koch, M., Sester, M., & Sommerer, C. (2012). The influence of immunosuppressive agents on BK virus risk following kidney transplantation, and

- implications for choice of regimen. *Transplantation Reviews (Orlando, Fla.)*, 26(3), 201–211. <https://doi.org/10.1016/j.trre.2011.05.002>
- Suzuki, M., Kato, C., & Kato, A. (2015). Therapeutic antibodies: Their mechanisms of action and the pathological findings they induce in toxicity studies. *Journal of Toxicologic Pathology*, 28(3), 133–139. <https://doi.org/10.1293/tox.2015-0031>
- Takasaka, T., Goya, N., Tokumoto, T., Tanabe, K., Toma, H., Ogawa, Y., Hokama, S., Momose, A., Funyu, T., Fujioka, T., Omori, S., Akiyama, H., Chen, Q., Zheng, H.-Y., Ohta, N., Kitamura, T., & Yogo, Y. (2004). Subtypes of BK virus prevalent in Japan and variation in their transcriptional control region. *Journal of General Virology*, 85(10), 2821–2827. <https://doi.org/10.1099/vir.0.80363-0>
- Takemoto, K. K., & Mullarkey, M. F. (1973). Human papovavirus, BK strain: Biological studies including antigenic relationship to simian virus 40. *Journal of Virology*, 12(3), 625–631. <https://doi.org/10.1128/JVI.12.3.625-631.1973>
- Takemoto, K. K., Rabson, A. S., Mullarkey, M. F., Blaese, R. M., Garon, C. F., & Nelson, D. (1974). Isolation of Papovavirus From Brain Tumor and Urine of a Patient With Wiskott-Aldrich Syndrome. *JNCI: Journal of the National Cancer Institute*, 53(5), 1205–1207. <https://doi.org/10.1093/jnci/53.5.1205>
- Tepper, S., Mortusewicz, O., Członka, E., Bello, A., Schmidt, A., Jeschke, J., Fischbach, A., Pfeil, I., Petersen-Mahrt, S. K., Mangerich, A., Helleday, T., Leonhardt, H., & Jungnickel, B. (2019). Restriction of AID activity and somatic hypermutation by PARP-1. *Nucleic Acids Research*, 47(14), 7418–7429. <https://doi.org/10.1093/nar/gkz466>
- Teunissen, E. A., de Raad, M., & Mastrobattista, E. (2013). Production and biomedical applications of virus-like particles derived from polyomaviruses. *Journal of Controlled Release*, 172(1), 305–321. <https://doi.org/10.1016/j.jconrel.2013.08.026>
- Throsby, M., van den Brink, E., Jongeneelen, M., Poon, L. L. M., Alard, P., Cornelissen, L., Bakker, A., Cox, F., van Deventer, E., Guan, Y., Cinatl, J., ter Meulen, J., Lasters, I., Carsetti, R., Peiris, M., de Kruif, J., & Goudsmit, J. (2008). Heterosubtypic neutralizing monoclonal antibodies cross-protective against H5N1 and H1N1 recovered from human IgM+ memory B cells. *PloS One*, 3(12), e3942. <https://doi.org/10.1371/journal.pone.0003942>
- Tian, Y.-C., Li, Y.-J., Chen, H.-C., Wu, H.-H., Weng, C.-H., Chen, Y.-C., Lee, C.-C., Chang, M.-Y., Hsu, H.-H., Yen, T.-H., Hung, C.-C., & Yang, C.-W. (2014). Polyomavirus BK-encoded microRNA suppresses autoregulation of viral replication. *Biochemical and Biophysical Research Communications*, 447(3), 543–549. <https://doi.org/10.1016/j.bbrc.2014.04.030>
- Tikhanovich, I., & Nasheuer, H. P. (2010). Host-Specific Replication of BK Virus DNA in Mouse Cell Extracts Is Independently Controlled by DNA Polymerase α -Primase and Inhibitory Activities. *Journal of Virology*, 84(13), 6636–6644. <https://doi.org/10.1128/JVI.00527-10>
- Tonnerre, P., Gérard, N., Gavlovsky, P.-J., Mazalrey, S., Hourmant, M., Cheneau, M.-L., Cesbron-Gautier, A., Renaudin, K., Bressollette-Bodin, C., & Charreau, B. (2016). MICA Mutant A5.1 Influences BK Polyomavirus Reactivation and Associated Nephropathy After Kidney Transplantation. *The Journal of Infectious Diseases*, 214(5), 807–816. <https://doi.org/10.1093/infdis/jiw168>
- Trapnell, C., Cacchiarelli, D., Grimsby, J., Pokharel, P., Li, S., Morse, M., Lennon, N. J., Livak, K. J., Mikkelsen, T. S., & Rinn, J. L. (2014). The dynamics and regulators of cell fate decisions are revealed by pseudotemporal ordering of single cells. *Nature Biotechnology*, 32(4), 381–386. <https://doi.org/10.1038/nbt.2859>

- Trydzenskaya, H., Juerchott, K., Lachmann, N., Kotsch, K., Kunert, K., Weist, B., Schönemann, C., Schindler, R., Nickel, P., Melzig, M. F., Hugo, C., Thomsch, O., Neumann, A. U., Reinke, P., & Babel, N. (2013). The genetic predisposition of natural killer cell to BK virus-associated nephropathy in renal transplant patients. *Kidney International*, *84*(2), 359–365. <https://doi.org/10.1038/ki.2013.59>
- Vago, L., Cinque, P., Sala, E., Nebuloni, M., Caldarelli, R., Racca, S., Ferrante, P., Trabottoni, G., & Costanzi, G. (1996). JCV-DNA and BKV-DNA in the CNS tissue and CSF of AIDS patients and normal subjects. Study of 41 cases and review of the literature. *Journal of Acquired Immune Deficiency Syndromes and Human Retrovirology: Official Publication of the International Retrovirology Association*, *12*(2), 139–146. <https://doi.org/10.1097/00042560-199606010-00006>
- Vajdy, M., & Lycke, N. (1993). Stimulation of antigen-specific T- and B-cell memory in local as well as systemic lymphoid tissues following oral immunization with cholera toxin adjuvant. *Immunology*, *80*(2), 197–203.
- Vasudev, B., Hariharan, S., Hussain, S. A., Zhu, Y.-R., Bresnahan, B. A., & Cohen, E. P. (2005). BK virus nephritis: Risk factors, timing, and outcome in renal transplant recipients. *Kidney International*, *68*(4), 1834–1839. <https://doi.org/10.1111/j.1523-1755.2005.00602.x>
- Vats, A., Shapiro, R., Singh Randhawa, P., Scantlebury, V., Tuzuner, A., Saxena, M., Moritz, M. L., Beattie, T. J., Gonwa, T., Green, M. D., & Ellis, D. (2003). Quantitative viral load monitoring and cidofovir therapy for the management of BK virus-associated nephropathy in children and adults. *Transplantation*, *75*(1), 105–112. <https://doi.org/10.1097/00007890-200301150-00020>
- Velay, A., Solis, M., Benotmane, I., Gantner, P., Soulier, E., Moulin, B., Caillard, S., & Fafi-Kremer, S. (2019). Intravenous Immunoglobulin Administration Significantly Increases BKPyV Genotype-Specific Neutralizing Antibody Titers in Kidney Transplant Recipients. *Antimicrobial Agents and Chemotherapy*, *63*(8). <https://doi.org/10.1128/AAC.00393-19>
- Vettermann, C., & Schlissel, M. S. (2010). Allelic exclusion of immunoglobulin genes: Models and mechanisms. *Immunological Reviews*, *237*(1), 22–42. <https://doi.org/10.1111/j.1600-065X.2010.00935.x>
- Victora, G. D., Dominguez-Sola, D., Holmes, A. B., Deroubaix, S., Dalla-Favera, R., & Nussenzweig, M. C. (2012). Identification of human germinal center light and dark zone cells and their relationship to human B-cell lymphomas. *Blood*, *120*(11), 2240–2248. <https://doi.org/10.1182/blood-2012-03-415380>
- Vidarsson, G., Dekkers, G., & Rispens, T. (2014). IgG Subclasses and Allotypes: From Structure to Effector Functions. *Frontiers in Immunology*, *5*. <https://doi.org/10.3389/fimmu.2014.00520>
- Virtanen, E., Seppälä, H., Helanterä, I., Laine, P., Lautenschlager, I., Paulin, L., Mannonen, L., Auvinen, P., & Auvinen, E. (2018). BK polyomavirus microRNA expression and sequence variation in polyomavirus-associated nephropathy. *Journal of Clinical Virology*, *102*, 70–76. <https://doi.org/10.1016/j.jcv.2018.02.007>
- Vladutiu, A. O. (2000). Immunoglobulin D: Properties, Measurement, and Clinical Relevance. *Clinical and Diagnostic Laboratory Immunology*, *7*(2), 131–140. <https://doi.org/10.1128/CDLI.7.2.131-140.2000>
- Wadei, H. M., Rule, A. D., Lewin, M., Mahale, A. S., Khamash, H. A., Schwab, T. R., Gloor, J. M., Textor, S. C., Fidler, M. E., Lager, D. J., Larson, T. S., Stegall, M. D., Cosio, F. G., & Griffin, M. D. (2006). Kidney transplant function and histological clearance of virus following

- diagnosis of polyomavirus-associated nephropathy (PVAN). *American Journal of Transplantation: Official Journal of the American Society of Transplantation and the American Society of Transplant Surgeons*, 6(5 Pt 1), 1025–1032. <https://doi.org/10.1111/j.1600-6143.2006.01296.x>
- Walker, P. J., Siddell, S. G., Lefkowitz, E. J., Mushegian, A. R., Adriaenssens, E. M., Dempsey, D. M., Dutilh, B. E., Harrach, B., Harrison, R. L., Hendrickson, R. C., Junglen, S., Knowles, N. J., Kropinski, A. M., Krupovic, M., Kuhn, J. H., Nibert, M., Orton, R. J., Rubino, L., Sabanadzovic, S., ... Davison, A. J. (2020). Changes to virus taxonomy and the Statutes ratified by the International Committee on Taxonomy of Viruses (2020). *Archives of Virology*, 165(11), 2737–2748. <https://doi.org/10.1007/s00705-020-04752-x>
- Wang, Y., Rowley, K. J., Booth, B. J., Sloan, S. E., Ambrosino, D. M., & Babcock, G. J. (2011). G glycoprotein amino acid residues required for human monoclonal antibody RAB1 neutralization are conserved in rabies virus street isolates. *Antiviral Research*, 91(2), 187–194. <https://doi.org/10.1016/j.antiviral.2011.06.002>
- Wang, Z., Lorenzi, J. C. C., Muecksch, F., Finkin, S., Viant, C., Gaebler, C., Cipolla, M., Hoffmann, H.-H., Oliveira, T. Y., Oren, D. A., Ramos, V., Nogueira, L., Michailidis, E., Robbiani, D. F., Gazumyan, A., Rice, C. M., Hatzioannou, T., Bieniasz, P. D., Caskey, M., & Nussenzweig, M. C. (2021). Enhanced SARS-CoV-2 neutralization by dimeric IgA. *Science Translational Medicine*, 13(577). <https://doi.org/10.1126/scitranslmed.abf1555>
- Wei, C., Anolik, J., Cappione, A., Zheng, B., Pugh-Bernard, A., Brooks, J., Lee, E.-H., Milner, E. C. B., & Sanz, I. (2007). A new population of cells lacking expression of CD27 represents a notable component of the B cell memory compartment in systemic lupus erythematosus. *Journal of Immunology (Baltimore, Md.: 1950)*, 178(10), 6624–6633. <https://doi.org/10.4049/jimmunol.178.10.6624>
- Weill, J.-C., Weller, S., & Reynaud, C.-A. (2009). Human Marginal Zone B Cells. *Annual Review of Immunology*, 27(1), 267–285. <https://doi.org/10.1146/annurev.immunol.021908.132607>
- Weiss, G. E., Crompton, P. D., Li, S., Walsh, L. A., Moir, S., Traore, B., Kayentao, K., Ongoiba, A., Doumbo, O. K., & Pierce, S. K. (2009). Atypical Memory B Cells Are Greatly Expanded in Individuals Living in a Malaria-Endemic Area. *The Journal of Immunology*, 183(3), 2176–2182. <https://doi.org/10.4049/jimmunol.0901297>
- Weist, B. J. D., Schmueck, M., Fuehrer, H., Sattler, A., Reinke, P., & Babel, N. (2014). The role of CD4+ T cells in BKV-specific T cell immunity. *Medical Microbiology and Immunology*, 203(6), 395–408. <https://doi.org/10.1007/s00430-014-0348-z>
- Weist, Benjamin J. D., Wehler, P., Ahmad, L. E., Schmueck-Henneresse, M., Millward, J. M., Nienen, M., Neumann, A. U., Reinke, P., & Babel, N. (2015). A revised strategy for monitoring BKV-specific cellular immunity in kidney transplant patients. *Kidney International*, 88(6), 1293–1303. <https://doi.org/10.1038/ki.2015.215>
- Weller, S., Braun, M. C., Tan, B. K., Rosenwald, A., Cordier, C., Conley, M. E., Plebani, A., Kumararatne, D. S., Bonnet, D., Tournilhac, O., Tchernia, G., Steiniger, B., Staudt, L. M., Casanova, J.-L., Reynaud, C.-A., & Weill, J.-C. (2004). Human blood IgM “memory” B cells are circulating splenic marginal zone B cells harboring a prediversified immunoglobulin repertoire. *Blood*, 104(12), 3647–3654. <https://doi.org/10.1182/blood-2004-01-0346>
- Weller, S., Mamani-Matsuda, M., Picard, C., Cordier, C., Lecoeuche, D., Gauthier, F., Weill, J.-C., & Reynaud, C.-A. (2008). Somatic diversification in the absence of antigen-driven

- responses is the hallmark of the IgM+IgD+CD27+ B cell repertoire in infants. *The Journal of Experimental Medicine*, 205(6), 1331–1342. <https://doi.org/10.1084/jem.20071555>
- White, M. K., Safak, M., & Khalili, K. (2009). Regulation of Gene Expression in Primate Polyomaviruses. *Journal of Virology*, 83(21), 10846–10856. <https://doi.org/10.1128/JVI.00542-09>
- Williams, J. W., Javaid, B., Kadambi, P. V., Gillen, D., Harland, R., Thistlewaite, J. R., Garfinkel, M., Foster, P., Atwood, W., Millis, J. M., Meehan, S. M., & Josephson, M. A. (2005). Leflunomide for polyomavirus type BK nephropathy. *The New England Journal of Medicine*, 352(11), 1157–1158. <https://doi.org/10.1056/NEJM200503173521125>
- Williams, L. D., Ofek, G., Schätzle, S., McDaniel, J. R., Lu, X., Nicely, N. I., Wu, L., Loughheed, C. S., Bradley, T., Louder, M. K., McKee, K., Bailer, R. T., O’Dell, S., Georgiev, I. S., Seaman, M. S., Parks, R. J., Marshall, D. J., Anasti, K., Yang, G., ... Haynes, B. F. (2017). Potent and broad HIV-neutralizing antibodies in memory B cells and plasma. *Science Immunology*, 2(7). <https://doi.org/10.1126/sciimmunol.aal2200>
- Wiseman, A. C. (2009). Polyomavirus nephropathy: A current perspective and clinical considerations. *American Journal of Kidney Diseases: The Official Journal of the National Kidney Foundation*, 54(1), 131–142. <https://doi.org/10.1053/j.ajkd.2009.01.271>
- Womer, K. L., Huang, Y., Herren, H., Dibadj, K., Peng, R., Murawski, M., Shraybman, R., Patton, P., Clare-Salzler, M. J., & Kaplan, B. (2010). Dendritic cell deficiency associated with development of BK viremia and nephropathy in renal transplant recipients. *Transplantation*, 89(1), 115–123. <https://doi.org/10.1097/TP.0b013e3181bc6096>
- Wu, S. W., Chang, H. R., Hsieh, M. C., Chiou, H. L., Lin, C. C., & Lian, J. D. (2008). Early diagnosis of polyomavirus type BK infection in tailoring immunosuppression for kidney transplant patients: Screening with urine qualitative polymerase chain reaction assay. *Transplantation Proceedings*, 40(7), 2389–2391. <https://doi.org/10.1016/j.transproceed.2008.06.025>
- Wu, S.-W., Chang, H.-R., & Lian, J.-D. (2009). The effect of low-dose cidofovir on the long-term outcome of polyomavirus-associated nephropathy in renal transplant recipients. *Nephrology, Dialysis, Transplantation: Official Publication of the European Dialysis and Transplant Association - European Renal Association*, 24(3), 1034–1038. <https://doi.org/10.1093/ndt/gfn675>
- Yang, R. C., & Wu, R. (1979). BK virus DNA: Complete nucleotide sequence of a human tumor virus. *Science (New York, N.Y.)*, 206(4417), 456–462. <https://doi.org/10.1126/science.228391>
- Yogo, Y., Zhong, S., Suzuki, M., Shibuya, A., & Kitamura, T. (2007). Occurrence of the European subgroup of subtype I BK polyomavirus in Japanese-Americans suggests transmission outside the family. *Journal of Virology*, 81(23), 13254–13258. <https://doi.org/10.1128/JVI.01018-07>
- Zeng, G., Huang, Y., Huang, Y., Lyu, Z., Lesniak, D., & Randhawa, P. (2016). Antigen-Specificity of T Cell Infiltrates in Biopsies With T Cell-Mediated Rejection and BK Polyomavirus Viremia: Analysis by Next Generation Sequencing. *American Journal of Transplantation: Official Journal of the American Society of Transplantation and the American Society of Transplant Surgeons*, 16(11), 3131–3138. <https://doi.org/10.1111/ajt.13911>
- Zhao, L., & Imperiale, M. J. (2017). Identification of Rab18 as an Essential Host Factor for BK Polyomavirus Infection Using a Whole-Genome RNA Interference Screen. *MSphere*, 2(4). <https://doi.org/10.1128/mSphereDirect.00291-17>

- Zhao, L., Marciano, A. T., Rivet, C. R., & Imperiale, M. J. (2016). Caveolin- and clathrin-independent entry of BKPyV into primary human proximal tubule epithelial cells. *Virology*, *492*, 66–72. <https://doi.org/10.1016/j.virol.2016.02.007>
- Zheng, H.-Y., Nishimoto, Y., Chen, Q., Hasegawa, M., Zhong, S., Ikegaya, H., Ohno, N., Sugimoto, C., Takasaka, T., Kitamura, T., & Yogo, Y. (2007). Relationships between BK virus lineages and human populations. *Microbes and Infection*, *9*(2), 204–213. <https://doi.org/10.1016/j.micinf.2006.11.008>
- Zhou, W., Sharma, M., Martinez, J., Srivastava, T., Diamond, D. J., Knowles, W., & Lacey, S. F. (2007). Functional characterization of BK virus-specific CD4+ T cells with cytotoxic potential in seropositive adults. *Viral Immunology*, *20*(3), 379–388. <https://doi.org/10.1089/vim.2007.0030>
- Zhou, Y., Liu, Z., Wang, Z., Zhang, Q., Mayer, C. T., Schoofs, T., Nussenzweig, M. C., de Jong, Y. P., & Wang, Q. (2020). Single-Cell Sorting of HBsAg-Binding Memory B Cells from Human Peripheral Blood Mononuclear Cells and Antibody Cloning. *STAR Protocols*, *1*(3), 100129. <https://doi.org/10.1016/j.xpro.2020.100129>
- Zinkernagel, R. M. (2001). Maternal antibodies, childhood infections, and autoimmune diseases. *The New England Journal of Medicine*, *345*(18), 1331–1335. <https://doi.org/10.1056/NEJMra012493>

INTRODUCTION

Le polyomavirus BK (BKPyV) est un virus ubiquitaire qui infecte 80% de la population humaine. La primo-infection a lieu lors de la petite enfance, puis le virus établit une infection latente dans le rein et persiste probablement tout au long de la vie chez son hôte. Bien que cette infection soit généralement asymptomatique, la réactivation du BKPyV chez les receveurs de greffe de rein est la cause de pathologies rénales sévères telles que la néphropathie associée au polyomavirus (PyVAN), qui survient chez 1 à 10% des receveurs de greffe, selon la cohorte étudiée. Une PyVAN incontrôlée peut provoquer le dysfonctionnement ou même la perte du greffon. Il n'existe actuellement aucun traitement antiviral approuvé ayant une efficacité clinique contre le BKPyV. La PyVAN est donc gérée par modulation de la thérapie immunosuppressive, qui permet aux réponses immunitaires de l'hôte de contrôler à nouveau la multiplication virale.

En l'absence d'enzymes virales qui pourraient être des cibles pharmacologiques pour des antiviraux à action directe, l'immunothérapie peut avoir un potentiel pour la prophylaxie ou le traitement de PyVAN chez les receveurs de transplantation rénale. En ce qui concerne la réponse humorale spécifique du BKPyV, il a été observé que l'incidence de PyVAN est plus élevée chez les receveurs de rein avec de faibles titres d'anticorps neutralisants. En outre, certaines études ont indiqué que la perfusion d'immunoglobulines intraveineuses (IVIG) contenant des anticorps neutralisants spécifiques du BKPyV peut empêcher la réplication virale chez les greffés rénaux, et traiter avec succès la PyVAN. Ainsi, les données existantes indiquent que les thérapies à base d'anticorps peuvent également être efficaces contre le BKPyV. Cependant, l'IVIG est un produit sanguin qui contient un mélange complexe d'anticorps non contrôlé, et bien que rare, un rejet aigu médié par un anticorps après perfusion d'IGIV contenant des anticorps spécifiques du donneur, a été rapporté dans la littérature. Dans ce cadre,

le développement d'anticorps monoclonaux neutralisants constitue une alternative qui permet de combiner la puissance antivirale de l'IVIg avec un risque moindre d'effets secondaires indésirables. En particulier, la génération d'anticorps neutralisants à spectre large, capables d'inhiber les quatre génotypes de BKPyV, pourrait représenter une avancée thérapeutique importante dans le traitement ou la prévention de la PyVAN.

Dans ce projet, nous avons cherché à isoler et à caractériser des anticorps monoclonaux neutralisants à partir de receveurs de rein ayant développé une forte réponse humorale spécifique au BKPyV, et à caractériser le répertoire des récepteurs aux cellules B spécifiques du BKPyV (BCR).

METHODES

Des capsides virales vides ("Virus-Like Particles", ou VLPs) de génotype Ia du BKPyV portant des fluorophores ont été utilisées pour cibler les lymphocytes B mémoires spécifiques du virus et circulants dans le sang de différents patients greffés. Une fois purifiés, les séquences des récepteurs B exprimés par ces lymphocytes B ainsi que leur transcriptome ont été définies par single-cell RNA seq et analysées par bioinformatique. Six greffés rénaux présentant des augmentations significatives de titres d'anticorps neutralisants après réactivation du BKPyV ont été sélectionnés pour cette expérience. 17 échantillons de cellules mononucléées sanguines (PBMC) congelés (au moins deux échantillons indépendants par patient) ont été décongelés. Les lymphocytes B totaux, présents dans ces échantillons, ont été enrichis par tri magnétique, puis marqués avec des VLPs couplées à différents fluorochromes (VLP BKPyV gla couplées à l'AF555 et l'AF647, VLPs du polyomavirus murin (MPyV) couplées à l'AF488), et un cocktail d'anticorps anti CD3 et anti CD19 (anti CD3-BV510, CD19-BV421) afin de pouvoir identifier et sélectionner, à l'échelle de cellules uniques (plateforme chromium), les lymphocytes B spécifiques du virus. Les 17 échantillons de PBMC ont par ailleurs été préalablement marqués à l'aide de deux anticorps couplés à des séquences oligonucléotidiques variables : Anticorps de type "hashtag" permettant

d'associer les données RNAseq obtenues (appareil Illumina) pour chaque cellule à l'un des 17 échantillons de PBMC initiaux. Cette méthode nous a permis d'identifier un certain nombre d'anticorps neutralisants du virus BK.

RESULTATS

1. Production et validation des VLPs couplées

Afin de générer des VLP, des vecteurs d'expression codant pour la protéine de capsid majeur du virus, la VP1, du BKPyV de génotype Ia, ou du MPyV ont été transfectés de manière transitoire dans des cellules HEK 293TT. Les lysats cellulaires contenant les VLPs du BKPyV ont été couplés à l'AF555 ou AF647, tandis que le lysat du MPyV a été couplé avec l'AF488. Les VLPs marquées ont ensuite été purifiées par ultracentrifugation dans un gradient d'Optiprep, qui a été ensuite éliminé par plusieurs lavages en PBS et passage sur filtres Amicon de 100 kDa. Les VLP fluorescentes 1) avaient une morphologie homogène de type polyomavirus en microscopie électronique à coloration négative, 2) contenaient une seule bande protéique correspondant à la VP1 sur gel SDS-PAGE, et 3) n'avaient pas de réactivation sérologique croisée entre les VLPs du BKPyV et les VLPs du MPyV par ELISA. Par conséquent, les VLPs marquées du MPyV peuvent être utilisées comme contrôle négatif pour éliminer les lymphocytes B non spécifiques du BKPyV.

Ensuite, nous avons testé la capacité des VLPs marquées du BKPyV à cibler les cellules B mémoire spécifiques du virus parmi différents groupes d'individus : les donneurs sains, et les receveurs de greffe de rein séronégatifs et séropositifs pour le BKPyV après la transplantation. Nous avons observé que seuls les receveurs séropositifs présentant une virurie et une virémie élevée, avaient un pourcentage de cellules B spécifiques du BKPyV supérieur à 0,1% au sein de la population de lymphocytes B CD19⁺, ce qui était au moins 10 fois plus élevé que dans les autres groupes. Les VLP fluorescentes du BKPyV pouvaient donc être utilisées comme des sondes pour trier les lymphocytes B circulants spécifiques du BKPyV.

2. Tri des lymphocytes B spécifiques du BKPyV à partir de plusieurs receveurs de greffe de rein

Afin d'obtenir un nombre suffisant de lymphocytes B spécifiques du BKPyV pour l'expérience de single-cell RNA seq, nous avons dû traiter plusieurs échantillons de PBMC congelés le même jour. Sur un total d'environ 270 millions de PBMC congelés, environ 10^5 cellules CD19⁺ ont été isolées (population de lymphocytes B totaux, ou TotB) et environ 10^4 cellules CD19⁺ spécifiques du BKPyV (population SpecB) ont été triées.

3. Répertoire BCR de lymphocytes B spécifiques du BKPyV

2105 séquences BCR ont été obtenues, avec une distribution très inégale entre les patients. Plus de 1500 séquences d'anticorps ont été dérivées du patient 3.1, tandis que seulement 13 séquences d'anticorps du patient 3.12 et 12 du patient 3.3 ont été obtenues. Cependant, au moins 50 séquences de BCR spécifiques du BKPyV ont été obtenues à partir de chacun des trois autres patients. De plus, chez les mêmes patients, des centaines de séquences BCR ont été déterminées à partir de lymphocytes B CD19⁺ circulants. Chez les quatre patients avec au moins 50 séquences d'anticorps spécifiques, la plupart des cellules B spécifiques du BKPyV portaient des chaînes légères Lambda, tandis que le répertoire TotB des mêmes patients avait une prédominance d'anticorps avec des chaînes légères Kappa. De plus, seule une minorité de lymphocytes B spécifiques du BKPyV exprimait des anticorps de type IgA ou de type IgG, même si la proportion d'anticorps ayant une commutation isotypique était supérieure à celle observée dans la population de TotB chez trois des quatre patients.

En termes d'utilisation du gène V, les quatre patients ont présenté un enrichissement supérieur à deux fois en IGVH4-39 dans le répertoire SpecB par rapport au répertoire TotB du même patient. Chez les patients 3.1, 3.4 et 2.6, le gène V IGVH4-39 était dominant et présent dans au moins 20% des lymphocytes B spécifiques du BKPyV. En ce qui concerne la chaîne légère, aucun gène V unique ne s'est démarqué,

bien que l'IGVL2-11 a montré un enrichissement supérieur à deux fois, chez trois des quatre patients.

La diversité des clonotypes, mesurée par la diversité de Shannon et l'indice D50, était significativement plus faible dans le répertoire SpecB par rapport au répertoire TotB, tandis que l'inégalité du répertoire, mesurée par le coefficient de Gini, était significativement plus élevée. Ces caractéristiques sont attendues pour les répertoires de lymphocytes B biaisés vers la reconnaissance d'un antigène connu. Suffisamment de données étaient disponibles à partir des échantillons des patients 3.1 et 3.2 pour analyser le chevauchement du répertoire spécifique du BKPyV dans des échantillons indépendants de PBMC du même individu. Le chevauchement du répertoire spécifique du BKPyV trouvé entre les deux échantillons du patient 3.2 était de 51%. Concernant les trois échantillons du patient 3.1, le chevauchement moyen du répertoire était de 68%. La disponibilité d'échantillons répétés de ces deux patients nous a permis de calculer la diversité α du répertoire BCR spécifique du BKPyV en utilisant l'estimateur Chao1. Le nombre total de clonotypes spécifiques du BKPyV était de 437 ± 25 chez le patient 3.1 et de 599 ± 99 chez le patient 3.2. Entre différents patients, le chevauchement de répertoire s'est avéré faible (environ 3%) indiquant que le répertoire BCR spécifique du BKPyV de chaque patient est principalement privé, avec seulement quelques clonotypes publics partagés entre deux individus.

Ensuite, nous avons étudié les caractéristiques des anticorps IgM et IgG spécifiques du BKPyV. Comme attendu, le nombre moyen de mutations somatiques non-synonymes était plus faible dans les lymphocytes B exprimant une IgM ou une IgD par rapport aux lymphocytes B ayant subi une commutation de classe. Nous avons néanmoins observé des IgM avec un nombre très élevé de mutations somatiques, et dans les clonotypes qui contenaient à la fois des anticorps IgG et IgM, il n'y avait aucune différence dans le nombre moyen de mutations entre les clones IgG et IgM. La relation entre la commutation de classe et le nombre de mutations somatiques au sein des clonotypes dans le jeu de données SpecB a été analysée systématiquement chez les patients 3.1 et 3.2. Chez les deux patients, un cluster de clones IgM avec un faible taux

de mutation somatique, qui semblait indiquer une forte réponse primaire, a été observé. Nous avons également observé des clonotypes avec une proportion progressivement plus élevée de lymphocytes B ayant une commutation de classe et un nombre progressivement plus élevé de mutations somatiques, culminant dans un cluster de clonotypes exclusivement d'IgG, représentant des lymphocytes B mémoire à IgG (MBG). En outre, les deux patients présentaient également un certain nombre de clonotypes avec des niveaux élevés de SHM qui étaient principalement des IgM, vraisemblablement des lymphocytes B mémoire à IgM (MBM). Ces MBM comprenaient le clonotype dominant chez le patient 3.1, qui montrait une activité neutralisante spécifique du génotype I lors des tests sur des cellules 293TT et des cellules RS, une lignée de cellules épithéliales tubulaires rénales humaines immortalisées.

Nous avons ensuite comparé l'utilisation des gènes V au sein des MBM et MBG spécifiques du BKPyV exprimant des anticorps avec au moins 5 mutations somatiques dans la chaîne lourde. Chez les patients 3.1 et 3.2, les MBM et MBG spécifiques du BKPyV ont montré des profils distincts d'utilisation des gènes V des chaînes lourdes et légères. Chez le patient 3.1, les gènes de chaîne lourde IGHV1-3, IGHV3-53 et IGHV4-61, et les gènes de chaîne légère IGKV3-11, IGKV3-20 et IGLV3-21 étaient plus fréquents dans le MBG que dans le MBM. Un schéma similaire a été observé chez le patient 3.2, avec les gènes IGHV2-5 et IGHV4-61, et IGKV3-11 et IGLV3-2. Inversement, l'IGHV5-51 et l'IGLV3-1 ont été préférentiellement utilisés par les MBM spécifiques de BKPyV chez les patients 3.1 et 3.2. Le gène IGHV4-39 qui a montré le plus grand enrichissement dans le répertoire BCR global spécifique du BKPyV a été retrouvé dans les MBG et le MBM. Ces résultats indiquent que les anticorps IgG et IgM spécifiques du BKPyV utilisent des répertoires BCR distincts.

En comparant les gènes différentiellement exprimés entre le MBM et le MBG par bio-informatique, nous avons observé une baisse de la régulation de 5 gènes et une augmentation pour 14 gènes dans les MBM par rapport aux MBG. Parmi les gènes sous-exprimés se trouvaient le *CD83*, un marqueur de cellules dendritiques matures et de lymphocytes B activés dans le centre germinatif, et l'*IGLC3*, gène de la région constante

3 de la chaîne légère lambda. Parmi les gènes sur-exprimés, nous avons trouvé *CD79B* qui, associé au *CD79A* et à l'immunoglobuline membranaire, forme le complexe BCR mature. Un autre gène plus fortement exprimé chez les MBM était le *PARP-1*. Ce gène agit dans de nombreux événements importants au cours de la maturation des cellules B. En général, bien que nous ayons trouvé divers gènes exprimés de manière significative (*p-value* inférieure à 0,05), le niveau d'expression différentielle était faible, ce qui indique que les profils d'expression des lymphocytes B mémoire commutées et non-commutées spécifiques du BKPyV étaient très similaires.

4. Identification d'une famille d'anticorps « 41F17-like » neutralisant à spectre large

Afin d'identifier les anticorps possédant des propriétés neutralisantes semblables aux monoclonaux 41F17 et 27O24 identifiés par une équipe de recherche de la société Novartis, les anticorps avec moins de 5 SHM de chaînes lourdes ont été exclus, puis les séquences d'acides aminés CDR3 des chaînes lourdes et légères ont été associées, puis alignées. Les séquences alignées ont été regroupées sous forme d'un arbre phylogénétique par l'algorithme de Neighbor-Joining.

Bien que nous n'ayons pas détecté de séquence voisine de l'anticorps 27O24, nous avons pu identifier un cluster d'anticorps IgG à chaîne légère kappa partageant un motif de CDR3 avec l'anticorps 41F17. Lorsqu'ils ont été clonés et exprimés, les anticorps des clonotypes 120, 160 et 198 se liaient spécifiquement aux quatre génotypes de BKPyV, une propriété qu'ils partagent avec l'anticorps 41F17, et qui n'a été retrouvée que dans l'un des neuf autres anticorps testés. Les clonotypes 120, 160 et 198 avaient une utilisation identique des gènes V des chaînes lourdes et légères (IGHV4-39 / IGKV3-11), qui différait de celle trouvée dans 41F17 (IGHV4-31 / IGKV3-11). Comme décrit dans la section précédente, le gène IGKV3-11 était utilisé préférentiellement par les MBG. En effet, les clonotypes 120, 160 et 198 étaient caractérisés par une proportion de plus de 85% d'IgG. Par conséquent, malgré la

dominance des IgM dans le répertoire spécifique du BKPyV, ce cluster d'anticorps neutralisants à spectre large était majoritairement de type IgG.

L'avidité de liaison aux VLPs mesurée par la SPR était dans la gamme sous-nanomolaire, les clonotypes 120 et 160 se lient aux quatre génotypes du BKPyV avec une avidité similaire à celle observée pour l'anticorps 41F17. En termes de neutralisation, comme le 41F17, les anticorps 120 et 160 neutralisaient les quatre génotypes du BKPyV dans les cellules 293TT, alors que seuls le clonotype 120 et le monoclonal 41F17 possédaient une activité de neutralisation à spectre large dans les cellules RS avec des concentrations inhibitrices (IC50) sous-nanomolaire. Concernant l'anticorps 198, un test de neutralisation réalisé avec des surnageants contenant des anticorps sécrétés par les cellules transfectées en plaque 96 puits, a démontré que cet anticorps était également capable de neutraliser les quatre génotypes du BKPyV dans les cellules RS. Cependant, en raison d'un problème technique inconnu, le rendement de la production en flasques T175 était toujours inférieur à 10 µg/mL. Par conséquent, nous n'avons pas pu jusqu'à présent purifier l'anticorps 198 pour des analyses plus approfondies, y compris pour la mesure de l'avidité et la mesure de son titre neutralisant contre les quatre génotypes du virus.

CONCLUSION

En réponse à l'objectif principal du projet, nous avons généré plusieurs anticorps neutralisants à spectre large contre le BKPyV. Parmi eux, l'anticorps 120 a montré une forte activité antivirale, comparable, voire légèrement plus élevée que celle de l'anticorps 41F17 de chez Novartis. Il existe actuellement un anticorps monoclonal spécifique du BKPyV, le MAU 868, qui est actuellement en essai clinique de phase 2 financé par la société Amplyx Pharmaceuticals, qui a racheté la licence d'exploitation du MAU 868 à la société Novartis.





Notre anticorps monoclonal 120 semble donc être un excellent candidat pour un développement clinique, seul ou en combinaison avec d'autres monoclonaux.

ANNEX

ANNEX

Article

Persistent BK Polyomavirus Viruria Is Associated with Accumulation of VP1 Mutations and Neutralization Escape

Dorian McIlroy ^{1,2,3,*} , Mario Hönemann ⁴, Ngoc-Khanh Nguyen ^{1,2}, Paul Barbier ^{1,2}, Cécile Peltier ^{1,2}, Audrey Rodallec ⁵, Franck Halary ^{1,2} , Emilie Przyrowski ⁵, Uwe Liebert ⁴ , Maryvonne Hourmant ^{2,6} and Céline Bressollette-Bodin ^{1,2,5,7} 

¹ Centre de Recherche en Transplantation et Immunologie (CRTI), UMR 1064, INSERM, Université de Nantes, 44093 Nantes, France; ngoc-khanh.nguyen@univ-nantes.fr (N.-K.N.); paul.barbier@univ-nantes.fr (P.B.); cecile.peltier@univ-nantes.fr (C.P.); franck.halary@univ-nantes.fr (F.H.); celine.bressollette@univ-nantes.fr (C.B.-B.)

² Institut de Transplantation Urologie-Néphrologie (ITUN), CHU Nantes, 44093 Nantes, France; maryvonne.hourmant@chu-nantes.fr

³ Faculté des Sciences et des Techniques, Université de Nantes, 44322 Nantes, France

⁴ Institut für Virologie, Universität Leipzig, 04103 Leipzig, Germany; Mario.Hoenemann@medizin.uni-leipzig.de (M.H.); liebert@medizin.uni-leipzig.de (U.L.)

⁵ Service de Virologie, CHU Nantes, 44093 Nantes, France; Audrey.RODALLEC@chu-nantes.fr (A.R.); EmPrzyrowski@chu-angers.fr (E.P.)

⁶ Service de Néphrologie et Immunologie Clinique, CHU Nantes, 44093 Nantes, France

⁷ Faculté de Médecine, Université de Nantes, 44093 Nantes, France

* Correspondence: dorian.mcilroy@univ-nantes.fr; Tel.: +33-2-40-41-28-39

Received: 19 July 2020; Accepted: 28 July 2020; Published: 29 July 2020



Abstract: To investigate the relationship between neutralization escape and persistent high-level BK polyomavirus replication after kidney transplant (KTx), VP1 sequences were determined by Sanger and next-generation sequencing in longitudinal samples from KTx recipients with persistent high-level viruria (non-controllers) compared to patients who suppressed viruria (controllers). The infectivity and neutralization resistance of representative VP1 mutants were investigated using pseudotype viruses. In all patients, the virus population was initially dominated by wild-type VP1 sequences, then non-synonymous VP1 mutations accumulated over time in non-controllers. BC-loop mutations resulted in reduced infectivity in 293TT cells and conferred neutralization escape from cognate serum in five out of six non-controller patients studied. When taken as a group, non-controller sera were not more susceptible to neutralization escape than controller sera, so serological profiling cannot predict subsequent control of virus replication. However, at an individual level, in three non-controller patients the VP1 variants that emerged exploited specific “holes” in the patient’s humoral response. Persistent high-level BK polyomavirus replication in KTx recipients is therefore associated with the accumulation of VP1 mutations that can confer resistance to neutralization, implying that future BKPyV therapies involving IVIG or monoclonal antibodies may be more effective when used as preventive or pre-emptive, rather than curative, strategies.

Keywords: polyomavirus; transplantation; immunity; neutralization

1. Introduction

The BK polyomavirus PyV (BKPyV) is a typical opportunistic pathogen. Following asymptomatic primary infection during childhood, it establishes a latent infection in the kidney, which appears

to persist throughout life. Approximately 7% of healthy adults excrete BKPyV in the urine [1], and this proportion increases during natural, acquired [2], or iatrogenic [3] immunosuppression. Its pathogenic potential is manifested in kidney transplant (KTx) recipients, in whom uncontrolled BKPyV replication can result in polyomavirus nephropathy (PyVAN) and graft loss or dysfunction. PyVAN can only be diagnosed definitively by histology, but it is correlated with viremia greater than 10^4 genome copies/mL [4], and high-level viremia is generally classified as presumptive PyVAN [5]. Recent results indicate that at least 90% of BKPyV genomes in plasma are DNase sensitive, that is, represent free DNA and not infectious virions [6], which explains why BKPyV replication remains restricted to the graft and does not spread to the native kidneys. There is currently no approved antiviral therapy with clinical efficacy against BKPyV, so presumptive or biopsy-confirmed PyVAN is managed by modulation of immunosuppressive therapy, which allows host immune responses to clear the virus [7]. The virological response rate to this intervention appears to vary between centres, with recent publications reporting clearance of viremia in response to modulation of immunosuppression in proportions varying from 30% [8,9] up to more than 75% [10] of PyVAN patients. In the single-centre study with the longest follow-up and the largest cohort, clearance of viremia was attained by 44 (92%) of 48 patients with presumptive PyVAN following a standard three-stage protocol for reduction of immunosuppressive therapy [11]. However, the interquartile range for time to viremia clearance was 65–414 days, meaning that at least 25% of these PyVAN patients had viremia that persisted for more than 1 year, despite modulation of immunosuppressive therapy. Similarly, the Banff working group on PyVAN, analyzing data from nine transplant centres in Europe and North America, found that PyVAN persisted for more than 24 months in 39 of 149 (26%) patients [12].

The importance of the neutralizing antibody response in controlling BKPyV replication in KTx recipients has been highlighted by the observation that higher neutralizing titres at the time of graft are correlated with lower risk of BKPyV reactivation in the 12 months following KTx [13]. Surprisingly, the strong humoral response that develops in KTx recipients after BKPyV reactivation [13,14] does not correlate with subsequent viral clearance, and several studies have implicated CTL rather than antibodies as playing the dominant role [15–17] in the resolution of BKPyV infection after modulation of immunosuppressive therapy. In HIV [18,19] and HCV [20,21] infection, persistent viremia in the face of a robust humoral response is the result of the selection of escape mutations in viral glycoproteins, leading to an evolutionary arms race between the virus and the host neutralizing response, in which host responses continually struggle to keep up with a rapidly evolving virus population. Because polyomaviruses are generally considered to be slowly evolving DNA viruses, a similar process was not thought to be plausible during BKPyV infection. Nevertheless, mutations in the major BKPyV capsid protein, VP1, have been observed in patients with PyVAN [22,23], and appear to accumulate in the typing region of the VP1 gene [24,25], which distinguishes the four different BKPyV genotypes, and codes for the BC-loop on the surface of the virus capsid. Results published in 2018 provided an elegant explanation of how these mutations arise and the first description of their functional impact [26]. In two KTx patients with PyVAN caused by genotype IV BKPyV, Peretti et al. showed firstly, that mutations in VP1 carried the signature of cytosine deamination on the antisense strand by the apolipoprotein B mRNA editing, catalytic polypeptide-like (APOBEC) 3B enzyme; secondly, that these mutations led to resistance against neutralization; and thirdly, that APOBEC3 enzymes are expressed in renal biopsies from KTx recipients. However, the patients included in this study were both characterized by a rather uncommon clinical presentation of clear cell renal carcinoma concomitant with, or subsequent to PyVAN. In addition, both patients cleared their BKPyV viremia, despite the presence of apparent neutralization escape mutations. Therefore, it is not entirely clear whether the results of the study by Peretti et al. can be generalized to other BKPyV genotypes and to more frequent clinical situations, and the relationship between the presence of VP1 mutations and viral clearance remains an open question. In order to address these points, we first investigated the presence of mutations in the VP1 typing region in KTx recipients with persistent or transient high-level

BKPyV viruria, then analyzed the functional impact of BC-loop mutations in genotype I and genotype IV VP1 proteins on infectivity and resistance to neutralization.

2. Materials and Methods

2.1. Patients and Clinical Samples

Patients in the present study were included retrospectively in Nantes and in Leipzig, based on duration of viral load and BKPyV genotype recorded in the hospital laboratory databases. Patients in Nantes were transplanted between 2011 and 2014 and had previously been included in a prospective observational study, approved by the local ethics committee (approval date: 8 November 2011) and declared to the French Commission Nationale de l'Informatique et des Libertés (CNIL, n°1600141). Patients in Leipzig were transplanted between 2009 and 2012. Retrospective analysis was approved by the local ethics committee (Leipzig University ethical review committee ref.-no. 300/16-ek, approval date: 26 September 2016). All patients in Nantes and Leipzig gave informed consent authorizing the use of archived urine and blood samples for research protocols. Anonymised clinical and biological data for these patients were extracted from the hospital databases. Patients 3.16, 3.17 and 3.18 were recruited in Leipzig; all other patients were recruited in Nantes.

In order to define two clearly distinct patient groups, KTx recipients in Nantes and Leipzig with peak viruria $>7 \log_{10}$ copies/mL were stratified into controllers, who showed a drop in viruria of greater than $2 \log_{10}$ copies/mL at 6 months following peak viruria, and a reduction of greater than $3 \log_{10}$ copies at 12 months following peak viruria ($n = 12$, Figure 1A), and non-controllers who had a drop in viruria less than $2 \log_{10}$ copies/mL over 12 months ($n = 12$, Figure 1B). Patients with high-level viruria that lasted more than 6 months, but less than 12 months, were considered “intermediate”, and not included. Presence of viremia was not used as an inclusion criterion as preliminary investigations had shown that VP1 mutations could be detected in patients with persistent viruria in the absence of viremia.

2.2. VP1 Sequence Analysis

For Sanger sequencing, the typing region was amplified from urine and whole-blood extracted DNA using primers described in Takasaka et al. [27], and the full-length VP1 gene was amplified using primers described in Sharma et al. [28]. After Sanger sequencing of PCR products, VP1 sequences were analyzed using SeqScape™ software v3.0 (ThermoFisher Scientific). BKPyV genotypes were identified, and nucleotide polymorphisms were accepted only if present on both sense and antisense sequences. Sequences containing at least one non-synonymous BC-loop mutation were selected, and in the case of multiple sequences from the same patient, the sequence containing the most mutations was retained, so that each observed mutation represented an independent event. The prevalence of each mutation was calculated as the number of times each mutation was observed divided by the number of sequences.

To illustrate the positions of these mutated amino acids on the virus capsid, BKPyV VP1 pentamers were visualized using Pymol 1.8.4.0 under a Ubuntu Linux operating system. The 4MJ0 crystal structure of wild-type genotype I VP pentamer in complex with GD3 oligosaccharide was loaded, then rotated in order to present the sialic-acid binding pocket with its associated oligosaccharide ligand at the centre of the figure. The surfaces of the central (C), clockwise (CW), and counter-clockwise (CCW) VP1 subunits were rendered using the “show surface” command, and coloured light green, light blue, and light grey, respectively. The GD3 oligosaccharide was shown in a yellow stick representation. Since no three-dimensional structure of genotype IV BKPyV VP1 has been described, for visualization purposes, the genotype IV-specific amino acids were introduced using the Wizard/Mutagenesis function. Specifically, the S71T, N74T, D75A, and S77D mutations were introduced on the CW VP1 subunit, and the E61N, F66Y, K69R, and E82D mutations were introduced on the C subunit. Finally, amino acid residues that were found to be mutated in patients were coloured on a scale from light orange to red,

according to the prevalence of mutations found at each site. Specifically, positions 59, 60, 61, 62, 68, 69, and 82 were coloured on the C subunit, positions 72, 73, 75, 66, and 170 were coloured on the CW subunit, and positions 138 and 139 were coloured on the CCW subunit.

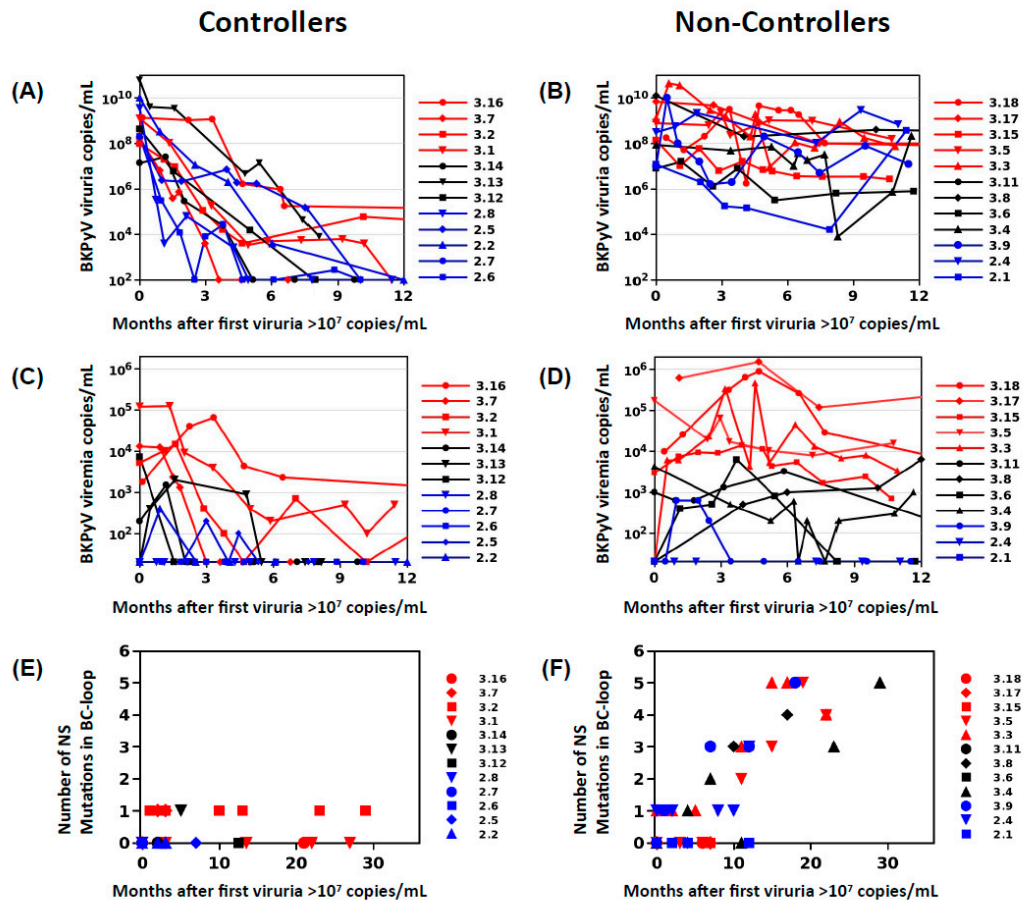


Figure 1. Evolution of viruria and VP1 mutations in controller and non-controller groups. Urine (A,B) and blood (C,D) viral load over time in controller (A,C) and non-controller (B,D) patients. Symbol colours correspond to high ($>4\log_{10}$ copies/mL, red), intermediate (between $3\log_{10}$ and $4\log_{10}$ copies/mL, black), and low ($<3\log_{10}$ copies/mL, blue) peak viremia. Accumulation of non-synonymous VP1 BC-loop mutations in non-controller (F), but not in controller patients (E). For each sample analyzed by PCR and Sanger sequencing, the number of differences compared to wild-type was plotted against time after first viruria $>10^7$ copies/mL. Blue symbols in panel E show patients who accumulate BC-loop mutations in the absence of viremia.

For next-generation sequencing (NGS) of the typing region, eight different unique and base-balanced 8bp barcodes were added to the 5' end of each forward and reverse primer, respectively. This provided a 16 primer set from which each forward and reverse primer were used in combination to create a dual barcode sample index. Barcoded VP1 sequences were amplified in a reaction volume of 25 μ L containing 5 μ L extracted viral DNA, 0.5 U Platinum SuperFi DNA Polymerase (Thermo Fisher, Courtaboeuf, France), 200 μ M each dNTP, 0.5 μ M primers, and 1x PCR buffer. After initial denaturation at 98 $^{\circ}$ C for 3 min, amplification was performed for 35 cycles on a LifePro Thermal Cycler (Dutscher, Issy-les-Moulineaux, France). Cycling conditions were 98 $^{\circ}$ C for 30 s, 54 $^{\circ}$ C for 30 s, and 72 $^{\circ}$ C for 30 s, with final extension at 72 $^{\circ}$ C for 5 min. PCR products were purified using columns (NucleoSpin Gel and PCR Clean-up, Macherey-Nagel, Hoerd, France) and eluted into 5 mM Tris/HCl, pH 8.5 buffer. Amplicon lengths and concentrations were measured with a LabChip GX (PerkinElmer, Villebon-sur-Yvette, France) using a high sensitivity 1K chip. PCR products were then

pooled in equimolar proportions then sent for DNA library preparation and Illumina sequencing at GENEWIZ, Inc. (South Plainfield, NJ, USA).

Illumina PE raw reads were quality trimmed, checked for N content and length filtered using Cutadapt version 2.3 [29]. Reads were then 5' trimmed and assigned to each patient's sample using Flexbar [30] version 3.3.0, and Illumina reads one and two were merged with NGmerge [31]. Mutations and their associated frequencies were predicted by running the breseq pipeline version 0.33.0 [32] with targeted-sequencing and polymorphism-mode options with default parameters using the Dunlop BKPyV genome (Accession Number NC_001538.1) as reference. After quality trimming and alignment 1263–8163 (mean 3449 ± 1543), merged sequences were analyzed per sample. NGS data has been deposited as a Targeted Locus Study in the following NCBI Bioproject PRJNA633999: Intra patient evolution of Human polyomavirus 1 (BKPyV).

2.3. Cell Culture

Vero cells and HEK 293TT cells, purchased from the National Cancer Institute's Developmental Therapeutics Program, were maintained in DMEM High Glucose (Thermo-Fisher) containing 10% FBS (Dutscher), 100 U/mL penicillin, 100 µg/mL streptomycin (Thermo-Fisher), 1x Glutamax (Thermo-Fisher), and 250 µg/mL Hygromycin (Sigma-Aldrich, Lyon, France). RS cells (Evercyte, Vienna, Austria), which are immortalized human renal tubular epithelial cells, were cultured in Proxup-3 medium (Evercyte, Vienna, Austria) supplemented with 100 U/mL penicillin and 100 µg/mL streptomycin (Thermo-Fisher) in tissue-culture plasticware coated with 50 µg/mL collagen I (Thermo-Fisher). 293TT and RS cells were grown at 37 °C with 5% CO₂ in a humidified incubator, and passaged at confluence by trypsinization for 10 min with 1x Trypsin-EDTA in PBS (Thermo-Fisher). Cultures were routinely tested for mycoplasma contamination by PCR [33] and were consistently negative.

2.4. Plasmids

The VP2 and VP3 expression plasmids ph2b and ph3b (#32109 and #32110) were obtained from Addgene (Cambridge, MA, USA). VP1 expression plasmids for genotypes Ia, Ib2 and IVc2 were kindly provided by Dr Christopher Buck, National Cancer Institute (NCI), Bethesda, MD. The plasmid pEGFP-N1 (Clontech) was used as the reporter gene. Mutations were introduced into the relevant VP1 plasmids by site-directed mutagenesis using the Q5 Site-directed mutagenesis kit (New England Biolabs, Evry, France). Primer pairs used for mutagenesis were selected using the NEBasechanger tool. After each mutagenesis reaction, miniprep DNA from four colonies was screened by Sanger sequencing (Eurofins Genomics, Ebersberg, Germany) with the EF1a-F primer. The full-length VP1 sequence of clones incorporating the desired mutations was confirmed by sequencing with the WPRE-R primer. The BKPyV-MM genome cloned into the pBR322 vector (pBKV 35-1, ATCC 45026) was obtained from the ATCC, and VP1 mutations were introduced using the Q5 Site-directed mutagenesis kit (New England Biolabs).

2.5. Pseudotype BKPyV Production

Pseudotype BKPyV (PSV) particles were prepared following a slightly modified version of protocols developed by the Buck lab [34,35]. Briefly, 293TT cells were seeded at 1×10^7 cells in a 75 cm² flask in DMEM 10% FBS without antibiotics, then co-transfected using Lipofectamine 2000 reagent (Thermo-Fisher) according to manufacturer's instructions. A total of 36 µg plasmid DNA comprising 16 µg VP1 plasmid, 4µg ph2b, 8 µg ph3b, and 8 µg pEGFP-N1 was mixed with 1.5 mL of Opti-MEM I (Thermo-Fisher). Eighty-five microlitres of Lipofectamine 2000 was diluted in 1.5 mL of Opti-MEM I and incubated for 5 min at room temperature, then mixed with the diluted plasmid DNA. After 20 min at room temperature, DNA-Lipofectamine complexes were added to each flask containing pre-plated 293TT cells.

Producer cells were harvested by trypsinisation 48 h after transfection. The pellet was washed once in cold PBS then resuspended in 800 μ L hypotonic lysis buffer consisting of 25 mM Sodium Citrate pH 6.0, 1 mM CaCl_2 , 1 mM MgCl_2 , and 5mM KCl. Cells were sonicated in a Bioruptor Plus device (Diagenode, Seraing, Belgium) for 10 min at 4 $^\circ\text{C}$ with 5 cycles of 1 min ON/1 min OFF. Type V neuraminidase (Sigma-Aldrich) was added to a final concentration of 1 U/mL and the extract was incubated for 30 min. at 37 $^\circ\text{C}$. The pH was neutralized by adding 100 μ L of 1M HEPES buffer pH 7.4, then 1 μ L (250 U) Pierce Nuclease (Thermo-Fisher) was added followed by 2 h incubation at 37 $^\circ\text{C}$. The lysate was clarified by centrifuging twice at 5000 $\times g$ for 5 min at 4 $^\circ\text{C}$, then layered onto an Optiprep 27%/33%/39% step gradient prepared in DPBS/0.8M NaCl. Gradients were centrifuged overnight at 175,000 $\times g$ at 4 $^\circ\text{C}$ in an SwTi55 rotor. Tubes were punctured with a 25G syringe needle, and 10 fractions of each gradient were collected into 1.5 mL microcentrifuge tubes. Eight microlitres of each fraction was removed for qPCR, and PBS 5% BSA was then added to each fraction to give a final concentration of 0.1% BSA as a stabilizing agent before tubes were transferred to -80°C . The two or three peak fractions from each pseudo-virus preparation were pooled and aliquoted for use in infectivity and neutralisation assays.

For quantification of reporter plasmid, 8 μ L of each fraction was mixed with 2 μ L of proteinase K buffer containing 100 mM Tris-HCl pH 7.5 (Thermo-Fisher), 100 mM DTT (Sigma), 25 mM EDTA (Sigma), 1% SDS (Sigma) and 200 $\mu\text{g}/\text{mL}$ proteinase K (Qiagen, Courtaboeuf, France). This solution was incubated at 50 $^\circ\text{C}$ for 60 min, then heated to 95 $^\circ\text{C}$ for 10 min and diluted 80-fold in water. One microlitre of this diluted solution was used for qPCR using Applied Biosystems 2 \times Sybr Mix (Applied Biosystems, Villebon-sur-Yvette, France). Primers were CMV-F 5'-CGC AAA TGG GCG GTA GGC GTG-3' and pEGFP-N1-R 5'-GTC CAG CTC GAC CAG GAT G-3'. Thermal cycling was initiated with a first denaturation step at 95 $^\circ\text{C}$ for 10 min to activate the polymerase, followed by 35 cycles of 95 $^\circ\text{C}$ for 15 s and 55 $^\circ\text{C}$ for 40 s. Standard curves were constructed using serial dilutions from 10^2 to 10^7 copies of the pEGFP-N1 plasmid.

2.6. Infectivity Assay

Cells were seeded at 10^4 cells/well in 96-well Falcon plates (BD Falcon, Le Pont de Claix, France) then left to adhere at 37 $^\circ\text{C}$ for at least 1 h. Serial dilutions of each type of BK pseudo-virus were prepared in DMEM 10% FBS + antibiotics, then added to plated 293TT or RS cells so as to inoculate from 1×10^7 to 8×10^4 pEGFP-N1 copies per well of each VP1 variant in quadruplicate. Plates were incubated in a humidified 5% CO_2 incubator at 37 $^\circ\text{C}$ for 72 h (293TT cells), or 96 h (RS cells) after which, cells were washed once in PBS 0.5 mM CaCl_2 , 0.5 mM MgCl_2 , then fixed and stained in PBS 0.5 mM CaCl_2 , 0.5 mM MgCl_2 , 1% paraformaldehyde, and 10 $\mu\text{g}/\text{mL}$ Hoechst 33342. The number and percentage of GFP⁺ cells was quantified using a Celloomics ArrayScan VTI HCS Reader (Thermo Scientific, Courtaboeuf, France). Twelve to twenty-five fields containing 5000–20,000 cells were acquired for each well using HCS Studio Celloomics Scan Version 6.5.0 software. The log₁₀ percentage of GFP⁺ cells was plotted against the log₁₀ inoculated dose (Supplementary Figure S1), and the linear part of the curve was used to calculate the dose required to infect 1% of the plated cells, and hence the ratio of infectious particles to pEGFP-N1 copies in the pseudovirus stock. Control experiments (Supplementary Figure S1) showed that the infectious particle/pEGFP-N1 ratio was reproducible across different quadruplicates set up in the same experiment, and that independent PSV preparations with wild-type VP1 had identical infectious particle/pEGFP-N1 ratios, when measured in the same experiment. To test the dependence of PSV entry on sialic acid, RS or 293TT cells were plated at 10^4 cells/well in 96-well plates, cultured overnight, then parallel series of wells were either left untreated, or incubated with 0.5 U/mL Type V neuraminidase (Sigma) in DMEM supplemented with 0.1% BSA and 25 mM HEPES pH 7.4 for 1 h at 37 $^\circ\text{C}$. Cells were washed three times in PBS 5% FCS, then incubated with PSV at 5×10^7 copies EGFP per well in culture medium for 1 h at 37 $^\circ\text{C}$. Medium was removed, cells were washed three times in PBS 5% FCS, then culture medium was added and cells were incubated for 48–72 h (293TT cells) or 72–96 h (RS cells) before quantification of GFP⁺ cells as described above. For each PSV,

the percentage of GFP+ cells observed in the presence and absence of neuraminidase was used to calculate the percentage inhibition of infectious entry by neuraminidase treatment.

To test infectivity of the whole virus, 50 µg of the pBKV 35-1 plasmid carrying wild-type or mutant VP1 was digested with BamHI and PvuI (New England Biolabs) in CutSmart buffer. Cleavage products were purified on DNA Nucleospin columns (Macherey-Nagel), quantified using a Nanodrop spectrophotometer, then 20 µg of cut DNA were recircularized by ligation with T4 ligase overnight at 16 °C in a reaction volume of 1.2 mL to favour self-ligation. Ligation products were precipitated with isopropanol, then redissolved in sterile 10 mM Tris pH 8, 1 mM EDTA. For transfection, Vero cells were seeded into a 96-well plate at 1×10^4 cells per well, then transfected the next morning with 200 ng/well religated pBKV 35-1 using the Lipofectamine 2000 reagent (Thermo-Fisher). Twenty-four hours after transfection, medium was removed, cells were washed in PBS to remove excess plasmid, and fresh medium was added to wells. At day 7 and 14 post transfection, cells were washed in PBS, then fixed in 2% PFA in PBS for 20 min at room temperature (RT), washed three times in PBS, then permeabilized with 1% Triton X-100 in PBS for 15 min at 37 °C. After three washes in PBS, cells were blocked with 0.5% BSA in PBS for 1 h at RT, then incubated with the mouse monoclonal anti-SV40 TAg (PAb416 clone, Abcam, Cambridge, UK) diluted 1/200 in PBS 0.1% BSA for 1 h at RT. After three washes in PBS 0.05% Tween-20, cells were incubated with Alexa-488 conjugated goat anti-mouse IgG (Thermo Scientific) diluted 1/200 in PBS 0.1% BSA for 1 h at RT before three final washes in PBS 0.05% Tween-20, then counterstaining with PBS 0.5 mM CaCl₂, 0.5 mM MgCl₂, 1% paraformaldehyde and 10 µg/mL Hoechst 33342. The percentage of cells positive for TAg staining was quantified using a Cellomics ArrayScan VTI HCS Reader (Thermo Scientific) as described above.

2.7. Neutralization Assay

Cells were seeded as for an infectivity assay, and during adhesion, pseudovirus stocks were diluted in DMEM supplemented with 0.1% BSA and 25 mM HEPES pH 7.4, and distributed in a 96-well U-bottom plate. Depleted patient serum was added to the first well, then serially diluted in the plate before incubation for 60 min at 4 °C. Pseudotype virus incubated with diluted serum was then transferred onto pre-plated cells. Plates were incubated in a humidified 5% CO₂ incubator at 37 °C for 72 h (293TT cells), or 96 h (RS cells), then fixed and analyzed as described above. A sufficient number of fields were acquired in order to count a minimum of 200 GFP+ cells in control wells incubated in the absence of serum. Percentages of positive cells in test wells were normalized with respect to these control wells, and log₁₀ neutralizing titers were calculated using Prism 5™ software. To compare the effects of different VP1 mutations on neutralization escape, neutralizing titres in each serum were normalized by subtracting the log₁₀ neutralizing titre against wild-type VP1 from the log₁₀ neutralizing titre observed against the variant in the same serum sample.

2.8. Statistical Analysis

Between patient groups, categorical variables were compared by Fisher's exact test and continuous variables were compared by unpaired t-test. Infectious particle/pEGFP-N1 ratios were compared by one-way ANOVA followed by Dunnett's post-hoc test, using the wild-type gIb2-E⁷³E⁸², gIVc2, or gIVc2-S⁶¹ PSV as control for all comparisons. Fisher's exact test was performed using the <http://statpages.info/ctab2x2.html> webpage, and all other tests were performed using Graphpad Prism 5.

3. Results

3.1. VP1 Mutations Accumulate in KTx Recipients with Persistent BKPyV Viruria

In order to examine the relationship between the intensity and duration of BKPyV replication, the presence of non-synonymous VP1 mutations, and the neutralizing antibody response, we studied BKPyV VP1 sequences obtained from the urine of KTx recipients in Nantes and Leipzig with peak

viruria $>7 \log_{10}$ copies/mL. Patients who showed a rapid and sustained reduction in viruria ($>3 \log_{10}$ drop in viruria at 12 months after peak) were defined as the controller group ($n = 12$, Figure 1A), and those who had a drop in viruria less than $2 \log_{10}$ copies/mL over the same period were defined as non-controllers ($n = 12$, Figure 1B).

BKPyV controllers and non-controllers had comparable age, male–female sex ratio, and received similar induction and maintenance immunosuppressive therapies (Table 1). Concerning virological parameters, the delay from graft to first positive viruria, peak viruria, peak viremia, and the proportion of patients with detectable viremia and histologically confirmed PyVAN, were all similar in controllers and non-controllers, and BKPyV genotype I viruses predominated in both groups. The cold ischemia time (CIT) was significantly shorter in the non-controller group (8.7 ± 4.8 h compared to 17.9 ± 6.6 h, $p < 0.001$), and this difference remained significant after excluding three kidneys that came from living donors in the non-controller group. Furthermore, the mean number of HLA mismatches was higher in non-controllers than in controllers.

Table 1. Clinical and biological characteristics of BKPyV Controller and Non-controller groups. For continuous variables, mean \pm standard deviation are shown for each group. Means were compared by unpaired Student t-test, and categorical variables were compared by Fisher’s exact test.

	Controllers ($n = 12$)	Non-Controllers ($n = 12$)	<i>p</i>
Age (years)	56.2 ± 14.5	50.4 ± 12.8	0.308
Sex (M/F)	7/5	10/2	0.371
Kidney donor deceased/living	12/0	9/3	0.217
Cold ischemia time (hours) all donors	17.9 ± 6.6	8.7 ± 4.8	<0.001
Cold ischemia time (hours) deceased donors	17.9 ± 6.6	10.9 ± 3.2	0.008
Number of HLA mismatches	2.7 ± 1.5	4.1 ± 1.4	0.028
Induction therapy Basiliximab/ATG	9/3	7/4	0.667
Immunosuppressive regimen base MMF or MPA plus Tacrolimus	12	11	1.000
Maintenance immunosuppression included corticoids	6	8	0.680
Modification of immunosuppressive regimen following BKPyV reactivation	7	10	0.371
Received IVIG post graft	2	0	0.478
Rejection within 12 months post-graft	1	1	1.000
Months post-graft at first positive viruria	2.9 ± 2.5	3.5 ± 2.9	0.606
Peak viruria (Log ₁₀ copies/mL)	8.8 ± 1.0	8.8 ± 1.1	0.947
Viremia positive	9	10	1.000
Peak viremia (Log ₁₀ copies/mL)	3.7 ± 1.0	4.4 ± 1.2	0.238
Confirmed PyVAN	3	6	0.400
BKPyV genotype I/IV	12/0	10/2	0.478

In controllers, the kinetics of viruria clearance could be modelled as a single-phase ($n = 10$) or two-phase ($n = 2$) exponential decay curve preceded in some cases by a plateau of up to 90 days, with a mean viruria half-life of 6.4 ± 3.2 days, corresponding to a reduction in urine viral load greater than $1 \log_{10}$ per month during the decay phase. In contrast, viruria remained higher than $7 \log_{10}$ copies/mL for more than 12 months in 10 of 12 non-controllers, and the mean reduction in viruria over that time

was less than 0.5 log₁₀. Changes in viremia mirrored changes in viruria. In controllers, viremia was durably suppressed (Figure 1C), whereas in non-controllers, viremia remained close to initial values: patients with high (>4 log₁₀ copies/mL) peak viremia maintained plasma viral loads varying from 3 to 6 log₁₀ copies/mL; patients with intermediate (>3 log₁₀ copies/mL) peak viremia had durable viremia from 2.3 to 4 log₁₀ copies per mL, while three non-controllers had low or undetectable viremia throughout, despite persistent high-level viruria (Figure 1D).

Sequential urine samples were subjected to PCR and Sanger sequencing, and the number of non-synonymous *VP1* mutations in the BC-loop (amino acids 59-84) was plotted against time following initial viruria > 7 log₁₀ copies/mL (Figure 1E,F). The BC-loop sequence was identical to the reference wild-type sequence at the first time point analyzed in 11 out of 12 controllers and 10 out of 12 non-controllers, and sequences in the three remaining patients differed by only one amino acid. The virus population in both controllers and non-controllers was therefore dominated by wild-type virus at early time points. Subsequently, there was a clear correlation between the number BC-loop mutations and the duration of high-level viruria in non-controllers ($r^2 = 0.67$, $p < 0.0001$). Comparing *VP1* sequences in sequential samples from the same patient confirmed that BC-loop mutations accumulated over time in non-controllers (Figure 1F), but this was not observed in the rare controller patients with persistent low-level viruria (Figure 1E). Furthermore, the accumulation *VP1* mutations over time was also observed in patients with undetectable or low viremia (blue symbols, Figure 1E). When possible, *VP1* sequences were analyzed from blood drawn on the same day as the urine sample (18 pairs of samples from 8 patients). In all but one case, the same *VP1* sequences were found in blood and urine. The exception was the last blood-urine pair in patient 3.3, sampled at 23 months post KTx. At this time point, the blood *VP1* sequence carried three new non-synonymous BC-loop mutations in addition to the four mutations that were present in the paired urine sample, or had been detected in previous urine samples.

Furthermore, *VP1* sequences were obtained from urine samples of KTx recipients in Nantes and Leipzig, and pooling these results with the longitudinal data, 71 patients (54 with genotype I including 28 full-length *VP1* sequences; 17 with genotype IV virus) with one or more BC-loop mutation were identified. In this cross-sectional sample, the pattern of mutations in the BC-loop differed slightly between genotype I and genotype IV viruses (Figure 2A). The most frequently mutated amino acids were D60, A72, E73, D75, and E82 in genotype I viruses, and D62, R69, E73, and D77 in genotype IV viruses. In genotype I viruses, A72V was strongly correlated with the presence of a mutation at E73 ($p = 0.002$, Fisher's exact test). In genotype IV viruses, mutation at E73 was associated with R69K ($p = 0.009$) as well as A72V, although in the latter case, the association did not reach statistical significance ($p = 0.051$) due to small sample size. Outside the BC-loop, the only major mutation in genotype I *VP1* was observed at H139. Projecting these amino-acids onto the *VP1* pentamer showed that mutations in both genotype I and genotype IV *VP1* were concentrated at sites forming a ring around the sialic acid binding pocket (Figure 2B,C).

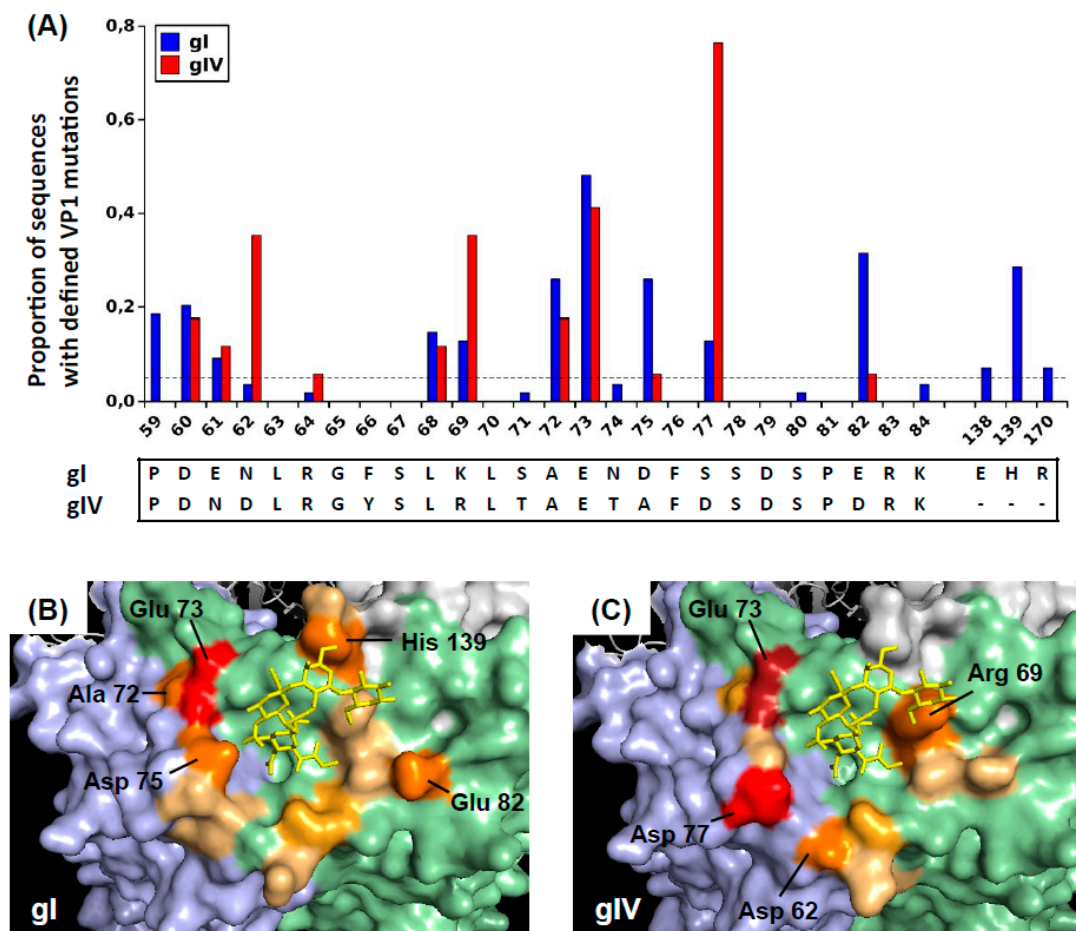


Figure 2. Distribution of VP1 mutations observed in patients with genotype I and genotype IV virus. (A) Prevalence of VP1 mutations among sequences from 54 patients with genotype I BKPyV (26 typing region sequences AA 55–110, 28 full-length VP1 sequences) and 17 patients with genotype IV virus (typing region sequences only). Localisation of observed mutations on genotype I (B) and genotype IV (C) VP1 pentamers. BKPyV VP1 pentamers (4MJ0 [36]) were visualized with Pymol, and the genotype IV-specific BC-loop residues were added using the mutate function. Adjacent VP1 monomers are coloured light blue, light green and light grey, and the GD3 oligosaccharide is shown in a yellow stick representation. Mutations with prevalence >5% are coloured in progressively darker shades on the following scale: mutation prevalence 5–15% lightorange; 15–25% brightorange; 25–35% orange; 35–45% firebrick; >45% red. The files used to prepare panels (B) gI_VP1Muts_Orange.pse and (C) gIV_VP1Muts_Orange.pse are included in the Supplementary Materials.

To further investigate the kinetics of BC-loop evolution in non-controller patients, we analyzed VP1 sequences in sequential urine samples from four non-controller and four controller patients by NGS. At early time points, virus populations were dominated by wild-type VP1 sequences, with <5% mutant sequences detected in all patients. BC-loop mutations then rose to frequencies >10% in non-controller patients after several months of persistent viruria and viremia (Figure 3). A recurring pattern was the emergence of one BC-loop mutation (E73Q in patient 3.5, E73A in patient 3.4, and D77N in patient 3.3) followed by the addition of further mutations to the same mutant VP1 allele. In contrast, BC-loop mutations were not detected at greater than 5% prevalence in the rare controller patients who had a peak of intense virus replication, then subsequently had prolonged low-level viruria and viremia (patients 3.1, 3.2 and 3.12).

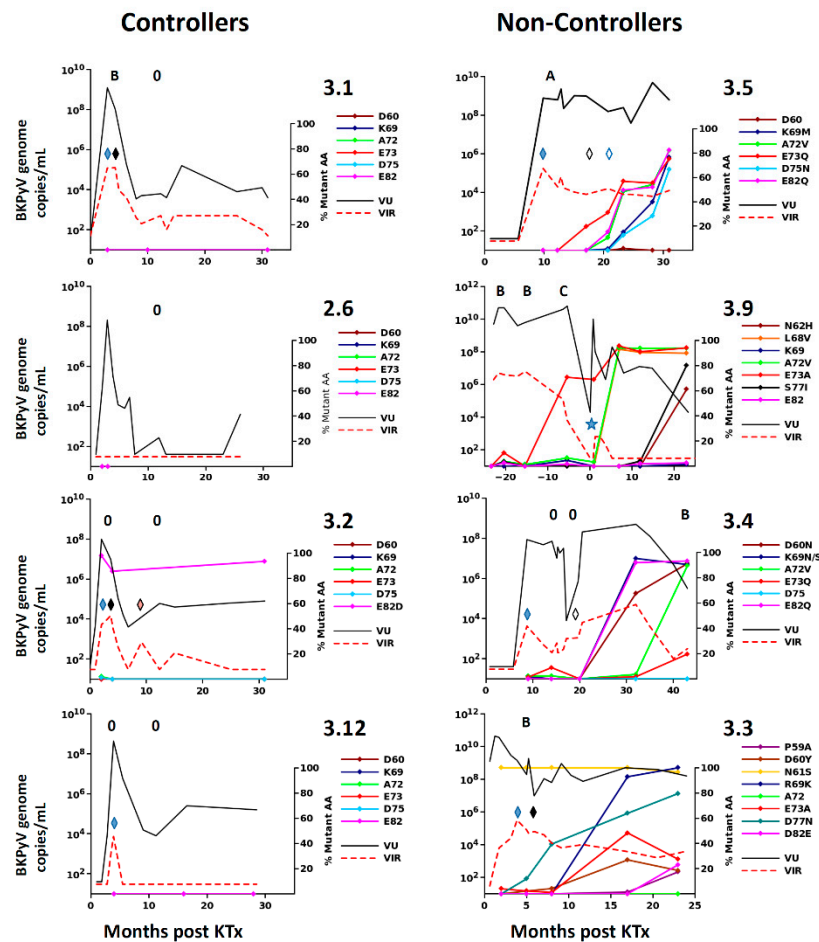


Figure 3. Prevalence of BC-loop mutations in virus population studied longitudinally in controllers and non-controllers. In each panel, urine viral load (VU) and viremia (VIR) are shown against time after Ktx with the scale on the left axis, together with the proportion of selected BC-loop mutations (right axis) detected in the urine at different times. Left panels: controllers; right panels: non-controllers. In non-controllers, the BC-loop mutations that made up at least 10% of the virus population in at least one sample are shown. In controllers, the most frequent BC-loop mutations observed in non-controllers are shown. Mutations at other sites were not detected in controllers. Absence (0) or presence of stage A, B, or C PyVAN in graft biopsies is indicated. Modifications of immunosuppression are indicated by lozenges. Filled blue—MMF reduced by 50%; filled black—MMF discontinued; open black—switch to MPO; open blue—MPO dose reduced by 50%; pink—MMF resumed at 50% dose. In patient 3.9, time is indicated in months post second KTx. Viral load and biopsy results before T = 0 refer to the first KTx. No biopsies were performed for the second graft, since renal function was normal and viremia was negative. The star symbol indicates the initiation of a reduced immunosuppression regime of azathioprine plus low dose MMF.

3.2. Effects of VP1 Mutations on Infectivity of Genotype I and Genotype IV PSV

To investigate the functional impact of BC-loop mutations, four different genotype Ib2 VP1 variants and two different genotype IVc2 VP1 variants observed in non-controller patients were selected for further study (Supplementary Table S1). Firstly, the combinations of different BC-loop mutations were incorporated into expression vectors coding for genotype Ib2 and IVc2 VP1 proteins, then these plasmids were used to prepare pseudotype viruses (PSV) as previously described [35]. We noted that the genotype Ib2 plasmid [37] coded for a VP1 protein carrying two mutations (E73K and E82D). These were reverted to the wild-type amino-acids before incorporating further mutations. Some mutant VP1 plasmids failed to support PSV production, or were produced at very low titres that precluded

their use (Supplementary Table S1), so it was not possible to examine the biological properties of all the VP1 variants observed in vivo.

Infectivity, quantified by the ratio of infectious particles to reporter gene copies in purified PSV stocks, was measured for wild-type PSV, and PSV carrying different VP1 variants. In all cases, the VP1 variants that emerged in patients were associated with reduced infectivity in 293TT cells (Figure 4A,D). The variants Ib2-V⁶⁸V⁷²A⁷³, Ib2-V⁷²K⁷³, and Ib2-V⁷²Q⁷³Q⁸² all had approximately 50-fold lower infectivity than the wild-type Ib2-E⁷³E⁸² PSV in 293TT cells, while Ib2-N⁶⁰N⁶⁹V⁷²Q⁸² resulted in only a 5-fold loss in infectivity. Mutations at the conserved E73 residue significantly reduced PSV infectivity, particularly for E73K (Figure 4B), and an incremental effect of the accumulation of multiple mutations was observed for the Ib2-V⁷²Q⁷³Q⁸² variant (Figure 4C).

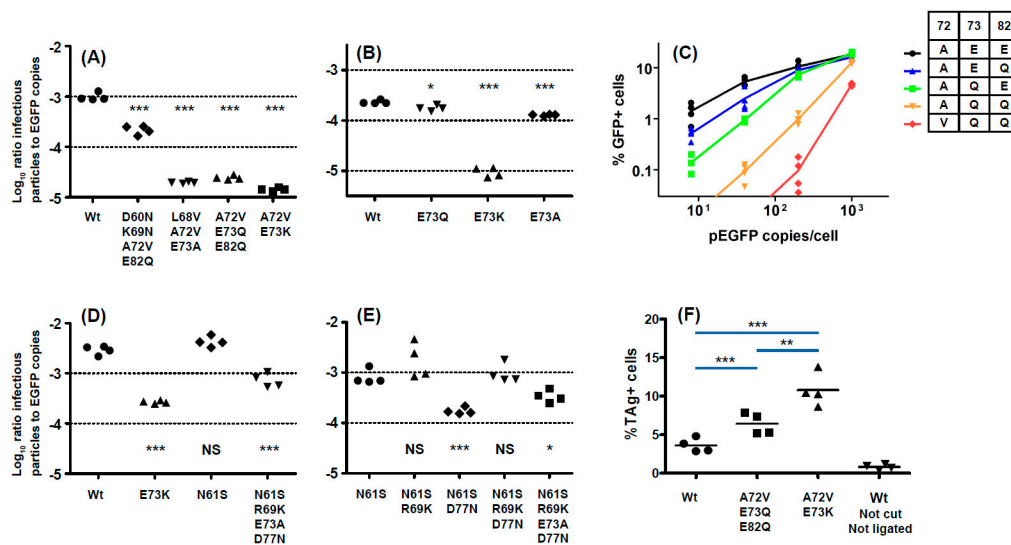


Figure 4. Effects of BC-loop mutations on pseudotype and virus infectivity. Infectivity in 293TT cells of PSV with wild-type genotype Ib2 VP1, and VP1 with multiple (A) or individual (B) BC-loop mutations. Cumulative effect of A72V, E73Q, and E82Q mutations on infectivity of genotype Ib2 PSV in 293TT cells (C). Infectivity in 293TT cells of PSV with wild-type genotype IVc2 VP1, and VP1 with multiple BC-loop mutations (D). Cumulative effect of R69K, E73A and D77N mutations on infectivity of genotype IVc2 PSV in 293TT cells (E). Replication in Vero cells of wild-type BK-MM virus, and mutant viruses incorporating A72V, E73K and A72V, E73Q, E82Q VP1 mutations (F). The uncut pBKV 35-1 plasmid was used as a negative control. Significant differences between groups were tested by one-way ANOVA followed by Tukey's post-hoc test *** $p < 0.001$; ** $p < 0.01$, * $p < 0.05$. All results shown are from one representative experiment of at least two independent experiments.

Similar, though less severe, effects were observed in the two genotype IV variants that were analyzed. In a genotype IV context, the E73K mutation resulted in a 10-fold reduction in infectivity in 293TT cells (Figure 4D), while the IVc2-S⁶¹K⁶⁹A⁷³N⁷⁷ variant had only 3 to 4-fold lower infectivity than wild-type IVc2-N⁶¹R⁶⁹E⁷³D⁷⁷ or the IVc2-S⁶¹R⁶⁹E⁷³D⁷⁷ single mutant (Figure 4D). The N61S mutation, which was present at the initial peak of viremia, appeared to be a neutral polymorphism, as it did not affect infectivity in 293TT cells. D77N reduced infectivity in 293TT cells, and this was mitigated by the R69K mutation. The addition of the E73A mutation slightly reduced infectivity to that seen in the gIVc2-S⁶¹R⁶⁹E⁷³N⁷⁷ variant (Figure 4E).

All of the variants tested were found in VP1 sequences from patients with high viral loads in which the mutant variant dominated the viral population and, therefore, represented viruses that replicated efficiently in vivo. To confirm that VP1 variants with strongly reduced infectivity in 293TT cells were derived from replication-competent viruses, the genotype I BKPyV-MM virus was mutated to incorporate V⁷²K⁷³, and the V⁷²Q⁷³Q⁸² VP1 mutations. Circularized genomic DNA was

transfected into Vero cells, and efficient replication of both these mutant viruses was observed at 14 days post-transfection by nuclear staining for LT antigen (Figure 4F and Supplementary Figure S2). Indeed, both variants reproducibly gave a higher percentage of LT antigen positive cells than wild-type plasmid in this assay, with the V⁷²K⁷³ variant seemingly replicating more efficiently than V⁷²Q⁷³Q⁸². Since VP1 variants with reduced infectivity in 293TT retained infectivity in renal epithelial cells, we then measured the infectivity of PSV incorporating different VP1 variants in the RS cell line, which are human renal tubular epithelial cells (RTEC) immortalized by the SV40 LT antigen and, therefore, a better model for primary RTEC than 293TT cells. VP1 mutations had a markedly reduced impact on PSV infectivity in RS cells (Figure 5A,B). Among genotype Ib2 variants, Ib2-N⁶⁰N⁶⁹V⁷²Q⁸² had 3-fold lower infectivity in RS cells compared to Ib2-E⁷³E⁸², whereas Ib2-V⁶⁸V⁷²A⁷³, Ib2-V⁷²K⁷³, and Ib2-V⁷²Q⁷³Q⁸² all had infectivity close to wild-type in RS cells (Figure 5A). Similarly, the IVc2-S⁶¹K⁶⁹A⁷³N⁷⁷ and IVc2 K73 variants had infectivity close to wild-type IVc2. (Figure 5B). Furthermore, at PSV doses greater than 200 pEGFP copies per cell, the percentage of GFP⁺ RS cells observed after infection with Ib2-V⁷²Q⁷³Q⁸² and IVc2-S⁶¹K⁶⁹A⁷³N⁷⁷ variant PSV was significantly higher than for the corresponding wild-type PSV (Figure 5C,D). In contrast, in 293TT cells, the percentage of GFP⁺ cells compared to wild-type was significantly lower at all tested doses (Figure 5E,F). Therefore, the Ib2-V⁷²Q⁷³Q⁸² and IVc2-S⁶¹K⁶⁹A⁷³N⁷⁷ variants showed increased capacity to infect RS cells, but reduced infectivity in 293TT cells compared to wild-type gI and gIV PSV.

Treatment of cells with neuraminidase prior to infection with PSV fully inhibited Infectious entry of Ib2-E⁷³E⁸² and Ib2-V⁷²Q⁷³Q⁸² PSV into both 293TT cells and RS cells (Figure 6A), indicating that the Ib2-V⁷²Q⁷³Q⁸² VP1 variant remained sialic acid dependent. In contrast, entry of genotype IVc2 PSV into 293TT cells was only partially inhibited by neuraminidase treatment (Figure 6B), while infection by IVc2-S⁶¹K⁶⁹A⁷³N⁷⁷ PSV in RS cells was significantly more resistant to neuraminidase treatment than the corresponding wild-type PSV (Figure 6B).

3.3. Effects of Mutations on Neutralization

Since some VP1 variant PSV had drastically reduced infectivity in 293TT cells, it was necessary to use high doses of these PSV in neutralization assays. Control experiments showed that when used at 5×10^6 and 1×10^6 EGFP copies per well, the neutralizing titre against gIb2-E⁷³E⁸² PSV measured in a panel of six patient sera was significantly lower at the higher PSV dose. However, when neutralizing titres against Ib2-E⁷³E⁸² and gIa PSV (which carry the same BC-loop sequence) were compared at the same input dose, neutralizing titres were not significantly different (Supplementary Figure S3). Neutralizing assays comparing PSV with wild-type and variant VP1 were therefore conducted at the same input dose of PSV against a panel of sera drawn at 12 months post-KTx from six controllers and six non-controllers. To compare the effects of different VP1 mutations on neutralization escape, variant-specific neutralizing titres in each serum were normalized by subtracting the log₁₀ neutralizing titre against wild-type VP1 from the log₁₀ neutralizing titre observed against the variant in the same serum sample. Neutralization escape, defined by a lower neutralizing titre against the variant than against the wild-type, therefore gives negative values on this scale.

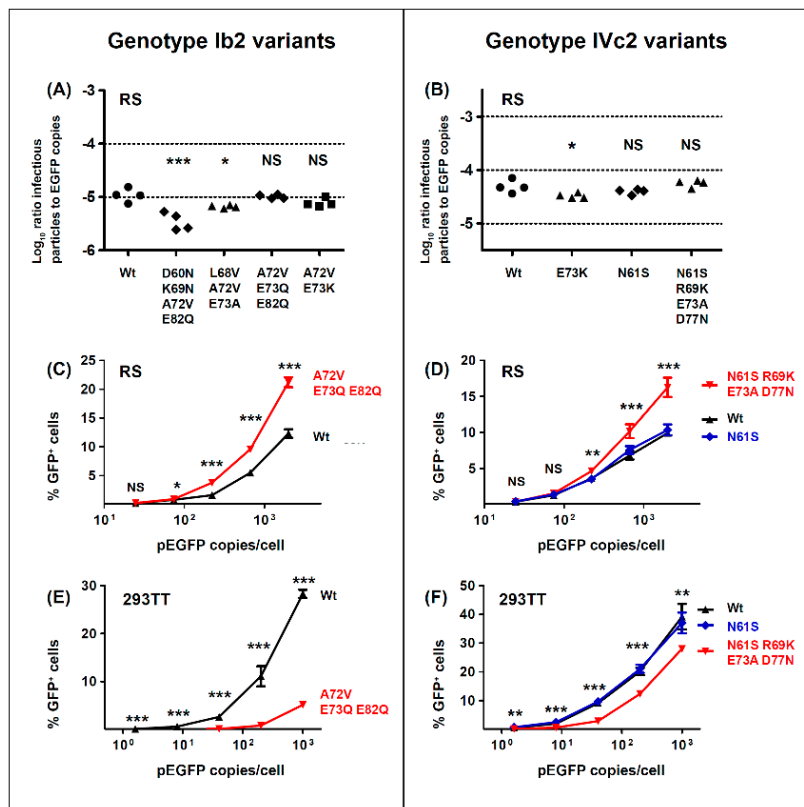


Figure 5. Opposite effects of BC-loop mutations on pseudo-type infectivity in RS and 293TT cells. Infectivity in RS cells of PSV with genotype Ib2 (A) and genotype IVc2 (B) VP1 variants. Percentage of infected RS cells as a function of input PSV dose for wild type gIb2 PSV compared to the V⁷²Q⁷³Q⁸² mutant (C) and wild type gIVc2 PSV compared to the S⁶¹ and S⁶¹K⁶⁹A⁷³N⁷⁷ mutants (D). Percentage of infected GFP⁺ 293TT cells for the same gIb2 (E) and gIVc2 PSV (F). In the experiments shown, the gIb2 Wt and V⁷²Q⁷³Q⁸² PSV were produced in parallel in the same production lot, as were the gIVc2 Wt S⁶¹ and S⁶¹K⁶⁹A⁷³N⁷⁷ PSV. The percentage of GFP⁺ cells at each PSV dose was compared by two-tailed t-test (C,E) or by ANOVA followed by Dunnett’s post-hoc test (D,F). *** *p* < 0.001; ** *p* < 0.01, * *p* < 0.05. The results of one representative experiment of at least two independent experiments are shown. Error bars indicate the StDev of quadruplicates.

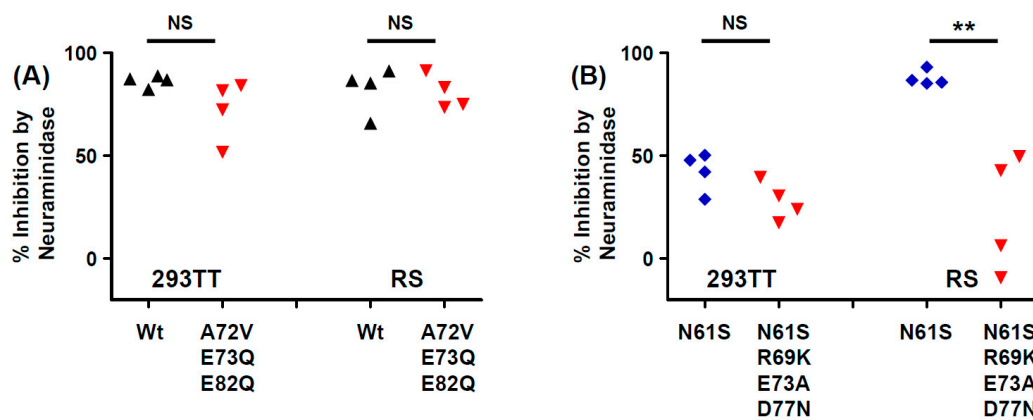


Figure 6. Sialic acid dependence of genotype I and genotype IV VP1 variants. Percentage inhibition of infectious entry of wild-type and V⁷²Q⁷³Q⁸² genotype Ib2 PSV (A), and S⁶¹ and S⁶¹K⁶⁹A⁷³N⁷⁷ genotype IVc2 PSV into 293TT and RS cells (B). One of three independent experiments is shown, with groups compared by two-tailed t-test. ** *p* < 0.01.

Taken as a group, sera from non-controllers were not more susceptible to neutralization escape than sera from controllers (Figure 7A,B). However, in three non-controllers (3.3, 3.4 and 3.8), neutralization escape of the patient's VP1 variant (red symbols, Figure 7A,B) by cognate serum was much clearer than in any of the 11 other sera tested against that variant. The Ib2-N⁶⁹Q⁸² variant that emerged in patient 3.4 was 10-fold more resistant to neutralization by cognate serum than wild-type, while the Ib2-N⁶⁰N⁶⁹V⁷²Q⁸² variant was fully resistant to neutralization (Figure 7C). Similarly, the IVc2-S⁶¹K⁶⁹A⁷³N⁷⁷ variant from patient 3.3 was 17-fold more resistant to neutralization by cognate serum than wild-type IVc2 PSV. Similar results were obtained in RS cells (Supplementary Figure S4), although due to the lower infectivity of the Ib2-N⁶⁹Q⁸² and the Ib2-N⁶⁰N⁶⁹V⁷²Q⁸² variants in RS cells, it was not possible to determine whether these VP1 variants were resistant to neutralization in this cell line. Further experiments confirmed that the combination R69K plus D77N found in patient 3.3 only conferred resistance to neutralization by cognate serum (Supplementary Figure S5). These VP1 mutations were therefore specifically adapted to the neutralizing profile of the host's serum.

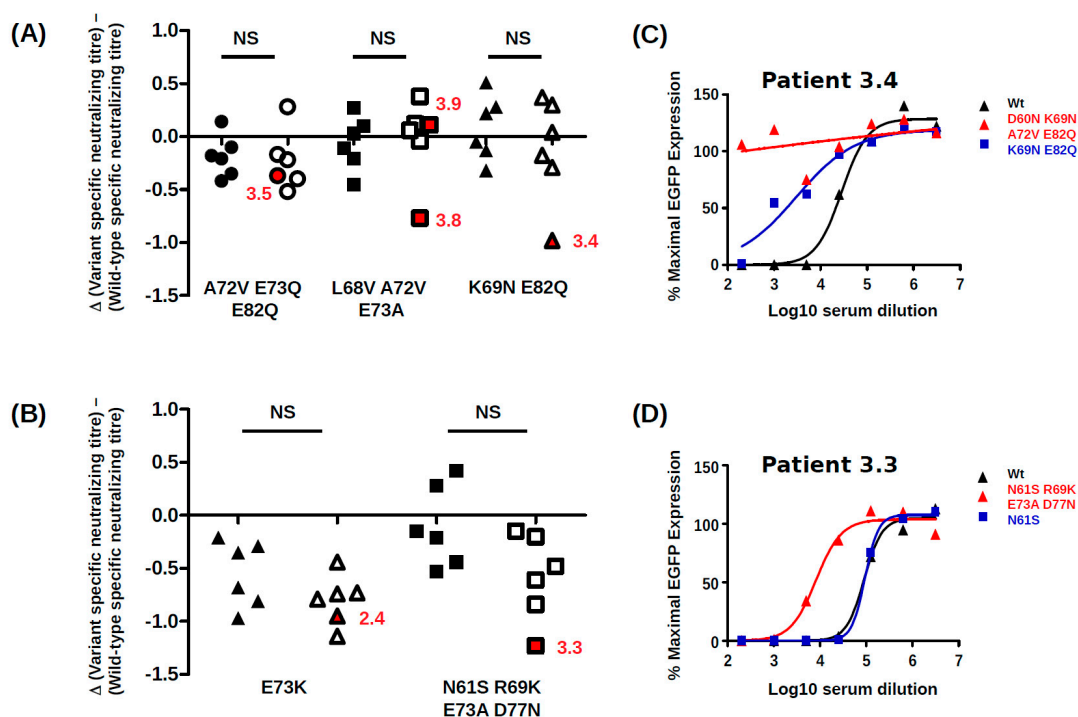


Figure 7. Impact of BC-loop mutations on neutralization by sera from controllers and non-controllers. Neutralizing titres in controller ($n = 6$, filled symbols) and non-controller ($n = 6$, open symbols) sera at 12 months post-KTx were measured against PSV carrying wild type VP1 and different VP1 variants. Experiments were performed in 293TT cells. For each serum, the log10 neutralizing titre against the wild-type virus was subtracted from the log10 neutralizing titre against the VP1 variant measured at the same PSV dose, and the result is plotted for each PSV variant. (A) genotype Ib2 variants; (B) genotype IVc2 variants. Red symbols and adjacent patient codes indicate the cognate non-controller serum for each VP1 variant. Input PSV doses were 500 pEGFP copies/cell for Ib2-V⁷²Q⁷³Q⁸² and Ib2-V⁶⁸V⁷²A⁷³, 200 pEGFP copies/cell for Ib2-N⁶⁹Q⁸² and 100 pEGFP copies/cell for genotype IV variants. (C) Neutralization curves for wild-type Ib2-E73E82, Ib2-N⁶⁹Q⁸² and Ib2-N⁶⁰N⁶⁹V⁷²Q⁸² PSV in serum from patient 3.4 at 12 months post-KTx. (D) Neutralization curves for wild-type IVc2, IVc2-S⁶¹K⁶⁹A⁷³N⁷⁷ PSV in serum from patient 3.3 at 12 months post-KTx.

4. Discussion

In the present work, we investigated the evolution of BKPyV VP1 in patients who showed no virological response to modulation of immunosuppressive therapy compared to controllers, whose viral load dropped more than 1000-fold in the 6 months following peak viruria. In a prospective cohort of

KTx patients recruited in Nantes in 2011–2014, non-controllers made up approximately 30% of the patients (7 out of 24) in whom viremia was greater than 7 log₁₀ copies/mL. Although the patient group definitions are different, this proportion is similar to the 26% rate of persistent PyVAN reported by the Banff working group on PyVAN [12]. Importantly, recent analysis indicates that persistent PyVAN is associated with an increased risk of graft failure and that graft loss occurs almost exclusively in patients with persistent PyVAN [38]. Understanding the physiological basis of persistent, high-level BKPyV replication in KTx recipients is therefore important in order to mitigate these adverse clinical outcomes.

In the present work, most clinical and biological parameters were similar in controllers and non-controllers, and in particular there was no difference in induction or maintenance immunosuppression between the two groups. However, CIT was two times longer in controllers compared to non-controllers, and this difference remained significant after exclusion of live donor transplants. Although this result should be interpreted with caution due to the small sample size, it suggests that when high-level BKPyV replication occurs, it may persist longer in KTx recipients whose transplant was characterized by short CIT. The biological basis of this observation is not clear, since cold ischemia time has not been reproducibly identified as a risk factor for BKPyV reactivation post-graft [39,40]. However, longer CIT is a clear risk factor for delayed graft function and acute rejection [41] and is also related to chronic graft damage [42]. If the same immunological mechanisms, such as higher levels of intra-graft inflammation and T-cell infiltration [43], are involved in graft rejection and control of BKPyV reactivation, this could lead to an association between longer CIT and more rapid control of BKPyV replication.

We found that in all KTx recipients with BKPyV reactivation, the virus population was initially dominated by wild-type *VP1* sequences and that non-synonymous *VP1* mutations then accumulate over time. The emergence of *VP1* mutations was directly related to the duration of high-level BKPyV replication, with the accumulation of non-synonymous BC-loop mutations observed both by Sanger and NGS sequencing. The accumulation of *VP1* mutations over time was initially reported in sequential biopsies from KTx recipients with PyVAN [22], and more recently, Peretti et al. found that *VP1* mutations were present in blood and urine from two patients with PyVAN, but not in plasma or urine samples from 16 KTx recipients with ongoing BKPyV replication in the absence of PyVAN [26], suggesting that BC-loop mutations are a specific hallmark of PyVAN. Our results do not support this interpretation, since BC-loop mutations also emerged in patients with persistent high-level viremia in the absence of viremia and with normal graft function (eg. patients 2.4 and 3.9 Figure 1F), who had no suspicion of PyVAN. Furthermore, *VP1* variants were only found at a prevalence of less than 5% in the viral population in patients with acute PyVAN, accompanied by transient high-level viremia and viremia (eg. patient 3.1 and patient 3.5 at initial peak viremia Figure 3). Therefore, BC-loop mutations are not found in all patients with PyVAN, nor are they restricted to patients with PyVAN. In fact, patient 3.9 illustrated both of these characteristics in the same individual (Figure 3). This patient had two consecutive kidney grafts, with the second following graft loss due to PyVAN. At the time of the first histological PyVAN diagnosis, the E73A mutation was only rarely detected (PyVAN without prevalent *VP1* mutations). Following the second graft, the initial virus persisted, and accumulated several BC-loop mutations, even though graft function was normal and viremia was undetectable (*VP1* mutations without signs of PyVAN). These counterexamples convince us that the duration of continuous BKPyV replication, and not the presence of PyVAN, is the key determinant for the emergence of BC-loop mutations in KTx recipients. Our data are consistent with the first longitudinal study [22] of *VP1* variability, which also demonstrated the accumulation of mutations over time, and two subsequent studies that did not find a relationship between PyVAN and the presence of BC-loop mutations [23,44]. Some inconsistency between studies may be caused by patient stratification into PyVAN/viremia/viremia groups, which are then compared cross-sectionally. Most patients with viremia and/or viremia without PyVAN rapidly control virus replication, while many patients only develop PyVAN after a prolonged period of virus replication, and this may lead to some degree of confounding between cross-sectional groups and the duration of virus replication. To the best of our

knowledge, the present work is the first study in which the duration of virus replication was specifically taken into account in addition to the distinction between PyVAN/viremia/viruria, and this is what allowed us to document the accumulation of VP1 mutations in patients with persistent viruria in the absence of viremia, and the absence of VP1 mutations in patients with acute PyVAN. Whether VP1 evolves more rapidly in patients with PyVAN than in patients with only persistent viruria, and whether the rate of VP1 evolution differs between genotypes are open questions that will require the study of a larger patient cohort.

With respect to the functional impact of BC-loop mutations, very few neutral mutations (only N61S and R69K in gIV) were identified. All other variants, and in particular mutations that modified the conserved E73 residue, resulted in a significant loss of infectivity in 293TT cells. Wild-type gI and gIV VP1 sequences therefore appear to occupy a fitness peak, and this could be related to the high degree of VP1 conservation that is observed in BKPyV genomes. In most cases, however, the diminished infectivity we observed in 293TT cells was not recapitulated in either Vero cells or RS cells, which is consistent with previous data on the infectivity of patient-specific VP1 variants in Vero cells [45]. Indeed, both the Ib2-V⁷²Q⁷³Q⁸² and IVc2-S⁶¹K⁶⁹A⁷³N⁷⁷ variants showed significantly higher infectivity in RS cells than gIb2 and gIVc2 wild-type PSV, despite having significantly lower infectivity in 293TT cells. These results suggest that entry receptors on 293TT cells and RTEC may not be the same, and our results are consistent with the observation that BC loop mutants are able to engage a different spectrum of cell surface glycans than the WT pseudovirus [26]. The one exception was the Ib2-N⁶⁰N⁶⁹V⁷²Q⁸² variant, which had a similar loss of infectivity in both 293TT and RS cells (Figure 5A). Unlike JCPyV, in which VP1 mutations have been shown to switch virus tropism to non-sialylated entry receptors [46], we found that infectious entry of PSV with the Ib2-V⁷²Q⁷³Q⁸² variant was still sialic acid-dependent in both 293TT and RS cells (Figure 6A). Genotype IV viruses may, however, use some non-sialylated entry receptors, since entry of PSV with both gIVc2-Wt and IVc2-S⁶¹K⁶⁹A⁷³N⁷⁷ into 293TT was not fully blocked by neuraminidase treatment, and entry into RS cells mediated by IVc2-S⁶¹K⁶⁹A⁷³N⁷⁷ mutant VP1 was almost entirely insensitive to neuraminidase (Figure 6B). The nature of these potential non-sialylated entry receptors, and the putative receptors for VP1 variants such as Ib2-V⁷²Q⁷³Q⁸², remains to be determined.

BC-loop mutations conferred neutralization escape from cognate serum in five out of six non-controller patients studied. In three of these patients (3.3, 3.4 and 3.8), the mutations that arose in vivo were specifically adapted to the host's humoral response, strongly indicating that VP1 mutations accumulate through positive selection for neutralization escape variants in these individuals. In the two other patients (3.5, 2.4), the VP1 mutations that were observed did confer some degree of neutralization escape from cognate serum, but this was not greater than that seen with serum from other controller or non-controller patients. Only the Ib2-N⁶⁰N⁶⁹V⁷²Q⁸² variant observed in patient 3.4 conferred complete neutralization escape, and this was also the only VP1 variant that displayed markedly reduced infectivity in RS cells, implying that the resistance of this mutant to host neutralization constituted a sufficient selective advantage to compensate its loss of infectivity in RTEC. Unfortunately, it was not possible to confirm that the Ib2-N⁶⁰N⁶⁹V⁷²Q⁸² variant was able to infect RS cells in the presence of serum from patient 3.4, since the infectivity of this variant was too low in RS for neutralization assays to be carried out successfully. Nevertheless, since neutralization assays gave comparable results in 293TT cells and RS cells (compare Figure 7 and Supplementary Figure S4) for the other VP1 variants, it is likely that the neutralization escape observed in 293TT cells for Ib2-N⁶⁰N⁶⁹V⁷²Q⁸² is relevant to neutralization resistance of this variant in RTEC.

For the five other variants studied, the quantitative level of neutralization resistance was relatively modest, ranging from roughly 2 to 3-fold (0.3–0.5 log₁₀) lower neutralizing titres for Ib2-V⁷²Q⁷³Q⁸², to more than 10-fold (1.1–1.2 log₁₀) lower neutralizing titres for gIV variants. The minor impact of Ib2-V⁷²Q⁷³Q⁸² on neutralization by serum from patient 3.5 and the susceptibility of Ib2-V⁶⁸V⁷²A⁷³ to neutralization by serum from patient 3.9 are not consistent with neutralization escape as a significant factor in VP1 evolution in these patients. However, it should be noted that in both these patients,

further VP1 mutations accumulated at later time points (K69M and D77N in patient 3.5 and S77I and N62H in patient 3.9, Figure 2), and it is possible that significant neutralization escape would have been observed if it had been possible to prepare PSV, incorporating these further mutations. It is perhaps also pertinent that the serum from patient 3.9 used in neutralization assays was drawn at 23 months post-KTx, at which point Ib2-V⁶⁸V⁷²A⁷³ had been the dominant variant for more than 12 months, and it is therefore possible that patient 3.9 had generated a specific response against this variant. Alternatively, since Ib2-V⁷²Q⁷³Q⁸² PSV showed enhanced infectivity in RS cells compared to wild type, this variant might have emerged by outcompeting wild-type virus for infection of RTEC, independently of any selection pressure exerted by the humoral response. Previously published modelling work has indicated that the majority of virus shed into the urine originates from infected cells in the urothelium rather than the tubular epithelium in the kidney [47]. If the entry receptors on urothelial cells are slightly different from those present on RTEC, this could explain the otherwise puzzling observation that the highly conserved wild-type VP1 sequences of both genotype I and genotype IV BKPyV are highly adapted to entry into 293TT cells, but do not represent the optimal solution for infecting RS cells. In this scenario, PSV entry into 293TT cells would be a model for BKPyV infection of urothelial cells, whereas PSV entry into RS cells would more closely represent infection of RTEC, and the accumulation of VP1 mutations observed in patient 3.5 could reflect a progressive specialisation of the virus towards RTEC rather than escape from neutralization. Of course, these two processes are not mutually exclusive, for example the IVc2-S⁶¹K⁶⁹A⁷³N⁷⁷ variant showed both resistance to neutralization and enhanced infectivity in RS cells.

Overall, our results confirm and extend the findings of Peretti et al. [26] and underline the role of the humoral response as a driver of VP1 evolution in patients. Neutralizing antibodies therefore can exert selection pressure on BKPyV in patients with persistent viraemia, but appear not to be sufficient, on their own, to eradicate the virus. This may occur because the concentration of IgG in urine, and presumably the glomerular filtrate, of healthy adults is at least 1000-fold lower than in serum [48], so high neutralizing titres in the serum may not fully block virus transmission in the urothelium or renal tubules [49]. Of course, the humoral response is not deployed in isolation, and one important limitation of the present work is that BKPyV-specific CTL responses were not measured. However, in the light of several previous studies that have shown the importance of the antiviral CTL response for BKPyV clearance [15–17], it is likely that our non-controller patients did not mount an effective BKPyV-specific CTL response. This may in fact be the key event that allows the virus capsid to evolve, in the sense that if CTL fail to kill infected cells, then neutralizing antibodies become the last line of defence, and their impact on viral fitness becomes more important. If cellular and humoral responses both fail—in the latter case, due to the selection of VP1 mutants that confer viruses with a competitive advantage in terms of neutralization escape—the result is the persistent high level BKPyV replication that characterizes the non-controller group.

Clinical management of PyVAN currently relies on diminution of immunosuppressive therapy, but this strategy does not always lead to control of virus replication and resolution of nephropathy. It would therefore be useful to identify predictors of the virological and clinical response to modulation of immunosuppression. For this reason, we compared the specificity of the neutralizing response in a panel of BKPyV controllers and non-controllers, working under the hypothesis that serum from non-controllers would have a narrower neutralizing response than serum from controllers. Contrary to our hypothesis, however, no clear difference in specificity between controller and non-controller sera was observed. For example, the Ib2-V⁷²Q⁷³Q⁸² and IVc2-K⁷³ variants were partially resistant to neutralization by sera from both controller and non-controller patients. Therefore, the neutralizing profile of sera from KTx recipients patients with BKPyV reactivation is unlikely to have clinical value as a predictor of persistent high-level virus replication. On the other hand, the existence of escape mutations has implications for therapy of BKPyV with IVIG [50] or monoclonal antibodies. For example, the D60N mutation observed in patient 3.4 disrupts the epitope bound by the broadly neutralizing monoclonal 41F17 [51] and may confer neutralization escape to this antibody. Firstly,

this implies that a combination of different monoclonals recognizing distinct neutralizing epitopes may be required for optimal PyVAN therapy. Secondly, since escape mutations accumulate over time, preventive or pre-emptive use of neutralizing monoclonal antibodies may prove more effective than a curative approach.

Supplementary Materials: The following are available online at <http://www.mdpi.com/1999-4915/12/8/824/s1>, Figure S1: Calculation of ratio of infectious particles to pEGFP copies for pseudotype virus with different VP1 variants in HEK 293TT cells. Figure S2. TAG expression in Vero cells transfected with recircularized pBKV 35-1 plasmid carrying either Wild-type or mutant VP1. Figure S3: Increased pseudotype virus dose significantly reduces measured neutralizing titre. Figure S4. Neutralization of PSV carrying VP1 variants in RS cells. Figure S5: Cumulative effect of VP1 mutations on neutralization escape. Table S1: VP1 mutants produced and analyzed during this study. Data files: gI_VP1Muts_Orange.pse; gIV_VP1Muts_Orange.pse.

Author Contributions: Conceptualization, D.M., C.B.-B. and M.H. (Mario Hönemann); methodology, D.M., N.-K.N., P.B.; formal analysis, P.B., D.M.; investigation, D.M., C.P., A.R., E.P., P.B., N.-K.N.; resources, M.H. (Mario Hönemann), U.L., M.H. (Maryvonne Hourmant), C.B.-B.; data curation, P.B., D.M.; writing—original draft preparation, D.M.; writing—review and editing, M.H. (Mario Hönemann), F.H., C.B.-B.; visualization, D.M.; supervision, D.M., F.H., C.B.-B.; project administration, D.M., C.B.-B.; funding acquisition, D.M., C.B.-B. All authors have read and agreed to the published version of the manuscript.

Funding: This research was funded by grants from the Agence de la Biomedecine (AO Recherche et Greffe 2017) the Fondation Centaure (PAC10, 2017), and the Agence Nationale de la Recherche (Project ANR-17-CE17-0003). Recruitment of Nantes patients into a prospective cohort was made possible by funding from the CHU Nantes (AO Interne CHU Nantes 2011).

Acknowledgments: The authors would like to thank Chris Buck for advice and discussion at several stages of this work, as well as the staff of the MicroPicell platform for help in setting up the HCS analysis.

Conflicts of Interest: The authors declare no conflict of interest. The funders had no role in the design of the study; in the collection, analyses, or interpretation of data; in the writing of the manuscript, or in the decision to publish the results.

References

1. Egli, A.; Infanti, L.; Dumoulin, A.; Buser, A.; Samaridis, J.; Stebler, C.; Gosert, R.; Hirsch, H.H. Prevalence of polyomavirus BK and JC infection and replication in 400 healthy blood donors. *J. Infect. Dis.* **2009**, *199*, 837–846. [[CrossRef](#)] [[PubMed](#)]
2. Sundsfjord, A.; Flaegstad, T.; Flø, R.; Spein, A.R.; Pedersen, M.; Permin, H.; Julsrud, J.; Traavik, T. BK and JC viruses in human immunodeficiency virus type 1-infected persons: Prevalence, excretion, viremia, and viral regulatory regions. *J. Infect. Dis.* **1994**, *169*, 485–490. [[CrossRef](#)] [[PubMed](#)]
3. Leung, A.Y.; Suen, C.K.; Lie, A.K.; Liang, R.H.; Yuen, K.Y.; Kwong, Y.L. Quantification of polyoma BK viremia in hemorrhagic cystitis complicating bone marrow transplantation. *Blood* **2001**, *98*, 1971–1978. [[CrossRef](#)] [[PubMed](#)]
4. Nickleit, V.; Klimkait, T.; Binet, I.F.; Dalquen, P.; Del Zenero, V.; Thiel, G.; Mihatsch, M.J.; Hirsch, H.H. Testing for polyomavirus type BK DNA in plasma to identify renal-allograft recipients with viral nephropathy. *N. Engl. J. Med.* **2000**, *342*, 1309–1315. [[CrossRef](#)] [[PubMed](#)]
5. Hirsch, H.H.; Randhawa, P.S. AST Infectious Diseases Community of Practice BK polyomavirus in solid organ transplantation-Guidelines from the American Society of Transplantation Infectious Diseases Community of Practice. *Clin. Transplant.* **2019**, e13528. [[CrossRef](#)]
6. Leuzinger, K.; Naegele, K.; Schaub, S.; Hirsch, H.H. Quantification of plasma BK polyomavirus loads is affected by sequence variability, amplicon length, and non-encapsidated viral DNA genome fragments. *J. Clin. Virol.* **2019**, *121*, 104210. [[CrossRef](#)] [[PubMed](#)]
7. Babel, N.; Volk, H.-D.; Reinke, P. BK polyomavirus infection and nephropathy: The virus-immune system interplay. *Nat. Rev. Nephrol.* **2011**, *7*, 399–406. [[CrossRef](#)]
8. Garofalo, M.; Pisani, F.; Lai, Q.; Montali, F.; Nudo, F.; Gaeta, A.; Russo, G.; Natilli, A.; Poli, L.; Martinelli, C.; et al. Viremia Negativization After BK Virus Infection in Kidney Transplantation: A National Bicentric Study. *Transplant. Proc.* **2019**, *51*, 2936–2938. [[CrossRef](#)]
9. Bruminhent, J.; Srisala, S.; Klinmalai, C.; Pinsai, S.; Watcharananan, S.P.; Kantachavesiri, S.; Hongeng, S.; Apiwattanakul, N. BK Polyomavirus-specific T cell immune responses in kidney transplant recipients diagnosed with BK Polyomavirus-associated nephropathy. *BMC Infect. Dis.* **2019**, *19*, 974. [[CrossRef](#)]

10. Mühlbacher, T.; Beck, R.; Nadalin, S.; Heyne, N.; Guthoff, M. Low-dose cidofovir and conversion to mTOR-based immunosuppression in polyomavirus-associated nephropathy. *Transplant. Infect. Dis.* **2020**, *22*, e13228. [[CrossRef](#)]
11. Bischof, N.; Hirsch, H.H.; Wehmeier, C.; Amico, P.; Dickenmann, M.; Hirt-Minkowski, P.; Steiger, J.; Menter, T.; Helmut, H.; Schaub, S. Reducing calcineurin inhibitor first for treating BK polyomavirus replication after kidney transplantation: Long-term outcomes. *Nephrol. Dial. Transplant.* **2019**, *34*, 1240–1250. [[CrossRef](#)] [[PubMed](#)]
12. Nickenleit, V.; Singh, H.K.; Randhawa, P.; Drachenberg, C.B.; Bhatnagar, R.; Bracamonte, E.; Chang, A.; Chon, W.J.; Dadhania, D.; Davis, V.G.; et al. The Banff Working Group Classification of Definitive Polyomavirus Nephropathy: Morphologic Definitions and Clinical Correlations. *J. Am. Soc. Nephrol.* **2018**, *29*, 680–693. [[CrossRef](#)] [[PubMed](#)]
13. Solis, M.; Velay, A.; Porcher, R.; Domingo-Calap, P.; Soulier, E.; Joly, M.; Meddeb, M.; Kack-Kack, W.; Moulin, B.; Bahram, S.; et al. Neutralizing Antibody-Mediated Response and Risk of BK Virus-Associated Nephropathy. *J. Am. Soc. Nephrol.* **2018**, *29*, 326–334. [[CrossRef](#)] [[PubMed](#)]
14. Wunderink, H.F.; van der Meijden, E.; van der Blij-de Brouwer, C.S.; Zaaier, H.L.; Kroes, A.C.M.; van Zwet, E.W.; Rotmans, J.I.; Feltkamp, M.C.W. Stability of BK polyomavirus IgG seroreactivity and its correlation with preceding viremia. *J. Clin. Virol.* **2017**, *90*, 46–51. [[CrossRef](#)] [[PubMed](#)]
15. Binggeli, S.; Egli, A.; Schaub, S.; Binet, I.; Mayr, M.; Steiger, J.; Hirsch, H.H. Polyomavirus BK-specific cellular immune response to VP1 and large T-antigen in kidney transplant recipients. *Am. J. Transplant.* **2007**, *7*, 1131–1139. [[CrossRef](#)] [[PubMed](#)]
16. Schachtner, T.; Müller, K.; Stein, M.; Diezemann, C.; Sefrin, A.; Babel, N.; Reinke, P. BK virus-specific immunity kinetics: A predictor of recovery from polyomavirus BK-associated nephropathy. *Am. J. Transplant.* **2011**, *11*, 2443–2452. [[CrossRef](#)] [[PubMed](#)]
17. Leboeuf, C.; Wilk, S.; Achermann, R.; Binet, I.; Golshayan, D.; Hadaya, K.; Hirzel, C.; Hoffmann, M.; Huynh-Do, U.; Koller, M.T.; et al. BK Polyomavirus-Specific 9mer CD8 T Cell Responses Correlate With Clearance of BK Viremia in Kidney Transplant Recipients: First Report From the Swiss Transplant Cohort Study. *Am. J. Transplant.* **2017**. [[CrossRef](#)]
18. Richman, D.D.; Wrin, T.; Little, S.J.; Petropoulos, C.J. Rapid evolution of the neutralizing antibody response to HIV type 1 infection. *Proc. Natl. Acad. Sci. USA* **2003**, *100*, 4144–4149. [[CrossRef](#)]
19. Wei, X.; Decker, J.M.; Wang, S.; Hui, H.; Kappes, J.C.; Wu, X.; Salazar-Gonzalez, J.F.; Salazar, M.G.; Kilby, J.M.; Saag, M.S.; et al. Antibody neutralization and escape by HIV-1. *Nature* **2003**, *422*, 307–312. [[CrossRef](#)]
20. Von Hahn, T.; Yoon, J.C.; Alter, H.; Rice, C.M.; Rehmann, B.; Balfe, P.; McKeating, J.A. Hepatitis C virus continuously escapes from neutralizing antibody and T-cell responses during chronic infection in vivo. *Gastroenterology* **2007**, *132*, 667–678. [[CrossRef](#)]
21. Dowd, K.A.; Netski, D.M.; Wang, X.-H.; Cox, A.L.; Ray, S.C. Selection pressure from neutralizing antibodies drives sequence evolution during acute infection with hepatitis C virus. *Gastroenterology* **2009**, *136*, 2377–2386. [[CrossRef](#)] [[PubMed](#)]
22. Randhawa, P.S.; Khaleel-Ur-Rehman, K.; Swalsky, P.A.; Vats, A.; Scantlebury, V.; Shapiro, R.; Finkelstein, S. DNA sequencing of viral capsid protein VP-1 region in patients with BK virus interstitial nephritis. *Transplantation* **2002**, *73*, 1090–1094. [[CrossRef](#)] [[PubMed](#)]
23. Krautkrämer, E.; Klein, T.M.; Sommerer, C.; Schnitzler, P.; Zeier, M. Mutations in the BC-loop of the BKV VP1 region do not influence viral load in renal transplant patients. *J. Med. Virol.* **2009**, *81*, 75–81. [[CrossRef](#)] [[PubMed](#)]
24. Luo, C.; Hirsch, H.H.; Kant, J.; Randhawa, P. VP-1 quasispecies in human infection with polyomavirus BK. *J. Med. Virol.* **2012**, *84*, 152–161. [[CrossRef](#)] [[PubMed](#)]
25. McIlroy, D.; Halary, F.; Bressollette-Bodin, C. Intra-patient viral evolution in polyomavirus-related diseases. *Philos. Trans. R. Soc. Lond. B Biol. Sci.* **2019**, *374*, 20180301. [[CrossRef](#)] [[PubMed](#)]
26. Peretti, A.; Geoghegan, E.M.; Pastrana, D.V.; Smola, S.; Feld, P.; Sauter, M.; Lohse, S.; Ramesh, M.; Lim, E.S.; Wang, D.; et al. Characterization of BK Polyomaviruses from Kidney Transplant Recipients Suggests a Role for APOBEC3 in Driving In-Host Virus Evolution. *Cell Host Microbe* **2018**, *23*, 628–635.e7. [[CrossRef](#)]
27. Takasaka, T.; Goya, N.; Tokumoto, T.; Tanabe, K.; Toma, H.; Ogawa, Y.; Hokama, S.; Momose, A.; Funyu, T.; Fujioka, T.; et al. Subtypes of BK virus prevalent in Japan and variation in their transcriptional control region. *J. Gen. Virol.* **2004**, *85*, 2821–2827. [[CrossRef](#)]

28. Sharma, P.M.; Gupta, G.; Vats, A.; Shapiro, R.; Randhawa, P. Phylogenetic analysis of polyomavirus BK sequences. *J. Virol.* **2006**, *80*, 8869–8879. [[CrossRef](#)]
29. Martin, M. Cutadapt removes adapter sequences from high-throughput sequencing reads. *EMBnet. J.* **2011**, *17*, 10–12. [[CrossRef](#)]
30. Dodt, M.; Roehr, J.T.; Ahmed, R.; Dieterich, C. FLEXBAR-Flexible Barcode and Adapter Processing for Next-Generation Sequencing Platforms. *Biology* **2012**, *1*, 895–905. [[CrossRef](#)]
31. Gaspar, J.M. NGmerge: Merging paired-end reads via novel empirically-derived models of sequencing errors. *BMC Bioinform.* **2018**, *19*, 536. [[CrossRef](#)] [[PubMed](#)]
32. Deatherage, D.E.; Barrick, J.E. Identification of mutations in laboratory-evolved microbes from next-generation sequencing data using breseq. *Methods Mol. Biol.* **2014**, *1151*, 165–188. [[CrossRef](#)] [[PubMed](#)]
33. Wong-Lee, J.G.; Lovett, M. Rapid and Sensitive PCR method for identification of Mycoplasma species in tissue culture. In *Diagnostic Molecular Microbiology*; American Society for Microbiology: Washington, DC, USA, 1993; pp. 257–260. ISBN 1-55581-056-X.
34. Buck, C.B.; Pastrana, D.V.; Lowy, D.R.; Schiller, J.T. Generation of HPV pseudovirions using transfection and their use in neutralization assays. *Methods Mol. Med.* **2005**, *119*, 445–462. [[CrossRef](#)] [[PubMed](#)]
35. Pastrana, D.V.; Brennan, D.C.; Cuburu, N.; Storch, G.A.; Viscidi, R.P.; Randhawa, P.S.; Buck, C.B. Neutralization serotyping of BK polyomavirus infection in kidney transplant recipients. *PLoS Pathog.* **2012**, *8*, e1002650. [[CrossRef](#)] [[PubMed](#)]
36. Neu, U.; Allen, S.-A.A.; Blaum, B.S.; Liu, Y.; Frank, M.; Palma, A.S.; Ströh, L.J.; Feizi, T.; Peters, T.; Atwood, W.J.; et al. A structure-guided mutation in the major capsid protein retargets BK polyomavirus. *PLoS Pathog.* **2013**, *9*, e1003688. [[CrossRef](#)] [[PubMed](#)]
37. Pastrana, D.V.; Ray, U.; Magaldi, T.G.; Schowalter, R.M.; Çuburu, N.; Buck, C.B. BK polyomavirus genotypes represent distinct serotypes with distinct entry tropism. *J. Virol.* **2013**, *87*, 10105–10113. [[CrossRef](#)] [[PubMed](#)]
38. Nickenleit, V.; Singh, H.K.; Dadhania, D.; Cornea, V.; El-Husseini, A.; Castellanos, A.; Davis, V.G.; Waid, T.; Seshan, S.V. The 2018 Banff Working Group Classification of Definitive Polyomavirus Nephropathy: A Multi Center Validation Study in the Modern Era. *Am. J. Transplant.* **2020**. [[CrossRef](#)]
39. Bressollette-Bodin, C.; Coste-Burel, M.; Hourmant, M.; Sebille, V.; Andre-Garnier, E.; Imbert-Marcille, B.M. A prospective longitudinal study of BK virus infection in 104 renal transplant recipients. *Am. J. Transplant.* **2005**, *5*, 1926–1933. [[CrossRef](#)]
40. Demey, B.; Tinez, C.; François, C.; Helle, F.; Choukroun, G.; Duverlie, G.; Castelain, S.; Brochet, E. Risk factors for BK virus viremia and nephropathy after kidney transplantation: A systematic review. *J. Clin. Virol.* **2018**, *109*, 6–12. [[CrossRef](#)]
41. Mikhalski, D.; Wissing, K.M.; Ghisdal, L.; Broeders, N.; Touly, M.; Hoang, A.-D.; Loi, P.; Mboti, F.; Donckier, V.; Vereerstraeten, P.; et al. Cold ischemia is a major determinant of acute rejection and renal graft survival in the modern era of immunosuppression. *Transplantation* **2008**, *85*, S3–S9. [[CrossRef](#)]
42. Yilmaz, S.; McLaughlin, K.; Paavonen, T.; Taskinen, E.; Monroy, M.; Aavik, E.; Vamvakopoulos, J.; Häyry, P. Clinical predictors of renal allograft histopathology: A comparative study of single-lesion histology versus a composite, quantitative scoring system. *Transplantation* **2007**, *83*, 671–676. [[CrossRef](#)] [[PubMed](#)]
43. Quintella, A.H.D.S.; Lasmar, M.F.; Fabreti-Oliveira, R.A.; Nascimento, E. Delayed Graft Function, Predictive Factors, and 7-Year Outcome of Deceased Donor Kidney Transplant Recipients With Different Immunologic Profiles. *Transplant. Proc.* **2018**, *50*, 737–742. [[CrossRef](#)] [[PubMed](#)]
44. Tremolada, S.; Delbue, S.; Castagnoli, L.; Allegrini, S.; Miglio, U.; Boldorini, R.; Elia, F.; Gordon, J.; Ferrante, P. Mutations in the external loops of BK virus VP1 and urine viral load in renal transplant recipients. *J. Cell. Physiol.* **2010**, *222*, 195–199. [[CrossRef](#)] [[PubMed](#)]
45. Tremolada, S.; Akan, S.; Otte, J.; Khalili, K.; Ferrante, P.; Chaudhury, P.R.; Woodle, E.S.; Trofe-Clark, J.; White, M.K.; Gordon, J. Rare subtypes of BK virus are viable and frequently detected in renal transplant recipients with BK virus-associated nephropathy. *Virology* **2010**, *404*, 312–318. [[CrossRef](#)] [[PubMed](#)]
46. Geoghegan, E.M.; Pastrana, D.V.; Schowalter, R.M.; Ray, U.; Gao, W.; Ho, M.; Pauly, G.T.; Sigano, D.M.; Kaynor, C.; Cahir-McFarland, E.; et al. Infectious Entry and Neutralization of Pathogenic JC Polyomaviruses. *Cell Rep.* **2017**, *21*, 1169–1179. [[CrossRef](#)] [[PubMed](#)]
47. Funk, G.A.; Gosert, R.; Comoli, P.; Ginevri, F.; Hirsch, H.H. Polyomavirus BK replication dynamics in vivo and in silico to predict cytopathology and viral clearance in kidney transplants. *Am. J. Transplant.* **2008**, *8*, 2368–2377. [[CrossRef](#)] [[PubMed](#)]

48. Trinick, T.R.; Laker, M.F. Measurement of urinary immunoglobulins G, A and M by an enzyme linked immunosorbent assay (ELISA). *Clin. Chim. Acta* **1984**, *139*, 113–117. [[CrossRef](#)]
49. Kaur, A.; Wilhelm, M.; Wilk, S.; Hirsch, H.H. BK polyomavirus-specific antibody and T-cell responses in kidney transplantation: Update. *Curr. Opin. Infect. Dis.* **2019**, *32*, 575–583. [[CrossRef](#)]
50. Vu, D.; Shah, T.; Ansari, J.; Naraghi, R.; Min, D. Efficacy of intravenous immunoglobulin in the treatment of persistent BK viremia and BK virus nephropathy in renal transplant recipients. *Transplant. Proc.* **2015**, *47*, 394–398. [[CrossRef](#)]
51. Lindner, J.M.; Cornacchione, V.; Sathe, A.; Be, C.; Srinivas, H.; Riquet, E.; Leber, X.-C.; Hein, A.; Wrobel, M.B.; Scharenberg, M.; et al. Human Memory B Cells Harbor Diverse Cross-Neutralizing Antibodies against BK and JC Polyomaviruses. *Immunity* **2019**, *50*, 668–676.e5. [[CrossRef](#)]



© 2020 by the authors. Licensee MDPI, Basel, Switzerland. This article is an open access article distributed under the terms and conditions of the Creative Commons Attribution (CC BY) license (<http://creativecommons.org/licenses/by/4.0/>).

Titre : Caractérisation des anticorps monoclonaux spécifiques au BKPyV chez les greffés de rein après la réactivation du BKPyV

Mots clés : BKPyV, virus, monoclonal, anticorps, neutralisant, thérapie

Résumé : Le polyomavirus BK (BKPyV) est ubiquitaire et persiste asymptomatiquement dans le rein. La réactivation virale peut être observée chez les greffés du rein qui reçoivent des traitements d'immunosuppression. La réplication active peut causer une morbidité significative. Puisqu'aucune thérapie antivirale à action directe n'est disponible, les anticorps neutralisants représentent des thérapies possibles. L'objectif principal de ma thèse a été de générer des monoclonaux neutralisants à potentiel thérapeutique ainsi que de caractériser le répertoire des récepteurs de cellules B spécifiques de BKPyV (BCR) chez les receveurs de rein avec une réactivation virale. Pour cela, nous avons utilisé des particules virales de BKPyV couplées aux fluorochromes pour isoler une population de cellules B spécifiques de BKPyV. Nous avons obtenu 2158 séquences d'anticorps spécifiques, via

single-cell RNA seq. Après analyse bioinformatique, nos résultats montrent que le répertoire BCR est très diversifié en termes de clonotypes et d'utilisation du gène V. La réponse anticorps spécifique au BKPyV est dominée par l'IgM, puis l'IgG. Bien que les cellules B mémoires de types IgG et IgM soient hypermutées somatiquement et expriment des répertoires BCR distincts, le profil d'expression génique de ces deux sous-populations est très similaire. En outre, le regroupement basé sur la séquence nous a permis d'identifier un groupe d'anticorps neutralisants 41F17-like. Après expression *in vitro* et caractérisation de plus de 20 candidats, nous avons trouvé l'anticorps 120 représentant un anticorps puissant à des fins thérapeutiques en raison de son activité antivirale neutralisante plus forte que le 41F17.

Title : Characterization of BKPyV-specific monoclonal antibodies in kidney transplant recipients after BKPyV reactivation

Keywords : BKPyV, virus, monoclonal, antibody, neutralizing, therapy

Abstract : The BK polyomavirus (BKPyV) is ubiquitous and persists asymptotically in the kidney. BKPyV reactivation can be seen in kidney transplant (KTx) recipients who receive immunosuppression treatments. The active replication can cause significant morbidity. Since no directly acting antiviral therapies are available, neutralizing antibodies represent possible therapeutics. The main objective of my PhD was, therefore, to generate neutralizing monoclonals with therapeutic potential. We also wanted to characterize the BKPyV-specific B-cell receptor (BCR) repertoire in KTx recipients with BKPyV reactivation. For that, we used fluorescence-labeled BKPyV virus-like particles (VLPs) to isolate a population of BKPyV-specific B cells. Using single-cell RNA seq technique, we obtained 2158 BKPyV-specific antibody

sequences which were subsequently submitted to bioinformatic analysis. Our results show that the BCR repertoire was highly diverse in terms of both V-gene usage and clonotype diversity. The BKPyV-specific antibody response was dominated by IgM, then IgG. Although memory IgG and memory IgM B-cells were somatically hypermutated and expressed distinct BCR repertoires, the gene expression profile of these two B-cell subsets was highly similar. Furthermore, sequence-based clustering allowed us to identify a group of 41F17-like broadly neutralizing antibodies. After *in vitro* expression and characterization of more than 20 candidates, we found the antibody 120 representing a potent antibody for therapeutic purposes due to its stronger neutralizing antiviral activity compared to 41F17.